

University of Warwick institutional repository: <http://go.warwick.ac.uk/wrap>

**A Thesis Submitted for the Degree of PhD at the University of Warwick**

<http://go.warwick.ac.uk/wrap/3158>

This thesis is made available online and is protected by original copyright.

Please scroll down to view the document itself.

Please refer to the repository record for this item for information to help you to cite it. Our policy information is available from the repository home page.

**GLOBAL PERSPECTIVES ON THE  
MOLECULAR ECOLOGY OF  
PHOTOSYNTHETIC PICOEUKARYOTES**

Amy R. KIRKHAM

A thesis submitted in fulfilment of the requirements for the degree of  
Doctor of Philosophy

**University of Warwick, Coventry, United Kingdom**

**Department of Biological Sciences**

*September 2009*

## Table of contents

<b>Table of contents</b> .....	<b>i</b>
<b>List of Figures</b> .....	<b>iv</b>
<b>List of Tables</b> .....	<b>vii</b>
<b>Acknowledgements</b> .....	<b>viii</b>
<b>Declaration</b> .....	<b>ix</b>
<b>Publications in preparation</b> .....	<b>x</b>
<b>Summary</b> .....	<b>xi</b>
<b>Abbreviations</b> .....	<b>xii</b>
<b>1. Introduction</b> .....	<b>1</b>
1.1. Biogeochemistry of the oceans .....	2
1.2. Evolution of photosynthesis and the global carbon cycle.....	4
1.3. Evolution of phytoplankton diversity .....	7
1.3.1. Phytoplankton diversity as a feature of complex plastid evolution .....	7
1.3.2 Niche partitioning in the continuous marine environment.....	12
1.3.3 Evolutionary mechanisms revealed by PPE genomics .....	13
1.4. The relative importance of primary producers.....	14
1.5. The fate of carbon fixed by the picophytoplankton .....	16
1.6. Eukaryotic versus prokaryotic picophytoplankton .....	18
1.7. PPE diversity studies.....	21
1.8. Aims of this work.....	30
<b>2. Materials and methods</b> .....	<b>32</b>
2.1. Cruise transects analysed .....	33
2.2. DNA sample collection and extraction .....	34
2.3. Polymerase chain reaction (PCR) .....	35
2.4. Agarose gel electrophoresis .....	36
2.5. Dot blot hybridisation analysis .....	36
2.5.1. Preparation of DNA for hybridisation .....	36
2.5.2. Preparation of dot blot hybridisation membranes.....	37
2.5.3. Dot blot hybridisation probe labelling and purification.....	39
2.5.4. Probing, washing, exposure and stripping of dot blot hybridisation membranes .....	39
2.6. Clone library construction/ TA cloning .....	41
2.7. Restriction Fragment Length Polymorphism (RFLP) analysis.....	41
2.8. DNA purification .....	42
2.9. DNA sequencing.....	42
2.10. Fluorescent in situ hybridisation (FISH) analysis.....	42
2.10.1. FISH sample collection.....	42
2.10.2. FISH probing of filters.....	43
2.10.3. Epifluorescent microscopy.....	44
2.11. Bioinformatic analysis .....	45
2.11.1. Illustration of dot blot hybridisation and environmental data.....	45
2.11.2. Phylogenetic analysis.....	45
2.11.3. Statistical analyses .....	45
<b>3. Photosynthetic picoeukaryote community structure along the Atlantic Meridional Transect (AMT15)</b> .....	<b>48</b>
3.1. Introduction.....	49
3.1.1. History of the Atlantic Meridional Transect.....	49

3.1.2. Characteristics of the phytoplankton along the AMT .....	50
3.1.3. Aims of this work .....	52
3.2. Results .....	53
3.2.1. Chemical and physical characteristics of AMT15 .....	53
3.2.2. Flow cytometric data .....	55
3.2.3. Basin-scale distribution patterns of PPE classes along AMT15 .....	56
3.2.4. A comparison of 16S and 18S rRNA clone libraries .....	63
3.2.4.1. Representation of classes in clone libraries .....	63
3.2.4.2. Phylogenetic relatedness of sequences from clone libraries .....	71
3.3. Discussion .....	82
<b>4. Photosynthetic picoeukaryote community structure along an extended Ellett Line transect .....</b>	<b>91</b>
4.1. Introduction .....	92
4.1.1. History of the Ellett Line and physical oceanographic findings .....	92
4.1.2. Biological features of the Rockall Trough .....	93
4.1.3. Studies of the phytoplankton .....	94
4.1.4. Aims of this work .....	95
4.2. Results .....	96
4.2.1. Physical and chemical characteristics along the extended Ellett Line .....	96
4.2.2. Picophytoplankton abundance along the extended Ellett Line .....	98
4.2.3. Photosynthetic picoeukaryote community structure along the extended Ellett Line assessed using dot blot hybridisation analysis .....	99
4.2.4. Taxonomic composition of photosynthetic picoeukaryotes at two sites along the extended Ellett Line transect .....	104
4.2.5. Phylogenetic analysis .....	106
4.2.6. Photosynthetic picoeukaryote community composition along the extended Ellett Line transect evidenced by fluorescent in situ hybridisation (FISH) analysis .....	115
4.3. Discussion .....	118
<b>5. Photosynthetic picoeukaryote community structure across major ocean basins .....</b>	<b>127</b>
5.1. Introduction .....	128
5.1.1. Introduction to the Arctic Ocean cruise .....	128
5.1.2. Introduction to the Indian Ocean Cruise VANC10MV .....	131
5.1.3. Introduction to the 'Blue EArth GLobal Expedition' (BEAGLE) cruise .....	133
5.1.4. The 'Analysing the Microbial BIodiveriTy of the Indian Ocean' (AMBITION) and 'BIogeochemistry and Optic SOuth Pacific Experiment' (BIOCOPE) cruises. ....	136
5.1.5. Aims of this work .....	137
5.2. Results .....	140
5.2.1. The Arctic Ocean cruise .....	140
5.2.1.1. Arctic Ocean environmental parameters .....	140
5.2.1.2. Picophytoplankton community structure in the Arctic Ocean .....	140
5.2.1.3. PPE distribution patterns in the Arctic Ocean .....	142
5.2.2. The Indian Ocean transect (VANC10MV) .....	147
5.2.2.1. Environmental parameters along the Indian Ocean transect .....	147
5.2.2.2. Picophytoplankton community structure along the Indian Ocean transect .....	148
5.2.2.3. PPE distribution patterns along the Indian Ocean transect .....	149

5.2.3. The BEAGLE transect .....	152
5.2.3.1. Environmental parameters along the BEAGLE transect .....	152
5.2.3.2. Picophytoplankton community structure along the BEAGLE transect .....	152
5.2.3.3. PPE distribution patterns along the BEAGLE transect.....	155
5.2.4. Global perspectives on PPE class distributions .....	158
5.2.5. Phylogenetic analysis of environmental sequences from the Arctic Ocean .....	164
5.3. Discussion .....	168
5.3.1. PPE class distribution patterns along the Arctic Ocean transect.....	168
5.3.2. PPE class distribution patterns along the Indian Ocean transect .....	171
5.3.3. PPE class distribution patterns along the BEAGLE transect.....	172
5.3.4. Global perspectives on PPE class distributions .....	173
<b>6. General discussion and future perspectives.....</b>	<b>177</b>
6.2. Future perspectives .....	182
<b>Bibliography .....</b>	<b>184</b>
<b>Appendix .....</b>	<b>200</b>

## List of Figures

<b>Figure 1.1.</b> Map illustrating the 54 oceanic provinces defined by Longhurst (2007).	2
<b>Figure 1.2.</b> Illustration of static and dynamic province boundaries in the north-east Atlantic Ocean.....	3
<b>Figure 1.3.</b> Schematic representation of the fluxes of carbon in the global carbon cycle .....	6
<b>Figure 1.4.</b> Schematic representation of the origin of plastids by primary and secondary endosymbioses. ....	10
<b>Figure 1.5.</b> Geological timeline.....	11
<b>Figure 1.6.</b> Schematic representation of the biological pump.....	17
<b>Figure 1.7.</b> Flow cytometric signatures of members of the picophytoplankton.....	20
<b>Figure 1.8.</b> Light micrographs of some PPE species .....	23
<b>Figure 2.1.</b> World map showing the position of transects used in this work. ....	33
<b>Figure 2.2.</b> Example phosphorimager picture dot blot hybridisation membranes ...	40
<b>Figure 3.1.</b> Cruise tracks of AMT cruises 1-17.....	50
<b>Figure 3.2.</b> AMT15 cruise track.....	53
<b>Figure 3.3.</b> Contour plots showing chemical and physical parameters along AMT15 .....	54
<b>Figure 3.4.</b> Contour plots of flow cytometry data.....	56
<b>Figure 3.5.</b> Histogram showing the percent relative hybridisation for probes which reached above 2% relative hybridisation along AMT15.....	58
<b>Figure 3.6.</b> Contour plots of dot blot hybridisation data showing the distribution patterns of PPE classes along the AMT15 track .....	59
<b>Figure 3.7.</b> Venn diagram, drawn to scale by the eigenvalues calculated for the total variation in dot blot hybridisation along AMT15 (white) with the amount of variation that can be explained by physical (blue), chemical (red) and biological (yellow) parameters .....	61
<b>Figure 3.8.</b> CCA plot for PPE class distributions along AMT15 in relation to environmental variables .....	62
<b>Figure 3.9.</b> Pie-charts representing the proportion of clones assigned to different classes in clone libraries constructed for samples from AMT15 .....	67
<b>Figure 3.10.</b> Rarefaction curves for clone libraries constructed for samples from AMT15.....	70
<b>Figure 3.11.</b> Phylogenetic relationships amongst the Prymnesiophyceae using nuclear 18S rRNA gene sequences .....	72
<b>Figure 3.12.</b> Phylogenetic relationships amongst the Prymnesiophyceae using plastid 16S rRNA gene sequences.....	73
<b>Figure 3.13.</b> Phylogenetic relationships amongst the Chrysophyceae using nuclear 18S rRNA gene sequences.....	75
<b>Figure 3.14.</b> Phylogenetic relationships amongst the Chrysophyceae using plastid 16S rRNA gene sequences.....	76
<b>Figure 3.15.</b> Phylogenetic relationships amongst the Chlorophyceae using nuclear 18S rRNA gene sequences.....	77
<b>Figure 3.16.</b> Phylogenetic relationships amongst the Chlorophyceae using plastid 16S rRNA gene sequences.....	79
<b>Figure 3.17.</b> Phylogenetic relationships amongst the Cryptophyceae using nuclear 18S rRNA gene sequences.....	81

<b>Figure 3.18.</b> Phylogenetic relationships amongst the Cryptophyceae using plastid 16S rRNA gene sequences .....	81
<b>Figure 4.1.</b> Cruise track of the Extended Ellett Line.....	92
<b>Figure 4.2.</b> The extended Ellett Line track taken by cruise D321b in 2007.....	95
<b>Figure 4.3.</b> Contour plots showing chemical and physical parameters along the extended Ellett Line 2007 .....	97
<b>Figure 4.4.</b> Contour plots of flow cytometry data along the extended Ellett Line....	98
<b>Figure 4.5.</b> Histogram showing the percent relative hybridisation for probes which reached above 2% relative hybridisation along the extended Ellett Line .....	100
<b>Figure 4.6.</b> Contour plots of dot blot hybridisation data showing the distribution patterns of PPE classes along the extended Ellett Line transect .....	101
<b>Figure 4.7.</b> Venn diagram, drawn to scale by the eigenvalues calculated for the total variation in dot blot hybridisation along the extended Ellett Line (white) with the amount of variation that can be explained by physical (blue), chemical (red) and biological (yellow) parameters.....	102
<b>Figure 4.8.</b> CCA plot of the environmental variables (blue) that are associated with the variation in dot blot hybridisation data (red) along the extended Ellett Line ....	103
<b>Figure 4.9.</b> Pie-charts representing the proportion of clones assigned to different classes in clone libraries constructed for samples from the extended Ellett Line....	105
<b>Figure 4.10.</b> Rarefaction curves for clone libraries constructed from samples along the extended Ellett Line .....	106
<b>Figure 4.11.</b> Phylogentic relationships amongst the Prymnesiophyceae using plastid 16S rRNA gene sequences .....	107
<b>Figure 4.12.</b> Phylogenetic relationships amongst the Chrysophyceae using plastid 16S rRNA gene sequences .....	109
<b>Figure 4.13.</b> Phylogenetic relationships amongst the Dictyochophyceae using plastid 16S rRNA gene sequences .....	110
<b>Figure 4.14.</b> Phylogenetic relationships amongst the Bacillariophyceae using plastid 16S rRNA gene sequences .....	111
<b>Figure 4.15.</b> Phylogenetic relationships amongst the Chlorophyceae using plastid 16S rRNA gene sequences .....	112
<b>Figure 4.16.</b> Phylogenetic relationships amongst the Cryptophyceae using plastid 16S rRNA gene sequences .....	114
<b>Figure 4.17.</b> Phylogenetic relationships amongst the Pelagophyceae using plastid 16S rRNA gene sequences .....	115
<b>Figure 5.1.</b> Map illustrating the position of stations sampled in the Arctic Ocean in 2002 used for dot blot hybridisation analysis .....	129
<b>Figure 5.2.</b> Map illustrating the position of stations sampled in the Indian Ocean in 2003 used for dot blot hybridisation analysis .....	132
<b>Figure 5.3.</b> Map displaying the cruise track (yellow line) taken by the BEAGLE project August 2003 - January 2004 .....	134
<b>Figure 5.4.</b> Map showing the position of stations sampled at the surface of the BEAGLE cruise transect for dot blot hybridisation analysis.....	136
<b>Figure 5.5.</b> Map showing the location of cruises analysed by dot blot hybridisations to give global perspectives on PPE community structure.....	138
<b>Figure 5.6.</b> Contour plots showing chemical and physical parameters along the Arctic cruise .....	141
<b>Figure 5.7.</b> Contour plots of flow cytometry data along the Arctic cruise.....	143
<b>Figure 5.9.</b> Venn diagram, drawn to scale by the eigenvalues calculated for the total variation in dot blot hybridisation along the Arctic Ocean cruise (white) with the	

amount of variation that can be explained by physical (blue), chemical (red) and biological (yellow) parameters.....	145
<b>Figure 5.10.</b> Canonical correspondence analysis (CCA) plot for PPE class distribution in the Arctic Ocean in relation to environmental variables .....	146
<b>Figure 5.11.</b> Contour plots showing the chemical and physical parameters measured along the Indian Ocean cruise .....	147
<b>Figure 5.12.</b> Contour plots of flow cytometry data along the Indian Ocean cruise	148
<b>Figure 5.13.</b> Contour plots of dot blot hybridisation data showing the distribution patterns of PPE classes along the Indian Ocean transect .....	149
<b>Figure 5.14.</b> Venn diagram, drawn to scale by the eigenvalues calculated for the total variation in dot blot hybridisation along the Indian Ocean cruise (white) with the amount of variation that can be explained by physical (blue), chemical (red) and biological (yellow) parameters.....	150
<b>Figure 5.15.</b> CCA plot for PPE class distribution in the Indian Ocean in relation to environmental variables .....	151
<b>Figure 5.16.</b> Physical and chemical parameters measured along the BEAGLE transect .....	153
<b>Figure 5.17.</b> Flow cytometry data along the BEAGLE cruise .....	154
<b>Figure 5.18.</b> Percent relative hybridisation (top) and relative proportion (bottom) for probes which reached above 2% relative hybridisation for the BEAGLE transect .	156
<b>Figure 5.19.</b> Venn diagram, drawn to scale by the eigenvalues calculated for the total variation in dot blot hybridisation along the BEAGLE transect (white) with the amount of variation that can be explained by physical (blue), chemical (red) and biological (yellow) parameters.....	157
<b>Figure 5.20.</b> CCA plot for PPE class distribution along the BEAGLE transect in relation to environmental variables.....	158
<b>Figure 5.21.</b> Average relative proportion of PPE classes detected by dot blot hybridisations for each cruise used in this study.....	159
<b>Figure 5.22.</b> Global distribution patterns of PPE classes in samples as determined by dot blot hybridisations.....	160
<b>Figure 5.23.</b> Venn diagram, drawn to scale by the eigenvalues calculated for the total variation in dot blot hybridisation in the global dataset (white) with the amount of variation that can be explained by physical (blue), chemical (red) and biological (yellow) parameters.....	162
<b>Figure 5.24.</b> CCA plot for global PPE class distribution in relation to environmental variables .....	163
<b>Figure 5.25.</b> Pie-chart representing the proportion of clones assigned to different classes in the clone library constructed for station Z59 of the Arctic cruise .....	164
<b>Figure 5.26.</b> Phylogenetic relationships amongst the Prymnesiophyceae using plastid 16S rRNA gene sequences .....	165
<b>Figure 5.27.</b> Phylogenetic relationships amongst the Chrysophyceae using plastid 16S rRNA gene sequences .....	167
<b>Figure 5.28.</b> Phylogenetic relationships amongst the Cryptophyceae using plastid 16S rRNA gene sequences .....	168



## List of Tables

<b>Table 1.1.</b> Contribution of different aquatic ecosystems to primary productivity estimated by Pauly and Christensen (1995).....	4
<b>Table 1.2.</b> List of described PPE species from Vaultot <i>et al.</i> (2008).....	24
<b>Table 2.1.</b> Probes used for dot blot hybridisation analysis.....	38
<b>Table 2.2.</b> Probes used in FISH analyses.....	44
<b>Table 3.1.</b> Summary of clone libraries constructed with nuclear SSU rRNA and plastid 16S rRNA gene amplicons for stations 1, 15, 27 and 33 along AMT15.....	63
<b>Table 3.2.</b> Approximate fragment lengths of potentially photosynthetic classes from RFLP analysis of 18S SSU rRNA gene libraries from AMT15.....	64
<b>Table 3.3.</b> Approximate fragment lengths of potentially photosynthetic classes from RFLP analysis of 16S SSU rRNA gene libraries from AMT15.....	65
<b>Table 3.4.</b> Number of RFLP types, and clones in brackets, identified within each algal class observed in the plastid 16S and nuclear SSU rRNA gene clone libraries from AMT15.....	69
<b>Table 4.1.</b> Number of RFLP types and clones identified within each algal class observed in the two plastid 16S rRNA gene clone libraries from the extended Ellett Line.....	105
<b>Table 4.2.</b> Results of fluorescent in situ hybridisation (FISH) along the extended Ellett Line.....	116
<b>Table 4.3.</b> Fluorescent microscope images of cells observed for each class identified by FISH along the extended Ellett Line transect.....	117
<b>Table 5.1.</b> Summary of cruises sampled in this work.....	139

## **Acknowledgements**

I would like to thank my supervisor Prof Dave Scanlan for all of his help and support during my PhD, I feel very lucky to have worked with you. I also thank my advisory committee: Prof Nick Mann, Dr Hendrik Schaefer and Prof Laura Green.

I need to thank Ludwig Jardillier for always being on hand to provide me with endless support and encouragement, and Sophie Mazard for generously sharing her vast knowledge of all sorts of molecular biology and marine microbiology problems and ideas, and both of them for their friendship over the last four years. Similarly I thank my micro II labmates past and present who have given me great support, with special mention to Cécile, Martin, Martha, Katrin, Andy, Fran, Yi, Ed, Sam, Colin and Steve.

I am indebted to Mike Zubkov who managed to find me an opportunity to work onboard a research ship – a major highlight of my PhD experience. I also thank the Principle Scientific Officer on this cruise, Prof Toby Sherwin for his support and for promptly but patiently helping me out with my queries relating to the cruise as well as aspects of physical oceanography. I am extremely grateful to Ross Holland and Rachel Gibson for their support and company on the cruise, and I thank the Master and Crew of RRS Discovery.

I am also grateful to Andrew Mead who expertly taught me everything I needed to know about multivariate statistics; despite my initial statistics-phobia I understood every single thing – he's a great teacher.

I thank and acknowledge Ana Tiganescu who constructed two of the plastid 16S rRNA gene libraries for AMT15.

I thank the fabulous friends that I have made at Warwick, Phil, Pete, Alicia, Ricci, Ollie, Alex, Siân M. Rob and Andy, and my lovely supportive friends outside Warwick, Siân H., Liza, Lisa, Zoe, Alison and Julia, you are stars.

Thank you to Tony Prior whose advice 4 years ago was pivotal.

Thank you to my family, my wonderful Mum and Dad for everything they've done for me, and Adam my tremendous little brother of whom I am immensely proud.

I thank the Kirkmans for their generosity and support over the last eight months.

Finally I must thank Joe who has put up with so much and been incredibly supportive and patient, teaching me how to deal with all sorts of computer issues, helping me format my work, looking after me and being generally wonderful.

## **Declaration**

I declare the the work presented in this thesis was conducted by myself under the direct supervision of Professor Dave J. Scanlan, with the exception of those instances where contribution of others has been specifically acknowledged. None of the work presented has been previously submitted for any other degree.

Amy Kirkham

## **Publications in preparation**

A.R. Kirkham, L.E. Jardillier, K. Zwirgmaier, A. Tigenescue & D.J. Scanlan. Basin-scale distribution patterns of photosynthetic picoeukaryotes in the Atlantic. For *ISME Journal*.

A.R. Kirkham, L.E. Jardillier, D.J. Scanlan. Photosynthetic picoeukaryote community structure along the Ellett Line in the North Atlantic. For *Environ. Microbiol.*

A.R. Kirkham, C. Lepère, N.J. Fuller, L.E. Jardillier, A. Mead, D.J. Scanlan. A global study of photosynthetic picoeukaryote distribution. For *ISME Journal*.

## Summary

Photosynthetic picoeukaryotes (PPEs) are single celled algae of <math><3\mu\text{m}</math> diameter, present in both marine and freshwater environments. Marine PPEs have begun to gain increasing recognition as important, ubiquitous primary producers, after largely being overlooked in favour of the more numerous picocyanobacteria for many years. Molecular studies have shown the group to be extremely diverse. However, most molecular studies have used PCR with general primers targeting the nuclear 18S rRNA gene to construct clone libraries and have been dominated by heterotrophic picoeukaryotes. To overcome this problem, more recent molecular studies have targeted the 16S rRNA gene of marine algal plastids, an approach which essentially excludes heterotrophic organisms.

In this PhD thesis, the molecular diversity of the PPE community was analysed over broad spatial scales using both 16S and 18S rRNA gene markers to begin to draw global conclusions on the phylogenetic composition of this group and identify the major players in marine CO<sub>2</sub> fixation. Moreover, distributions of various PPE classes were also analysed along a range of cruise transects with dot blot hybridisation of PCR amplified DNA using class-specific plastid 16S rRNA gene targeted oligonucleotide probes. All major ocean basins were analysed, encompassing a range of nutrient regimes and latitudes.

The dot blot hybridisation approach revealed that the classes Prymnesiophyceae and Chrysophyceae appeared to be ubiquitous and dominated the PPE community throughout large expanses of the global ocean. Furthermore, these classes showed strongly complementary distributions along some of the transects analysed. Clone library construction demonstrated that both classes are comprised of an array of genetic lineages, many with no close cultured counterpart. For one cruise transect, the extended Ellett Line in the North Atlantic Ocean, a fluorescent *in situ* hybridisation approach was used as a PCR-independent assessment of the PPE community. This approach largely supported the dot blot hybridisation data.

Other classes, Cryptophyceae, Pinguiphyceae, Pelagophyceae, Eustigmatophyceae, Pavlovophyceae, Trebouxiophyceae, Chlorarachniophyceae and Prasinophyceae clade VI, were detected at lower abundances by dot blot hybridisation, with some classes restricted to specific sites. Multivariate statistics indicated that the distribution patterns of PPE classes were influenced by both temperature and nutrient concentrations. However, at the global scale, a large proportion of the variation in dot blot hybridisation data could not be explained by the environmental parameters measured. It is likely that the classes harbour different ecotypes which are individually influenced by environmental factors. Furthermore, biotic parameters not measured in this work e.g. viral lysis, predation or parasitic infection may have been important in controlling the PPE community.

## Abbreviations

ALSK	Alaska Downwelling Coastal Province
AMBITION	Analysing the Microbial Biodiversity of The Indian Ocean
AMT	Atlantic Meridional Transect
ANTA	Antarctic Province
APLR	Austral Polar Province
ARAB	Northwestern Arabian Upwelling Province
ARCH	Archipelagic Deep Basins Province
ARCT	Atlantic Arctic Province
ATP	adenosine triphosphate
AUSE	East Australian Coastal Province
AUSW	Australia-Indonesia Coastal Province
BEAGLE	Blue Earth Global Expedition
BENG	Benguela Current Coastal Province
BERS	North Pacific Epicontinental Sea Province
BIOCOPE	Biochemistry and Optics South Pacific Experiment
BPLR	Boreal Polar Province
BRAZ	Brazil Current Coastal Province
BSA	bovine serine albumin
CAMR	Central American Coastal Province
CARB	Caribbean Province
CCA	canonical correspondence analysis
CCAL	California Upwelling Coastal Province
CCMP	Provasoli-Guillard National Centre for Culture of Marine Phytoplankton
CHIL	Chile-Peru Current Coastal Province
CHIN	China Sea Coastal Province
CNRY	Eastern Canary Coastal Province
CTD	conductivity temperature depth
DAPI	4', 6- diamidino-2-phenylindole
DNA	deoxyribonucleic acid
DOM	dissolved organic matter
EAFR	Eastern Africa Coastal Province
EDTA	ethylenediaminetetraacetic acid
ETRA	Eastern Tropical Atlantic Province
Fe-SOD	Iron-superoxide dismutase
FISH	fluorescent <i>in situ</i> hybridisation
FITC	Fluorescein isothiocyanate
FKLD	Southwest Atlantic Shelves Province
GFST	Gulf Stream Province
GUIA	Guianas Coastal Province
GUIN	Guinea Current Coastal Province
HB	hybridisation buffer
HL	high light
HPLC	high performance liquid chromatography
INDE	Eastern India Coastal Province
INDW	Western India Coastal Province
IPTG	isopropyl $\beta$ -D-1-thiogalactopyranoside

ISSG	Indian South Subtropical Gyres Province
kb	kilo base
KURO	Kuroshio Current Province
LB	lysogeny broth
LL	low light
Mbp	mega base pairs
MEDI	Mediterranean Sea, Black Sea Province
MONS	Indian Monsoon Gyres Province
mya	million years ago
NADR	North Atlantic Drift Province
NAG	North Atlantic Gyre
NASE	North Atlantic Subtropical Gyral East Province
NASW	North Atlantic Subtropical Gyral West Province
NATR	North Atlantic Tropical Gyre Province
NECS	Northeast Atlantic Shelves Province
NEWZ	New Zealand Coastal Province
NPPF	North Pacific Transition Zone Province
NPSW	North Pacific Subtropical Gyre West
NPTG	North Pacific Tropical Gyre Province
NWCS	Northwest Atlantic Shelves Province
OTU	operational taxonomic unit
PCR	polymerase chain reaction
PEQD	Pacific Equatorial Divergence Province
PNE	photosynthetic nanoeukaryote
PNEC	North Pacific Equatorial Countercurrent Province
PNNL	Pacific Northwest National Laboratory
POC	particular organic carbon
PPE	photosynthetic picoeukaryote
PSAE	Pacific Subarctic Gyre East Province
PSAW	Pacific Subarctic Gyre West Province
<i>psbA</i>	gene encoding the D1 protein of photosystem II
qPCR	quantitative PCR
RCC	Roscoff Culture Collection
REDS	Red Sea, Persian Gulf Province
RFLP	restriction fragment length polymorphism
RNA	ribonucleic acid
rRNA	ribosomal RNA
SACZ	Sub-Antarctic Convergence Zone
SAG	South Atlantic Gyre
SANT	South Subtropical Convergence Province
SARC	Atlantic Subarctic Province
SATL	South Atlantic Gyral Province
SDS	sodium dodecyl sulphate
SSPE	sodium chloride, sodium hydrogen phosphate, EDTA buffer
SSU	small subunit
SUND	Sundra-Arafura Shelves Province
TASM	Tasman Sea Province
TBE	tris borate EDTA
TE	tris EDTA
TER	Tropics and Equatorial Region

TNT	Tris NaCl Tween® 20 buffer
WARM	Western Pacific Warm Pool Province
WB	washing buffer
WTRA	Western Tropical Atlantic Province



## **Chapter 1:**

## **Introduction**

## 1.1. Biogeochemistry of the oceans

Studies of marine ecology recognise that different regions of the world's oceans are characterised by different physical and biological parameters including the production and consumption of organic material (Longhurst, 2007). Attempts have been made to delineate the oceans into ecological provinces, as it is useful to have maps of major oceanic regions to refer to when considering fields of research in marine ecology (Watson *et al.*, 2003). These authors regard differences between regions of the sea to be governed by physical characteristics, and conclude that ocean frontal regions are linked to partitions in ecological geography.

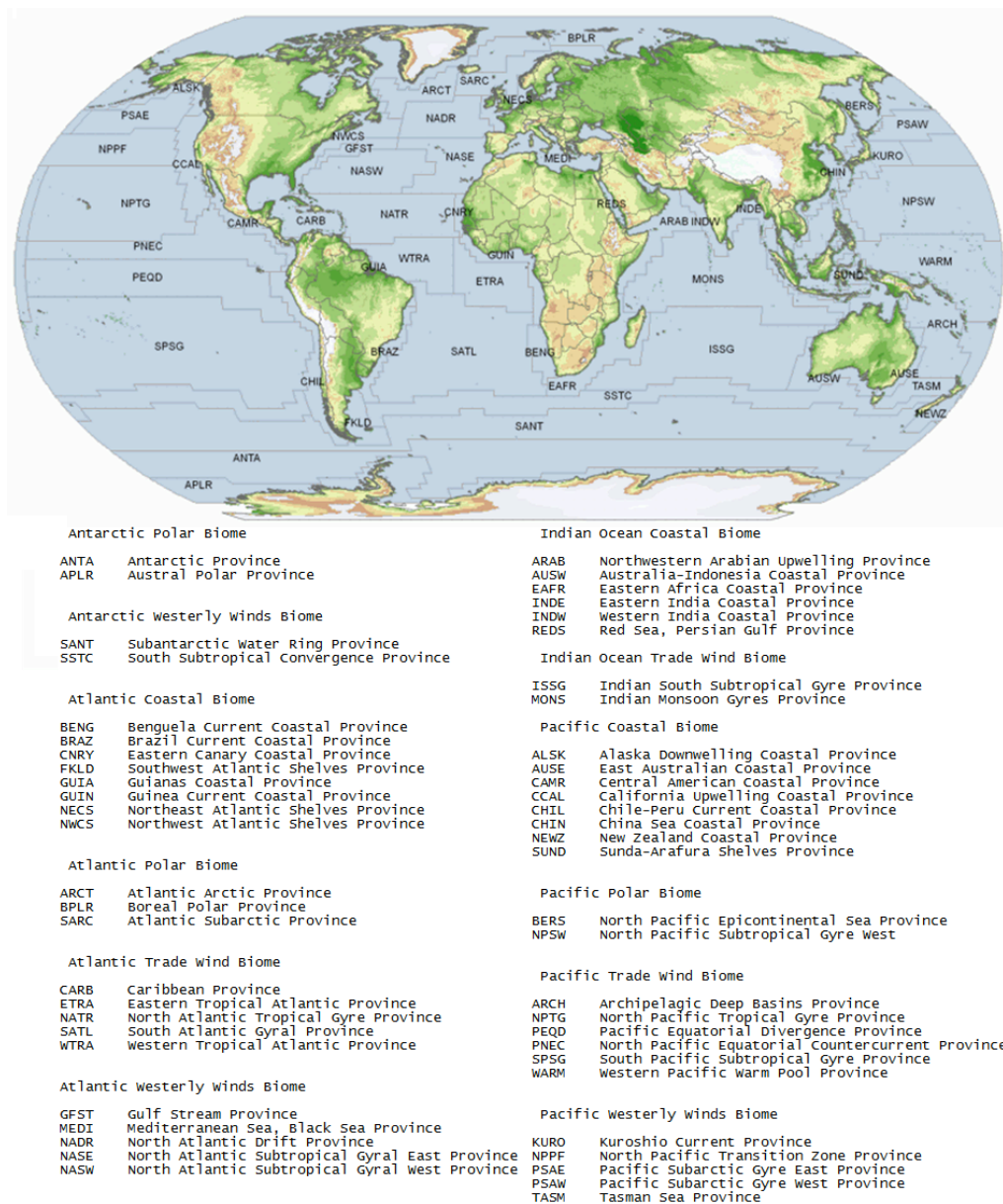


**Figure 1.1.** Map illustrating the 54 oceanic provinces defined by Longhurst (2007). Image retrieved from [www.vliz.be/vmdcdata/vlimar/downloads.php](http://www.vliz.be/vmdcdata/vlimar/downloads.php).

According to Longhurst (2007), the upper part of world's oceans are primarily categorised into four biomes, the polar, westerly winds, trade winds and coastal biomes. These are principally based on local physical processes affecting the stability of the upper ocean. The biomes are further subcategorised into provinces in order to reflect the regional structure of the pelagic ecosystem (Fig. 1.1), as different sea and shelf regions differ from each other in their ecology (Longhurst, 2007).

Physical ocean processes and biological parameters can be identified and monitored rapidly by satellite observations. In particular, sea surface temperature and chlorophyll *a* concentration can be monitored with remarkable accuracy and efficiency (Longhurst, 2007; Devred *et al.*, 2007). Such studies reveal the extent of the dynamic nature of oceanic provinces in actuality (Devred *et al.*, 2007) (Fig. 1.2). Thus, partitioning of pelagic ecology is a best-fit solution and not an exact science (Longhurst, 2007).

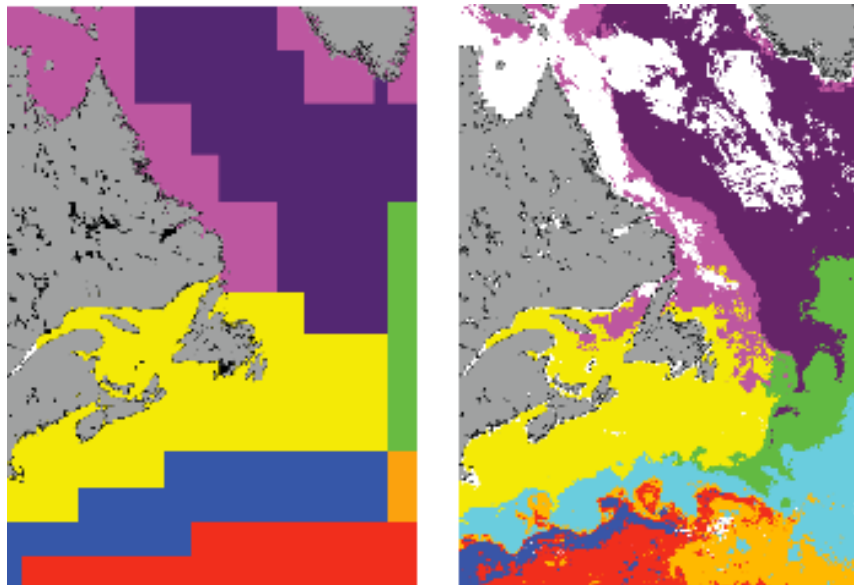


**Figure 1.2.** Illustration of static and dynamic province boundaries in the north-east Atlantic Ocean. Static boundaries as defined by Longhurst (2007) (left) compared with dynamic province boundaries computed for the last two weeks of April 2003 (right). Colours refer to domains (see key in Fig. 1.1): pale purple is BPLR domain, dark purple is ARCT, yellow is NWCS, green is NADR, blue is GFST, orange is NASE and red is NASW. Image retrieved from [www.emmanueldevred.net/research](http://www.emmanueldevred.net/research).

Chlorophyll *a* concentration is an important variable that gives an indication of the primary productivity of particular regions, and gives a proxy for biomass. Global

estimates of primary production, divided into basic ecosystem types, indicate that the open ocean is the site of approximately one third of global primary production, despite having low primary production rates per unit area. This is as a result of the vast area of the Earth's surface occupied by open ocean (Pauly and Christensen, 1995) (Table 1.1.). It is, therefore, important to study the ecology of the open ocean and the organisms responsible for this primary production.

**Table 1.1.** Contribution of different aquatic ecosystems to primary productivity estimated by Pauly and Christensen (1995).

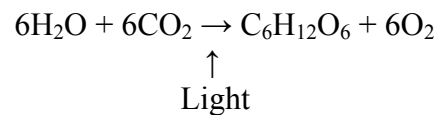
Ecosystem Type	Area (10 <sup>6</sup> km <sup>2</sup> )	Primary Productivity (gC m <sup>2</sup> /yr)	Contribution to Aquatic Productivity (%)	Contribution to Global Productivity (%)
Open Ocean				
Regions	332.0	103	75	31
Upwelling				
Regions	0.8	973	2	0.8
Tropical				
Shelves	8.6	310	6	2.4
Non-Tropical				
Shelves	18.4	310	12	5
Coastal/Reef				
Systems	2.0	890	4	1.7
Terrestrial				
Rivers/Lakes	2.0	290	1	0.4

## 1.2. Evolution of photosynthesis and the global carbon cycle

Oxygenic photosynthesis arose over 2500 million years ago, probably from a simpler anoxygenic form of photosynthesis. Genome comparison of cyanobacteria with members of the four extant anoxygenic photosynthetic phyla indicated the importance of extensive horizontal gene transfer between these phyla, crucial to the evolution of oxygenic photosynthesis (Raymond *et al.*, 2002). Oxygenic photosynthesis transformed the biochemistry of Earth. Accumulation of oxygen in the atmosphere lead to the formation of the ozone layer which shields the Earth's surface and would have allowed colonisation of land. Furthermore, oxygen was also used as an electron acceptor in metabolically efficient aerobic respiration. Both of these processes allowed the evolution of complex life (McFadden and Gilson, 1995). It has remained the most important process for the maintenance of life on Earth because

photosynthesis is the main source of metabolic energy and basis of food chains in almost all environments globally (Giovannoni and Stingl, 2005).

Although carbon is the basis of life on Earth, it is not a particularly abundant element in the atmosphere or the Earth's crust. However, carbon occurs in a huge diversity of naturally occurring compounds. Carbon compounds comprise the foundation of energy storage and respiration (the conversion of sugar to ATP) in organisms, as well as structural factors such as the 'backbone' of nucleic acids and cellulose cell walls of plants (Encyclopaedia Britannica, 1990). Carbon is supplied to most organisms through the ingestion of food sources and to photosynthetic organisms through uptake of inorganic carbon in the form of carbon dioxide (CO<sub>2</sub>) which is converted into organic carbon using light energy. In oxygenic photosynthesis, this process is described as follows:



C<sub>6</sub>H<sub>12</sub>O<sub>6</sub> being glucose.

Carbon is present in three reservoirs: the atmosphere, marine systems and terrestrial systems; and circulates between these reservoirs (Fig. 1.3). Photosynthetic organisms in marine and terrestrial environments form carbon sinks as CO<sub>2</sub> is taken up and incorporated into biomass. However, human activities of fossil-fuel burning and deforestation have returned hundreds of gigatonnes of carbon to the atmosphere (Post *et al.*, 1990). The action of photosynthesis is vital in removing CO<sub>2</sub> from the atmosphere. However, it is unlikely that photosynthesis can mitigate the effects of anthropological carbon release (Falkowski *et al.*, 2000).

Satellite-based estimates show that approximately half of global carbon fixation occurs in the marine environment (Field *et al.*, 1998). Oceans store carbon as dissolved inorganic carbon, dissolved organic carbon and particulate carbon (including carbon incorporated into biomass) and play a major role in influencing the concentration of CO<sub>2</sub> in the atmosphere (Post *et al.*, 1990). Carbon is readily exchanged between surface waters and the air, and an approximate equilibrium is

maintained at the sea-air interface (Post *et al.*, 1990).  $\text{CO}_2$  is moved down the water column by physical mixing as well as processes known as the biological pump (Ducklow *et al.*, 2001). This transfer of carbon to deeper waters allows the continued uptake of  $\text{CO}_2$  at the ocean surface. The biological pump is discussed with reference to photosynthetic picoeukaryotes (PPEs) below (section 1.5). This process results in the accumulation of organic carbon at depth in the marine environment, thus removing carbon from the system for thousands of years (Ducklow *et al.*, 2001). The amount of carbon taken out of the carbon cycle by the marine system is in the region of two gigatonnes annually (Post *et al.*, 1990; Fig. 1.3). Thus, the organisms responsible for carbon fixation in the oceans are the subject of a great deal of scientific interest.

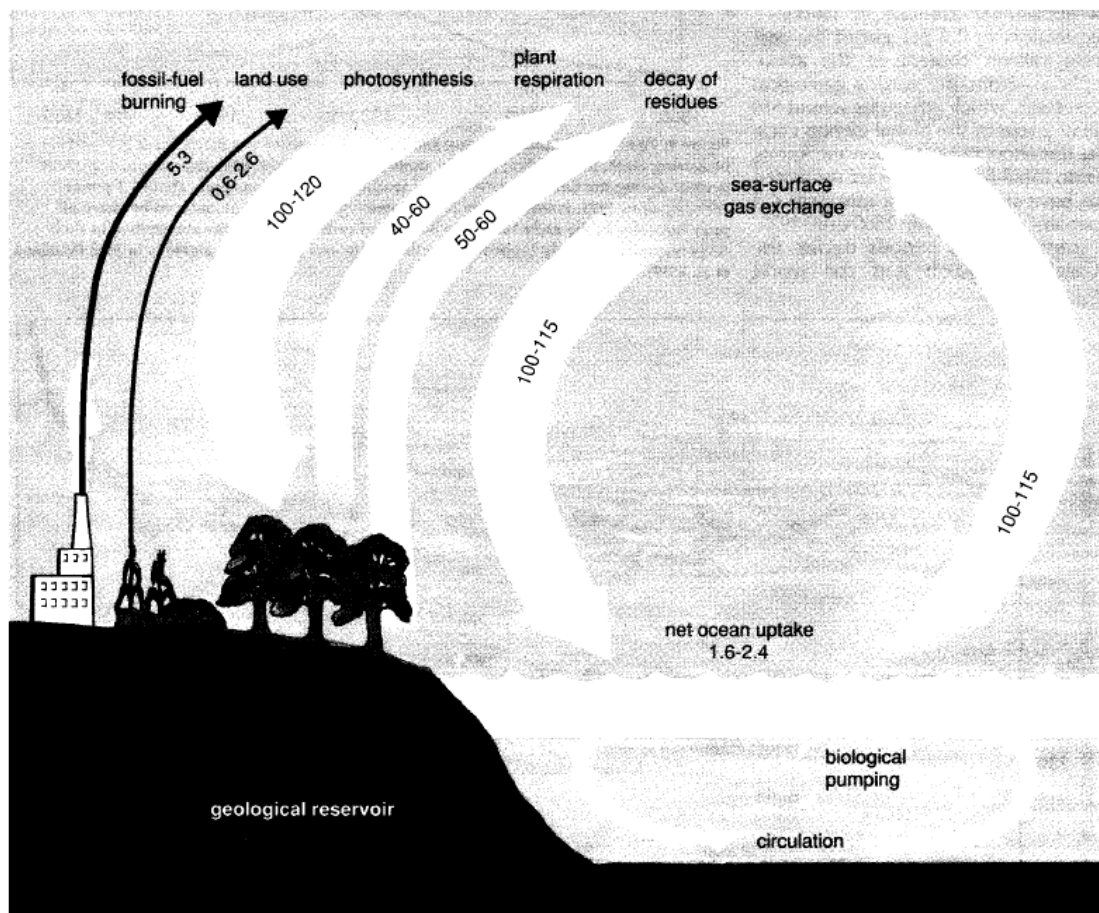


**Figure 1.3.** Schematic representation of the fluxes of carbon in the global carbon cycle with carbon fluxes annotated with amounts of carbon in gigatonnes based on 1980 estimates. Image used from Post *et al.* (1990).

### 1.3. Evolution of phytoplankton diversity

#### 1.3.1. Phytoplankton diversity as a feature of complex plastid evolution

The marine environment is understood to be a continuous habitat with the absence of barriers isolating groups of organisms traditionally thought to be vital in the evolution of new species (Tait and Dipper, 1998). Debate continues regarding limitations to evolution of marine protists based on lack of geographical boundaries. For example, some authors believe that microbial eukaryotes do not display biogeographies as a result of population sizes and their propensity to dispersal by environmental perturbations or oceanic currents. As a result, marine microbial species diversity is considered low with species maintaining consistent levels of rarity or abundance at the global scale (Finlay, 2002). However, despite global dispersal of marine phytoplankton it was shown that this doesn't imply reduced species richness. For example, isolates of the photosynthetic picoeukaryote (PPE) *Micromonas pusilla* (Prasinophyceae), considered to be a single species, actually comprise divergent lineages and cryptic species (Šlapeta *et al.*, 2006). The authors of this study show that some of this diversification is ancient, and suggest that global ocean currents did not always operate as they do today. Thus, geographic isolation may have driven diversification in evolutionary history when oceans were not globally mixed. However, sequence data suggests divergence has been ongoing in *Micromonas pusilla*, this cannot therefore be explained by reduced oceanic mixing (Šlapeta *et al.*, 2006).

A major factor in the diversity of phytoplankton may be the complex nature of plastid acquisition. Plastid evolution is a controversial subject and tracing this history is made extremely difficult by the fact that plastids have moved laterally between eukaryotic groups that are not closely related to each other (Archibald, 2009). Incorporation of permanent plastids would have been a complex process. The uptake of a cyanobacterial endosymbiont was followed by reduction of its genome through loss of genes no longer required given the endosymbiont's new environment, and horizontal transfer of genes required for maintenance of the plastid to the host's genome. The relocation of essential plastid genes to the host genome is dependent on complex import mechanisms for gene products into the plastid (Moreira and

Philippe, 2001). The establishment of these mechanisms is likely to have facilitated fixation of the plastid within the host, making it less likely to be lost (Moreira and Philippe, 2001). A primary endosymbiosis between a cyanobacterial cell and a phagotrophic eukaryote is thought to have occurred only once (or at least only became fixed and persisted once), as all extant plastids of eukaryotes appear to be monophyletic (Moreira and Philippe, 2001; Archibald and Keeling, 2002). The primary endosymbiosis was established by the Proterozoic period and resulted in the predecessors of Archeplastida, Glaucophyta (which retain a peptidoglycan cell wall, characteristic of cyanobacteria, around the plastid), Rhodophyta (red algae) and Chlorophyta (green algae) (Simon *et al.*, 2009; see Fig 1.4).

All other photosynthetic eukaryotes arose from secondary or tertiary endosymbioses as photosynthetic eukaryotes were themselves engulfed and maintained by heterotrophic eukaryotes (Moreira and Philippe, 2001). These events gave rise to cryptophytes, haptophytes, photosynthetic stramenopiles and peridinin-containing dinoflagellates from red algal endosymbioses; and euglenophytes and chlorarachniophytes from green algal endosymbioses (Fig.1.4). Despite the diversity in this group it is likely that secondary endosymbioses are rare and may have occurred as few as three times in history (Archibald and Keeling, 2002).

In the Mesozoic era, a radiation of diatoms, dinoflagellates and prymnesiophytes, evidenced by fossils, is thought to have resulted in a dominance of these groups in global oxgenic photosynthesis by eukaryotes (Simon *et al.*, 2009). These secondary endosymbioses have been described as a driving force in eukaryotic evolution (McFadden and Gilson, 1995). Secondary endosymbioses have been followed by the reduction of the genome of the endosymbiont. Plastid genes products encoded by the host nucleus are targeted to the plastid after translation, as a result of a transit peptide and signal-peptide secretion system, allowing proteins to cross the additional membranes (Archibald and Keeling, 2002). In some cases, secondary endosymbioses can be identified by the presence of multiple membranes around plastids. Furthermore, remnants of eukaryotic endosymbionts' nuclei, known as nucleomorphs, have been observed. However, in many cases the nucleus of the endosymbiont has disappeared, having transferred all essential genes to its host's nucleus, and extra membranes have also been lost due to reductive evolution



(Moreira and Philippe, 2001). In cases where the nucleomorph is still present they have persisted over millions of years and contain a few hundred genes, most of which necessary for the maintenance of the nucleomorph itself (Cavalier-Smith, 2006). The nucleomorph present in the plastid of the chlorarachniophyte *Bigeloviella* contains only 17 genes of benefit to the host (Cavalier-Smith, 2006).

Tertiary endosymbiosis is observed in some dinoflagellates which have apparently substituted their peridinin-containing plastids for a different type of plastid. Many different types of plastids have been observed in dinoflagellates including those related to cryptomonads, heterokonts and prymnesiophytes (Archibald and Keeling, 2002). Dinoflagellates are remarkable organisms since they have the largest genome sizes of any eukaryotes, with unique features such as permanently condensed chromosomes with many gene copies (Zhu *et al.*, 2005). About half are photosynthetic and these have acquired a wide diversity of plastids, from both the red and green algal lineages. Whereas plastid acquisition and loss has been rare in eukaryotic evolution, it seems to be a common event in the evolution of dinoflagellates, with five known types of plastid observed (Hackett *et al.*, 2004a) and loss of photosynthesis thought to have occurred eight times (Saldarriaga *et al.*, 2001). A further tertiary plastid within dinoflagellates *Peridinium foliaceum* and *P. balticum* is of diatom origin. These species grow autotrophically in culture and the endosymbiont is reduced (Chesnick *et al.*, 1996; Hackett *et al.*, 2004a). However, the endosymbiont retains a nucleus, mitochondria, ribosomes and plastids within the endoplasmic reticulum lumen. It is not clear whether the endosymbiont is reduced to plastid status but it is thought to represent an intermediate stage in establishment of tertiary plastids. Furthermore, this dinoflagellate contains a remnant of a typical peridinin-containing plastid, thought to be the ancestral plastid within dinoflagellates (Hackett *et al.*, 2004a). Some dinoflagellates are also thought to temporarily maintain plastids known as kleptoplasts which are not fixed, these include plastids of cryptophyte origin (Takishita *et al.*, 2002), and of prymnesiophyte origin (Gast *et al.*, 2007). These examples may illustrate initial steps in the evolution of plastids in eukaryotic cells (Hackett *et al.*, 2004a).

Now, lineages of photosynthetic eukaryotes are broadly mixed with non-photosynthetic eukaryotes as plastids have been secondarily lost over the course of

evolution. Vestigial plastids are observed in two heterotrophic species of the class Dictyochophyceae (order Stramenopiles) *Pteridomonas danica* and *Ciliophrys infusionum*. Their loss of photosynthetic capacity is likely to have arisen separately (Sekiguchi *et al.*, 2002). In some parasitic alveolates, belonging to the apicomplexan genera *Eimeria*, *Plasmodium* and *Toxoplasma*, unpigmented plastids are observed which are related to the plastids of red algae. They were likely to have been established in a common ancestor to apicomplexa and dinoflagellates. The relict plastids are thought to have been retained, despite the parasitic life-mode of these organisms which precludes the need for photosynthesis, because they provide a beneficial source of fatty acid synthesis enzymes (Moreira and Philippe, 2001).

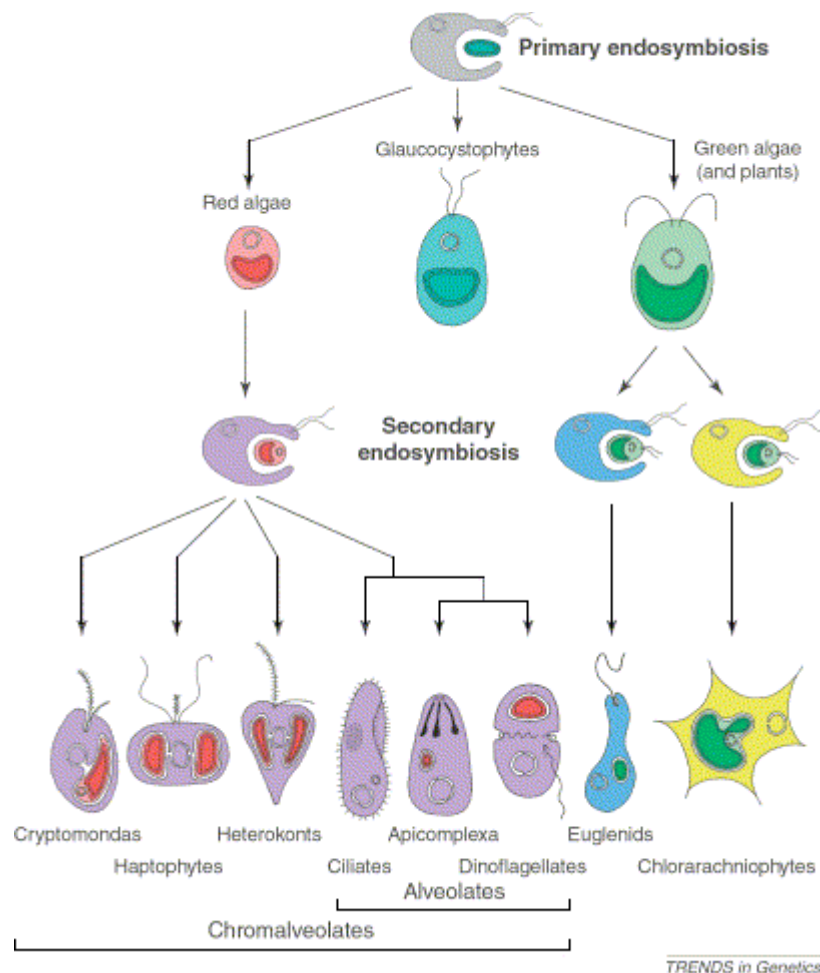


**Figure 1.4.** Schematic representation of the origin of plastids by primary and secondary endosymbioses. Image obtained from Archibald and Keeling (2002).

To some extent, diversity in photosynthetic eukaryotes can be explained by constructing evolutionary histories with evidence from the fossil record (Fig 1.5). This approach has shown that green algae dominated the oceans both in terms of abundance and diversity over 190 million years ago (mya). From the Triassic period

onwards, as the sea level rose, the phytoplankton became dominated by dinoflagellates, diatoms and coccolithophores (prymnesiophyceae), members of the red lineage. These groups dominated until the present. However, they have been declining in diversity since the early Eocene epoch (55 mya) (Falkowski *et al.*, 2004). The mass extinction event at the end of the Permian period provided the opportunity for the red algal lineage to radiate as new niches were made available for exploitation by new species, and it may have become a selective advantage for heterotrophic cells to take up a plastid as a means of retaining fixed nitrogen when it was scarce due to long-term euxinic conditions, whilst simultaneously obtaining organic carbon through photosynthesis. It is likely that this was exploited by the red lineage rather than the green lineage due to their differing trace-metal compositions (Falkowski *et al.*, 2004). The later radiations in diatoms at the beginning of the Oligocene and mid-way through the Miocene epochs is likely to have been a result of a co-evolution with grasses on land. Diatoms have a requirement for silica as their cells are surrounded by ornate silica frustules. Grasses produce a more soluble form of silica, with the proliferation of grasses, this would have become more available to be utilised by diatoms (Falkowski *et al.*, 2004).

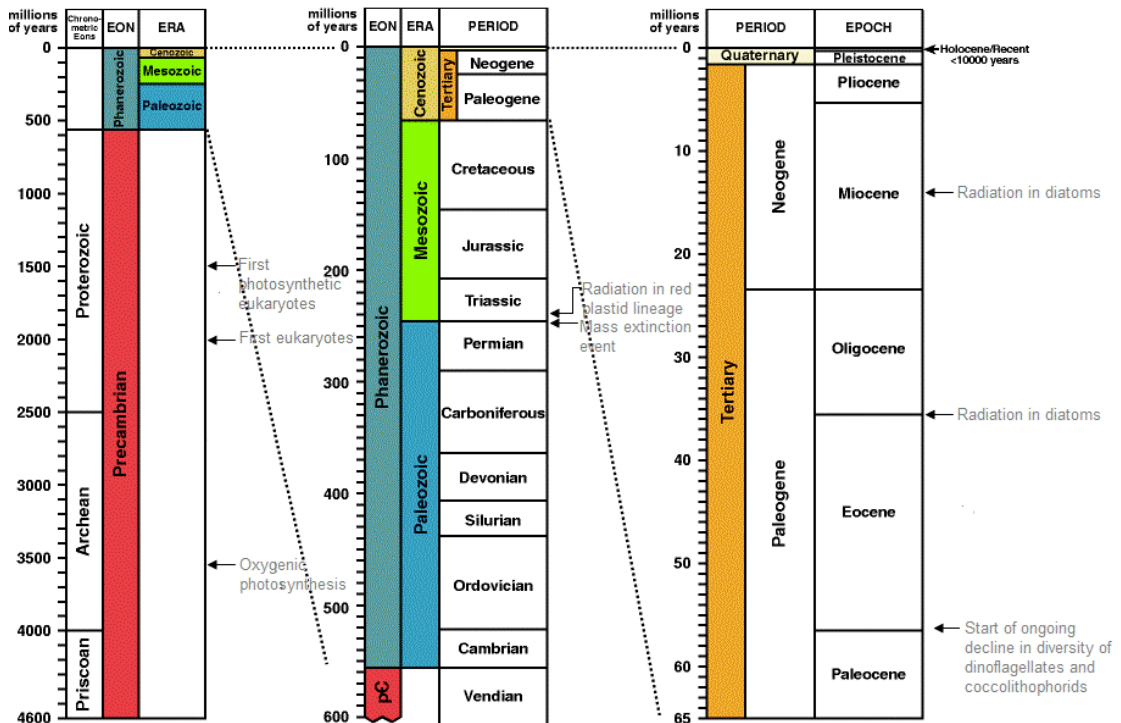


**Figure 1.5.** Geological timeline from [www.cbs.dtu.dk/staff/dave/roanoke/bio101\\_ch19a.htm](http://www.cbs.dtu.dk/staff/dave/roanoke/bio101_ch19a.htm), superimposed with approximate dates of significant events in PPE evolution taken from Katz (1998), Raymond *et al.* (2002) and Falkowski *et al.* (2004).

### 1.3.2 Niche partitioning in the continuous marine environment

Niche partitioning is a key factor in evolution, although this is not always easily explained for microbial phytoplankton in the marine environment, where traditional isolating barriers are not obvious. Light availability has been established as an important variable in niche partitioning for cyanobacteria, with high-light (HL) and low-light (LL) adapted clades of *Prochlorococcus* being partitioned down stratified water columns in various oceanic regions (West and Scanlan, 1999; Zwirgmaier *et al.*, 2007).

Similarly, differences between optimal light intensities for photosynthesis were shown for cultures of photosynthetic nanoeukaryotes: diatoms, prymnesiophytes and dinoflagellates (Falkowski and Owens, 1978). This was thought to include adaptation to shading which could extend the effective photic zone for the diatom *Skeletonema costatum* whereas the red-tide forming dinoflagellate *Gonyaulax tamarensis* could thrive in high light intensities which were prohibitive to other phytoplankton, but would be restricted to waters shallower than 10 m depth (Falkowski and Owens, 1978). A similar observation has been made within a single species indicating the existence of ecotypes within a photosynthetic picoeukaryote (PPE) species. *Ostreococcus tauri* cultures isolated from different depths were found to have different pigment composition, including the presence of an additional pigment in deep-water ecotypes (Rodríguez *et al.*, 2005). HL ecotypes have been found to have a greater capacity for photoacclimation compared to LL ecotypes, which instead benefit from a reduced requirement for nitrogen. A higher nitrogen cost is associated with plasticity in the light-harvesting antennae of photosystem II. HL ecotypes are, therefore, able to exploit a greater light range unless limited by nitrogen, whereas LL ecotypes are able to exploit lower-nitrogen regimes, but will suffer photoinhibition if exposed to excessive light (Six *et al.*, 2008). The light availability for phytoplankton can be highly variable in the oceans and thus it has been suggested that some phytoplankton have evolved a flexibility in photosynthesis based on carbon concentrating mechanisms, which allow efficiency of photosynthesis when light is not limiting. This is important for phytoplankton facing turbulent conditions (Rost *et al.*, 2006).

### 1.3.3 Evolutionary mechanisms revealed by PPE genomics

The first genome sequencing of a PPE species, the prasinophyte *Ostreococcus tauri*, provided insights into the specialisation of this remarkable PPE which is the smallest known, free-living eukaryote, as well as being an ancient member of the green lineage (Derelle *et al.*, 2006). The genome is 12.56 Mbp in size, the smallest eukaryotic genome known. Many of the features found reflected compaction of the genome by various mechanisms including reduction of intergenic regions, downsizing of gene families and gene fusion (Derelle *et al.*, 2006). A further striking, but unexplained, feature was the heterogeneity of the genome, with two of the eighteen chromosomes containing 77% of the transposable elements in the genome, and a lower GC content. One of these two chromosomes has features of sex chromosomes in other organisms, and whilst *Ostreococcus* has not been observed reproducing sexually in culture, it has been suggested that sexual reproduction may be a means of establishing and maintaining diversity in the marine environment (Derelle *et al.*, 2006).

A comparison of the genomes of *Ostreococcus tauri* (Derelle *et al.*, 2006) and the closely related *O. lucimarinus*, revealed mechanisms of divergence between them (Palenik *et al.*, 2007). Horizontal transfer of genes associated with sugar biosynthesis from prokaryotes is apparent, and some of these gene products may alter the surface glycosylation of these cells allowing some evasion of predators. Furthermore, *O. lucimarinus* has more potential selenium-containing enzymes which are more catalytically active than cysteine-containing alternatives and reduces the requirement for nitrogen, thus selenium availability may have been a factor driving speciation between these organisms. This study also showed that *Ostreococcus spp.* have achieved a smaller genome size than other eukaryotic phytoplankton through gene fusion events and reducing chromatin content. Moreover, they do not have iron-uptake mechanisms typical of other marine algae (suggesting they possess novel iron acquisition capability), and though they appear to have a mechanism for storing iron using ferritin they certainly have a reduced capacity for Fe-containing protein components, with an absence of cytochrome  $c_6$  and no Fe-superoxide dismutase (Fe-SOD) (Palenik *et al.*, 2007).

Other pico-sized members of Prasinophyceae clade II (Mamiellales), namely two strains of *Micromonas pusilla*, RCC299 isolated from the South Pacific and CCMP1545 isolated from the North Atlantic, have also been the subject of recent genomic sequence analysis (Worden *et al.*, 2009). These strains were found to share only 90% of their genes and thus are likely to be of different species. Their genomes are larger than those of *Ostreococcus* at 20.9 and 21.9 Mbp for RCC299 and CCMP1545 respectively. This appears to coincide with a broader habitat range than *Ostreococcus* and may be associated with the presence of genes such as those involved in defence against heavy metal toxicity and reactive oxygen species. Comparison of these genomes with those of the *Ostreococcus spp.*, *Chlamydomonas*, diatoms and higher plants has given insights into the ancestral state of the green lineage. For example, a relatively unknown carbon concentration mechanism that prevents CO<sub>2</sub> leaking from the chloroplast is likely to be a basic requisite of the lineage. Further, it appears that the common ancestor was capable of reproduction by sexual recombination (Worden *et al.* 2009). The genomic comparisons also suggest that the presumed primitive *Ostreococcus tauri*, with its tiny genome size is in fact more highly derived than *Micromonas* (Worden *et al.*, 2009).

#### **1.4. The relative importance of primary producers**

It has long been known that in the marine ecosystem, small autotrophs dominate primary production (e.g. Yentsch and Ryther, 1959; Saijo, 1964; Williams and Murdoch, 1966; Malone, 1971; Mommaerts, 1973). These early studies measured primary production by measuring the conversion of inorganic to organic carbon. The rate of conversion could be observed by supplying the inorganic carbon source with the radioactive isotope <sup>14</sup>C, in the form NaH<sup>14</sup>CO<sub>3</sub>. Early studies also showed the relative importance of smaller autotrophs in oceanic regions, with larger autotrophs becoming more important in coastal environments (Malone, 1971; Mommaerts, 1973).

These early studies often used various ‘cut-offs’ to target the appropriate cell diameters of nanoplankton by filtering water samples through nets with pore-sizes such as 65 µm (Yentsch and Ryther, 1959), 60 µm (Williams and Murdoch, 1966), 50 µm (Mommaerts, 1973), or 22 µm (Malone, 1971). However, Saijo (1964)

showed that approximately half of the productivity was attributed to a much smaller-sized fraction of cells, which passed a 5  $\mu\text{m}$  mesh at the surface of a site in the Indian Ocean. Comparatively recent studies show the most productive organisms are in the  $<3$   $\mu\text{m}$  size range, and identify these organisms as picoplankton (Herbland *et al.*, 1985).

Many studies have identified the most important primary producers in the ocean on the basis of size. Studies which determine the rates of primary production of size fractionated groups of phytoplankton have been carried out in a number of locations. They have consistently found the dominant primary producers in terms of chlorophyll *a* concentration, autotrophic biomass and integrated carbon fixation to be the community of cells which pass through a 3  $\mu\text{m}$  pore-sized mesh (e.g. Herbland *et al.*, 1985; Marañón *et al.*, 2001), 2  $\mu\text{m}$  mesh (Teira *et al.*, 2004; Poulton *et al.*, 2006), and in some specific sites, even as small as 1  $\mu\text{m}$  (Li, 1983; Herbland *et al.*, 1985).

As smaller organisms generally have higher rates of metabolism, they are also likely to exhibit a higher efficiency of photosynthesis, higher rates of primary productivity and higher growth rates than larger cells (Odum, 1956). Thus, it should not be surprising that size fractionation experiments attribute high proportions of carbon-uptake to the smallest photosynthetic organisms. Furthermore, high metabolic rates are related to high turnover rates, as such it is expected that these organisms may account for little biomass at any one time (Odum, 1956). Despite this, many studies show that in the sea, in contrast to on land, the smallest organisms represent the highest proportions of biomass (Giovannoni and Stingl, 2005).

From an ecological perspective, small organisms are resistant to sinking in the water, allowing to them stay towards the surface of the water column for longer, where they can utilise light for photosynthesis. This is important as light does not penetrate far into the water column (Tait and Dipper, 1998). Furthermore, small size, conveying a high surface area to volume ratio, facilitates nutrient acquisition, and may give small cells a competitive advantage over larger cells in nutrient limited waters (Raven).

### 1.5. The fate of carbon fixed by the picophytoplankton

Rather than going through a traditional food web, the carbon fixed by the picophytoplankton goes through a complex set of interactions known as the biological pump. This process describes a set of interactions involving the uptake of CO<sub>2</sub> by phytoplankton performing photosynthesis (as we have seen a large fraction of this is performed by PPEs), the food chain interactions between phytoplankton and grazers, as well as the sinking of cells, aggregates and detritus (Fig. 1.6). Up to 90% of the total net primary production (NPP) is supported by regenerated nutrients, of which the majority is produced by the small grazers and heterotrophic bacteria (Harrison, 1980 as cited in Ducklow, 2003). It is estimated that 5-50% of the carbon fixed is released as dissolved organic matter (DOM) (Larsson and Hagström, 1982). There is a close correlation between bacterial and primary production in marine and lake ecosystems as primary production makes carbon available to the bacterial community in the form of algal exudates, thus bursts in primary production are followed by bursts in bacterial production after a lag time of a couple of weeks (Larsson and Hagström, 1982; Lovell and Konopka, 1985). Nutrients, particularly carbon and nitrogen are thought to be rapidly recycled above the thermocline via the microbial loop (Azam *et al.*, 1983).

Phytoplankton produce DOM which is believed to be rapidly taken up by bacteria, and utilised as their energy source (Azam *et al.*, 1983). Compared to bacteria in sediments, those living in the water column are more likely to be motile and capable of actively maintaining positions close to phytoplankton cells (Azam *et al.*, 1983). Bacteria (and cyanobacteria) are consumed by heterotrophic flagellates of <10 µm in size (Azam *et al.*, 1983). Further, flagellates are consumed by microzooplankton in the same size range as the larger phytoplankton (10-80 µm). At each stage, nutrients are regenerated by 'sloppy grazing', as well as viral lysis of cells (e.g. Suttle, 2007). These processes are each responsible to the mortality of 20% of biomass per day (Suttle, 2007). DOM is released and used by bacteria, so this carbon is not efficiently passed to higher trophic levels in a traditional food-chain. A further complication in this process is that chemical nutrients released by viral lyses or sloppy grazing can stimulate photosynthesis as phytoplankton growth is often limited by nutrient availability (Suttle, 2007), this may effectively result in a positive feedback loop.



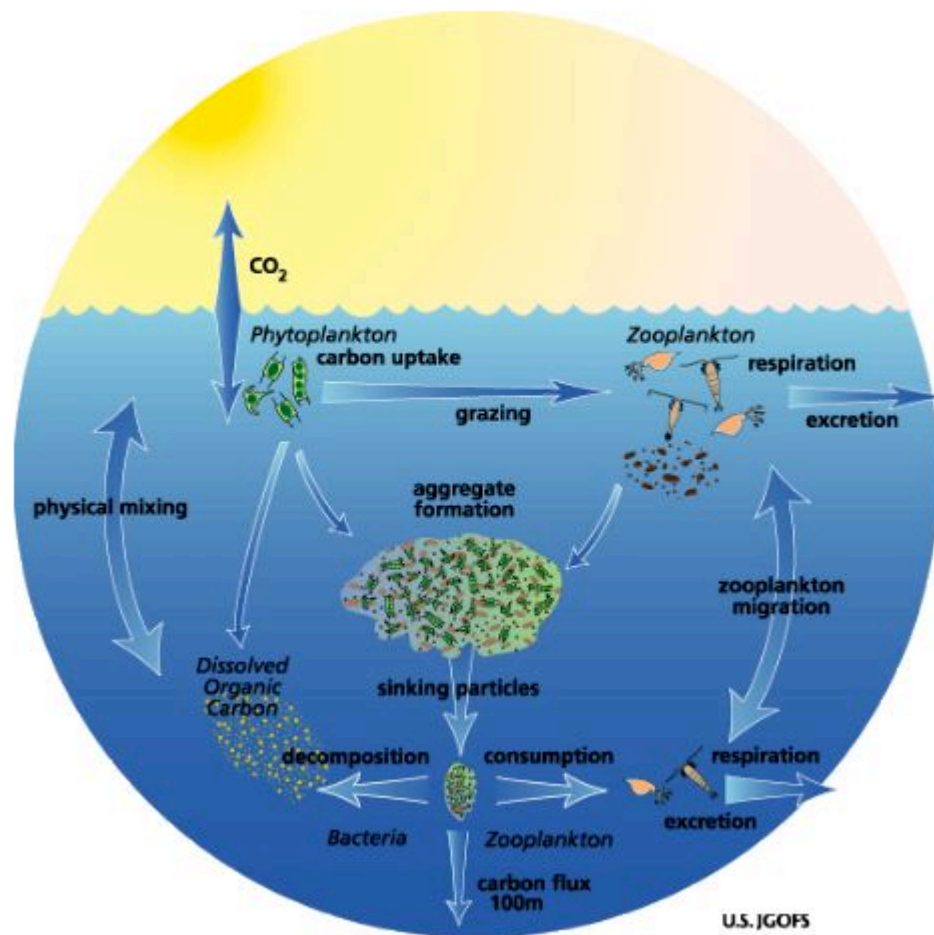


**Figure 1.6.** Schematic representation of the biological pump from the Joint Global Ocean Flux Study (JGOFS) retrieved from [http://www1.who.edu/general\\_info/gallery\\_modeling/slide4.html](http://www1.who.edu/general_info/gallery_modeling/slide4.html)

Picoplankton were believed to contribute relatively little to carbon export from surface layers due to their small size, making them less inclined to sink (Tait and Dipper, 1998) as well as their rapid utilisation in the microbial loop. However, the relative direct (aggregation into ‘marine snow’ and incorporation into settling detritus) and indirect (consumption of aggregates by higher trophic levels, or via micrograzers) contribution of picoplankton to export has recently been found to be proportional to their total net primary production (Richardson and Jackson, 2007). In the equatorial Pacific Ocean, picoplankton were responsible for >70% of the total net primary production, 87% of particulate organic carbon (POC) export via detritus and 76% of carbon exported through the mesozooplankton.

## 1.6. Eukaryotic versus prokaryotic picophytoplankton

Whilst it has long been appreciated that the smallest phytoplankton were the most important marine primary producers, it was not until the late 1970s that the first steps towards identifying the organisms comprising this group were made. In 1979, cyanobacteria, in particular orange-fluorescing *Synechococcus* cells, were observed and found to be widely distributed (Waterbury *et al.*, 1979). These cyanobacteria were discerned by epifluorescent microscopy and transmission electron microscopy revealing cells of  $<1 \mu\text{m}$  diameter containing thylakoid membranes, the lumen of which are the location of the photosynthetic reaction centres (Johnson and Sieburth, 1979). Previously, much of what was known about cyanobacteria was based on filamentous and colony-forming types. Hence, it was a significant breakthrough to suggest that microscopic photosynthetic cells were numerous (between  $10^4$  and  $10^5$  cells  $\text{ml}^{-1}$ ) and ubiquitous. This had major implications for our understanding of oceanic productivity.

Around this time, it began to be appreciated that eukaryotic autotrophs of a similar size were also present in diverse samples. Very small photosynthetic eukaryotes had been observed as early as 1773 (Müller as cited in Andersen, 1999), however it was not appreciated that PPEs were ubiquitous until the early 1980s, and the suggestion arose that PPEs may contribute significantly to global primary production when they were found to be abundant in samples from various marine habitats (Johnson and Sieburth, 1982; Joint and Pipe, 1984).

The number of cells comprising the picophytoplankton can be quickly counted by flow cytometry. A proportion of photons absorbed by photosynthetic pigments is re-emitted as fluorescence of different colour depending on the pigment. For example, chlorophyll *a* fluorescence is characteristically red and the photosynthetic accessory pigment phycoerythrin fluoresces orange. This fluorescence can be exploited to identify photosynthetic cells in marine samples (Yentsch and Horan, 1989). Flow cytometry involves running a sample in a very fine stream through a laser beam and detecting fluorescence and light scattering properties (associated with cell size). The stream is of such a size that cells are in single file. The fluorescence and light scattering properties of the cells are different between the three major groups within

the picophytoplankton (Fig. 1.7): the two main genera of marine unicellular cyanobacteria (*Synechococcus* and *Prochlorococcus*) and PPEs and can be rapidly distinguished and counted by flow cytometry (Olson *et al.*, 1985). *Prochlorococcus* are distinguished as small red fluorescing cells, *Synechococcus* are slightly larger orange-fluorescing cells due to the distinctive phycoerythrin pigmentation, and PPEs are larger red-fluorescing cells. Flow cytometry has allowed very rapid analysis of samples and can be used onboard ship as samples of interest are collected (Olson *et al.*, 1985). This technique has been exploited in research cruises all over the world and provided a rich dataset. These studies have confirmed the ubiquitous nature of PPEs in the marine euphotic zone as they were detected by flow cytometry over many horizontal and vertical (depth) profiles including in the Sargasso and Labrador Seas, tropical Pacific Ocean, along the Atlantic Meridional Transect (AMT) and East China Sea (Li, 1989; Campbell and Vaultot, 1993; Zubkov *et al.*, 1998 and Pan *et al.*, 2005, respectively). These studies also consistently showed that PPE cell numbers are several orders of magnitude lower than those of the cyanobacteria. In the North Pacific Ocean, for example, *Prochlorococcus* numbers peaked at  $2 \times 10^5$  cells ml<sup>-1</sup> whereas PPEs peaked at 100-1,000 cells ml<sup>-1</sup> (Campbell and Vaultot, 1993) and in the East China Sea average numbers for *Prochlorococcus*, *Synechococcus* and PPEs were  $10^5$ ,  $10^5$  and  $10^4$  cells ml<sup>-1</sup>, respectively (Pan *et al.*, 2005).

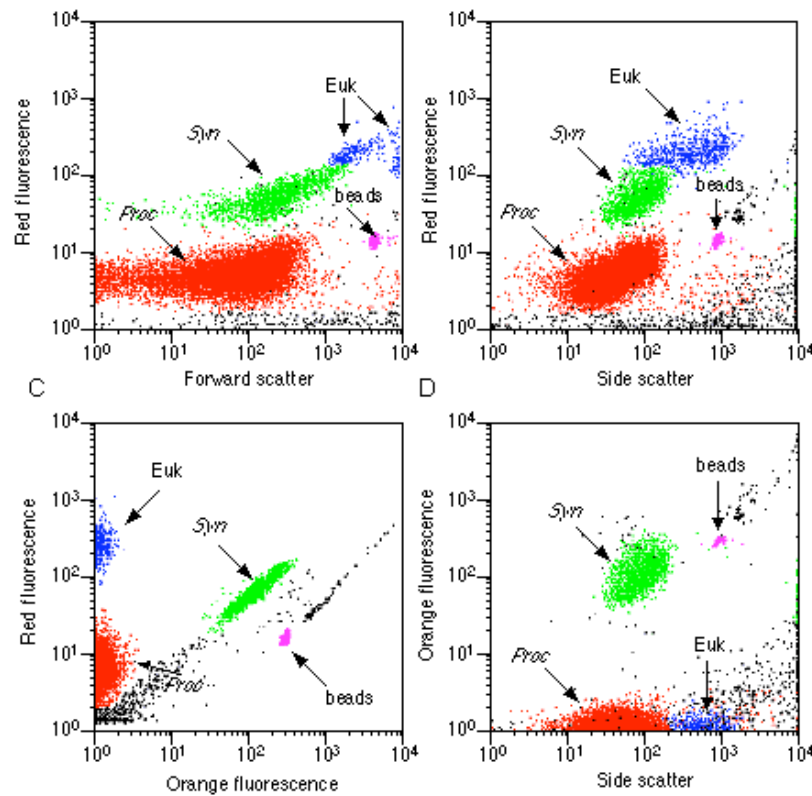


**Figure 1.7.** Flow cytometric signatures of members of the picophytoplankton. Photosynthetic eukaryotes (Euk), *Synechococcus* (Syn) and *Prochlorococcus* (Proc). Figure retrieved from [www.currentprotocols.com/protocol/cy1111](http://www.currentprotocols.com/protocol/cy1111).

There are few studies which have investigated the relative carbon fixation of these tiny photosynthetic prokaryotes and eukaryotes. A study in the North Atlantic directly measured the fixation of radioactive carbon by populations of cyanobacteria and photosynthetic picoeukaryotes by flow sorting samples following incubation with  $\text{NaH}^{14}\text{CO}_3$  (Li, 1994). Flow cytometric sorting is a version of flow cytometry where cells with diagnostic characteristics of fluorescence and light scattering properties are physically separated by electrical charging of droplets containing these cells (Yentsch and Horan, 1989). The sorted cells were harvested on membranes, inorganic  $^{14}\text{C}$  removed by fuming with HCl, and successive sorts of different numbers of cells allowed estimation of  $^{14}\text{C}$  per cell by plotting the slope of the radioactivity curve against cell numbers. This study concluded that although PPEs were by far the least numerous cells within the picophytoplankton, they were responsible for two-thirds of the carbon fixation of the group due to high cell-specific carbon uptake rates.

An indirect carbon-biomass estimation technique showed a similar partitioning of carbon amongst cyanobacteria and PPEs in the Pacific Ocean. Estimation of carbon biomass was based on calculating the volumes of cells using cell diameter data estimated from right-angle light scatter information collected by flow cytometry, assuming a spherical cell shape. The volume-dependent carbon biomass was extrapolated from measurements of cells in culture (Worden *et al.*, 2004). Similar studies also showed that PPEs could sometimes dominate carbon biomass in the picophytoplankton despite being numerically inferior at sites in the Atlantic and Pacific (Partensky *et al.*, 1996; Blanchot *et al.*, 2001).

As these data rely heavily on various assumptions, a recent study sought to clarify the role of members of the picophytoplankton in carbon fixation in a direct study, similar to that of Li (1994). Jardillier *et al.* (submitted) performed a more detailed analysis of group-specific CO<sub>2</sub> fixation using flow cytometric sorting at a series of stations in the tropical Atlantic Ocean. Flow cytometry facilitated the discrimination of two PPE groups, approximately 2 µm and 3 µm in size, as well as *Synechococcus* and *Prochlorococcus*. On average, the eukaryotes were found to be responsible for over 30% of the carbon fixation, and up to 44%. In particular, despite being the least numerous group, accounting for <0.5% of cells, the 3 µm eukaryotes were responsible for between 13 and 38% of the primary production. The use of fluorescent *in situ* hybridisation (FISH) allowed class-level taxonomic identification of the eukaryotic groups and revealed the 3 µm group to be primarily comprised of Prymnesiophyceae, a well known class that has been rarely observed within the pico size range (Jardillier *et al.*, submitted).

### **1.7. PPE diversity studies**

The diversity of PPEs has been a difficult subject to study due to the small size of individuals. PPEs have few distinguishing characteristics (Fig. 1.8) and those they have are likely to be too fragile to withstand sampling, preservation and examination procedures (Caron *et al.*, 1999). Even the simple characteristic of size is unreliable as it is known to vary depending on nutrient availability (van Leeuwe and Stefels, 1998). However, the study of the diversity of small eukaryotes has been an ongoing

area with a number of approaches applied, and recently our understanding of PPE diversity has grown exponentially.

A traditional method for understanding the diversity of microscopic organisms is to isolate them into culture. Establishing cultures of PPEs has often been achieved by a serial dilution approach where a species is isolated by sub-diluting a mixed culture in medium repeatedly until a final concentration of a single cell is obtained. Or more recently cultures have been established from single cells isolated by flow cytometric sorting. In an early study (Butcher, 1952), used the dilution method in the isolation of several small algal cultures of many classes, mainly from freshwater and of cells larger than 3  $\mu\text{m}$  in size. However, it was during this early work that the first marine PPE culture was isolated, the clade II prasinophyte *Micromonas pusilla*. The approach has been continually useful in the discovery of novel PPEs (Table 1.2). Recent discoveries of PPE classes that have been made using this approach include the Pelagophyceae and Bolidophyceae (Andersen *et al.*, 1993; Guillou *et al.*, 1999, respectively). However, this approach generally results in the isolation of only the most abundant species as rare species are diluted out of the culture long before it is diluted to the single-cell level (Vaulot *et al.*, 2008). Thus, the full diversity of PPEs cannot be appreciated with the use of this method.

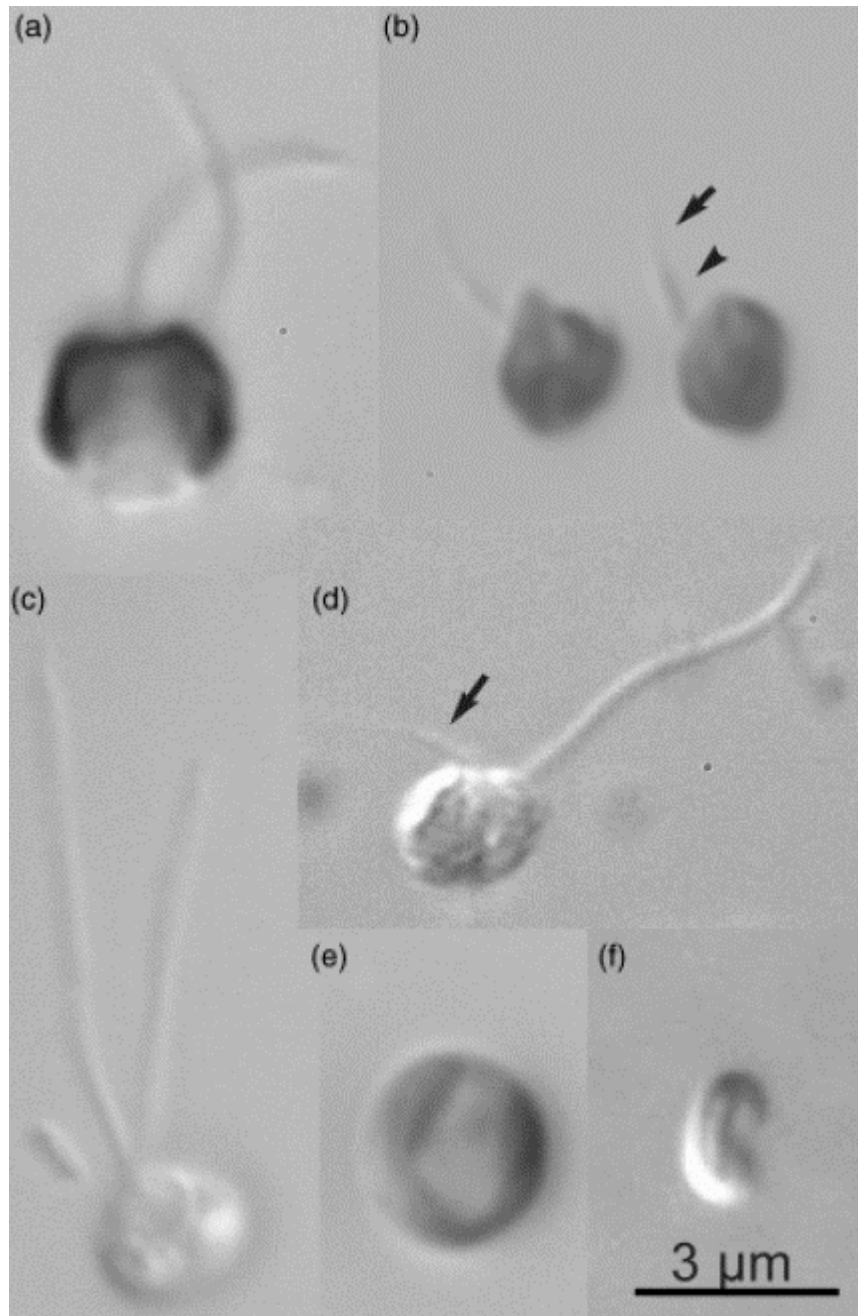


**Figure 1.8.** Light micrographs of some PPE species reproduced from Vaultot *et al.* (2008). (a) *Imantonia rotunda* fixed with osmium tetroxide vapour. (b) *Micromonas pusilla* fixed with Lugol's solution. (c) RCC391 (Mamiellales, Prasinophyceae clade II) fixed with osmium tetroxide vapour. (d) *Florenciella parvula* fixed with osmium tetroxide vapour. (e) RCC287 (Prasinophyceae clade VII) live cell. (f) *Bathycoccus prasinos* live cell.

**Table 1.2.** List of described PPE species from Vaultot *et al.* (2008)

Division	Class	Genus	Species	Authority	Year	Cell Length	Hydrography
Chlorophyta	Pedinophyceae	<i>Resultor</i>	<i>micron</i>	(Throndsen) Moestrup	1969	1.5-2.5	Marine
Chlorophyta	Prasinophyceae	<i>Bathycoccus</i>	<i>prasinus</i>	Eikrem and Throndsen	1990	1.5-2.5	Marine
Chlorophyta	Prasinophyceae	<i>Micromonas</i>	<i>pusilla</i>	(Butcher) Manton and Parke	1952	1.0-3.0	Marine
Chlorophyta	Prasinophyceae	<i>Ostreococcus</i>	<i>tauri</i>	Courties and Chrétiennot-Dinand	1995	0.8-1.1	Marine
Chlorophyta	Prasinophyceae	<i>Picocystis</i>	<i>salinarum</i>	Lewin	2001	2.0-3.0	Hypersaline
Chlorophyta	Prasinophyceae	<i>Pycnococcus</i>	<i>provasolii</i>	Guillard	1991	1.5-4.0	Marine
Chlorophyta	Trebouxiophyceae	<i>Chlorella</i>	<i>nana</i>	Andreoli <i>et al.</i>	1978	1.5-3.0	Marine
Chlorophyta	Trebouxiophyceae	<i>Picochlorum</i>	<i>atomus</i>	(Butcher) Henley <i>et al.</i>	1952	2.0-3.0	Brackish
Chlorophyta	Trebouxiophyceae	<i>Picochlorum</i>	<i>oklahomensis</i>	Henley <i>et al.</i>	2004	2.0-2.0	Hypersaline Brackish
Chlorophyta	Pedinophyceae	<i>Marsupiomonas</i>	<i>pelliculata</i>	Jones <i>et al.</i>	1994	3.0-3.0	marine
Chlorophyta	Prasinophyceae	<i>Crustomastix</i>	<i>stigmatica</i>	Zingone	2002	3.0-5.0	Marine
Chlorophyta	Prasinophyceae	<i>Dolichomastix</i>	<i>eurylepidea</i>	Manton	1977	3.0-3.0	Marine
Chlorophyta	Prasinophyceae	<i>Dolichomastix</i>	<i>lepidota</i>	Manton	1977	2.5-2.5	Marine
Chlorophyta	Prasinophyceae	<i>Dolichomastix</i>	<i>tenuilepis</i>	Throndsen and Zingone	1997	3.0-4.5	Marine
Chlorophyta	Prasinophyceae	<i>Mantoniella</i>	<i>squamata</i>	(Manton and Parke) Desikachary	1960	3.0-5.0	Marine
Chlorophyta	Prasinophyceae	<i>Prasinococcus</i>	<i>capsulatus</i>	Miyashita and Chihara	1993	3.0-5.5	Marine
Chlorophyta	Prasinophyceae	<i>Prasinoderma</i>	<i>coloniale</i>	Hasegawa and Chihara	1996	2.5-5.5	Marine
Chlorophyta	Prasinophyceae	<i>Pseudoscourfieldia</i>	<i>marina</i>	(Throndsen) Manton	1969	3.0-3.5	Marine
Chlorophyta	Prasinophyceae	<i>Pyramimonas</i>	<i>virginica</i>	Pennick	1977	2.7-3.5	Marine
Chlorophyta	Trebouxiophyceae	<i>Chlorella</i>	<i>spärckii</i>	Ålvik	1934	2.8-7.0	Marine
Chlorophyta	Trebouxiophyceae	<i>Picochlorum</i>	<i>eukaryotum</i>	(Wilhelm <i>et al.</i> ) Henley <i>et al.</i>	1982	3.0-3.0	Marine
Chlorophyta	Trebouxiophyceae	<i>Picochlorum</i>	<i>maculatus</i>	(Butcher) Henley <i>et al.</i>	1952	3.0-3.0	Brackish
Chlorophyta	Trebouxiophyceae	<i>Stichococcus</i>	<i>bacillaris</i>	Nägeli	1849	3.0-4.0	Marine
Cryptophyta	Cryptophyceae	<i>Hillea</i>	<i>marina</i>	Butcher	1952	2.0-2.5	Marine
Haptophyta	Prymnesiophyceae	<i>Chrysochromulina</i>	<i>tenuisquama</i>	Estep <i>et al.</i>	1984	2.0-5.0	Marine
Haptophyta	Prymnesiophyceae	<i>Imantonia</i>	<i>rotunda</i>	Reynolds	1974	2.0-4.0	Marine
Haptophyta	Prymnesiophyceae	<i>Trigonaspis</i>	<i>minutissima</i>	Thomsen	1980	2.0-3.6	Marine

Continued overleaf



Haptophyta	Prymnesiophyceae	<i>Chrysochromulina</i>	<i>apheles</i>	Moestrup and Thomsen	1986	3.0-4.0	Marine
Haptophyta	Prymnesiophyceae	<i>Chrysochromulina</i>	<i>minor</i>	Parke and Manton	1955	2.5-7.5	Marine
Haptophyta	Prymnesiophyceae	<i>Chrysochromulina</i>	<i>planisquama</i>	Hu <i>et al.</i>	2005	3.0-6.0	Marine
Haptophyta	Prymnesiophyceae	<i>Dicrateria</i>	<i>inornata</i>	Parke	1949	3.0-5.5	Marine
Haptophyta	Prymnesiophyceae	<i>Ericiolus</i>	<i>spiculiger</i>	Thomsen	1995	3.0-3.8	Marine
Haptophyta	Prymnesiophyceae	<i>Phaeocystis</i>	<i>cordata</i>	Zingone	1999	3.0-4.0	Marine
Haptophyta	Prymnesiophyceae	<i>Phaeocystis</i>	<i>pouchetii</i>	(Hariot) Lagerheim	1892	3.0-8.0	Marine
Handerokontophyta	Bacillariophyceae	<i>Arcocellulus</i>	<i>cornucervis</i>	Hasle <i>et al.</i>	1983	1.0-17.0	Marine
Handerokontophyta	Bacillariophyceae	<i>Chaetoceros</i>	<i>minimus</i>	(Levander) Marino <i>et al.</i>	1991	2.0-7.0	Marine
Handerokontophyta	Bacillariophyceae	<i>Chaetoceros</i>	<i>thronsenii</i>	(Marino <i>et al.</i> ) Marino <i>et al.</i>	1991	1.5-5.0	Marine
Handerokontophyta	Bacillariophyceae	<i>Minidiscus</i>	<i>comicus</i>	Takano	1981	2.0-7.0	Marine
Handerokontophyta	Bacillariophyceae	<i>Minutocellus</i>	<i>polymorphus</i>	(Hargraves and Guillard) Hasle <i>et al.</i>	1983	2.0-30.0	Marine
Handerokontophyta	Bacillariophyceae	<i>Skeletonema</i>	<i>grethae</i>	Zingone and Sarno	2005	2.0-10.5	Marine
Handerokontophyta	Bacillariophyceae	<i>Skeletonema</i>	<i>japonicum</i>	Zingone and Sarno	2005	2.0-10.0	Marine
Handerokontophyta	Bacillariophyceae	<i>Skeletonema</i>	<i>marinoi</i>	Sarno and Zingone	2005	2.0-12.0	Marine
Handerokontophyta	Bacillariophyceae	<i>Skeletonema</i>	<i>menzelii</i>	Guillard <i>et al.</i>	1974	2.0-7.0	Marine
Handerokontophyta	Bacillariophyceae	<i>Skeletonema</i>	<i>pseudocostatum</i>	Medlin	1991	2.0-9.0	Marine
Handerokontophyta	Bacillariophyceae	<i>Thalassiosira</i>	<i>bulbosa</i>	Syvertsen	1984	2.0-16.0	Marine
Handerokontophyta	Bacillariophyceae	<i>Thalassiosira</i>	<i>mala</i>	Takano	1965	2.0-10.0	Marine
Handerokontophyta	Bacillariophyceae	<i>Thalassiosira</i>	<i>proschkinae</i>	Makarova	1979	2.0-11.5	Marine
Handerokontophyta	Bolidophyceae	<i>Bolidomonas</i>	<i>mediterranea</i>	Guillou and Chrétiennot-Dinand	1999	1.0-1.7	Marine
Handerokontophyta	Bolidophyceae	<i>Bolidomonas</i>	<i>pacifica</i>	Guillou and Chrétiennot-Dinand	1999	1.0-1.7	Marine
Handerokontophyta	Eustigmatophyceae	<i>Nannochloropsis</i>	<i>granulata</i>	Karlson and Potter	1996	2.0-4.0	Marine
Handerokontophyta	Pelagophyceae	<i>Aureococcus</i>	<i>anophagefferens</i>	Hargraves and Sieburth	1988	1.5-2.0	Marine
Handerokontophyta	Pelagophyceae	<i>Pelagomonas</i>	<i>calceolata</i>	Andersen and Saunders	1993	2.0-3.0	Marine
Handerokontophyta	Pinguiochyceae	<i>Pinguiochrysis</i>	<i>pyriformis</i>	Kawachi	2002	1.0-3.0	Marine
Handerokontophyta	Bacillariophyceae	<i>Minidiscus</i>	<i>chilensis</i>	Rivera	1984	3.0-7.5	Marine
Handerokontophyta	Bacillariophyceae	<i>Minidiscus</i>	<i>spinulosus</i>	Gao <i>et al.</i>	1992	3.0-5.0	Marine
Handerokontophyta	Bacillariophyceae	<i>Minidiscus</i>	<i>trioculatus</i>	(F.J.R. Taylor) Hasle	1967	2.5-3.8	Marine
Handerokontophyta	Bacillariophyceae	<i>Minutocellus</i>	<i>scriptus</i>	Hasle <i>et al.</i>	1983	3.0-36.0	Marine
Handerokontophyta	Bacillariophyceae	<i>Thalassiosira</i>	<i>oceanica</i>	Hasle	1983	3.0-12.0	Marine

Continued overleaf

Handerokontophyta	Bacillariophyceae	<i>Thalassiosira</i>	<i>pseudonana</i>	Hasle and Heimdal	1970	2.3-5.5	Marine
Handerokontophyta	Chrysophyceae	<i>Ollicola</i>	<i>vangoorii</i>	(Conrad) Vørs	1938	3.0-5.0	Marine
Handerokontophyta	Chrysophyceae	<i>Tetraparma</i>	<i>insecta</i>	Bravo-Sierra and Hernández-Becerril	2003	2.8-3.8	Marine
Handerokontophyta	Chrysophyceae	<i>Tetraparma</i>	<i>pelagica</i>	Booth and Marchant	1987	2.2-2.8	Marine
Handerokontophyta	Chrysophyceae	<i>Triparma</i>	<i>columacea</i>	Booth	1981	2.3-4.7	Marine
Handerokontophyta	Chrysophyceae	<i>Triparma</i>	<i>laevis</i>	Booth	1981	2.2-3.1	Marine
Handerokontophyta	Chrysophyceae	<i>Triparma</i>	<i>retinervis</i>	Booth	1981	2.-4.5	Marine
Handerokontophyta	Dictyochophyceae	<i>Florenciella</i>	<i>parvula</i>	Eikrem	2004	3.0-6.0	Marine
Handerokontophyta	Eustigmatophyceae	<i>Nannochloropsis</i>	<i>oceanica</i>	Suda and Miyashita	2002	3.0-5.0	Marine
Handerokontophyta	Eustigmatophyceae	<i>Nannochloropsis</i>	<i>salina</i>	(Bourrelly) Hibberd	1958	3.0-4.0	Brackish
Handerokontophyta	Pelagophyceae	<i>Aureoumbra</i>	<i>lagunensis</i>	Stockwell <i>et al.</i>	1997	2.5-5.0	Marine
Handerokontophyta	Pelagophyceae	<i>Pelagococcus</i>	<i>subviridis</i>	Norris	1977	2.5-5.5	Marine
Handerokontophyta	Pinguiphyceae	<i>Pinguicoccus</i>	<i>pyrenoidosus</i>	Andersen <i>et al.</i>	2002	3.0-8.0	Marine

Pigment composition of environmental samples can be analysed by high performance liquid chromatography (HPLC) which separates and quantifies chlorophylls and carotenoids, some of which are considered diagnostic for certain PPE classes. Examples are: alloxanthin, associated with Cryptophyceae, and 19'-hexanoyloxyfucoxanthin associated with Prymnesiophyceae (Barlow *et al.*, 1999; Higgins and Mackey, 2000). However, the use of pigment analysis for taxonomic assignment has been criticised as cells with the same suites of pigments have been found to be distantly related, whilst members of the same taxonomic group have varying pigmentation. An example of this is that different strains of the nano-sized prymnesiophyte *Emiliana huxleyii* have considerable variation in pigment composition, with the importance of different carotenoids deviating and the total pigment content varying by an order of magnitude between strains (Stolte *et al.*, 2000). Furthermore, pigmentation varies depending on biochemical parameters and environmental stress, with light levels (Simon *et al.*, 1994) and nutrient limitation (Stolte *et al.*, 2000) having major influence over the pigment content of cells. Despite this, the analysis of PPE communities by HPLC has remained a popular approach and has been useful in providing information on distribution of PPEs at low taxonomic resolution (e.g. Gibb *et al.*, 2000).

The use of molecular techniques targeting the marine PPE community has led to a breakthrough in assessment of PPE diversity. In particular, the use of cloning and sequencing techniques, involving the amplification of the partial nuclear SSU (small subunit, 18S) rRNA gene by polymerase chain reaction (PCR) have been particularly successful, as reviewed by Moreira and López-García (2002). This approach is eukaryote-specific (bacteria possess 16S SSU rRNA genes) allowing researchers to target the eukaryotic community to the exclusion of the comparatively well studied bacterioplankton. The approach revealed that marine picoeukaryotes were more diverse than had previously been suspected (Moon van der Staay *et al.*, 2001; Díez *et al.*, 2001). Only a very small proportion of sequences from these studies had significant identity ( $\geq 99\%$ ) with described species. The other sequences could be assigned to their most likely class based on phylogenetic analysis. Most of the sequences obtained in studies of this nature were from heterotrophic lineages, in particular members of the order alveolata. Sequences obtained which were affiliated with the algae primarily belonged to the classes Prymnesiophyceae, Prasinophyceae

and Dinophyceae. Less frequently, sequences were observed which were related to Cryptophyceae, Pelagophyceae, Dictyochophyceae, Bolidophyceae and Chrysophyceae. These findings were recurrent in studies applying this approach to samples from around the world, including the equatorial Pacific Ocean (Moon van der Staay *et al.*, 2001); the North Atlantic Ocean, the Southern Ocean (Weddell and Scotia Seas) and Mediterranean Sea (Díez *et al.*, 2001); the coastal English Channel (Vaulot *et al.*, 2002); the northwest Mediterranean Sea (Massana *et al.*, 2004); the South China Sea (Yuan *et al.*, 2004); the coastal Pacific Ocean (Worden, 2006); the Arctic Ocean (Lovejoy *et al.*, 2006); and in the North Atlantic Ocean to Arctic Ocean convergence of water masses (Hamilton *et al.*, 2008).

Molecular approaches to studying PPE diversity have led to the discovery of a novel PPE class without the establishment of cultures. Novel sequences were found in clone libraries from the English Channel which grouped together in phylogenetic analysis. The sequence data were used to design probes to target sequences of this group, to the exclusion of all other sequences. These probes were fluorescently labelled and hybridised with fixed environmental samples to identify cells related to this group. The samples were also stained with 4', 6-diamidino-2-phenylindole (DAPI) which stains DNA. The positive cells were examined by epifluorescent microscopy and found to contain a plastid with orange fluorescence, indicative of phycobilins, and a nucleomorph. This group of cells were called picobiliphytes (Not *et al.*, 2007). Sequences related to this class were found to be the dominant photosynthetic group in the North Atlantic - Arctic convergence (Hamilton *et al.*, 2008).

Despite the large proportion of clones in the nuclear SSU rRNA gene libraries discussed being of heterotrophic lineages (in the English Channel less than 20% of clones were related to phototrophs (Vaulot *et al.*, 2002)), the abundance of heterotrophic eukaryote sequences does not equate to an abundance of heterotrophic eukaryotes in the environment (Vaulot *et al.*, 2008). This is because sequences from heterotrophs may be more easily amplified or these organisms may contain many copies of the target gene, giving rise to 'PCR bias'. In order to study PPEs more specifically, sequence information compiled from SSU rRNA environmental gene libraries and algal cultures can be used to design PCR primers to target specific PPE

classes. This has been achieved for the Prasinophyceae and a detailed study of diversity within this class was recently published (Viprey *et al.*, 2008). However, in order to study the overall diversity of the PPEs the exploitation of a photosynthetic gene may provide more relevant information. This approach has been applied by Zeidner *et al.* (2003), who targeted the *psbA* gene encoding the D1 protein of photosystem II. This approach afforded information on both PPEs and cyanobacteria from the Red Sea, Mediterranean and central North Pacific. However, given the greater abundance of cyanobacteria, as well as the presence of the *psbA* gene in the genome of cyanophages (Mann *et al.*, 2003), clone libraries contained few sequences related to the PPEs. Similarly, a clone library approach targeting the 16S rRNA gene of oxygenic photosynthetic organisms produced libraries also dominated by cyanobacterial sequences (Nübel *et al.*, 1997; West *et al.*, 2001). As a result, using sequence data obtained with general oxygenic phototroph 16S rRNA gene-targeted primers, a new primer, PLA491F was designed which, in combination with the oxygenic phototroph biased primer OXY1313R (West *et al.*, 2001) can be used to enrich the amplification of marine algal plastids, but not cyanobacteria (Fuller *et al.*, 2006b). Plastid-biased clone libraries subsequently constructed in the Arabian Sea contained many sequences related to Chrysophyceae, a class only occasionally identified in the 18S rRNA gene library studies discussed above. Prymnesiophyceae, Prasinophyceae clade II and Pelagophyceae were also well represented (Fuller *et al.*, 2006b), largely in agreement with trends in 18S rRNA gene library studies discussed above. This primer pair was also used to construct libraries over an annual cycle in the coastal Mediterranean Sea (McDonald *et al.*, 2008). This study found lower diversity in the summer when libraries were dominated by Chrysophyceae-, Cryptophyceae- and Prymnesiophyceae-related sequences. In the winter, when cell numbers were lower, libraries did not contain sequences related to the Chrysophyceae, but did contain sequences related to Cryptophyceae, Prymnesiophyceae, Bacilariophyceae, Prasinophyceae, Dictyochophyceae and Pelagophyceae. These studies showed a high level of taxonomic diversity within the observed classes revealed with this primer pair. This approach is the most targeted method for observing the diversity of PPEs, but has not been directly compared to the more commonly used nuclear SSU rRNA gene library approach.

Despite the advances made in comprehending the diversity of PPEs by molecular techniques, nutritional and biochemical studies of organisms require the isolation of pure cultures, without any bacteria (axenic) (Droop, 1954). The advantages of obtaining cultures of microbial algae are unmatched by molecular techniques as the ability to perform organism-based studies provides insights into the functional roles and ecology of the organisms. For example, Butcher (1952) was able to observe the mode of reproduction of species that he isolated, and even chemically induce the production of zoospores allowing him to describe life-cycle stages whilst being sure of their origin.

Studies comparing approaches using molecular cloning and the establishment of cultures have found that many of the most numerous sequences in DNA clone libraries represent the most frequently isolated organisms in culture (Massana *et al.*, 2004), supporting the notion that the most common organisms are the most likely to be isolated. However, some sequences were only found by one method or the other, indicating the presence of bias in both methods. For example, some organisms that are relatively rare in the environment grow more readily in culture than more common organisms, including members of the Pelagophyceae (Le Gall *et al.*, 2008).

### **1.8. Aims of this work**

The overall aim of this work was to assess the molecular diversity of PPEs at the ocean basin scale, and, following analysis of several open-ocean cruise transects, to evaluate the global distribution of various PPE classes. The work thus sought to provide i) insights into the major players in CO<sub>2</sub> fixation in this group, as well as ii) to begin to indentify the specific abiotic and biotic factors that influence the distribution of natural populations of specific PPE classes.

Specific aims:

To investigate PPE community structure at the basin scale along an Atlantic Meridional Transect (AMT15) using both dot blot hybridisation and clone library construction. In so doing, perform a comparison of plastid and nuclear markers for assessing PPE diversity (Chapter 3).

To 'extend' the AMT cruise data to colder, mesotrophic waters via analysis of PPE community structure along the extended Ellett Line transect. Moreover, to perform a fluorescent *in situ* hybridisation (FISH) approach to allow a PCR-independent comparison of PPE community structure with dot blot hybridisation and clone library data (Chapter 4).

To further characterise PPE community structure in Indian and Arctic Ocean environments. To utilise the information with data obtained in Chapters 3-4 (as well as previously published data) to identify more global PPE distribution patterns and to provide insight into the specific environmental parameters that influence the distribution of PPE classes at the global scale (Chapter 5).

## **Chapter 2:**

### **Materials and methods**



## 2.1. Cruise transects analysed

Samples were analysed from cruises of the Atlantic Meridional Transect (AMT), extended Ellett Line, Arctic Ocean and Indian Ocean as well as from the BEAGLE cruise which circumnavigated the world (Fig. 2.1). Samples from the extended Ellett Line cruise were taken by myself, with flow cytometry, nutrient and chlorophyll *a* measurements taken by R. Holland, T. Brand and S. Thomalla respectively (Sherwin *et al.*, 2007). Samples were collected from approximately six depths for all cruises except the BEAGLE cruise, for which samples were collected only from surface water. Analyses published for samples from the Arabian Sea (AMBITION, Fuller *et al.*, 2006a) and Pacific Ocean (BIOSOPE, Lepère *et al.*, 2009) were included for a synthesis of data to allow global perspectives to be drawn (Fig. 2.1).

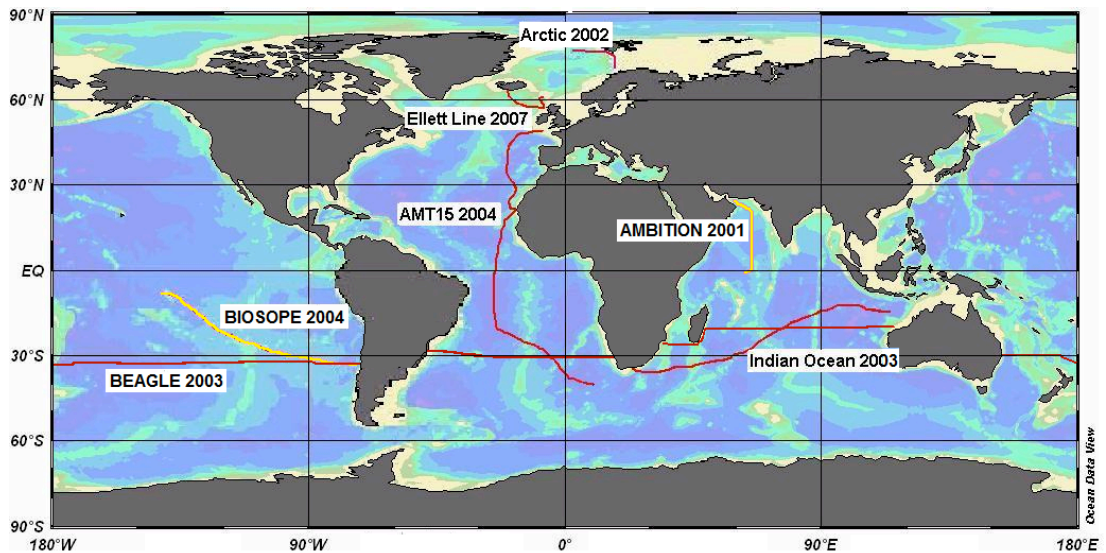


**Figure 2.1.** World map showing the position of transects used in this work. The Ambition and Biosope cruises, highlighted in yellow have been analysed previously, the Ambition cruise published (Fuller *et al.*, 2006a) and the Biosope in press (Lepère *et al.*, 2009). Cruises analysed in this work are highlighted in red.

Along these cruises, water temperature, salinity and dissolved oxygen concentration were measured by sampling rosette mounted sensor equipment. Measurements for dissolved oxygen were often calibrated using the Winkler titration technique on water samples drawn from Niskin Bottles on the sampling rosette (Sherwin *et al.*, 2007). Chlorophyll *a* concentrations were measured fluorometrically for water samples drawn from Niskin bottles. For most transects (except the Indian Ocean transect) concentrations of dissolved inorganic nutrients were measured using autoanalysers (e.g. a Lachat *Quik Chem 8000* flow injection autoanalyser was used

along the extended Ellett Line, Sherwin *et al.*, 2007). Cell numbers of photosynthetic eukaryotes, *Synechococcus* and *Prochlorococcus* were counted by ship-board flow cytometry on all cruises.

## 2.2. DNA sample collection and extraction

Seawater samples were collected using a rosette of 20 L Niskin bottles along the various cruise tracks (see section 2.1). 5-10 L of seawater was filtered through a 100  $\mu\text{m}$  pore-size mesh (Millipore) into a 25 L carboy to remove the largest clogging particles. Water was pre-filtered through 47 mm diameter, 3  $\mu\text{m}$  pore-size filters to target the pico-sized community. Samples were retained on 47 mm diameter, 0.45  $\mu\text{m}$  pore-size filters (polysulfone, Supor450, Gelman Sciences, AnnArbor, Mich) under gentle vacuum (10 mm Hg). DNA filters were put in 5 ml screw-top cryovials with 3 ml lysis buffer (20 mM EDTA, 400 mM NaCl, 0.75 M sucrose), flash-frozen in liquid nitrogen and stored at  $-80^{\circ}\text{C}$  until used.

DNA filters were thawed at room temperature, then 350  $\mu\text{l}$  of 10% (w/v) sodium dodecyl sulphate (SDS) was added to each cryovial and mixed. 0.335 mg proteinase K (Fermentas<sup>TM</sup>) was then added and the vials were incubated for 30 min at  $37^{\circ}\text{C}$ , followed by 10 min at  $55^{\circ}\text{C}$ . Lysate and filters were transferred to 15 ml falcon tubes with 3 ml phenol-chloroform-isoamyl alcohol (25:24:1) and vortex-mixed until the filters had dissolved in the phenol. Samples were then centrifuged for 5 min at  $6,000 \times g$  at  $4^{\circ}\text{C}$ . The upper layer was transferred to a new 15 ml tubes with 3 ml chloroform-isoamyl alcohol (24:1) and mixed before centrifuging for 5 min at  $6,000 \times g$  at  $4^{\circ}\text{C}$ . The aqueous phase was transferred to a fresh tube, then nucleic acids were precipitated with 1.2 ml 7.5 M ammonium acetate and 3 ml isopropanol, overnight at  $-20^{\circ}\text{C}$ . The following day, samples were centrifuged for 45 min at  $6,000 \times g$  at  $4^{\circ}\text{C}$ , the isopropanol was taken off and the remaining pellets washed with 2 ml 70% (v/v) ethanol, centrifuged for 15 min at  $6,000 \times g$  at  $4^{\circ}\text{C}$ , then the ethanol removed and the pellets left to dry. Pellets were resuspended in 50  $\mu\text{l}$  TE2 (10 mM Tris pH 8.0, 1 mM EDTA). 5  $\mu\text{l}$  aliquots were diluted 1:10 and stored at  $-80^{\circ}\text{C}$ .

### 2.3. Polymerase chain reaction (PCR)

PCR was performed slightly differently for dot blot hybridisations and for 16S/18S rRNA gene clone libraries, as much more DNA was required for the dot blot hybridisation technique. For the dot blot hybridisations and 16S rRNA gene clone libraries, a region of the 16S rRNA gene of approximately 830 bp of marine algal plastids was amplified using the algal plastid biased primer PLA491F (Fuller *et al.*, 2006b) coupled with the general oxygenic phototroph primer OXY1313R (West *et al.*, 2001).

For dot blot hybridisations, PCR amplification was carried out using a hot-start method. 1  $\mu\text{l}$  of environmental DNA was suspended in 25.85  $\mu\text{l}$  sterile milliQ water with 4  $\mu\text{l}$  of enzyme buffer, 1.4  $\mu\text{l}$   $\text{MgCl}_2$  (50 mM) and 2.5  $\mu\text{l}$  BSA (20 mg/ml) (Roche™), and heated to 95°C for 10 min before cooling to 80 °C at which point a second mixture was added containing dNTPs, Taq polymerase (Invitrogen™), primers and the remaining enzyme buffer and  $\text{MgCl}_2$ . This gave a final volume of 50  $\mu\text{l}$ , containing 1 mg  $\text{ml}^{-1}$  bovine serine albumin (BSA), 1 $\times$  enzyme buffer, 1.2 mM  $\text{MgCl}_2$ , 200  $\mu\text{M}$  concentrations of dNTPs, 0.8  $\mu\text{M}$  concentrations of primers and 2.5 U Taq polymerase. The following amplification conditions consisted of 30 cycles of 95 °C for 30 s, 60 °C for 30 s and 72 °C for 40 s. There was a final extension step of 72 °C for 6 min. For the 16S rRNA gene clone libraries the same conditions were used except that primers were at concentrations of only 0.2  $\mu\text{M}$  and 1.2 U Taq polymerase was used.

18S rRNA gene fragments were amplified for clone libraries using the general eukaryote primer pair 7F and 1534R (Moon van der Staay *et al.*, 2001) yielding 1.8 kbp products. PCRs were performed in a total volume of 50  $\mu\text{l}$ , with 1 mg  $\text{ml}^{-1}$  BSA, 1 $\times$  enzyme buffer, 1.5 mM  $\text{MgCl}_2$ , 200  $\mu\text{M}$  concentrations of dNTPs, 0.5  $\mu\text{M}$  concentrations of primers and 2.5 U HotStarTaq® (Qiagen™) Taq polymerase. The amplification conditions were 95 °C for 15 min followed by 35 cycles of 95 °C for 1 min, 57 °C for 1 min 30 s and 72 °C for 1 min 30 s, and a final extension step of 72 °C for 10 min.

## 2.4. Agarose gel electrophoresis

PCR-amplified DNA fragments were visualised by agarose gel electrophoresis, using 1% (w/v) ultra-pure agarose (Helena) dissolved in 1 × TBE (89 mM Tris, 89 mM boric acid, 2 mM Na<sub>2</sub>EDTA) after heating in a microwave. Ethidium bromide was added to the molten agarose to give a final concentration of 0.5 µl ml<sup>-1</sup>. PCR amplicons were mixed with loading buffer (6 ×: 15% Ficoll® 400, 0.03% (w/v) bromophenol blue, 0.03% (w/v) xylene cyanol FF, 10 mM Tris/HCl pH7.5) to give a 1 × concentration of loading buffer. Amplicons were electrophoresed alongside Generuler™ 1kb DNA ladder (Fermentas). Gels were electrophoresed in 1 × TBE buffer with a constant voltage of 80 V for 30 min. Fragments were visualised using Bio imaging gene flash documentation system (Synegene Synoptics group) with shortwave ultraviolet light.

7 µl of RFLP digests (section 2.7) were mixed with 3 µl of loading buffer, then electrophoresed on 2.5% (w/v) agarose gels with 0.5 µl ml<sup>-1</sup> ethidium bromide, in 1 × TBE. Gels were electrophoresed at 60 V for a minimum of 2 h, before visualising as above.

## 2.5. Dot blot hybridisation analysis

### 2.5.1. Preparation of DNA for hybridisation

As well as the sample DNA, control DNA from relevant algal classes were PCR amplified from cultures obtained from the Provasoli-Guillard National Centre for Culture of Marine Phytoplankton (CCMP) and the Roscoff Culture Collection (RCC) (see Table 2.1). In both cases, PCR was carried out as above in triplicate and pooled together using the Wizard PCR Prep DNA Purification System (Promega™). PCR amplified DNA was added to 100 µl of Direct PCR Amplification Buffer and mixed. 1 ml of resin was added and mixed by vortexing briefly 3 times over a 1 min interval. The resin and DNA was applied to a Wizard Minicolumn and the liquid pulled through a Promega vacuum manifold at <200 mm Hg pressure. 2 ml of 80% (v/v) isopropanol was added to the column and pulled through by applying the vacuum to wash the DNA in the column. The vacuum was applied for a further 30 sec to dry the

resin. DNA was eluted in 50  $\mu$ l nuclease-free water after standing at room temperature for 1 min by centrifuging at  $10,000 \times g$  for 1 min. DNA was stored at  $-20^{\circ}\text{C}$  until ready to use.

### **2.5.2. Preparation of dot blot hybridisation membranes**

Purified 16S rRNA PCR amplicons were quantified by NanoDrop spectrophotometer. Six copies of each membrane were produced containing each sample in triplicate. 50 ng of DNA was denatured for at least 10 min at room temperature using 0.2 M sodium hydroxide in TE buffer in a total volume of 200  $\mu$ l per dot (for six membranes with dots in triplicate 1  $\mu$ g of DNA in a total volume of 4 ml allowing for pipetting error). Control DNA amplicons from cultured species targeted by each probe (Table 3.1) in a dilution series of 5 to 70 ng per spot were prepared as above. DNA was blotted onto Zeta-probe® nylon membrane (Biorad™) using a microsample filtration manifold (Schleicher and Schuell™) under low pressure vacuum. The blotted DNA was then washed with  $2\times$  SSPE (0.3 M sodium chloride, 0.02 M sodium hydrogen phosphate, 0.002 M EDTA, pH 7.4) to remove sodium hydroxide. Membranes were placed on Whatman™ 3MM paper and left in the dark, overnight to dry. Membranes were then cross-linked at 120 mJ each side in a Stratalinker (Stratgene™). Fixed membranes were kept in the dark in a folder, separated with Whatman™ 3MM paper until use.

**Table 2.1.** Probes used for dot blot hybridisation analysis. The temperature at which stringent washes were performed (Td), probe sequence, reference for publication, target class and strain used for control DNA dilution series are shown for each probe.

Probe	Td (°C)	Sequence (5'-3')	Target Class	Reference	Control Strain
CHLA768	49	CCA TTC TCT CCC CTC GCT	Chlorarachniophyceae	Fuller <i>et al.</i> , 2006a	CCMP 621
CHRY1037	52	GCA CCA CCT GTG TAA GAG	Chrysophyceae	Fuller <i>et al.</i> , 2006a	CCMP 296
CRYP862	42	GGA TAC TTA ACG CCT TAG	Cryptophyceae	Fuller <i>et al.</i> , 2006a	CCMP 1868
EUB908	35	CCG TCA ATT CCT TTG AGT TT	Eubacteria	Edwards <i>et al.</i> , 1989	All Strains Used
EUST985	49	CAC TTC TAG CAA ACC CTG	Eustigmatophyceae	Fuller <i>et al.</i> , 2006a	RCC 438
PAVL665	37	TAG AAA TTC CTC CTA CCC	Pavlovophyceae	Fuller <i>et al.</i> , 2006a	CCMP 609
PELA1035	52	ACC ACC TGT GTG TGT CTA	Pelagophyceae	Fuller <i>et al.</i> , 2006a	RCC 100
PING1024	47	ACG TAT TCC TTA CGG CAC	Pinguiophyceae	Fuller <i>et al.</i> , 2006a	RCC 503
PRAS826	58	GAT TCG CGT ATC CCC TAG	Prasinophyceae clade VI	Fuller <i>et al.</i> , 2006a	RCC 137
PRYM666	44	CTA GAA ATT CCC TCT ACC	Prymnesiophyceae	Fuller <i>et al.</i> , 2006a	RCC 186
TREB708	44	CCT TTG GTG TTC CTC CCG	Trebouxiophyceae	Fuller <i>et al.</i> , 2006a	CCMP 243

### 2.5.3. Dot blot hybridisation probe labelling and purification

HPLC grade purified oligonucleotide probes (30ng, Table 2.1) were end labelled with 20  $\mu\text{Ci}$   $\gamma^{32}\text{P}$ -ATP using 10 U T4 DNA kinase in 1 $\times$  forward kinase buffer (Fermentas<sup>TM</sup>) at 37°C for 30 min, after which a further 10 U was added and the probes were incubated at 37°C for a further 30 min. Radiolabelled probes were purified from unincorporated precursors with Quick-spin sephedex-50 columns (Roche<sup>TM</sup>) at 1,500  $\times g$  for 1 minute.

### 2.5.4. Probing, washing, exposure and stripping of dot blot hybridisation membranes

Blotted membranes were moistened with 2 $\times$  SSPE and placed on a sheet of mesh, rolled up, placed in hybridisation tubes and unrolled using a glass pipette to smooth the membranes against the inside of the tubes, avoiding bubbles. 5 ml of hybridisation buffer (0.5 M Sørensen's phosphate buffer solution pH7.2, 7% (w/v) SDS, 1.0 mM EDTA) was added to the tubes. The membranes were pre-hybridised in the tubes rotating in a hybridisation oven (Hybaid<sup>TM</sup>) at 30°C for at least 1 h. The buffer was then poured off and replaced with 5 ml of fresh, prewarmed buffer. The purified, labelled probe (Table 2.1) was added and the tube returned to the hybridisation oven at 30°C to hybridise overnight. Hybridisation buffer was poured off and the non-hybridised probes were washed off with three washes with 30 ml wash buffer (0.2 $\times$  SSPE, 0.1% (w/v) SDS) at 30°C for 15 min. Membranes were transferred to a container holding 100 ml wash buffer pre-warmed to the probe-specific wash temperature (Table 2.1) for a stringency wash at this temperature for 10 min. The membranes were placed in a plastic wallet and sealed, then placed in an imaging cassette with a phosphorimager screen which was exposed overnight (except EUB908, which was exposed for 4 h).

The exposed screen was read by a phosphorimager reader FLA-500 (Fujifilm). The digitised image (Fig. 2.2) was analysed using TotalLab software (Nonlinear Dynamics<sup>TM</sup>).

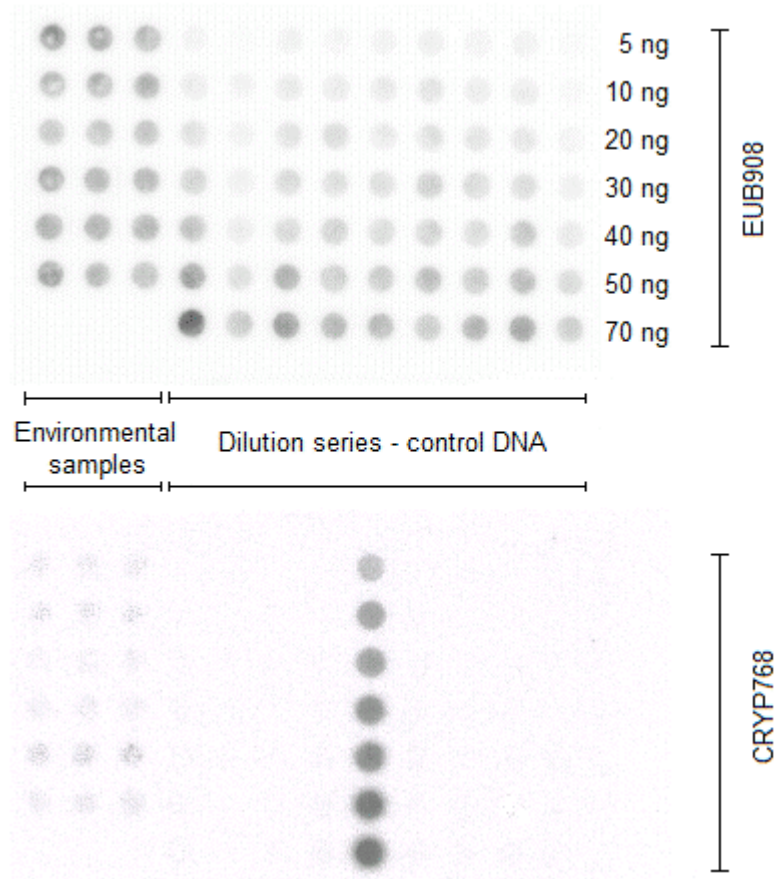


**Figure 2.2.** Example phosphorimager picture dot blot hybridisation membranes. Two copies of the same membrane are shown, probed with the eubacterial probe EUB908 (top) and with the Cryptophyceae- specific probe CRYP768 (bottom). The membranes were blotted with dilution series of control DNA (left) and environmental samples in triplicate (right).

The relative hybridisation of the specific probes to the total blotted DNA in the environmental samples was then calculated using the equation:

$$\text{Relative hybridisation (\%)} = \left[ \left( \frac{S_{env}}{E_{env}} \right) \cdot \left( \frac{S_{con}}{E_{con}} \right)^{-1} \right] \times 100$$

where  $S_{env}$  and  $E_{env}$  represent hybridisation to environmental DNA of the specific and eubacterial probes respectively, and  $S_{con}$  and  $E_{con}$  are the slopes of the specific and eubacterial probe-binding curves respectively, calculated by plotting the hybridization of each probe to the dilution series of homogenous control DNAs. The relative hybridisation of a given specific probe compared with that of the eubacterial probe to the control DNAs was averaged where more than one control DNA was used. Values above 2% were considered to be adequately above background levels for further analysis. Where, due to temperature differences in the stringent wash step, a probe gave readings in excess of 100% data were normalised such that the highest



value became 100%. The whole dataset, i.e. all probes and samples, was then normalised so that the sum of the relative hybridisation values for all probes across each sample never exceeded 100%.

## 2.6. Clone library construction/ TA cloning

The plastid 16S rRNA gene clone libraries for the upwelling and southern gyre stations were constructed by undergraduate student Ana Tiganescu. All clone libraries were created using pCR® 2.1-TOPO TA cloning kits (Invitrogen™), according to the manufacturer's instructions. Approximately 100 ng of DNA was added to 1 µl (10 ng µl<sup>-1</sup>) of linearised pCR® 2.1 vector, and 1 µl of supplied salt solution (1.2 M NaCl, 0.06 M MgCl<sub>2</sub>) in a total volume of 6 µl. This was mixed and incubated at room temperature for 30 min, then stored on ice or at -20°C until used. A 50 µl vial of chemically competent TOP10F' cells (stored at -80°C) were thawed on ice then mixed with 2 µl of recombinant plasmid DNA and incubated for 30 min. The mixture was heat-shocked at 42°C for 30 s and placed on ice. 250 µl room-temperature LB (10 g l<sup>-1</sup> tryptone, 5 g l<sup>-1</sup> yeast extract, 10 g l<sup>-1</sup> NaCl, pH7.0) was added and the mixture incubated for an hour at 37°C in an oscillating incubator at 200 rpm. 20-50 µl of cell suspension was spread on pre-warmed (37°C) LB 1.5% (w/v) agar plates prepared with 50 µg ml<sup>-1</sup> ampicillin and 50 µg ml<sup>-1</sup> kanamycin and spread with 40 µl of 40 mg ml<sup>-1</sup> X-gal in dimethylformamide and 40 µl of 100 mM IPTG in water. Plates were incubated overnight at 37°C.

## 2.7. Restriction Fragment Length Polymorphism (RFLP) analysis

50-200 white colonies were picked for analysis and grown on selective LB ampicillin and kanamycin plates overnight at 37°C. Colonies were suspended in water and 1 µl was PCR amplified as indicated in section 2.2 above. Amplification was checked by agarose gel electrophoresis and those with the expected amplicon size underwent RFLP analysis. For 16S rRNA gene libraries, 10 µl of amplicons were mixed with 2.5U each of *EcoRI* and *HaeIII* (Fermentas™) and 1× Tango buffer in a total volume of 20 µl and incubated at 37°C for 2 hours. For 18S rRNA gene libraries, 10 µl of amplicons were mixed with 5U of *HaeIII* (Fermentas™) with 1× *HaeIII* buffer and incubated at 37°C for 2 hours, before visualising using agarose gel electrophoresis

(see section 2.3 above). Clones with the same RFLP pattern were considered members of the same operational taxonomic unit (OTU). Amplicons of one or more members of each OTU were purified and sequenced.

## **2.8. DNA purification**

PCR amplicons were purified prior to sequencing using the QIAquick PCR purification kit (Qiagen™). Purification was performed on columns using the provided solutions and according to the manufacturer's instructions. DNA was eluted from the column with 30-50 µl of sterile MilliQ water.

## **2.9. DNA sequencing**

DNA sequencing was carried out using an ABI PRISM 3130xl Genetic Analyser® (Applied Biosystems™), using the primers that the clone libraries had been constructed with. A third primer, 528F (Elwood *et al.*, 1985) was used for sequencing the middle section of the 18S rRNA fragments to allow assembly of the full sequence. This also allowed a substantial amount of the fragment to be sequenced twice independently, increasing confidence in the sequence accuracy.

## **2.10. Fluorescent *in situ* hybridisation (FISH) analysis**

### **2.10.1. FISH sample collection**

Water samples were collected with a rosette of 20 L Niskin bottles, filtered through a 100 µm pore-size mesh (Millipore) to remove the largest clogging particles. Flow cytometry data collected on board ship was used to calculate the volume of water expected to contain approximately  $3.2 \times 10^6$  PPE cells. This volume of water was pre-filtered through a 47 mm diameter, 3 µm pore-size filter to target the pico-sized community. Samples were fixed with 1% (w/v) (final concentration) paraformaldehyde for 1 hour at 4°C before being retained on 47 mm diameter, 0.2 µm pore-size polycarbonate filters (Whatman) by vacuum at 200 mm Hg pressure. Samples were dehydrated with an ethanol series consisting of 3 min each of 50% (v/v), 80% (v/v) and 100% (v/v) ethanol before drawing through the filter under 200

mm Hg pressure, without allowing filters to dry between filtrations. Filters were stored at  $-80^{\circ}\text{C}$  until further analysis

### 2.10.2. FISH probing of filters

Filters were cut into pieces approx 1/10 of the size of the whole filter and marked with pencil on the side on which cells were fixed. Filters were placed face-down on a 10  $\mu\text{l}$  hybridisation buffer (HB) (40% (v/v) deionised formamide, 0.9 M NaCl, 20 mM Tris-HCl pH7.5, 0.01% (w/v) SDS, 2  $\times$  blocking agent for most probes except filters to be used with the probe targeting the Chrysophyceae which contained 20% (v/v) deionised formamide) droplet suspended on parafilm stretched over a microscope slide. Slides were placed in hybridisation chambers with a strip of Whatman paper moistened with approximately 1 ml HB and incubated at  $35^{\circ}\text{C}$  for 30 min. Filters were transferred, face down, to droplets of 9  $\mu\text{l}$  HB and 1  $\mu\text{l}$  probe, prelabelled with horseradish peroxidase (see Table 2.2), on parafilm stretched over fresh slides. These slides were placed in hybridisation chambers still containing the moistened Whatman paper, and hybridised at  $35^{\circ}\text{C}$  for 3 hours. Filters were washed twice by transferring to a preheated bijoux containing 3-4 ml of washing buffer (WB) (56 mM NaCl, 5 mM EDTA, 0.01% (w/v) SDS, 20 mM Tris-HCl pH 7.5) and incubating in a very slowly oscillating water-bath at  $37^{\circ}\text{C}$  for 20 min. Filters were then equilibrated in 3-4 ml TNT buffer (100 mM Tris-HCl pH7.5, 150 mM NaCl, 0.1% (v/v) Tween 20<sup>®</sup> for 20 min at room temperature in the dark. The tyramide signal amplification reaction, horseradish peroxidase activation of FITC fluorochromes, was carried out by placing a 20  $\mu\text{l}$  droplet of TSA solution (1:1 amplification diluent and dextran sulfate with 1:50 FITC tyramide with this mixture) on parafilm covered slides and placing filters face-down on these droplets and incubated in the dark at room temperature for 30 min. Filters were transferred to 2 successive baths of preheated TNT buffer at  $55^{\circ}\text{C}$  in the dark for 20 min each. The enzymatic reaction was stopped and dextran sulfate was removed by rinsing in distilled water. Filters were dried on Whatman paper in the dark and then counterstained with propidium iodide (10  $\mu\text{g ml}^{-1}$ ) in antifading mounting solution (Citifluor), face-up on slides and a coverslide added and sealed with nail varnish to prevent evaporation of mounting solution. Slides were stored at  $4^{\circ}\text{C}$  until analysed by epifluorescent microscopy.

**Table 2.2.** Probes used in FISH analyses

Probe	Sequence	Target	Reference
EUK1209r	GGG CAT CAC AGA CCT G	All eukaryotes	Giovanonni <i>et al.</i> , 1988
NCHLO01	GCT CCA CTC CTG GTG GTC	nuclear SSU rRNA	Simon <i>et al.</i> , 1995
CHLO02	CTT CGA GCC CCC AAC TTT		Simon <i>et al.</i> , 2000
PRYM02	GGA ATA CGA GTG CCC CTG AC	Prymnesiophyceae nuclear SSU rRNA	Simon <i>et al.</i> , 2000
CHRYSO01	GCA CCA CCT GTG TAA GAG	Chrysophyceae plastid SSU rRNA	Jardillier <i>et al.</i> , in press.
OSTREO01	CCT CCT CAC CAG GAA GC	Prasinophyceae clade II	Not <i>et al.</i> , 2004
PRAS02	CCC GTC CCG AGA CCA ACG	nuclear SSU rRNA	Biegala <i>et al.</i> , 2003
CRYPT13	CGA AAT ATA AAC GGC CCC AAC	Cryptophyceae nuclear SSU rRNA	Lepère <i>et al.</i> , 2008
PELA01	TAC CTA GGT ACG CAA ACC	Pelagophyceae nuclear SSU rRNA	Simon <i>et al.</i> , 2000

### 2.10.3. Epifluorescent microscopy

The hybridised and propidium iodide-stained filters were observed with a Zeiss Axioskop 40 (Germany) epifluorescence microscope equipped with a mercury light source and a Plan-Apochromat × 100 (Zeiss, Germany) objective. The green (FITC) and red emission (PI) fluorescence produced by the different fluorochromes was collected between 510 and 550 nm and above 585 nm. Fields were chosen at random and hybridised cells were counted. This value was converted to cells ml<sup>-1</sup> using the formula:

$$\text{cells ml}^{-1} = \frac{C S_1}{10/9 S_2 F V}$$

where C = number of positive cells counted.

S<sub>1</sub> = surface area of the filter.

S<sub>2</sub> = surface area of one field viewed under the microscope.

F = number of fields counted.

V = volume filtered.

## **2.11. Bioinformatic analysis**

### **2.11.1. Illustration of dot blot hybridisation and environmental data**

Dot blot hybridisation data and other environmental data were visualised using contour graphs. These were plotted using Ocean Data View software version 3.4.2 (ODV Schlitzer, R., <http://odv.awi.de>, 2006).

### **2.11.2. Phylogenetic analysis**

Sequences were assembled using SeqMan software (DNASTAR™) and initially checked for chimeras using the Check Chimera programme from the Ribosomal Database Project (Cole *et al.*, 2003). Sequences were then imported into laboratory-curated ARB databases (Ludwig *et al.*, 2004). Sequences were aligned using ARB and inserted into existing neighbour-joining phylogenetic trees using ARB parsimony. 16S rRNA sequences were inserted using a maximum frequency filter for plastids. Sequences were then manually checked again for chimeras by checking the phylogenetic position of subsections of the sequence in the trees. Sequences considered to be chimeras were excluded from further analysis. Bootstrap values (%) were obtained from 1000 replications. Trees were exported using XFig version 3.2.5 software and converted into scalable vector graphics files (.svg), then exported to Inkscape 0.46 software for editing.

### **2.11.3. Statistical analyses**

Rarefaction analyses were carried out using Analytic Rarefaction 1.3 (Holland, 2003). Graphs were drawn from the resulting data using Microsoft Excel.

Canonical correspondence analyses (CCAs) of diversity data (percent relative hybridisation data for individual PPE classes) were calculated using the vegan package (Legendre *et al.*, 1998) in the R software (<http://cran.r-project.org>). The value for the total variation in diversity was obtained as well as eigenvalues for each environmental variable from a CCA with the diversity data, and the variable with the highest eigenvalue was selected. This variable was then paired with each of the others in turn and the eigenvalue for both variables together obtained as well as eigenvalues for each variable as a constraining variable, allowing for the other as a conditional variable. From this, the percentage of variation explained by each variable alone, both together, the overlap between the variation explained by both variables and the remaining diversity variation not explained by either variable was calculated. The combination of variables with the highest value for total variation explained by both variables was considered the best 2 variable model. This process was repeated to find the best 3 variable model, and so on until the addition of variables had a negligible effect on the amount of variation in diversity that was explained by the model, and a CCA including all variables did not produce considerably higher eigenvalues. The model that explained most of the variation in diversity with few environmental variables was selected and CCA plots were drawn using R with biplot values of this combination of environmental variables and eigenvectors of dot blot hybridisation data group scores.

The CCA method was also used to calculate the amount of variation in dot blot hybridisation data explained by physical, chemical and biological parameters and the amount of overlap in variation explained by more than one set of parameters. Variables were grouped into physical, chemical and biological variables and the

eigenvalues calculated for each. The set of variables were then paired with each of the others in turn and the eigenvalue for both sets of variables together obtained as well as eigenvalues for each variable set as a constraining variable set, allowing for the other as a conditional variable set. From this, the percentage of variation explained by each variable set and the overlap of variation that could be explained by both variable sets were calculated. These data were plotted in Venn diagrams using VennDiagramPlotter Software from Pacific Northwest National Laboratory (PNNL) obtained from <http://omics.pnl.gov>.

## **Chapter 3:**

# **Photosynthetic picoeukaryote community structure along the Atlantic Meridional Transect (AMT15)**



### 3.1. Introduction

#### 3.1.1. History of the Atlantic Meridional Transect

The Atlantic Ocean is the second largest of the world's oceans, with an area of 77 million km<sup>2</sup> (Pidwirny and Duffy, 2008). The Atlantic Meridional Transect (AMT) project capitalises on the passage of the British Antarctic Survey vessel from the UK, typically twice yearly, allowing measurements and samples to be regularly taken over a large extent of the Atlantic Ocean (Aiken and Bale, 2000). The programme began in 1995 and has completed 19 transects up until November 2008 (Fig. 3.1). It therefore allows comparisons of data collected in subsequent years as well as between seasons. The AMT project was necessary to extrapolate ecosystem process and productivity research to basin scales as previous work had been hindered by under-sampling (Aiken *et al.*, 2000). Major goals have been to i) examine large scale phytoplankton processes, ii) validate the hypothesis of oceanographic provinces and determine their characteristic properties, and iii) evaluate the use of remotely-sensed ocean colour as an indicator of primary production (Aiken *et al.*, 2000).

The AMT extends between the UK and either the Falkland Islands or Cape Town in South Africa (and in future will end in Chile). It crosses 4 major circulation features of the Atlantic Ocean observed by Hooker *et al.* (2000): the North Atlantic Gyre (NAG), 50-25°N; the Tropics and Equatorial Region (TER) 25°N-15°S; the South Atlantic Gyre (SAG), 15-35°S; and the Sub-Antarctic Convergence Zone (SACZ) South of 35°S. These features are also characterised by particular temperature, salinity and mixed layer depth (Hooker *et al.*, 2000).

Over 10 years from its first cruise, the AMT programme has achieved findings in research areas as diverse as characterisation of oceanic domains; development of various measurement and sampling technologies; phytoplankton biomass, production and growth measurements; ratios of photosynthesis and respiration; heterotrophic nanoflagellate communities; nitrogen cycling; air-sea exchange of greenhouse gases; and aerosol input of nutrients (Aiken *et al.*, 2000; Robinson *et al.*, 2006).

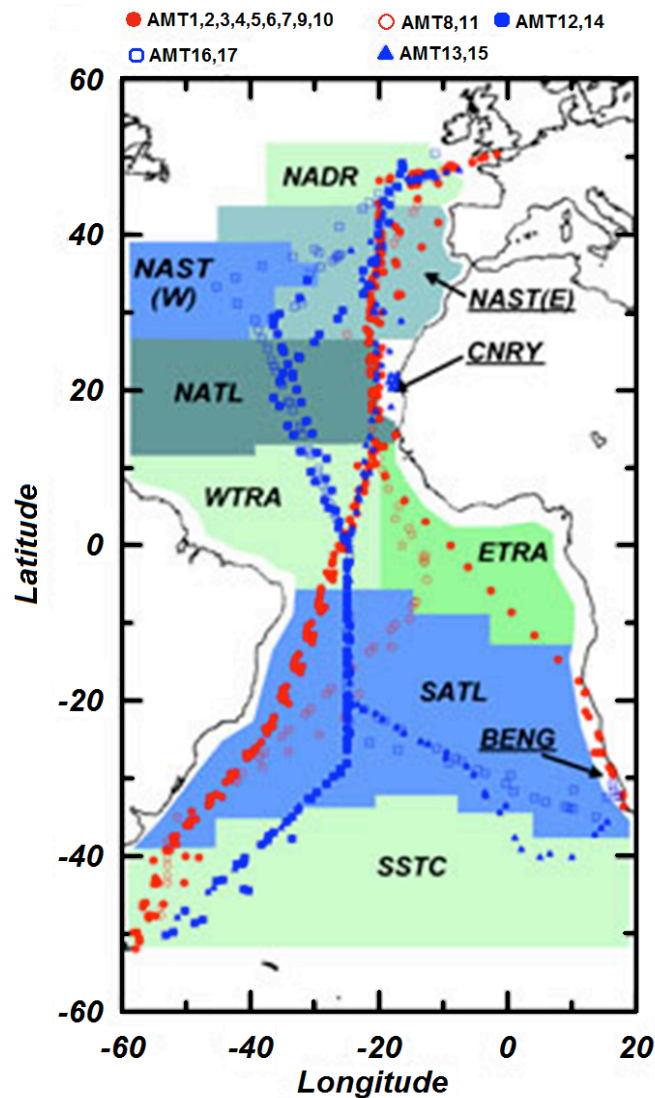


**Figure 3.1.** Cruise tracks of AMT cruises 1-17 from [www.amt-uk.org](http://www.amt-uk.org). Province boundaries are highlighted: North Atlantic Drift (NADR), North Atlantic Subtropical Gyral West and East (NAST(W) and (E)), North Atlantic Tropical Gyral (NATL), Canary Coastal (CNRY), Western Tropical Atlantic (WTRA), Eastern Tropical Atlantic (ETRA), South Atlantic Gyral (SATL), Benguela Coastal Current (BENG) and South Subtropical Convergence (SSTC) (Longhurst, 2007).

### 3.1.2. Characteristics of the phytoplankton along the AMT

The majority of primary producers along the AMT are smaller than  $3 \mu\text{m}$  in size (Zubkov *et al.*, 2000; Marañón *et al.*, 2001), as is the case for most open-ocean ecosystems (e.g. in the Pacific, Li *et al.*, 1983). Pigment analyses have shown biomass inferred by concentration of chlorophyll *a* was highest in the temperate shelf waters of the extreme north and south of the transect with  $>1 \text{ mg m}^{-3}$ . In contrast the tropical and subtropical regions had the lowest chlorophyll *a* concentrations, except

in the Canary current upwelling system where the concentration doubled from 0.5 to 1 mg m<sup>-3</sup> (Gibb *et al.*, 2000). In regions of highest chlorophyll *a* concentration, eukaryotes larger than 3 µm, such as diatoms and dinoflagellates are more important (Robinson *et al.*, 2006). Photosynthetic rates vary with nutrient availability, being lower in more oligotrophic regions, but in contrast to other parameters such as biomass, vary substantially between repeated transects (Marañón and Holligan, 1998).

Analysis of picophytoplankton community structure by flow cytometry revealed that *Prochlorococcus* was the dominant group in the oligotrophic gyres, in contrast to *Synechococcus* whose abundances were lowest in these regions. PPEs were observed in much lower numbers at all latitudes, but due to their larger size contributed significantly to biomass and tended to have higher abundances in temperate and upwelling areas as was the case for *Synechococcus* (Zubkov *et al.*, 1998). These characteristics were observed over multiple years (Heywood *et al.*, 2006) and led to the proposal of five provinces of the AMT, from north to south: northern temperate, northern Atlantic gyre, equatorial, southern Atlantic gyre and southern temperate (Zubkov *et al.*, 1998; Zubkov *et al.*, 2000). Seasonal comparison showed *Prochlorococcus*, *Synechococcus* and PPEs all appeared to have higher standing stocks in the spring than the autumn (Zubkov *et al.*, 2000). However, inter-annual study showed standing stocks of *Synechococcus* and *Prochlorococcus* in the gyres and equatorial region of the AMT did not vary significantly over 8 years (Heywood *et al.*, 2006).

At a higher resolution of prokaryotic picophytoplankton population study, the distributions of six *Prochlorococcus* ecotypes were elucidated along AMT13 using quantitative PCR (qPCR) data (Johnson *et al.*, 2006). Distribution of ecotypes was associated with adaptation to light, and temperature also appeared to be a major determinant of the presence of particular ecotypes. Specific lineages of both *Prochlorococcus* and *Synechococcus* were studied from the AMT cruise in the same season (boreal autumn) the following year (AMT15) (Zwirgmaier *et al.*, 2007). *Synechococcus* population structure varied between regions, but was very similar in equivalent regions in the northern and southern hemisphere. *Prochlorococcus* ecotype distribution was similar to the previous year, and shown to also be related to

light and temperature, suggesting that basin scale distribution patterns for *Prochlorococcus* ecotypes are remarkably reproducible from year to year.

Eukaryotic phototrophs along the AMT have been indicated by the presence of photosynthetic carotenoids and accessory pigments. 19'-hexanoyloxyfucoxanthin is a marker for the Prymnesiophyceae and was found throughout the extent of AMT2-5 (Gibb *et al.*, 2000). Fucoxanthin and peridinin were found at maximum concentrations in temperate and upwelling regions indicating the presence of diatoms and dinoflagellates. 19'-hexanoyloxyfucoxanthin, butanoyloxyfucoxanthin and chlorophyll *b*, indicative of prymnesiophytes, chlorophytes and chrysophytes had broader distribution patterns but were higher in temperate and upwelling regions (Gibb *et al.*, 2000).

PPEs, photosynthetic nanoeukaryotes (PNEs), cryptophytes and coccolithophores can all be identified by flow cytometry. This method was applied during AMT13 and 14 using the approximate parameters of 0.2-2.0  $\mu\text{m}$  diameter for PPEs and 2.0-10  $\mu\text{m}$  diameter for PNEs (Tarran *et al.*, 2006). This study found that PPEs were the major contributor to biomass, and PPE and PNE distributions matched the distribution of chlorophyll *a*. Cryptophytes were found to be at their most abundant in the southern temperate region. Coccolithophores were the least abundant group, and were often undetected. However, AMT14 encountered a bloom of coccolithophores within the northern temperate region (Tarran *et al.*, 2006).

### **3.1.3. Aims of this work**

Samples used in this work were collected by K. Zwirgmaier from 21 stations at 6 depths along AMT15 (Fig 3.2) in the boreal autumn of 2004. They were used in a clade-level survey of *Prochlorococcus* and *Synechococcus* community structure (Zwirgmaier *et al.*, 2007). The work presented here involves a comparable study of the PPE community, using dot blot hybridisation analysis to survey PPEs at the class level from the same DNA samples. Phylogenetic analysis of plastid-derived 16S rRNA genes and nuclear SSU rRNA genes was used to identify members of the PPE community in contrasting regions of the cruise, and these two approaches were compared for the first time directly from environmental samples.

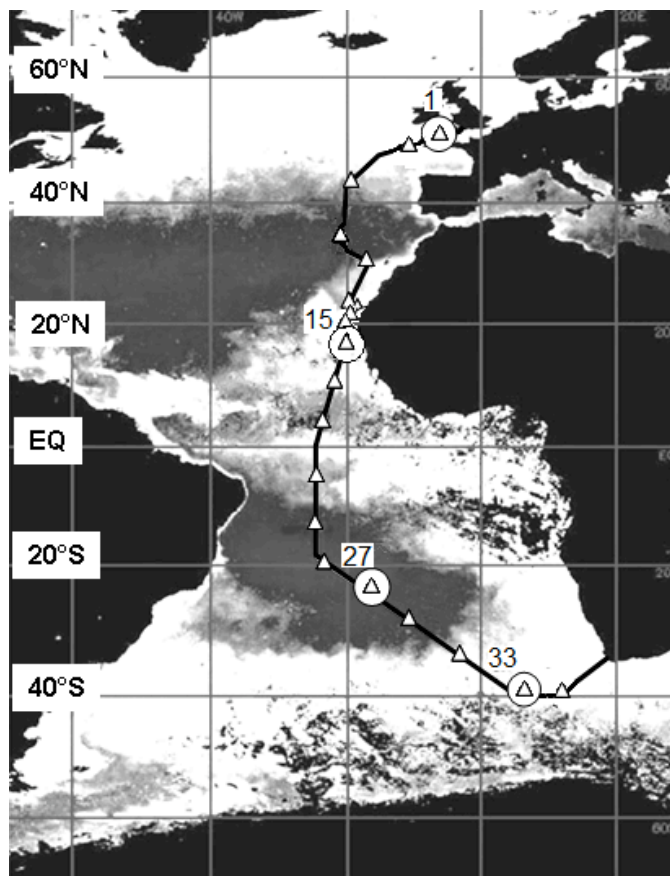


**Figure 3.2.** AMT15 cruise track. Triangles indicate the position of stations for which samples were used for dot blot hybridisations at 6 depths corresponding to the surface and 55, 33, 14, 1 and 0.1% of surface light intensity. Clone libraries were also created for samples from the depth corresponding to 55% surface light intensity at stations 1, 15, 27 and 33, marked with a circle.

## 3.2. Results

### 3.2.1. Chemical and physical characteristics of AMT15

The northern temperate region (48-39°N), the eastern edge of the northern gyre (38-30°N), Mauritanian upwelling (21°N), southern gyre (6-30°N) and southern temperate region (31-40°N) were characterised by particular physical and chemical profiles (Fig. 3.3). The temperate regions contained 0.0186 - 0.09  $\mu\text{M}$   $\text{NO}_2$ , 0.03 - 8.2  $\mu\text{M}$   $\text{NO}_3$  and 0.1676 - 0.62  $\mu\text{M}$   $\text{PO}_4$ ; gyres possessed lower concentrations at 0.0005 - 0.02  $\mu\text{M}$   $\text{NO}_2$ , 0.01 - 0.02951  $\mu\text{M}$   $\text{NO}_3$  and 0.0022 - 0.02  $\mu\text{M}$   $\text{PO}_4$  except at 1% light intensity and lower where concentrations peaked at 0.16  $\mu\text{M}$   $\text{NO}_2$  23.7  $\mu\text{M}$   $\text{NO}_3$  and 1.43  $\mu\text{M}$   $\text{PO}_4$ ; the upwelling region was the site of the highest nutrient concentrations of the transect with 0.0026 - 0.71  $\mu\text{M}$   $\text{NO}_2$ , 0.01 - 26.2  $\mu\text{M}$   $\text{NO}_3$  and 0.023 - 1.53  $\mu\text{M}$   $\text{PO}_4$ . Despite the elevated nutrient concentrations, characteristic of

upwelling regions, the temperature profile does not indicate deep mixing of the water column associated with upwelling. A clear thermocline is observed between depths corresponding to 14% and 1% surface light intensity along most of the length of the transect including the upwelling region, though the upwelling is cooler than surrounding waters. The position of the thermocline is less uniform when plotted against depth rather than percent of surface irradiance (see left and right panels in Fig 3.3). Stations south of 20°S appear to be characterised by deeper mixing with no thermocline observed over the depths sampled. Surface temperatures were 16-19°C in the northern temperate region and 12-13°C in the southern temperate region, 22-28°C in the gyres, and 21-23°C in the upwelling area (Zwirgmaier *et al.*, 2007).

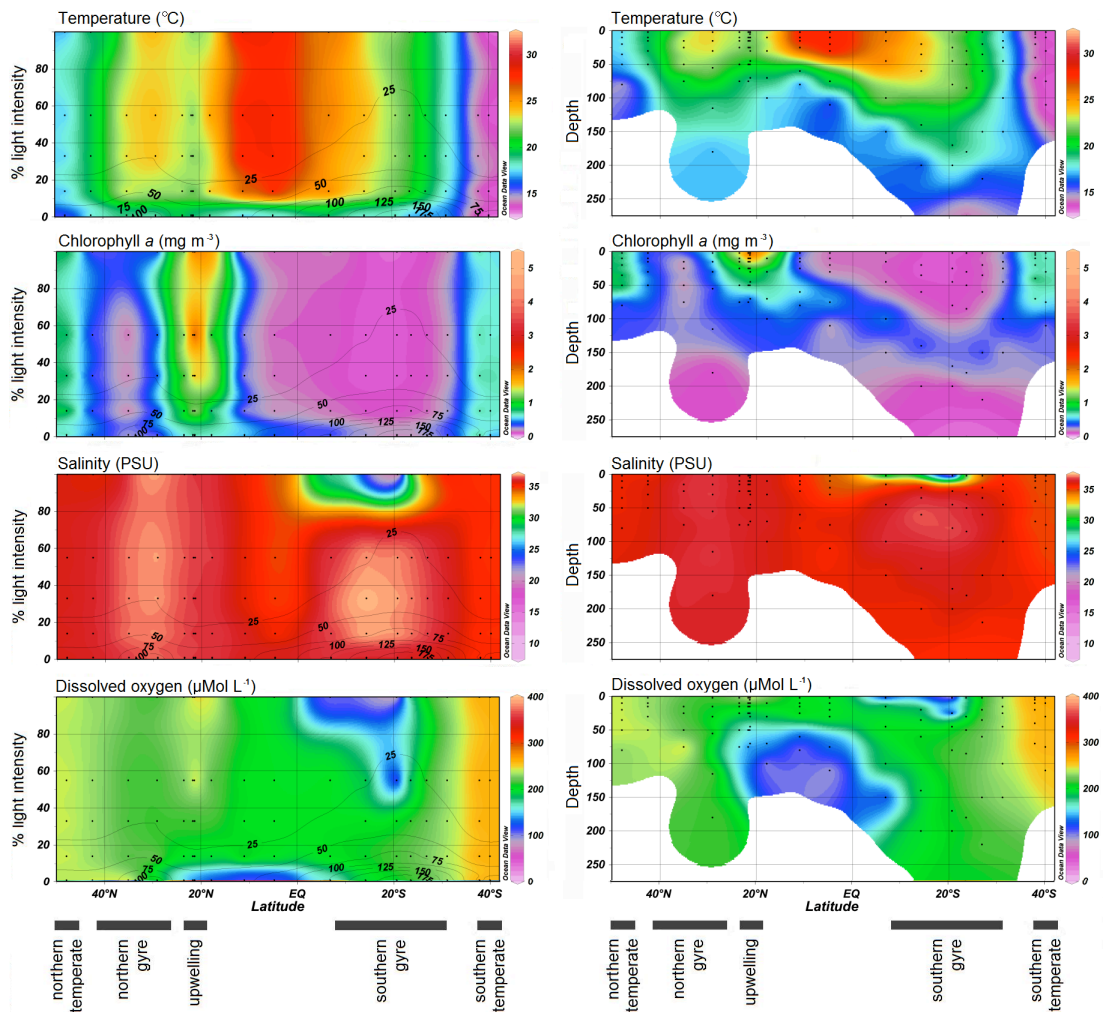


**Figure 3.3.** Contour plots showing chemical and physical parameters along AMT15. Latitude is plotted on the x axis, against light intensity on the y axis (left panels) or depth into water column (right panels). The colour represents the value of the environmental variable. Black contour lines indicate the depth in the water column corresponding to the light intensity value. Continued next page.

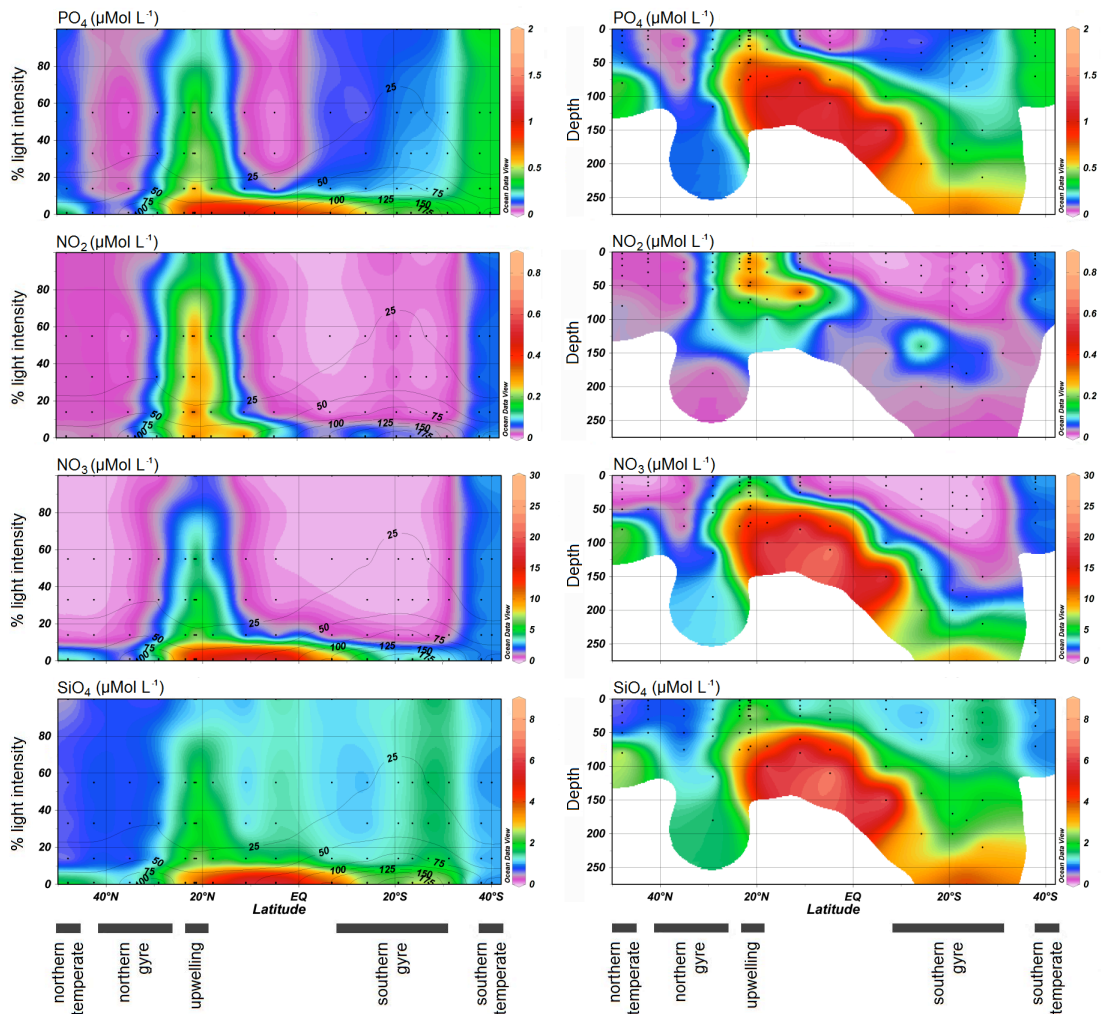


**Figure 3.3.** Continued.

An area of low salinity, corresponding with low dissolved oxygen, was encountered at the surface of a region in the Southern gyre. Here, a minimum salinity value of 8.5 PSU was recorded and dissolved oxygen reached undetectable levels as heavy rainfall gave rise to a pool of freshwater on top of the water column.

### 3.2.2. Flow cytometric data

Flow cytometry (Fig. 3.4) revealed peak abundance of photosynthetic eukaryotes towards the Northern (48°N) and Southern (40°S) extremes of the transect, reaching  $10 \times 10^3$  cells ml<sup>-1</sup> and  $8.5 \times 10^3$  cells ml<sup>-1</sup> respectively. The upwelling area (20°N), also had a peak in abundance of  $9 \times 10^3$  cells ml<sup>-1</sup>. Less than  $3.4 \times 10^3$  cells ml<sup>-1</sup> were found along the edge of the northern gyre, and in the southern gyre abundance remained below 900 cells ml<sup>-1</sup>. This distribution pattern appears to be similar to that

of *Synechococcus*, which had peaks of  $10^5$ ,  $3.6 \times 10^4$  and up to  $3 \times 10^5$  cells  $\text{ml}^{-1}$  in the northern and southern temperate and upwelling regions respectively. These distributions appear to reflect the distribution of chlorophyll *a* (Fig. 3.3), but are in contrast to *Prochlorococcus* flow cytometry data which shows peaks of  $1.5 \times 10^4$  and  $2 \times 10^5$  cells  $\text{ml}^{-1}$  in the northern and southern gyres respectively (Zwirgmaier *et al.*, 2007).

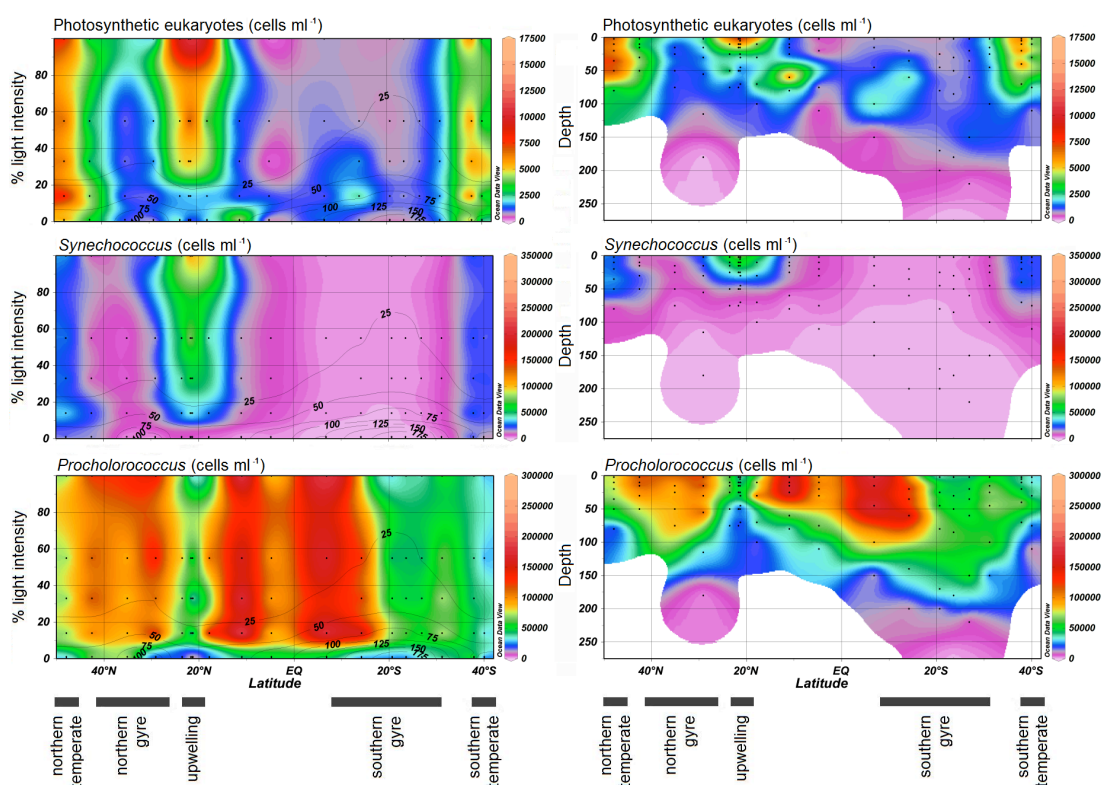


**Figure 3.4.** Contour plots of flow cytometry data along AMT15. Cells  $\text{ml}^{-1}$  have been measured for photosynthetic eukaryotes (top), *Synechococcus* (middle) and *Prochlorococcus* (bottom).

### 3.2.3. Basin-scale distribution patterns of PPE classes along AMT15

Of the ten class-specific probes used in dot blot hybridisation analysis, seven reached values above 2%. These were the probes detecting the classes Prymnesiophyceae, Chrysophyceae, Cryptophyceae, Pelagophyceae, Pinguiphyceae, Trebouxiophyceae and Eustigmatophyceae (Fig. 3.5).

The most abundant classes over the transect were the Prymnesiophyceae and the Chrysophyceae both of which had maximum values of 70% relative hybridisation.



These two major classes showed a strikingly complementary distribution (Fig. 3.6). Prymnesiophyceae had highest values in the northern gyre and lowest values in the southern gyre whereas Chrysophyceae had highest values in the northern temperate region and in the southern gyre, and very low values in the northern gyre. Both of these major classes showed decline in abundance below the depth corresponding to 14% light intensity, reflecting the position of the thermocline (Fig. 3.3).

The relative hybridisation values for the other classes were considerably lower. In one sample, Cryptophyceae reached a peak abundance of 23% relative hybridisation, at 0.1% light intensity at an upwelling station around 20°N. However, for the rest of the transect, relative hybridisation values for the Cryptophyceae values remained below 10%. Pelagophyceae reached 22% relative hybridisation at one northern gyre station at a depth corresponding to 1% light intensity, but was below the background level for much of the transect except in the northern gyre and upwelling regions. Pinguiphyceae, Trebouxiphyceae and Eustigmatophyceae reached peak relative hybridisation values of between 2 and 15% (Fig. 3.6). In contrast to the other classes, the Trebouxiphyceae reached peak values at depths corresponding to 1% and 0.1% light intensity (Fig. 3.6).

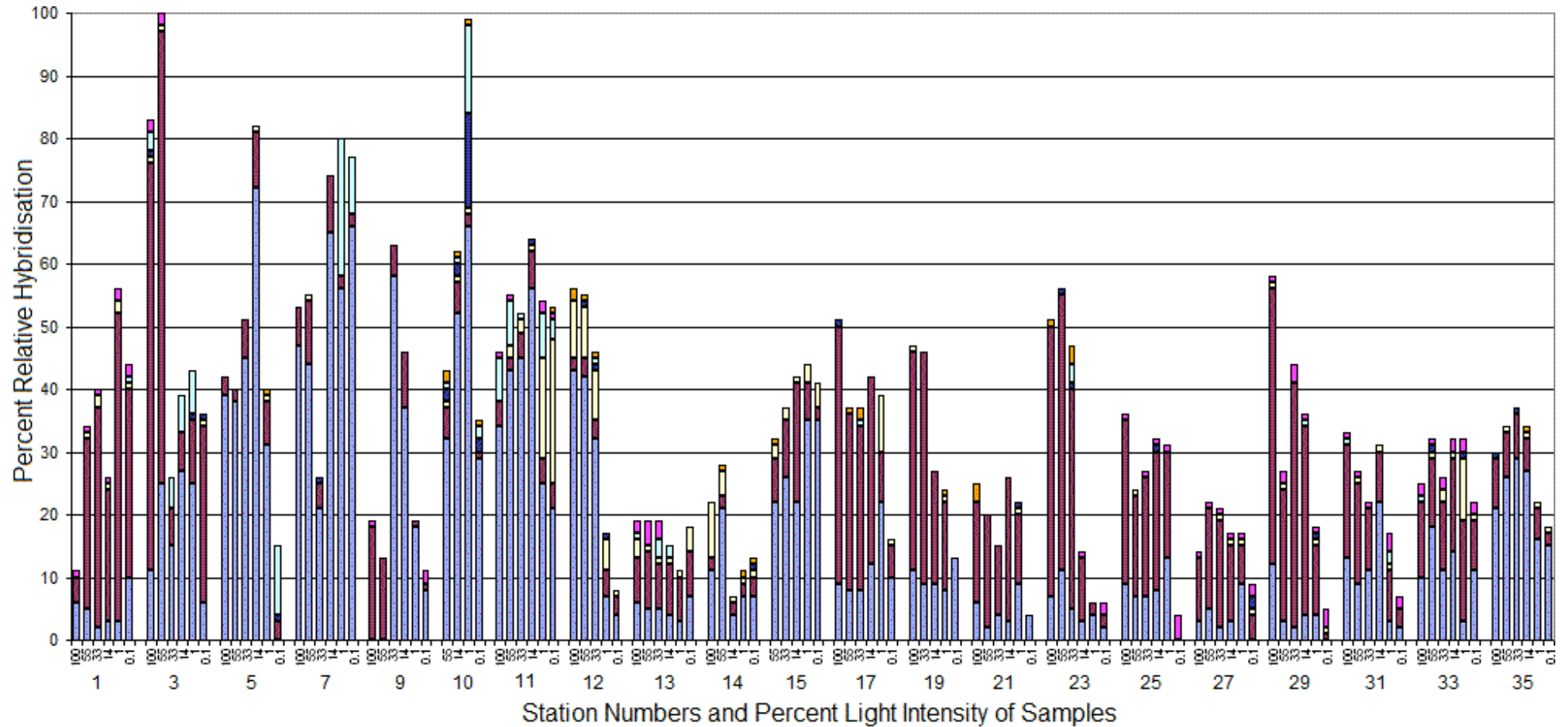


**Figure 3.5.** Histogram showing the percent relative hybridisation for probes which reached above 2% relative hybridisation along AMT15, targeting the Prymnesiophyceae (■), Chrysophyceae (■), Cryptophyceae (□), Eustigmatophyceae (■), Pelagophyceae (□), Trebouxiophyceae (■) and Pinguiohyceae (■) for each station and depth analysed.

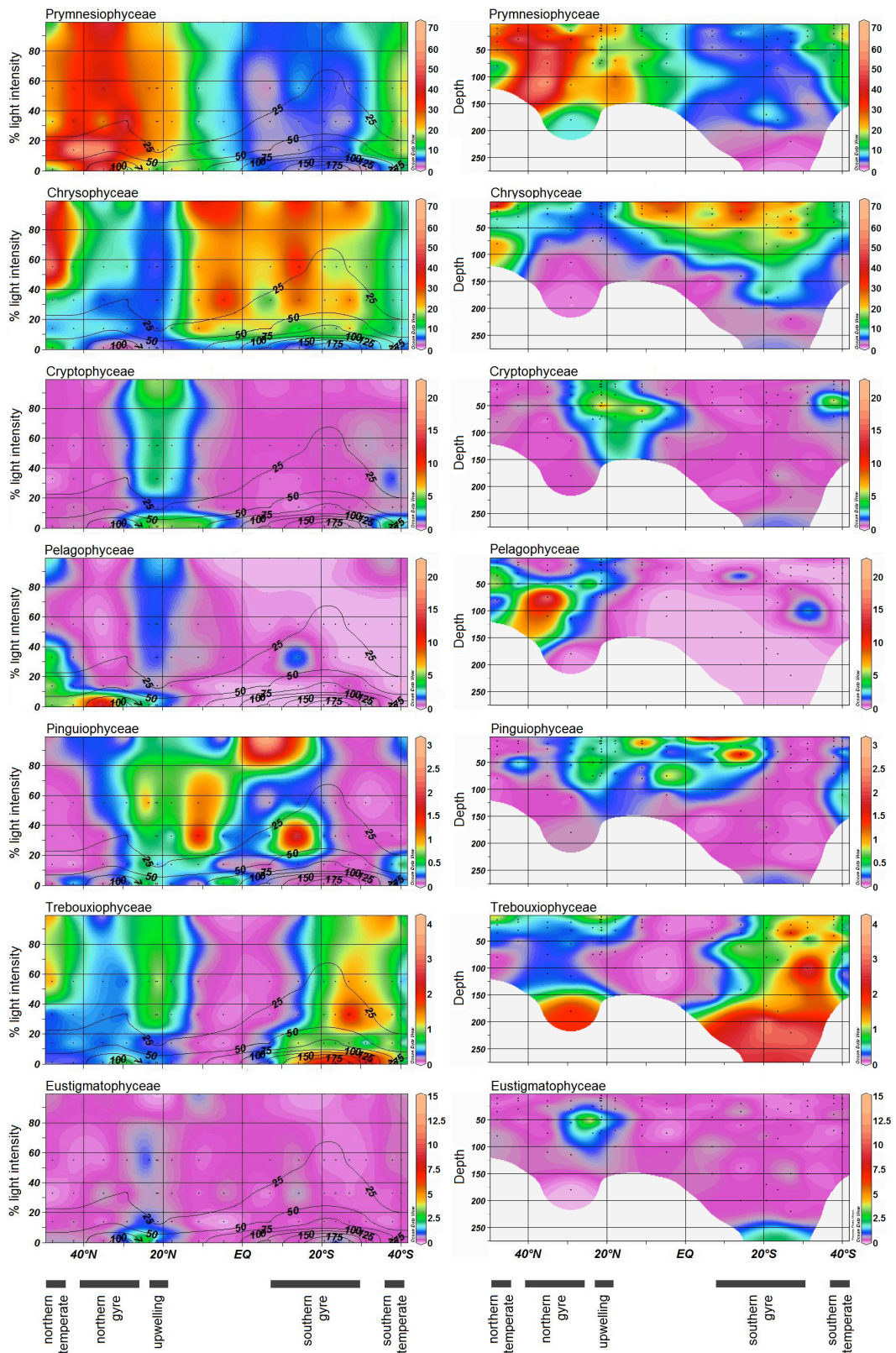


**Figure 3.6.** Contour plots of dot blot hybridisation data showing the distribution patterns of PPE classes along the AMT15 track. Colour represents the percent relative hybridisation (as a proportion of amplicons produced from primers PLA491F and OXY1313R, Fuller *et al.*, 2006b). Left panels: y-axis shows light intensity (% surface irradiance); right panels y-axis shows depth into water column.

Canonical Correspondence analysis (CCA) revealed that up to 48% of the variation in the dot blot hybridisation data could be explained by the environmental parameters considered: chemical i.e. nitrate, nitrite, phosphate, silicate and dissolved oxygen concentrations and salinity; physical i.e. temperature, depth, light intensity and density; and biological i.e. chlorophyll *a* concentration and the abundances of photosynthetic eukaryotes, *Synechococcus* and *Prochlorococcus*. The amount of variation explained by each of these groups of parameters is illustrated in the Venn diagram presented in Fig. 3.7. Chemical parameters appear to explain more of the differences in PPE class distribution patterns as indicated by dot blot hybridisations, with this group of variables able to explain up to 28% of the variation, whilst physical variables can explain up to 10% and biological variables up to 11% of the total variation in dot blot hybridisation data. The amount of variation explained by physical and chemical parameters overlapped by 3.5%, whereas the variation explained by biological parameters was separate from that explained by physical and chemical parameters (Fig. 3.7).

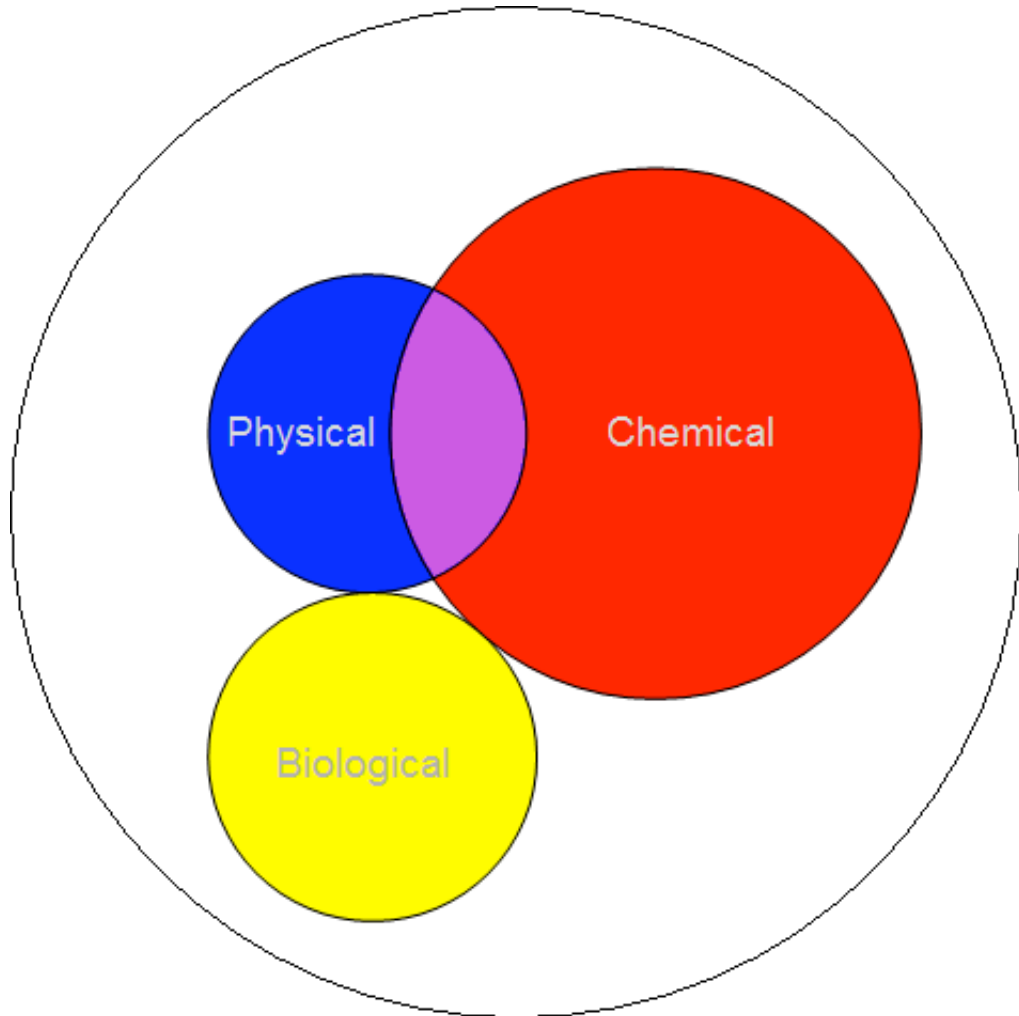


**Figure 3.7.** Venn diagram, drawn to scale by the eigenvalues calculated for the total variation in dot blot hybridisation along AMT15 (white) with the amount of variation that can be explained by physical (blue), chemical (red) and biological (yellow) parameters. These groups of parameters explain 10%, 28% and 11% of the total variation in dot blot hybridisation data. The overlap in the amount of variation explained by both physical and chemical parameters is also shown (3.5% of the total variation in dot blot hybridisation data). Physical parameters encompass light intensity, depth and temperature; chemical parameters encompass concentrations of nitrate, nitrite, phosphate, silicate, dissolved oxygen as well as salinity; biological parameters encompass chlorophyll *a* concentration and flow cytometry counts of *Prochlorococcus*, *Synechococcus* and photosynthetic eukaryotes.

Up to 44% of the variation in dot blot hybridisation data could be explained by a ten-variable model (Fig 3.8). The variables in this model consist of nitrite concentration, which was able to explain the most variation, when considered alone, at 8%; subsequent inclusion of further variables in the model increased the amount of variation in dot blot hybridisation data it explained by the following: light intensity – 4%; inclusion of temperature – 3%; abundance of photosynthetic eukaryotes – 5%;

chlorophyll *a* concentration – 3%; depth – 3%; *Synechococcus* abundance – 2%; nitrate concentration – 1%; phosphate concentration – 11%; and silicate concentration – 3%. The percentages of total variation explained by these variables are only accurate when added to the model in this order, in particular phosphate concentration had a small influence over the variation in dot blot hybridisation data in the absence of the other variables mentioned here, phosphate and nitrate concentrations explained substantially more data when considered together (9.5%) compared to the sum of each of these variables considered alone (3.5% and 2.8% respectively).

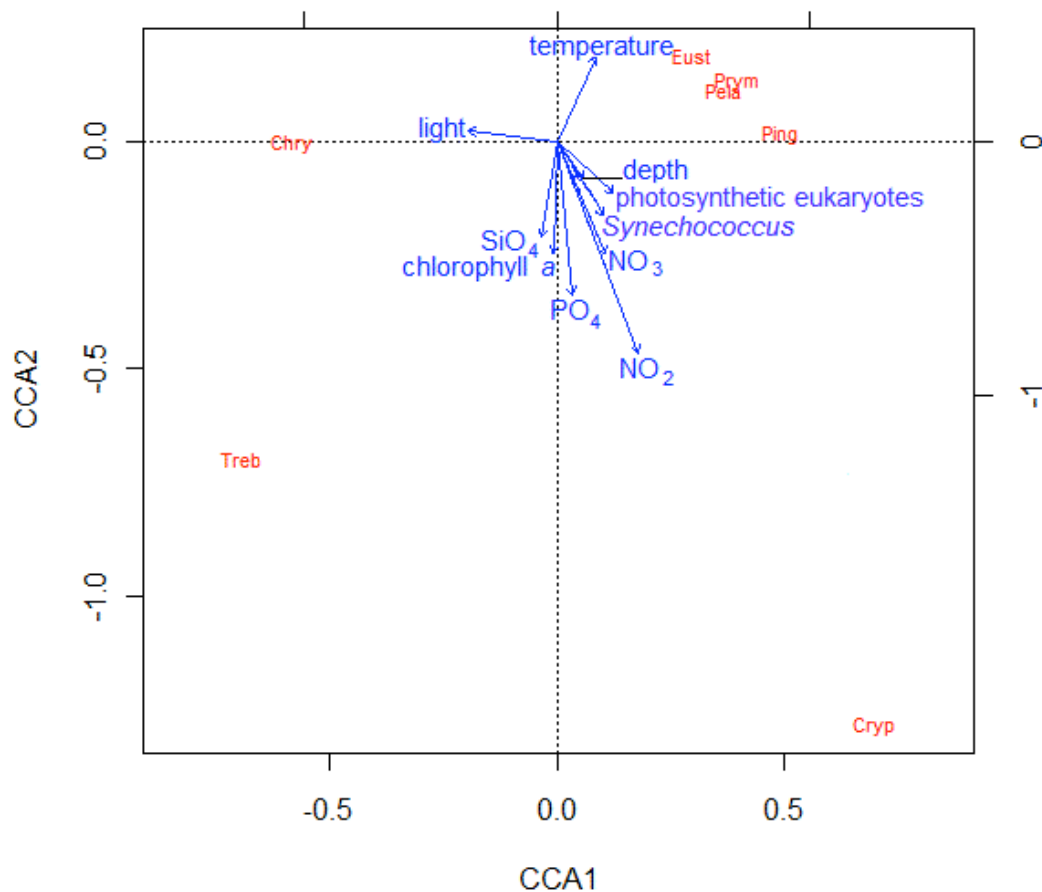


**Figure 3.8.** CCA plot for PPE class distributions along AMT15 in relation to environmental variables, from dot blot hybridisation results for classes: Prymnesiophyceae (Prym), Chrysophyceae (Chry), Cryptophyceae (Cryp), Pinguiphyceae (Ping), Pelagophyceae (Pela), Eustigmatophyceae (Eust) and Trebouxiophyceae (Treb). Axis 1 (CCA1) can explain 25% of the total variation in dot blot hybridisation data, axis 2 (CCA2) can explain a further 9%. Four additional axes (not shown) can explain a further 5, 3, 1 and 1% respectively.

The CCA shows that certain classes appear to be linked with particular environmental parameter (Fig 3.8). Where classes are observed in line with parameters they are likely to be linked to those parameters, whereas classes observed

at right angles to parameters are not linked to them. For example, Chrysophyceae appears to be linked to higher light intensities as the class is positioned close to this parameter. However, the parameters of silica, chlorophyll *a* and phosphate concentrations, as well as temperature are at right angles to the Chrysophyceae and thus are likely to have very minimal influence over the distribution of this class along AMT15. Conversely, Trebouxiophyceae is in line with temperature, but in the opposite quarter of the plot, indicating that this class is associated with low temperatures, possibly reflecting the peak in abundance of this class below the thermocline in Northern and Southern gyres.

### 3.2.4. A comparison of 16S and 18S rRNA clone libraries

#### 3.2.4.1. Representation of classes in clone libraries

Clone libraries were constructed for four stations in four distinct regions of the transect: the northern temperate, upwelling, southern gyre and southern temperate regions (Fig. 3.2, Table 3.1) using PCR products amplified with the general eukaryotic primers 7F and 1534R (Moon van der Staay *et al.*, 2001) targeting part of the nuclear SSU rRNA gene; and with algal plastid biased primers PLA491F (Fuller *et al.*, 2006b) and OXY1313R (West *et al.*, 2001). Clone libraries were analysed by restriction fragment length polymorphism (RFLP), and members representing each RFLP type were sequenced. The RFLP types representing potential PPEs (as opposed to heterotrophs or cyanobacteria) in the plastid 16S rRNA and nuclear 18S rRNA gene libraries are shown in Tables 3.2 and 3.3 respectively.

**Table 3.1.** Summary of clone libraries constructed with nuclear SSU rRNA and plastid 16S rRNA gene amplicons for stations 1, 15, 27 and 33 along AMT15.

Region	Station	Light intensity	Depth	No. clones analysed by RFLP (inc/excl chimeras)	
				18S rRNA library	16S rRNA library
Northern temperate	1	55%	10m	213 / 206	181 / 177
Upwelling	15	55%	10m	204 / 181	50
Southern gyre	27	55%	30m	119 / 106	50
Southern temperate	33	55%	5m	212 / 208	211 / 210

**Table 3.2.** Approximate fragment lengths of potentially photosynthetic classes from RFLP analysis of 18S SSU rRNA gene libraries from AMT15. Lengths are measured from sequence data with *in silico* analysis and by eye when visualised by agarose gel electrophoresis (see chapter 2).

<b>Class</b>	<b>Approximate fragment lengths (bp)</b>										
Bacillariophyceae	626	330	204	180	168	151	89	44	8		
Chlorarachniophyceae	474	443	382	253	173	75					
Chrysophyceae	492	451	340	295	179	43					
Chrysophyceae	594	345	325	212							
Chrysophyceae	492	450	341	338	179						
Chrysophyceae	494	423	312	296	221						
Chrysophyceae	490	451	370	179	168	142					
Chrysophyceae	821	492	450	433	242	179					
Chrysophyceae	492	450	367	269	179	43					
Cryptophyceae	451	316	305	256	177	100	63	53	47	32	
Dictyochophyceae	592	324	298	252	226	65	35	8			
Prasinophyceae	722	294	221	175	100	76	65	51	46	43	7
Prasinophyceae	612	329	323	314	100	76	46				
Prasinophyceae	612	323	320	260	176	63	46				
Prasinophyceae	937	269	186	176	123	63	46				
Prasinophyceae	612	423	304	239	100	76	46				
Prasinophyceae	625	612	284	100	76	57	46				
Prasinophyceae	937	325	312								
Prasinophyceae	620	323	320	315	176	46					
Prasinophyceae	594	478	302	283	258	33					
Prasinophyceae	501	377	332	292	178	66	54				
Prasinophyceae	612	535	325	212	98						
Prasinophyceae	937	345	325								
Prasinophyceae	566	376	355	283	94	84	42				
Prasinophyceae	633	351	271	176	155	151	63				
Prymnesiophyceae	630	312	274	193	178	133	63	17			
Prymnesiophyceae	504	479	345	180	162	66	64				
Prymnesiophyceae	942	331	215	178	134						
Prymnesiophyceae	612	350	341								



**Table 3.3.** Approximate fragment lengths of potentially photosynthetic classes from RFLP analysis of 16S SSU rRNA gene libraries from AMT15. Lengths are measured from sequence data with *in silico* analysis and by eye when visualised on gel.

Class	Approximate fragment lengths					
Chrysophyceae	278	103	187	254		
Chrysophyceae	280	103	188	251		
Chrysophyceae	275	150	130	115	110	40
Cryptophyceae	82	312	187	65	176	
Cryptophyceae	81	312	187	65	177	
Dictyochophyceae	105	200	78	187	251	
Dictyochophyceae	384	188	250			
Dictyochophyceae	312	255	157	56	42	
Dinophyceae	395	312	115			
Dinophyceae	490	230	60	42		
Dinophyceae	352	470				
Eustigmatophyceae	449	373				
Pelagophyceae	453	369				
Prasinophyceae	822					
Prasinophyceae	90	89	643			
Prasinophyceae	575	65	49	133		
Prasinophyceae	580	275				
Prymnesiophyceae	480	290	52			
Prymnesiophyceae	375	402	45			
Prymnesiophyceae	436	289	97			
Prymnesiophyceae	111	330	381			
Prymnesiophyceae	320	78	424			
Prymnesiophyceae	352	391	79			
Prymnesiophyceae	102	289	181	250		
Prymnesiophyceae	310	423	89			
Prymnesiophyceae	420	400				
Prymnesiophyceae	394	387	67			

The representation of classes in clone libraries, as assigned by BLAST and alignment in ARB, are illustrated in Fig. 3.9. 18S rRNA gene clone libraries revealed a greater number of different classes than the 16S rRNA clone libraries. However, most of these extra ‘classes’ belonged to heterotrophic lineages. As a result, the 16S rRNA gene clone libraries had higher coverage values and their rarefaction curves (Fig. 3.10) reached a plateau whereas those of 18S rRNA gene clone libraries did not, and as such would require analysis of a much greater number of clones to reveal the full extent of diversity in the libraries. The 18S rRNA gene clone libraries’ coverage values were 72, 55, 69 and 69% for the northern temperate, upwelling, southern gyre

and southern temperate libraries respectively, whereas the 16S rRNA clone libraries had coverage values of 89, 89, 94 and 90% for these sites.

The 18S rRNA gene clone libraries were highly dominated by heterotrophic alveolates, with 50, 67, 72 and 80% of clones in the northern temperate, upwelling, southern gyre and southern temperate libraries respectively. Of these, approximately 90% fell within the Syndiniales, parasites of the dinophyceae. These sequences have been extensively explored together with Syndiniales sequences from a range of other environments and the work subsequently published (see Guillou *et al.*, 2008). Other heterotrophic groups identified include labyrinthulida, pirsonia, bicosoecida, acantharea, taxapodida, polycystinea, apusozoa and metazoa.

Potentially photosynthetic classes accounted for only 11-33% of the clones in the 18S rRNA libraries. Of these, the most important classes appeared to be Prasinophyceae, Prymnesiophyceae and Chrysophyceae, which were present in all 18S rRNA gene libraries. Further photosynthetic classes were found more sporadically: one Dictyochophyceae clone was in the northern temperate library, one Cryptophyceae clone and two Chlorarachniophyceae clones were present in the upwelling library, one Chlorarachniophyceae and four Bacillariophyceae clones were found in the southern temperate library.

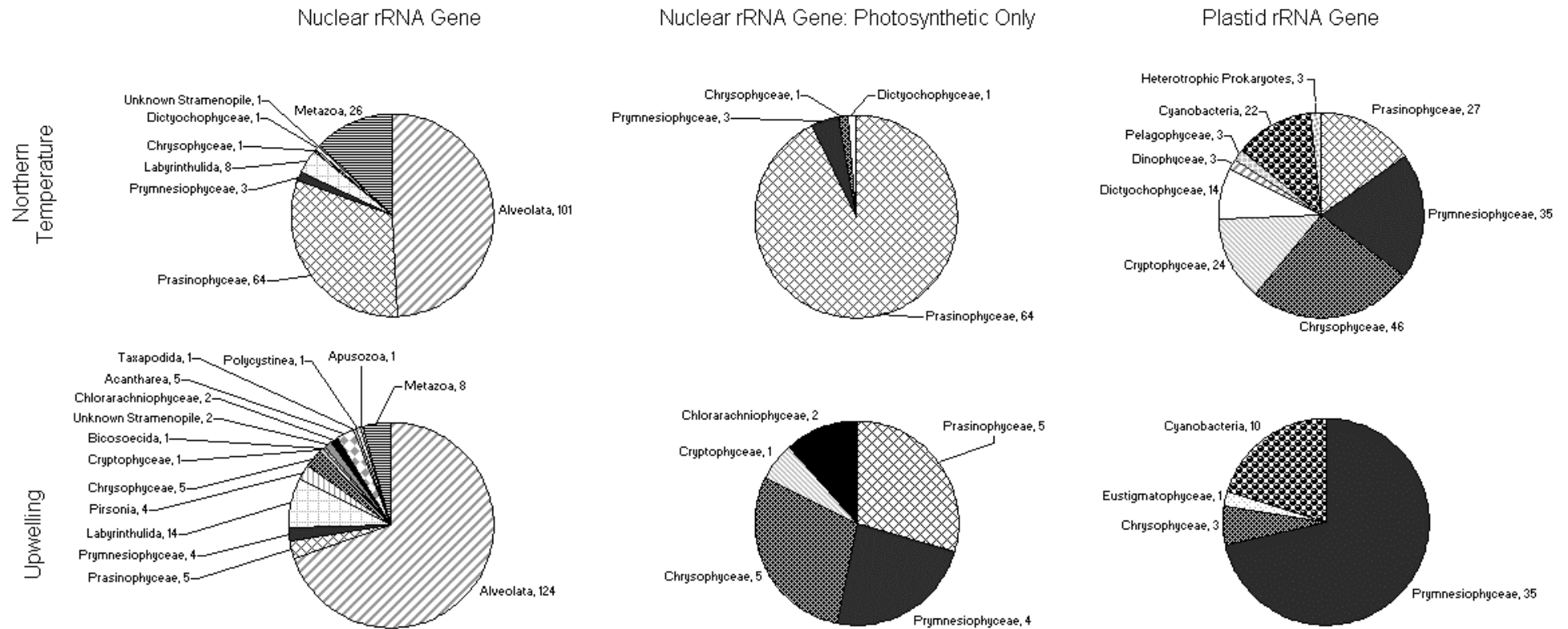


**Figure 3.9.** Pie-charts representing the proportion of clones assigned to different classes in clone libraries constructed for samples from AMT15 by RFLP analysis and BLAST and ARB alignments for representative sequences. Total results for 18S rRNA gene clone libraries are shown on the right, the results from potentially photosynthetic classes are shown in the middle and results for the 16S rRNA gene libraries are shown on the left. The pie-charts are annotated with the class and the number of clones assigned to each class. Continued next page.

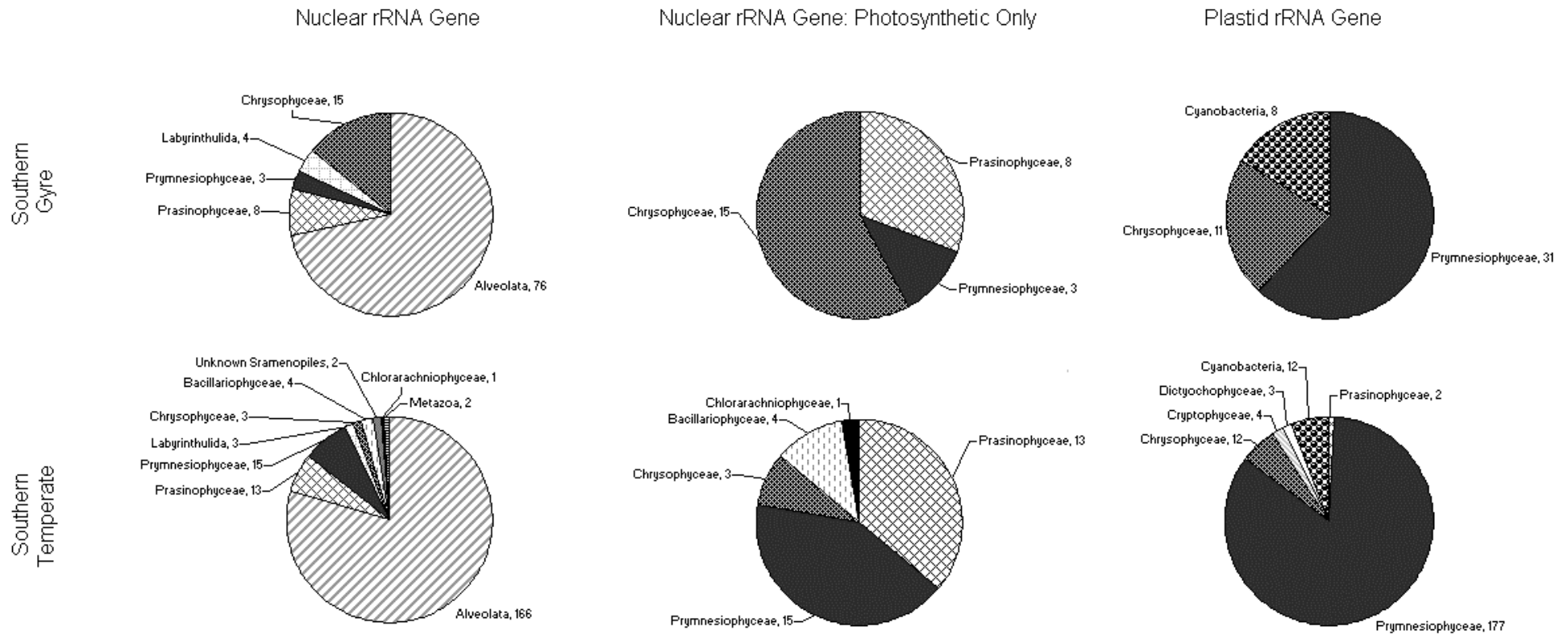
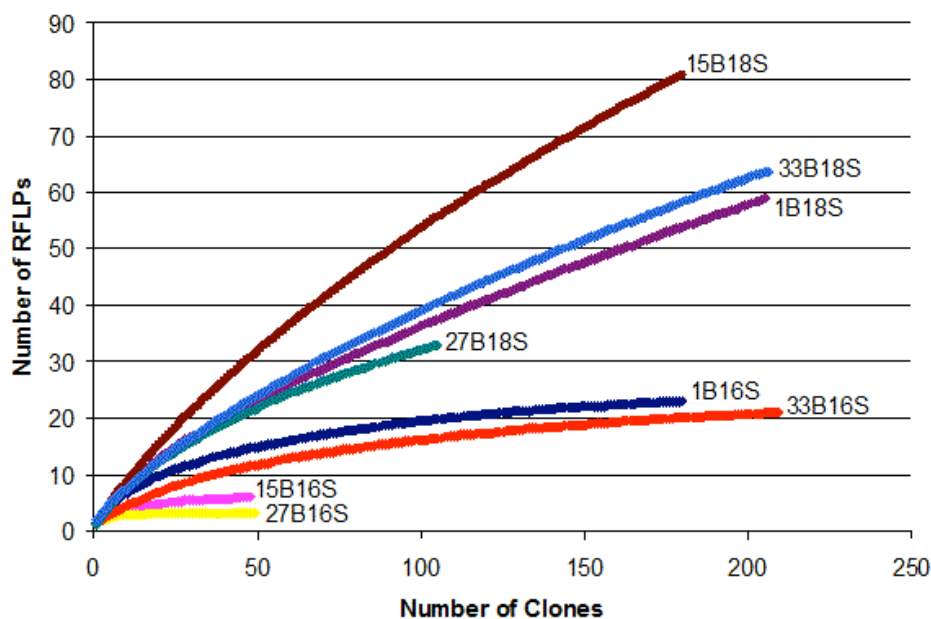


Figure 3.9. Continued.

**Table 3.4.** Number of RFLP types, and clones in brackets, identified within each algal class observed in the plastid 16S and nuclear SSU rRNA gene clone libraries from AMT15. 1B refers to libraries constructed from sample 1B collected from the northern temperate region; 15B refers to libraries from sample 15B from the Mauritanian upwelling; 27B refers to libraries from sample 27B from the southern gyre; and 33B refers to libraries from sample 33B from the northern temperate region.

Class	Number of RFLP types (clones) in each library							
	1B Plastid	1B Nuclear	15B Plastid	15B Nuclear	27B Plastid	27B Nuclear	33B Plastid	33B Nuclear
Prasinophyceae	3 (27)	15 (64)	-	3 (5)	-	2 (8)	1 (2)	8 (13)
Prymnesiophyceae	5 (35)	1 (3)	3 (35)	2 (4)	1 (31)	1 (3)	11 (177)	3 (15)
Chrysophyceae	2 (46)	1 (1)	1 (3)	2 (5)	1 (11)	4 (15)	3 (12)	2 (3)
Cryptophyceae	3 (24)	-	-	1 (1)	-	-	1 (4)	-
Dictyochophyceae	3 (14)	1 (1)	-	-	-	-	3 (2)	-
Eustigmatophyceae	-	-	1(1)	-	-	-	-	-
Dinophyceae	1 (3)	-	-	-	-	-	-	-
Pelagophyceae	1 (3)	-	-	-	-	-	-	-
Chlorarachniophyceae	-	-	-	2 (2)	-	-	-	1 (1)
Bacillariophyceae	-	-	-	-	-	-	-	1 (4)



**Figure 3.10.** Rarefaction curves for clone libraries constructed for samples from AMT15, from nuclear 18S and plastid 16S rRNA gene fragments from the northern temperate region (station 1) (1B18S and 1B16S respectively), upwelling region (station 15 – 15B18S and 15S16S), southern gyre (station 27 – 27B18S and 27B16S) and southern temperate (station 33 – 33B18S and 33B16S).

Slightly more photosynthetic classes were observed in 16S rRNA gene clone libraries, though these were largely dominated by Prymnesiophyceae clones, except for the northern temperate library which was not dominated by a particular class, but contained a range of classes represented with relative parity. Sequences related to the Chrysophyceae were detected in all of these libraries, accounting for between 4 and 34% of clones. Sequences relating to the Prasinophyceae accounted for 12% of clones in the northern temperate library, less than 1% in the southern temperate library (2 clones out of 210) and were absent from the upwelling and southern gyre libraries.

Less abundant PPE classes included 24 and 4 clones related to the Cryptophyceae and 14 and 1 clones related to the Dictyochophyceae in the northern and southern temperate libraries, respectively; 6 Dinophyceae- and 2 Pelagophyceae-related clones in the northern temperate library; and 1 Eustigmatophyceae-related clone in the upwelling library. Non-PPE clones (cyanobacteria, and heterotrophic bacteria) were also a minor part of the libraries, accounting for between 5 and 20% of clones.

Despite containing fewer photosynthetic classes, the nuclear 18S rRNA gene libraries contained clones related to photosynthetic classes Chlorarachniophyceae

and Bacilariophyceae which were absent in the plastid 16S rRNA gene clone libraries.

#### 3.2.4.2. Phylogenetic relatedness of sequences from clone libraries

The construction of phylogenetic trees revealed more within-class variation of PPE sequences in the 16S rRNA gene libraries than the 18S rRNA gene libraries. Many of the lineages apparent only in the plastid 16S rRNA gene libraries appear to be of novel (uncultured) lineages in many of the major classes.

Phylogenetic relationships amongst the Prymnesiophyceae (Figs. 3.11 and 3.12 for nuclear 18S and plastid 16S rRNA gene sequences, respectively) revealed sequences relating to *Chrysochromulina* sp. in both the 18S and 16S rRNA gene phylogenies. The nuclear SSU rRNA phylogeny shows a lineage at the base of the tree containing no sequences from described or cultured species. The plastid SSU rRNA gene tree has a lineage indicated between the cluster containing *Phaeocystis* sp. and the cluster containing *Emiliania huxleyi* and *Ochromonas* sp.

Phylogenetic relationships amongst the Chrysophyceae (Figs. 3.13 and 3.14) revealed the presence of heterotrophic sequences related to *Paraphysomonas* (nuclear sequences) or sequences whose closest cultured counterpart was *Hibberdia magna* or *Ochromonas* sp. However, particularly the plastid 16S rRNA environmental sequences clustered largely separately from these cultured representatives, which have all been isolated from freshwater environments.

Prasinophyceae-related sequences were present in all 18S rRNA libraries (Fig. 3.15), but were only seen in the plastid northern and southern temperate libraries (Fig. 3.16). Sequences from the plastid 16S rRNA northern temperate library fall within the *Micromonas* lineage of prasinophyte clade II, whilst another sequence, representing two clones, clusters within an extensive lineage containing no cultured representatives referred to as Pras16S-VIII (Lepère *et al.*, 2009). Many 18S rRNA gene sequences fell within a lineage containing no cultured representatives referred to as clade IX (Viprey *et al.*, 2008), which may represent the nuclear gene 'equivalent' of this plastid Pras16S-VIII clade.

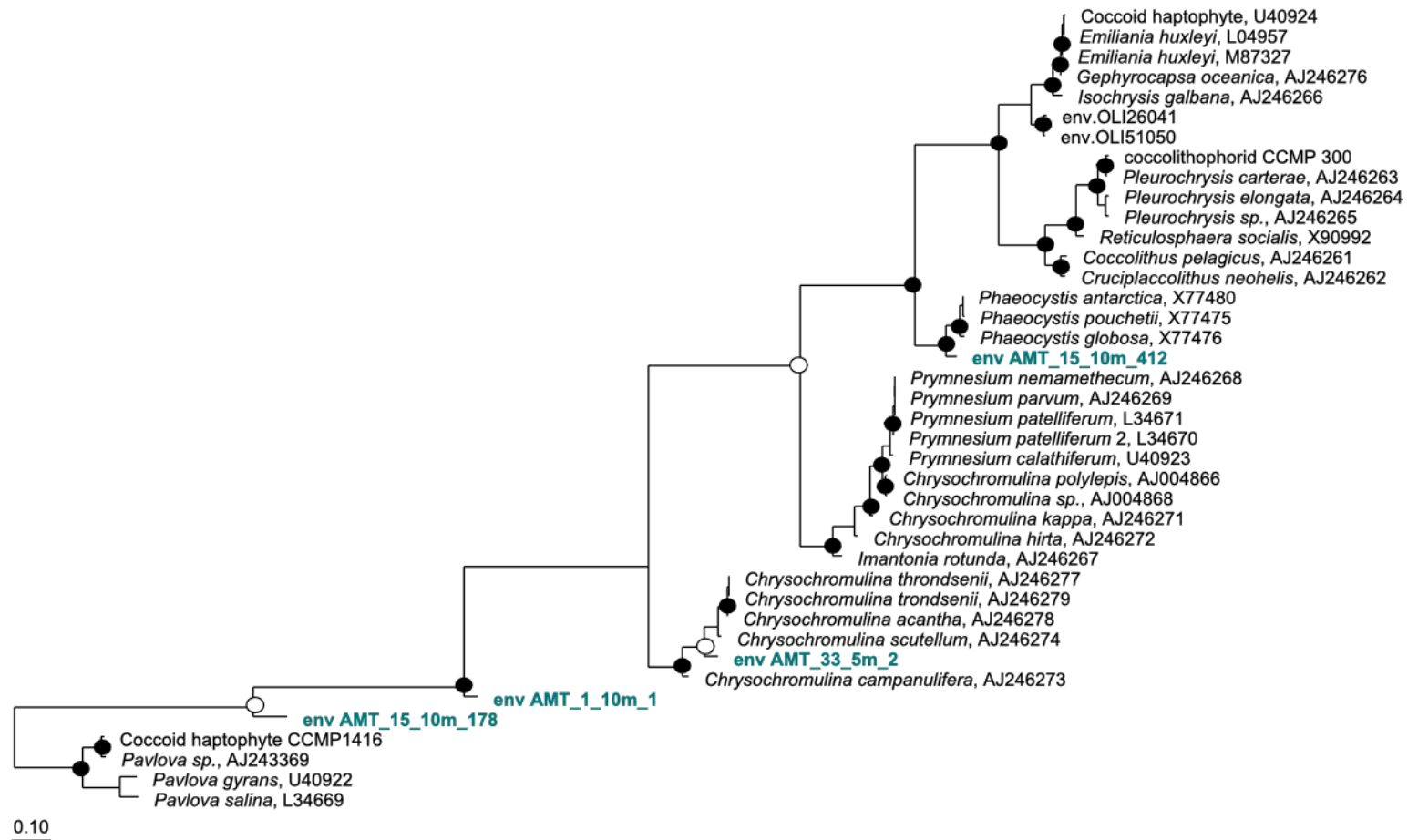


**Figure 3.11.** Phylogenetic relationships amongst the Prymnesiophyceae using nuclear 18S rRNA gene sequences and a neighbour-joining algorithm. Environmental sequences are approximately 1600 nucleotides long and added by ARB parsimony, without a filter. Bootstrap analysis was performed with ARB parsimony method (Ludwig *et al.*, 2004) values above 70% are marked with an open circle, values above 90% are marked with a filled circle. Environmental sequences from AMT15 are indicated in blue.



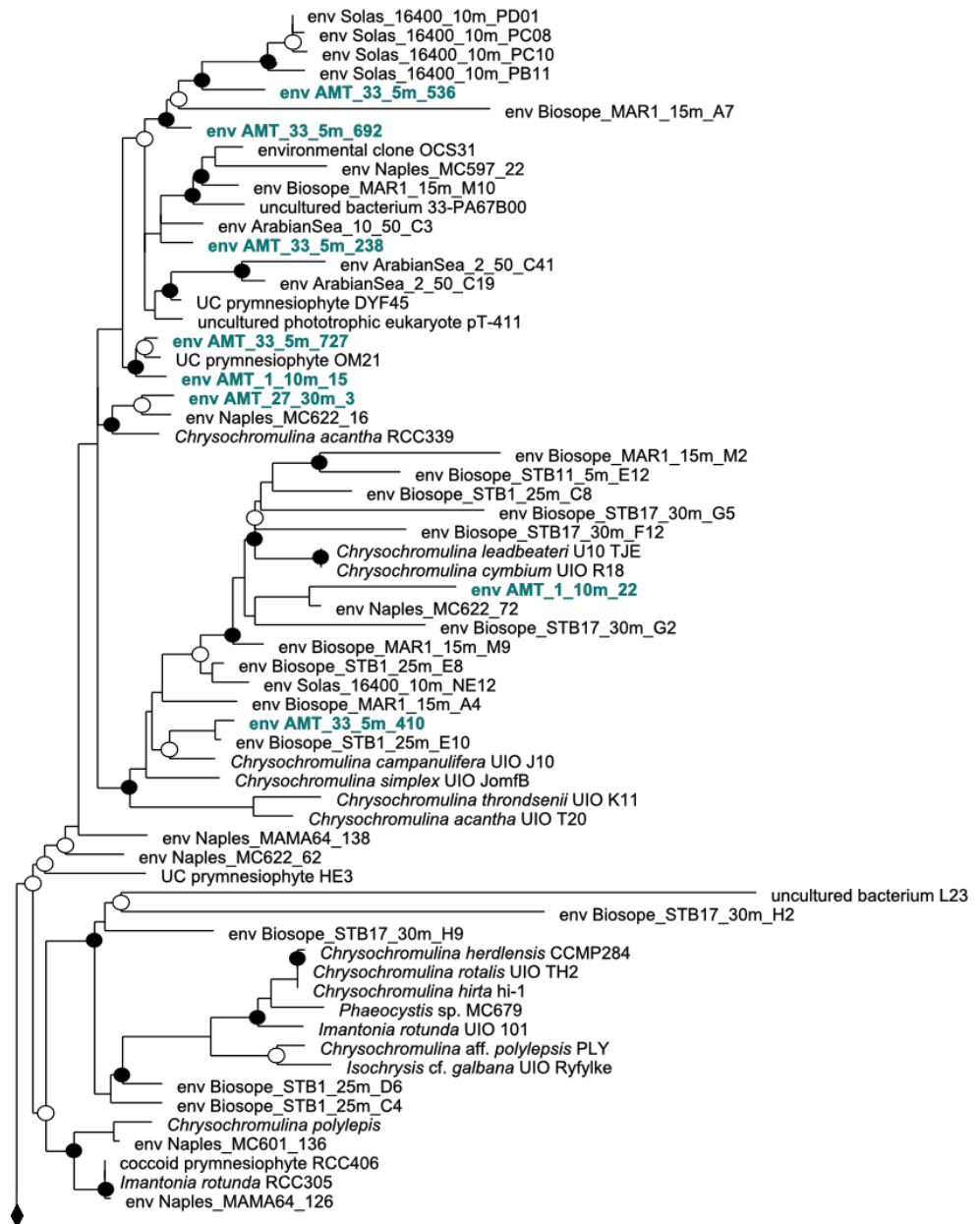


**Figure 3.12.** Phylogenetic relationships amongst the Prymnesiophyceae using plastid 16S rRNA gene sequences and a neighbour-joining algorithm. Environmental sequences are 600-800 nucleotides long and have been added to the tree by parsimony using a maximum frequency filter for plastids. Environmental sequences from AMT15 are indicated in blue. Bootstrap values above 70% are marked with an open circle, values above 90% are marked with a filled circle. Continued next page.

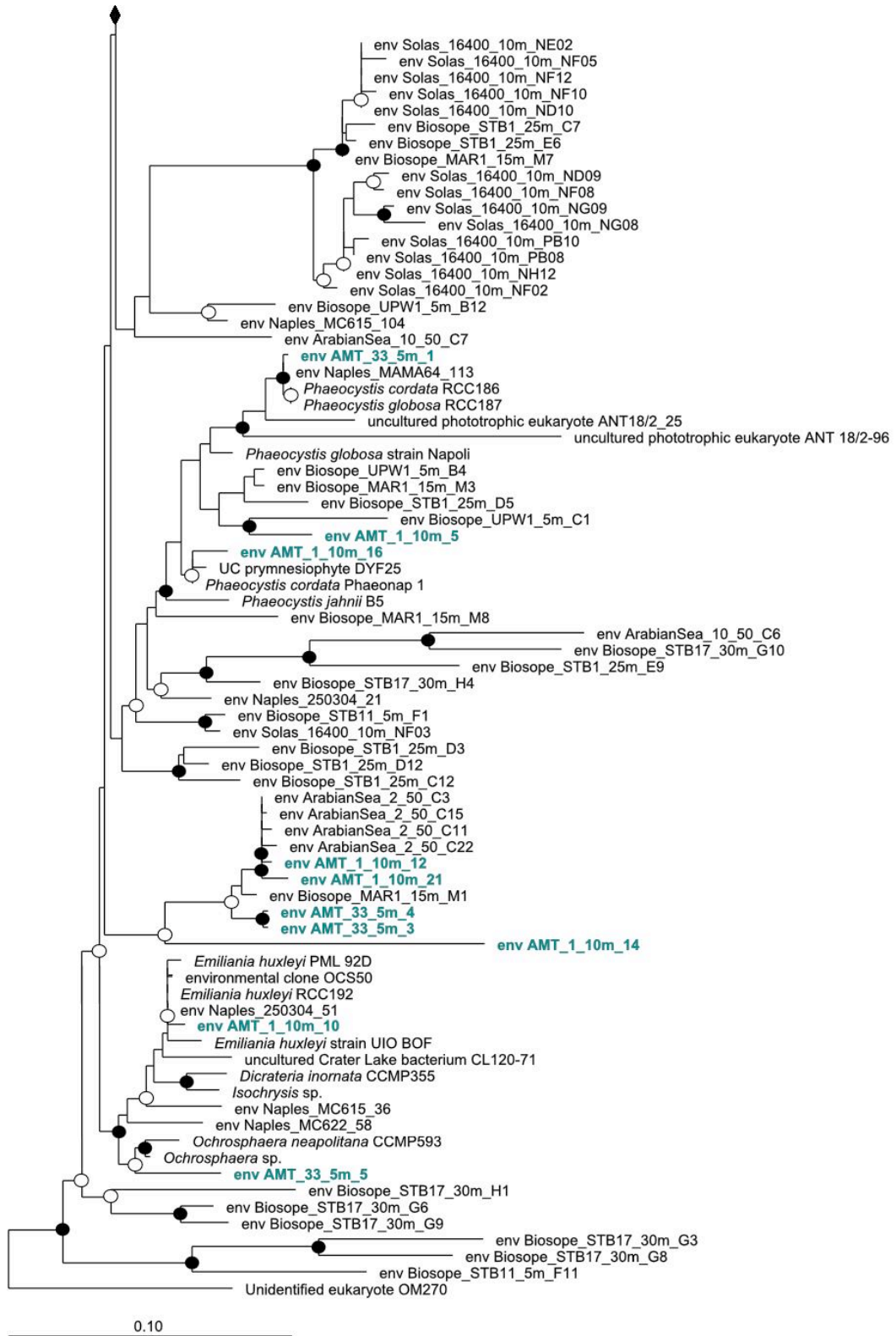
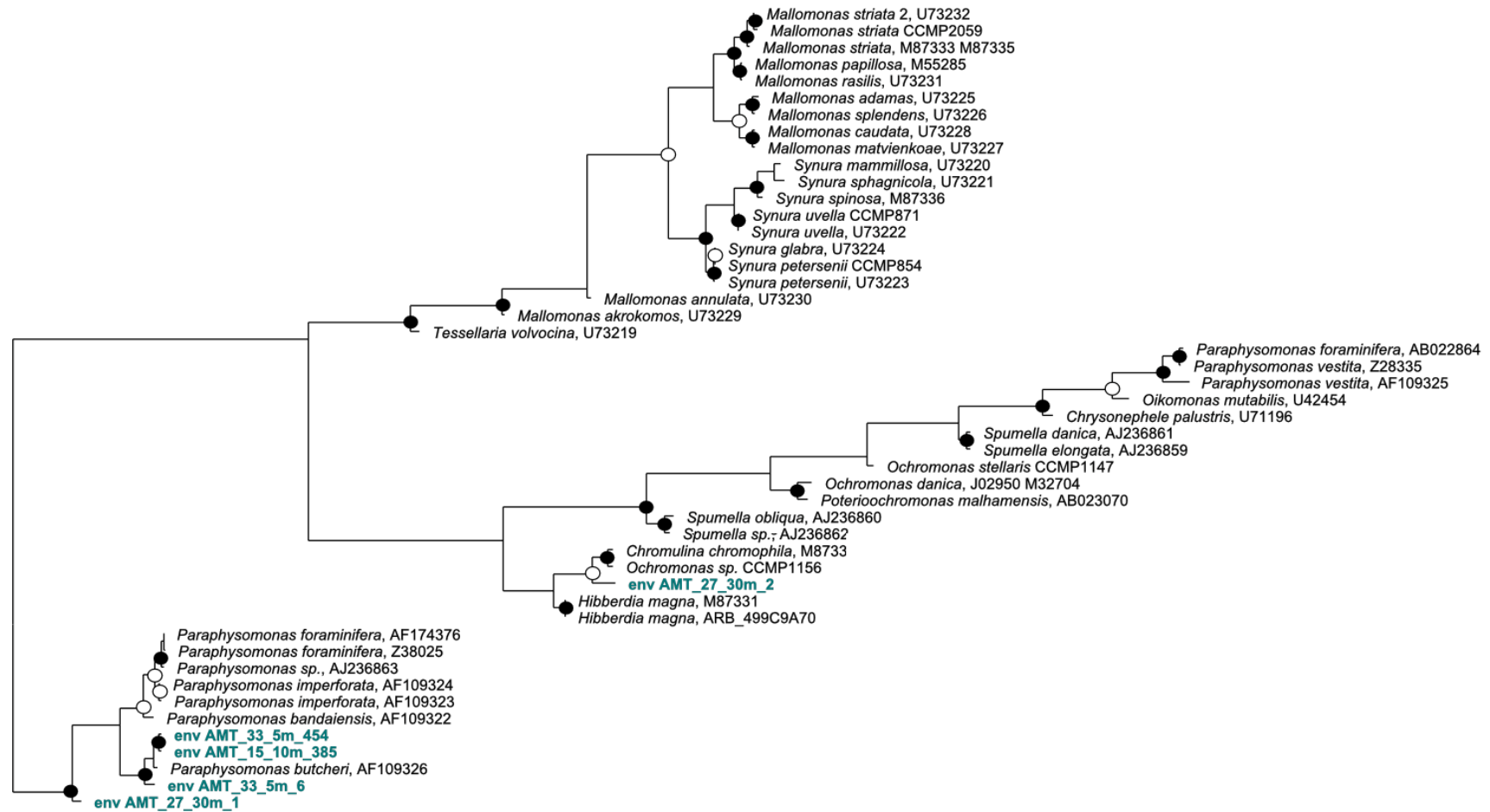
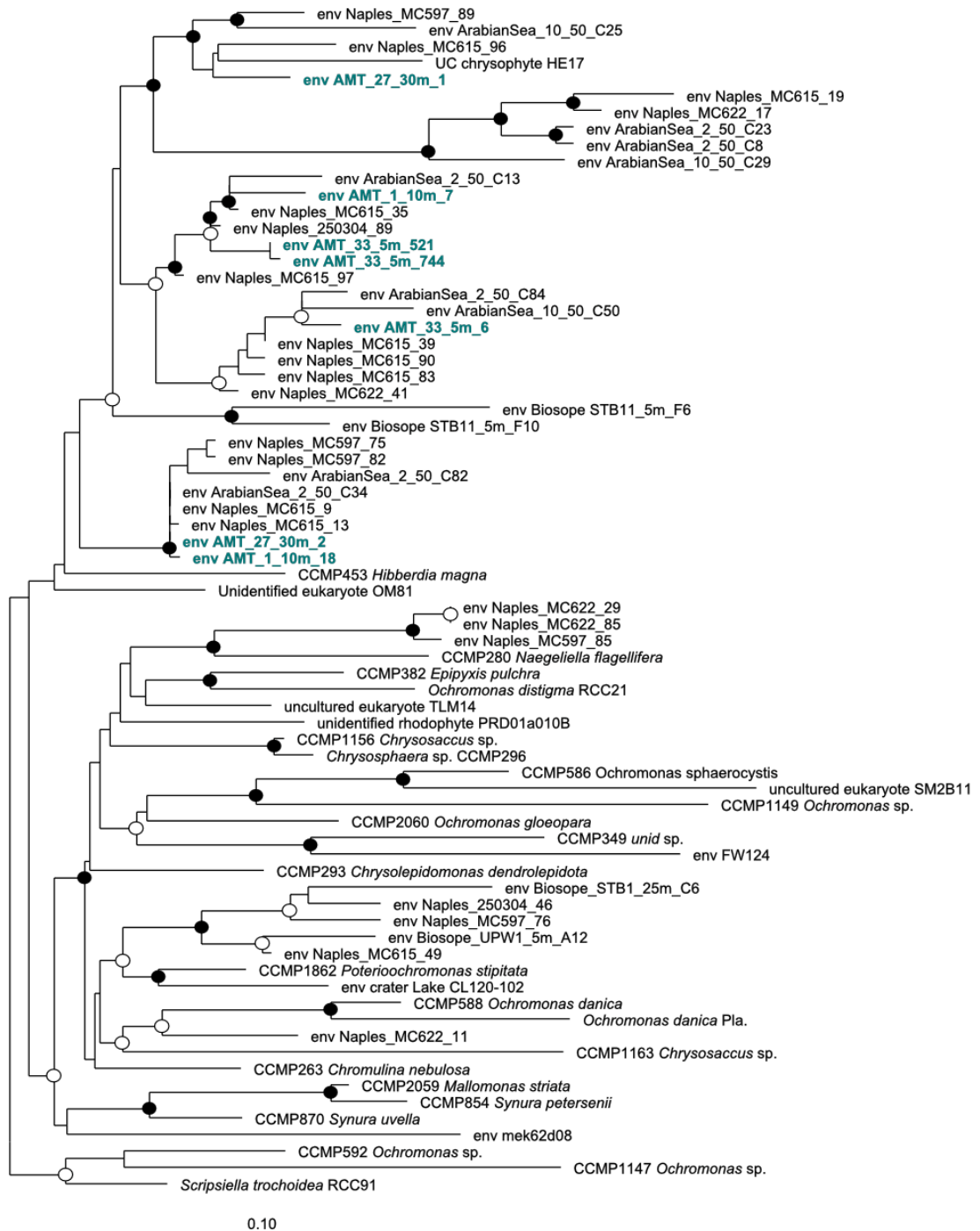


Figure 3.12. Continued



0.10

**Figure 3.13.** Phylogenetic relationships amongst the Chrysophyceae using nuclear 18S rRNA gene sequences and a neighbour-joining algorithm. Environmental sequences from AMT15 indicated in blue. Bootstrap values above 70% are marked with an open circle, values above 90% are marked with a filled circle.



**Figure 3.14.** Phylogenetic relationships amongst the Chrysophyceae using plastid 16S rRNA gene sequences and a neighbour-joining algorithm. Environmental sequences from AMT15 are indicated in blue. Bootstrap values above 70% are marked with an open circle, values above 90% are marked with a filled circle.

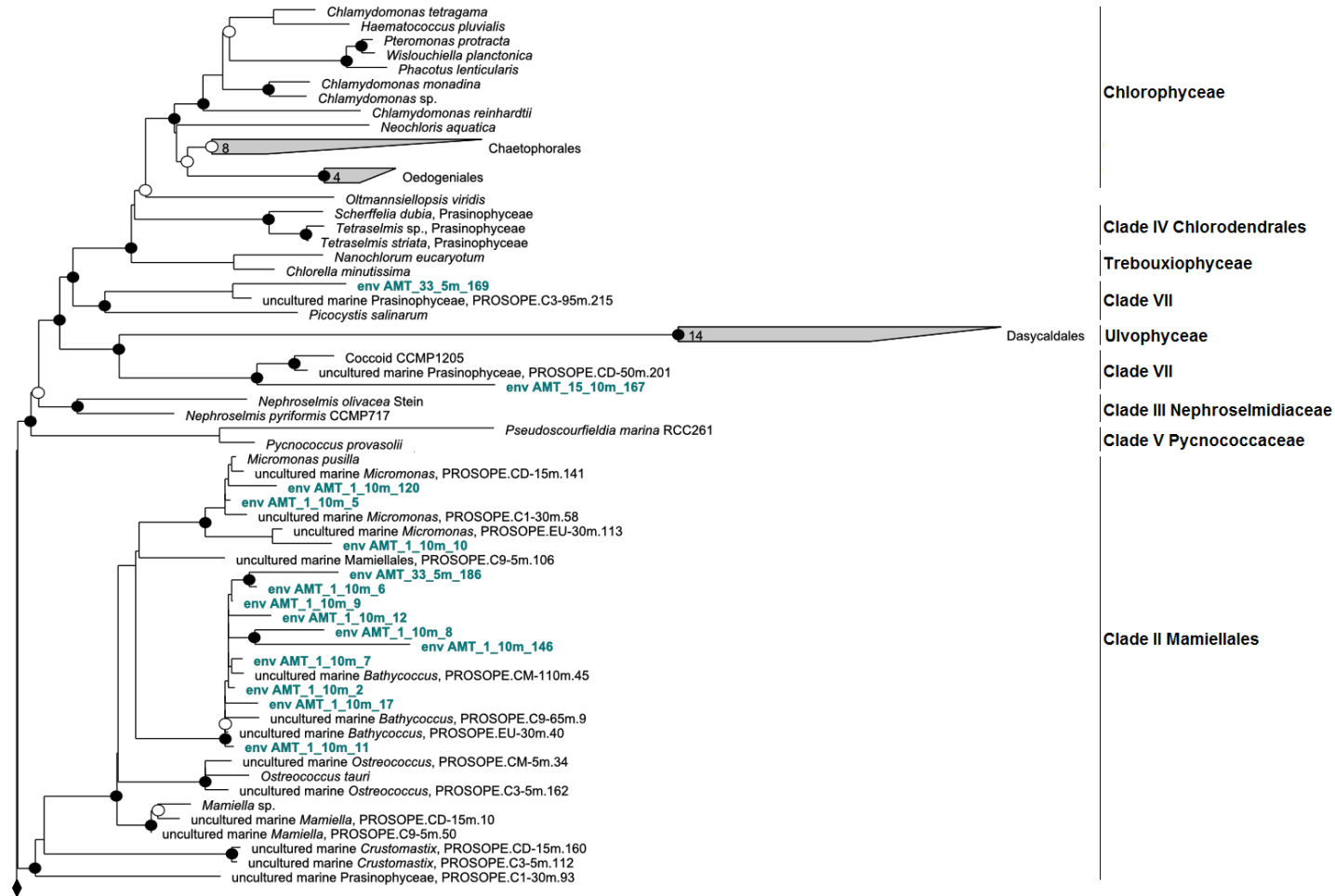


**Figure 3.15.** Phylogenetic relationships amongst the Chlorophyceae using nuclear 18S rRNA gene sequences and a neighbour-joining algorithm. Environmental sequences from AMT15 are indicated in blue. Prasinophyte clades are shown. Bootstrap values above 70% are marked with an open circle, values above 90% are marked with a filled circle. Continued next page.

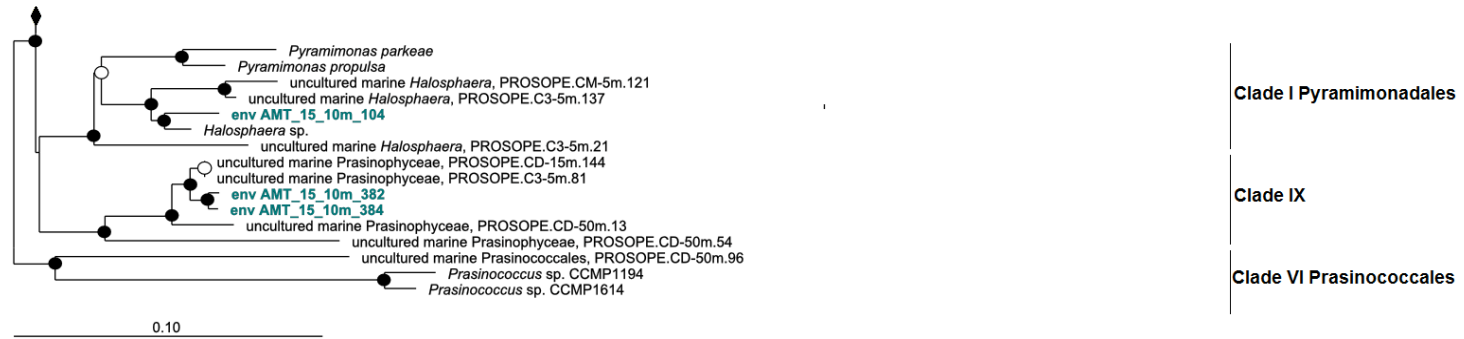


Figure 3.15. Continued.



**Figure 3.16.** Phylogenetic relationships amongst the Chlorophyceae using plastid 16S rRNA gene sequences and a neighbour-joining algorithm. Environmental sequences from AMT15 are indicated in blue. Prasinophyte clades are shown. Bootstrap values above 70% are marked with an open circle, values above 90% are marked with a filled circle. Continued next page.

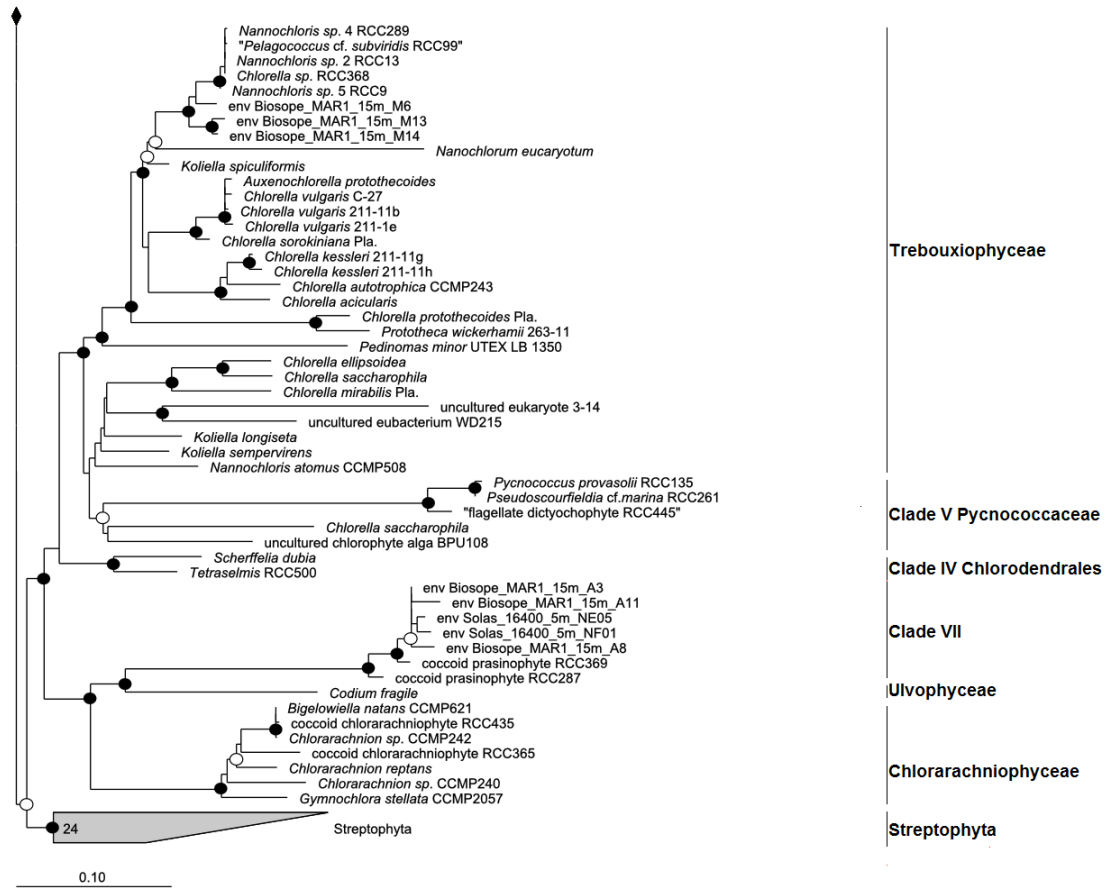
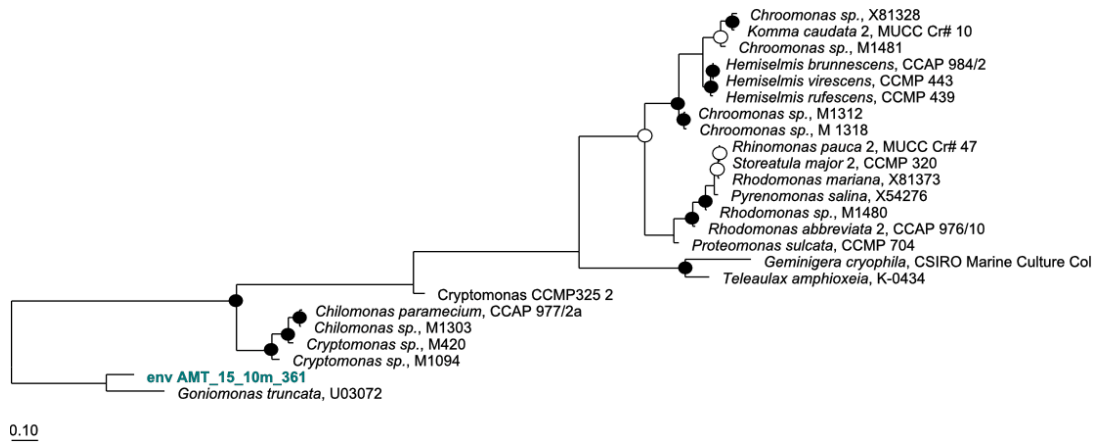


Figure 3.16. Continued.

The Cryptophyceae-related sequence found in the upwelling nuclear 18S rRNA gene library clustered fairly basally within the Cryptophyceae (Fig. 3.17), alongside *Goniomonas truncata*. There are three clearly separate branches within the Cryptophyceae plastid phylogeny (Fig. 3.18). The environmental sequences from AMT15 clustered within the lineage containing *Geminigera cryophila*, this lineage also contains sequences from cultured Dinophyceae species.





**Figure 3.17.** Phylogenetic relationships amongst the Cryptophyceae using nuclear 18S rRNA gene sequences and a neighbour-joining algorithm. Environmental sequences from AMT15 are indicated in blue. Bootstrap values above 70% are marked with an open circle, values above 90% are marked with a filled circle.

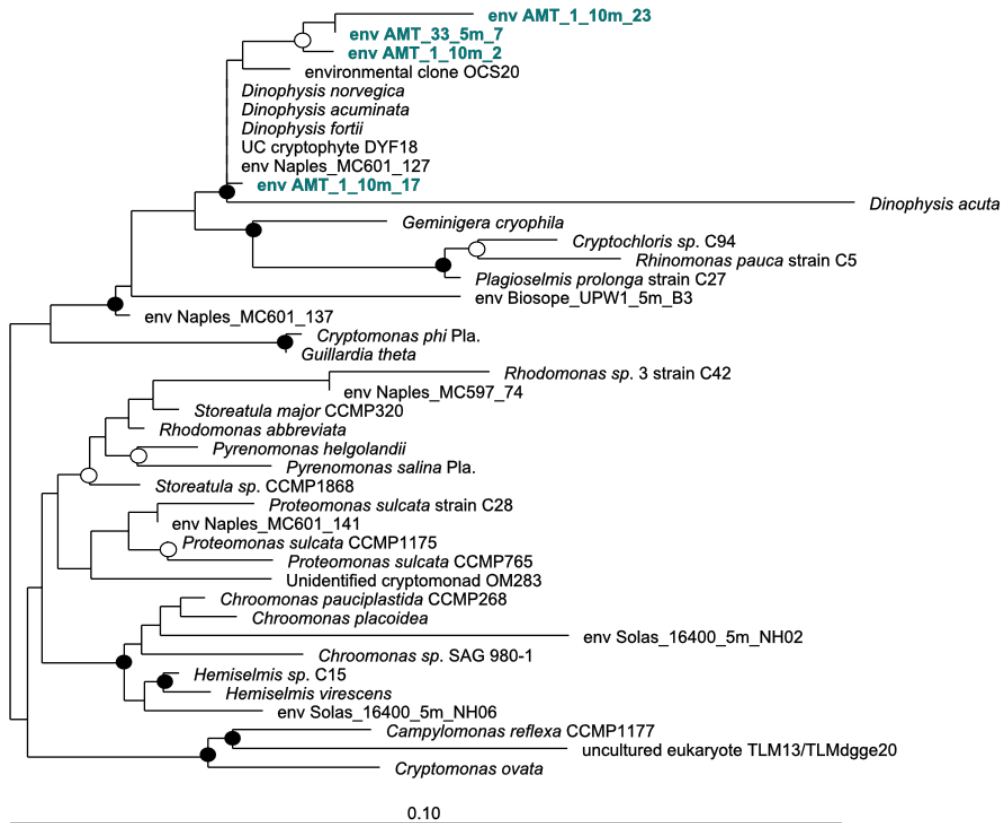


**Figure 3.18.** Phylogenetic relationships amongst the Cryptophyceae using plastid 16S rRNA gene sequences and a neighbour-joining algorithm. Environmental sequences from AMT15 are indicated in blue. Bootstrap values above 70% are marked with an open circle, values above 90% are marked with a filled circle.

Other sequences found in the AMT15 libraries included those related to the Dictyochophyceae which were present in both the nuclear and plastid libraries. A

sequence related to Bacillariophyceae, the diatom *Pseudo-nitzschia pungens*, (usually larger than 3  $\mu\text{m}$  diameter) was only present in the nuclear southern temperate library. A further sequence, representing three clones of the same RFLP type in the northern temperate plastid library clustered within the Pelagophyceae. Finally, one nuclear SSU rRNA gene sequence from the southern temperate station fell within the Chlorarachniophyceae, clustering alongside *Chlorarachnion reptans* and *Lotharella vacuolata* (data not shown). However, no Chlorarachniophyceae-related sequences were found in the plastid libraries.

### 3.3. Discussion

This chapter used various molecular approaches to target the PPE community along AMT 15. Before a detailed discussion of the observed diversity is undertaken some discussion of potential biases is appropriate. Thus, whilst filtration of samples under vacuum pressure biases samples toward the pico-sized community, it isn't possible to completely exclude organisms from the samples which are larger than 3  $\mu\text{m}$  diameter. These organisms may enter samples either in the form of broken cell matter passing through the filter, or whole cells which, though larger than 3  $\mu\text{m}$  in size, have the plasticity to pass through pores of a smaller size. The presence of a total of 36 clones related to the metazoa, particularly copepods, in nuclear SSU rRNA gene libraries, indicates this may have been the case with these samples. Conversely, a build up of larger cells clogging the 3  $\mu\text{m}$  pore-sized filter may exclude cells of the target size range.

The use of PCR to target the PPE community may also have inherent biases because some organisms amplify more readily than others due to greater primer binding efficiency. On top of this is variation in the number of copies of the target gene within the genome of a single organism. However, since the copy number of rRNA genes is directly related to the cell size of the organism (Zhu *et al.*, 2005), this is therefore likely to have only a minimal effect when studying communities of the smallest cells, as is the case here. Indeed, *Ostreococcus taurii*, a member of the PPE community, has the smallest genome of any known free-living eukaryote (Derelle *et al.*, 2006) and contains two copies of both the nuclear 18S rRNA gene and plastid 16S rRNA gene, with only a single plastid per cell. It is also likely then that, due to

their size, other PPEs also contain only one plastid per cell. Certainly, organisms containing multiple plastids would be likely to be over-represented in 16S rRNA gene libraries. However, the large number of 'heterotrophic' sequences in nuclear 18S rRNA gene libraries, particularly those affiliated to the Syndiniales, is likely to be due to higher rRNA gene copy numbers in these organisms.

Furthermore, the use of RFLP analysis on clone libraries, instead of sequencing all clones picked may mask some of the diversity present, as clones may appear to have the same fragment lengths on gels, but sequence identity may be different. Certainly the use of the term operational taxonomic units (OTUs), which usually have a 99% sequence identity, is not reliable when using RFLP screening.

With respect to the dot blot hybridisation data the fact that the sum of all relative hybridisation values corresponding to a particular sample rarely reached 100% (Fig. 3.5) indicates that sequences from other classes have likely been amplified in these samples, but were not targeted by the probes used. This is particularly notable for samples at depths corresponding to the lowest light intensity levels sampled, where photosynthetic cells may be much less abundant, as well as two of the stations in the upwelling regions (Fig 3.5). There are several known PPE classes which were not targeted by the dot blot hybridisation approach, for example the newly discovered picobiliphytes which have been found to be abundant in the extreme northern Atlantic Ocean (Hamilton *et al.*, 2008), as well as members of prasinophyte clade II and the new Pras16S-VIII clade which were relatively well presented in clone libraries. In addition, a small numbers of clones related to the Dictyochophyceae and Bacillariophyceae were also found in clone libraries, but for which no probes are currently available. Amplicons not targeted by dot blot hybridisation probes may also include non-PPE sequences such as cyanobacteria and heterotrophic bacteria which were occasionally found in the plastid gene libraries. Plastid libraries constructed from the same samples used in dot blot hybridisation thus revealed prasinophytes to be the major class which is not targeted by the majority of the dot blot probes used here (i.e. except prasinophyte clade VI), but it is unclear whether the numbers of prasinophyte sequences found in clone libraries is sufficient to explain % relative hybridisation totals of 71, 49, 45 and 51 for the northern temperate, upwelling, southern gyre and southern temperate regions respectively.

The flow cytometry data revealed that distributions of *Prochlorococcus*, *Synechococcus* and photosynthetic eukaryotes along AMT15 were very similar to those found in previous AMT studies where *Prochlorococcus* dominated the oligotrophic gyres and *Synechococcus* and photosynthetic eukaryotes had peak numbers in the temperate and upwelling regions (Zubkov *et al.*, 1998; Heywood *et al.*, 2006). A peak *Prochlorococcus* abundance of  $2 \times 10^5$  cells ml<sup>-1</sup> observed in the equatorial southern oligotrophic gyre matched that observed on AMT3, sampled in the boreal autumn of 1996 (Zubkov *et al.*, 1998). *Synechococcus* abundances have been more variable than *Prochlorococcus* (Heywood *et al.*, 2006).

Similarly, the observation that the distribution pattern of photosynthetic eukaryotes was mirrored by the concentration of chlorophyll *a* during AMT13 and 14 (Tarran *et al.*, 2006) is also apparent here (Figs. 3.3 and 3.4). However, in contrast to flow cytometry data of the distribution of the Cryptophyceae (Tarran *et al.*, 2006), the dot blot hybridisation analysis performed here showed a large peak in Cryptophyceae abundance in the upwelling region, as opposed to in the southern temperate region.

Whilst flow cytometry showed the distribution of photosynthetic eukaryotes to be similar to that of *Synechococcus* over broad nutrient profiles (e.g. northern and southern oligotrophic gyres and northern and southern temperate regions), at the class level, these peaks and troughs in photosynthetic eukaryote abundance along the cruise transect correspond to differing PPE class composition (Fig. 3.6). To some extent this contrasts with the distribution of different *Synechococcus* clades which sometimes co-occur in particular oceanic provinces e.g. clades I and IV both proliferate in northern and southern temperate regions along AMT15 (Zwirgmaier *et al.*, 2007). This may indicate that this photosynthetic prokaryotic community is governed by different environmental factors to the PPEs. However, it should be pointed out that this analysis of *Synechococcus* and *Prochlorococcus* community structure is at the clade and ecotype level, a much higher taxonomic resolution than the class-level used for PPEs here. Thus, study of PPEs at the clade level may uncover distribution patterns that are masked here.

Members of the Prymnesiophyceae were the major class detected along the AMT15 transect as assessed by dot blot hybridisation analysis (Fig 3.5) with a link to elevated temperatures indicated by the CCA (Fig 3.8). The prominence of members of the Prymnesiophyceae along the AMT transect is also supported by prior pigment studies that showed that 19'-hexanoyloxyfucoxanthin was the dominant photosynthetic carotenoid detected over AMT cruises 2-5 (Gibb *et al.*, 2000). The Prymnesiophyceae were also found to be an important class represented in the photosynthetic component of the nuclear 18S rRNA clone libraries constructed here, as well as dominating three of the four plastid libraries (Fig. 3.9). It has been suggested that clone libraries targeting the nuclear SSU rRNA gene of the marine picophytoplankton are biased against the Prymnesiophyceae due to the high GC content of their nuclear genomes (Liu *et al.*, 2009). Thus, it is likely that the results of the plastid gene libraries, in which the Prymnesiophyceae appear more numerous, and the plastid targeted dot blot hybridisation analysis provide a more accurate representation of the numerical abundance of this class. Furthermore, the plastid clone libraries revealed more diversity within the Prymnesiophyceae than the nuclear libraries as ten RFLP types related to this class were found in the former, in contrast to only four in the latter libraries. Previous dot blot hybridisation studies sampling the Arabian Sea (Fuller *et al.*, 2006a), Pacific Ocean (Lepère *et al.*, 2009) and a coastal Mediterranean Sea site (McDonald *et al.*, 2007) also found Prymnesiophyceae to be a major component of the PPE community. Similarly, Prymnesiophyceae were observed to be an abundant photosynthetic class found in nuclear SSU clone libraries from the oligotrophic, equatorial Pacific Ocean (Moon van der Staay *et al.*, 2001), the mesotrophic coastal Pacific (Worden, 2006), Weddell Sea, Scotia Sea and Mediterranean Sea (Díez *et al.*, 2001), as well as the Arctic Ocean (Lovejoy *et al.*, 2006), Arctic-Atlantic convergence area (Hamilton *et al.*, 2008), English Channel (Vaulot *et al.*, 2002) and North West Mediterranean Sea (Massana *et al.*, 2004), and as discussed above, these studies are likely to have underestimated their abundance.

Whilst members of the Prymnesiophyceae have been well studied and are known to be important in elemental cycling, for example *Emiliana huxleyi* is important in sulphur cycling, cultured representatives are generally larger than 3 µm in diameter. However, all the samples used here were pre-filtered through a 3 µm pore-size mesh

highlighting the importance of pico-size members of this class. Indeed, a recent study has identified prymnesiophytes  $<3 \mu\text{m}$  in size to be critical in oceanic  $\text{CO}_2$  fixation by coupling fluorescent *in situ* hybridisation analyses with radiotracer uptake and flow cytometric sorting (Jardillier *et al.*, submitted).

The other major class along AMT15, displaying a striking complementary distribution to the Prymnesiophyceae, was the Chrysophyceae. This class has traditionally been considered unimportant in marine systems, but had high relative hybridisation values in the northern temperate region and in the southern gyre. The Chrysophyceae have also been found to be important in other marine environments including the Pacific Ocean (Lepère *et al.*, 2009), the Arabian Sea (Fuller *et al.*, 2006a) and Mediterranean Sea (McDonald *et al.*, 2007). This latter study found Chrysophyceae abundance to be seasonal as this class was important largely during the summer months at a coastal site near Naples, as assessed by dot blot hybridisation analysis. This observation is supported in this study as Chrysophyceae reached values of up to 70% in the near-coast northern temperate region, where samples were collected in September. However, Chrysophyceae were found to be linked to elevated light levels in the CCA (Fig. 3.8), but not to elevated temperatures. Within the Chrysophyceae, the order Parmales is essentially the only documented marine group, comprising solitary cells 2 to 5  $\mu\text{m}$  in diameter each with a single chloroplast and a silicified cell wall composed of 5 to 8 plates, but lacking cultured representatives (Booth and Marchant, 1987; Bravo-Sierra and Hernández-Becerril, 2003). However, the CCA shows silica concentration is almost at a right angle to the position of Chrysophyceae (Fig. 3.8) indicating this factor has little or no influence on the distribution of this class along the AMT. Since other marine Chrysophyceae have not been characterised, their requirement for silicate is unknown. However, it would appear that the most abundant Chrysophyceae, certainly along the AMT, are unlikely to have a large requirement for silicate. Chrysophyceae also showed high relative hybridisation values in the Southern gyre and in the tropics, confirming the importance of Chrysophyceae in open ocean environments asserted by Fuller *et al.* (2006a). Sequences related to the Chrysophyceae have recently been observed in nuclear SSU clone libraries from the Sargasso Sea (Not *et al.*, 2007a) and South East Pacific Ocean (Shi *et al.*, submitted). Thus, members of the Chrysophyceae appear to be abundant in a range of marine environments. Interestingly, a marine chrysophyte

has recently been isolated into enrichment culture using seawater obtained from the Porcupine Abyssal Plain (PAP) site in the North Atlantic Ocean (L. Jardillier, personal communication). Using fluorescent *in situ* hybridisation with the chrysophyte plastid probe this enrichment culture appears to be photosynthetic (or mixotrophic) and along with the plastid 16S rRNA gene sequence data obtained here and elsewhere, this suggests that photosynthetic chrysophytes are abundant in marine waters. Given that described cultured members of the Chrysophyceae are virtually all from freshwater environments, it would be highly advantageous to further isolate and maintain marine chrysophytes in culture so that they may be more completely characterised.

Along AMT15, Cryptophyceae were found to be much less abundant than the Prymnesiophyceae and Chrysophyceae. This is in contrast to recent studies such as McDonald *et al.* (2007) and Lepère *et al.* (2009) who found Cryptophyceae to be as important as the Prymnesiophyceae in a Mediterranean Sea coastal site and across a transect in the South East Pacific Ocean, respectively, using dot blot hybridisation analysis. Cryptophyceae were also well represented in nuclear SSU clone libraries from a coastal site in the English Channel (Romari and Vaultot, 2004). In the Arabian Sea, Cryptophyceae were restricted to the coast and at 20-30 m depth elsewhere (Fuller *et al.*, 2006a). The latter is a similar pattern to that found here (Fig. 3.6). A study of photosynthetic eukaryote groups along AMT13 and 14 using flow cytometry (Tarran *et al.*, 2006) found Cryptophyceae to be most abundant in the temperate regions, whereas the dot blot hybridisation data presented here indicated they were most abundant in the upwelling region. However, AMT14 did not sample the upwelling region, but Cryptophyceae counts were elevated in the upwelling region of AMT13 though not to the extent of that in the Southern temperate region (Tarran *et al.*, 2006). These surveys indicate that the Cryptophyceae are associated with higher nutrient waters, which is clearly supported by a strong link between the concentrations of nitrate, nitrite and phosphate and this class highlighted by the CCA (Fig. 3.8).

The Pelagophyceae were a minor class found to be most abundant (22% relative hybridisation) at depth in the northern temperate region. CCA showed no clear links between the Pelagophyceae and environmental factors that were measured except for

light intensity, with Pelagophyceae appearing to be associated with lower light intensities, indicated by the opposing position of this factor and the Pelagophyceae distribution data (Fig. 3.8). Pelagophyceae were rarely detected in a seasonal study of a site in the Mediterranean Sea using dot blot hybridisation analysis (McDonald *et al.*, 2007), except in February when % relative hybridisation values for the class peaked at 6.75%. However, clones related to the Pelagophyceae were well represented in plastid 16S rRNA gene clone libraries from the Arabian Sea (Fuller *et al.*, 2006b). Furthermore, members of this class have regularly been isolated from the Pacific gyre (Andersen, 2007).

The distributions of other classes Pinguiphyceae, Trebouxiophyceae and Eustigmatophyceae, with low relative hybridisation values over small areas of AMT15 and often at depth is similar to their distribution in the Arabian Sea indicated by dot blot hybridisation data (Fuller *et al.*, 2006a). CCA shows the Pinguiphyceae to be associated with low light intensities, and potentially elevated numbers of photosynthetic eukaryotes. The Trebouxiophyceae appear to be linked with low temperatures and higher silicate and chlorophyll *a* concentrations and, reflecting their peak values below the thermocline in the gyres. Conversely, the Eustigmatophyceae appear to be linked with higher temperatures and lower silicate and chlorophyll *a* concentrations.

A wealth of phylogenetic information of the eukaryotic nuclear SSU rRNA gene has been amassed from the pico-sized eukaryotic community of many marine sites (e.g. Moon van der Staay *et al.*, 2001; Díez *et al.*, 2001). Recently, two studies have been published providing phylogenetic information of the plastid 16S rRNA gene from a coastal and open ocean site (McDonald *et al.*, 2008 and Fuller *et al.*, 2006b respectively). However, this is the first study to directly compare the information gleaned using both of these markers, particularly over the range of oceanic regimes spanned during AMT15.

Overall, the 16S rRNA gene provided more relevant information of the target group due to the presence of large numbers of heterotrophic sequences targeted by the 18S rRNA PCR primers used. The diversity of heterotrophic pico- and nano-eukaryotes is greater than their photosynthetic counterparts (Vaulot *et al.*, 2002) meaning



phototrophs are overshadowed in these libraries. However, constructing nuclear SSU rRNA gene libraries is still advantageous especially because there is a greater wealth of sequence information already available for this marker. Hence, it is easier to phylogenetically ‘place’ new environmental sequences.

The nuclear SSU rRNA gene libraries were dominated by marine alveolates, which are thought to have a parasitic life mode (Guillou *et al.*, 2008) potentially targeting dinoflagellates (Chambouvet *et al.*, 2008). The wide variety of sequences within this group means that they are likely to represent an important component of the picoeukaryote community. The phylogenetic significance of such sequences, including those obtained from this work has been critically examined elsewhere (Guillou *et al.*, 2008).

When only the ‘photosynthetic’ nuclear 18S rRNA gene sequences are considered, proportions of clones assigned to the major classes in 18S and 16S rRNA gene libraries largely correlated. However, an obvious exception was that sequences for the Prasinophyceae, particularly of clade II, were largely absent from the plastid clone libraries except for the northern temperate library. Whilst this group has been found to be important in nuclear SSU rRNA gene libraries from a range of sites (Moon van der Staay *et al.*, 2001; Romari and Vaultot, 2004; Worden, 2006; Medlin *et al.*, 2006), it was also absent from other studies using these plastid primers (Fuller *et al.*, 2006b; McDonald *et al.*, 2008) suggesting PCR bias against this prasinophyte clade. Indeed, McDonald *et al.* (2007) reported the appearance of clade II prasinophyte sequences related to *Micromonas* sp. only when the stringency of the PCR was reduced by increasing the concentration of MgCl<sub>2</sub> in the reaction. However, this caused libraries to be dominated by cyanobacteria. Further Prasinophyceae diversity is observed in nuclear SSU rRNA gene phylogenies, with sequences falling within clades I, VIII and IX (Viprey *et al.*, 2008). Although phylogenetic analysis of plastid 16S rRNA gene sequences revealed only a single sequence related to Pras16S-VIII (Lepère *et al.*, 2009), a novel lineage currently containing no cultured counterparts and potentially ‘equivalent’ to nuclear SSU rRNA clade IX (Viprey *et al.*, 2008), though where only two nuclear clones were obtained, the fact that these plastid Pras16S-VIII clade sequences are well

represented in plastid libraries from the South East Pacific suggests there is no obvious bias with this prasinophyte clade using the plastid primer set.

Despite the apparent bias of plastid clone libraries against prasinophyte clade II, a greater number of RFLP types assigned to the Prymnesiophyceae were obtained from these libraries as opposed to using the nuclear SSU rRNA gene marker. This is likely to be as a result of the apparent bias of 18S SSU rRNA gene approaches against the Prymnesiophyceae (Liu *et al.*, 2009). However, more diversity was also observed within the Cryptophyceae and Dictyochophyceae of the plastid libraries than the nuclear libraries (see Tables 3.2 and 3.3). This may be a direct result of the ‘overshadowing’ of photosynthetic diversity in nuclear clone libraries by the more numerous heterotrophic clones. As we saw, this resulted in lower coverage values for the nuclear SSU rRNA clone libraries than their plastid equivalents. Even so, Prymnesiophyceae phylogenies from both nuclear and plastid rRNA gene libraries contained sequences with similar affiliations. Whilst most cultured Prymnesiophyceae members are larger than 3  $\mu\text{m}$  in diameter, *Imantonia rotunda* and *Phaeocystis cordata* are observed to fall within this size range for at least part of their lifecycle whilst maintained in culture (Vaulot *et al.*, 2008), and indeed sequences clustering near to these species were observed in both the nuclear and plastid SSU rRNA gene phylogenies (Figs 3.11 and 3.12 respectively).

In contrast, more RFLP types related to the Chrysophyceae were found in nuclear libraries than plastid libraries presumably because nuclear sequences were also being obtained from heterotrophic species e.g. *Paraphysomonas* (Fig. 3.13). Indeed, Fuller *et al.* (2006b) failed to obtain PCR products with either of the heterotrophic chrysophyte species *Paraphysomonas* sp. CCMP1604 or *Picophagus flagellatus* (CCMP1953) using plastid 16S targeted primers suggesting that neither of these contain remnant plastids. Certainly, as mentioned above, the Chrysophyceae sequences obtained using the plastid 16S rRNA gene cluster separately from described chrysophyte species, which have virtually all been isolated from freshwater environments. Hence future culturing efforts attempting to isolate representative marine chrysophytes particularly of the pico-size range will be an important goal. The same can be said for the pico-sized prymnesiophytes which also appeared to be a key PPE group along AMT15.

**Chapter 4:**

**Photosynthetic picoeukaryote community structure along  
an extended Ellett Line transect**

## 4.1. Introduction

### 4.1.1. History of the Ellett Line and physical oceanographic findings

The North Atlantic is a fascinating area for the study of physical oceanography due to the North Atlantic Oscillation (NAO), a feature which affects wind speeds, evaporation, rainfall and heat exchange between the ocean and the atmosphere (Hughes *et al.*, 2008). In particular, the Rockall Trough is an area of deep ocean basin extensively studied by the late physical oceanographer David Ellett. The Ellett Line, named after him, originally crossed over the Rockall Trough and was repeatedly sampled from the 1970s onwards. From 1996, the area studied was extended to Iceland (Fig. 4.1).

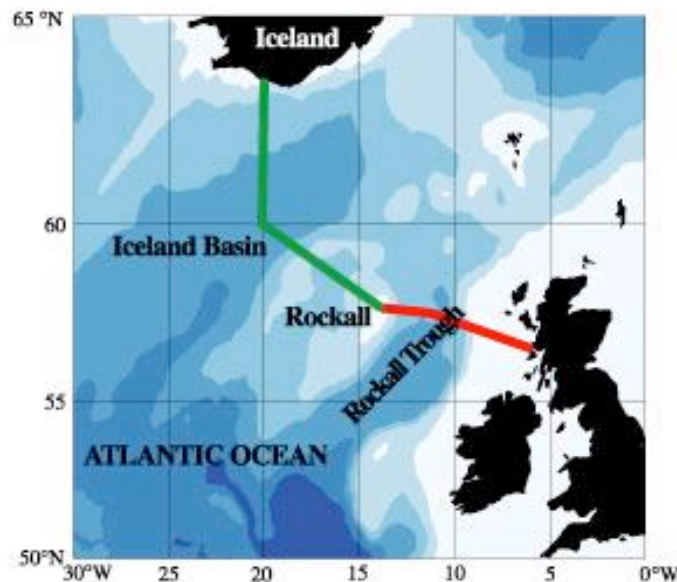


**Figure 4.1.** Cruise track of the Extended Ellett Line (<http://www.noc.soton.ac.uk/obe/PROJECTS/EEL/index.php>). The original Ellett Line along the Rockall Trough 1975-1995 is in red. The extension of the Ellett Line, sampled since 1996 is in green.

Measurements taken along the original and extended Ellett Line are primarily made from the point of view of physical oceanography. The Ellett Line has been the site of remarkable findings such as a freshening trend observed in the 1960s-90s, where salinity in the Ellett line area fell as the salinity of the subtropical Atlantic rose. This was thought to be due to changes in the balance of evaporation and precipitation over the Atlantic, as well as the effect of Arctic ice melting and changes in river discharge. However, this trend was rapidly reversed between 2003 and 2006

accompanied by a rise in water temperature, factors that generally co-vary in the upper ocean (Holliday *et al.*, 2008). Furthermore, the Ellett Line has been the site of some of the largest waves ever recorded (Holliday *et al.*, 2006; Turton and Fenna, 2008).

#### **4.1.2. Biological features of the Rockall Trough**

The extended Ellett Line lies across the Atlantic Subarctic Province (SARC) described by Longhurst (2007) as a complex region where warm Atlantic water penetrates to very high latitudes at variable rates, causing variation in physical and ecological processes. In this province, layers of water of different origins are associated with different zooplankton communities. The province is productive with extensive spring blooms as well as late summer blooms of coccolithophores (although when this transect was sampled in late August to September 2007, coccolithophores were very rarely detected by flow cytometry, R Holland personal communication).

The interesting physical features of the Rockall Trough have been shown to affect the biological features of the North Sea, as changes in the ecology recorded in the North Sea correspond with transport of large volumes of warm highly saline water in the Rockall Trough (Holliday and Reid, 2001). The Rockall Trough itself has some interesting biological features. Small coral banks known as Darwin mounds are present along the Rockall Trough of the sort that are thought to have resulted in giant carbonate structures observed at the Porcupine Seabight following thousands of years of sediment deposition (e.g. see Wheeler *et al.*, 2008). The zooplankton of the Rockall Trough has been investigated and marked seasonality was observed in the community progression (breeding and growth rates) of most crustaceans and fish species sampled (Mauchline, 1988).

The deep water area of the Rockall Trough has also been an area of ecological concern. The area has historically been an important area of study of deep-water ecology, and particularly the discovery of deep-water fish, but since 1989 has been over-exploited by commercial fishing (Gordon, 2003).

### 4.1.3. Studies of the phytoplankton

Despite the interest in this area, and the frequency of its study, the ecology of the picophytoplankton along the transect has been little studied. However, in areas close to part of the Ellett Line, to the south of the Icelandic Basin (59°N, 20°W) traversed by the PRIME cruise in 1996, standing stocks of picoplankton and nanophytoplankton were measured (Tarran *et al.*, 2001). Over the small area nearest to the transect of the extended Ellett Line, heterotrophic bacteria reached a peak of  $8.29 \times 10^8$  cells  $l^{-1}$ ; *Synechococcus* reached  $2.18 \times 10^8$  cells  $l^{-1}$ ; PPEs reached  $12.34 \times 10^6$  cells  $l^{-1}$ ; unidentified nanophytoplankton reached  $1.15 \times 10^7$  cells  $l^{-1}$ ; small coccolithophores (<8  $\mu m$ ) reached  $7.1 \times 10^5$  cells  $l^{-1}$ ; diatoms reached  $2.05 \times 10^5$  cells  $l^{-1}$ ; and dinoflagellates reached  $7.47 \times 10^3$  cells  $l^{-1}$ . *Prochlorococcus* cells were not detected in this area. This study revealed that PPEs contributed  $0.9 \text{ g C m}^{-2}$  to the biomass in this area, approximately twice that of *Synechococcus*. Thus, the PPEs were the most important component of the picophytoplankton at this site.

In contrast to the results of Tarran *et al.* (2001), the <2  $\mu m$ -sized photosynthetic community was deemed to be a minor contributor to the phytoplankton (<20% of biomass) during the spring bloom in an area partially overlapping the position of the extended Ellett Line (Moore *et al.*, 2005). This study measured physiological parameters of photosynthesis of the phytoplankton (excluding the < 2 $\mu m$ -sized members) and showed blooms were dominated by diatoms unless their growth was limited by silicate availability, in which case the large prymnesiophytes *Emiliania huxleyi* and *Phaeocystis globosa* were important. The study illustrated the changes in community size structure in response to environmental variability. The onset of the spring stratification of the water column provided favourable conditions for the proliferation of larger cells, which became more important to the biomass of the system than the underlying smaller cells that are more stable in nutrient limiting conditions (Moore *et al.*, 2005). However, full stratification of the water column causes a decline in larger cell abundance as they sink and are not returned to the surface at they would be under mixing conditions.

In the first leg of the cruise reported here, sampling an area very close to the Ellett Line, phytoplankton of <5  $\mu m$  diameter were found to have remarkably high rates of

bacterivory in pulse-chase experiments coupled with flow sorting (Zubkov and Tarran, 2008).

#### 4.1.4. Aims of this work

PPE community structure was investigated for the first time along the extended Ellett Line. At two sites, one in the Icelandic Basin and one at the Wyville-Thomson Ridge, the PPE community structure was investigated further with phylogenetic analysis targeting the plastid SSU rRNA gene. Further study involved the use of fluorescent *in situ* hybridisation (FISH) to identify PPEs at the class-level and assess their abundance. This method allowed comparison of dot blot hybridisation/clone library construction with a method independent of PCR, i.e. FISH. Seven stations along the extended Ellett Line were sampled at 5 or 6 depths between 26<sup>th</sup> August and 3<sup>rd</sup> September 2007, followed by two sites at the Wyville-Thomson Ridge (60.24°N, 9.01°W; and 60.64°N, 8.13°W) for size fractionated DNA samples and FISH filters (Fig. 4.2).

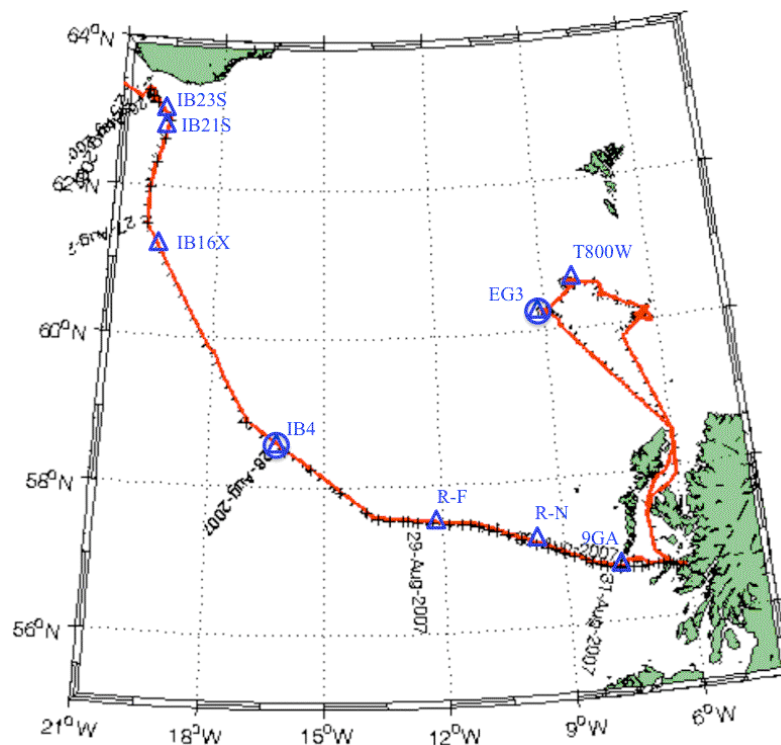


**Figure 4.2.** The extended Ellett Line track taken by cruise D321b in 2007 (Sherwin *et al.*, 2008). The positions of samples used in dot blot hybridisation analysis are marked with triangles, labelled with station names. Stations named “IB” are in the Icelandic Basin, R-(Rockall)-F and -N and 9GA are in the Rockall Trough, and EG3 and T800W are at the Wyville-Thomson Ridge. The positions of samples additionally used for the construction of clone libraries are also marked with circles.

## 4.2. Results

### 4.2.1. Physical and chemical characteristics along the extended Ellett Line

Physical and chemical variables measured along the extended Ellett Line are shown in Fig. 4.3. The Icelandic Basin, between 63.32°N 20.21°W and 58.5°N 16°W, was characterised by nutrient concentrations of 0.58 - 20.5  $\mu\text{M}$  nitrate, from undetectable levels to 0.84  $\mu\text{M}$  ammonium, 0.08 - 0.90  $\mu\text{M}$  phosphate, from undetectable levels to 5.89  $\mu\text{M}$  silicate and chlorophyll *a* concentrations 0.02 - 2.28  $\text{mg m}^{-3}$ . The Rockall Trough, between 57.51°N 12.25°W and 56.81°N 7.35°W, was characterised by concentrations of 0.1 - 14.62  $\mu\text{M}$  nitrate, 0.01 - 0.98  $\mu\text{M}$  ammonium, 0.06 - 0.62  $\mu\text{M}$  phosphate, <0.005 - 4.23  $\mu\text{M}$  silicate and 0.02 - 1.21  $\text{mg m}^{-3}$  chlorophyll *a*. Nutrient concentrations were not measured at the Wyville-Thomson Ridge, between 60.25°N 9.01°W and 60.64°N 8.13°W, but chlorophyll concentrations were much higher (chlorophyll *a* 12.08 - 78.31  $\text{mg m}^{-3}$ ). Temperatures were between 8.5 and 14.4 °C across the transect, with the highest values in the middle of the transect, from the southern end of the Icelandic basin across most of the Rockall Trough.



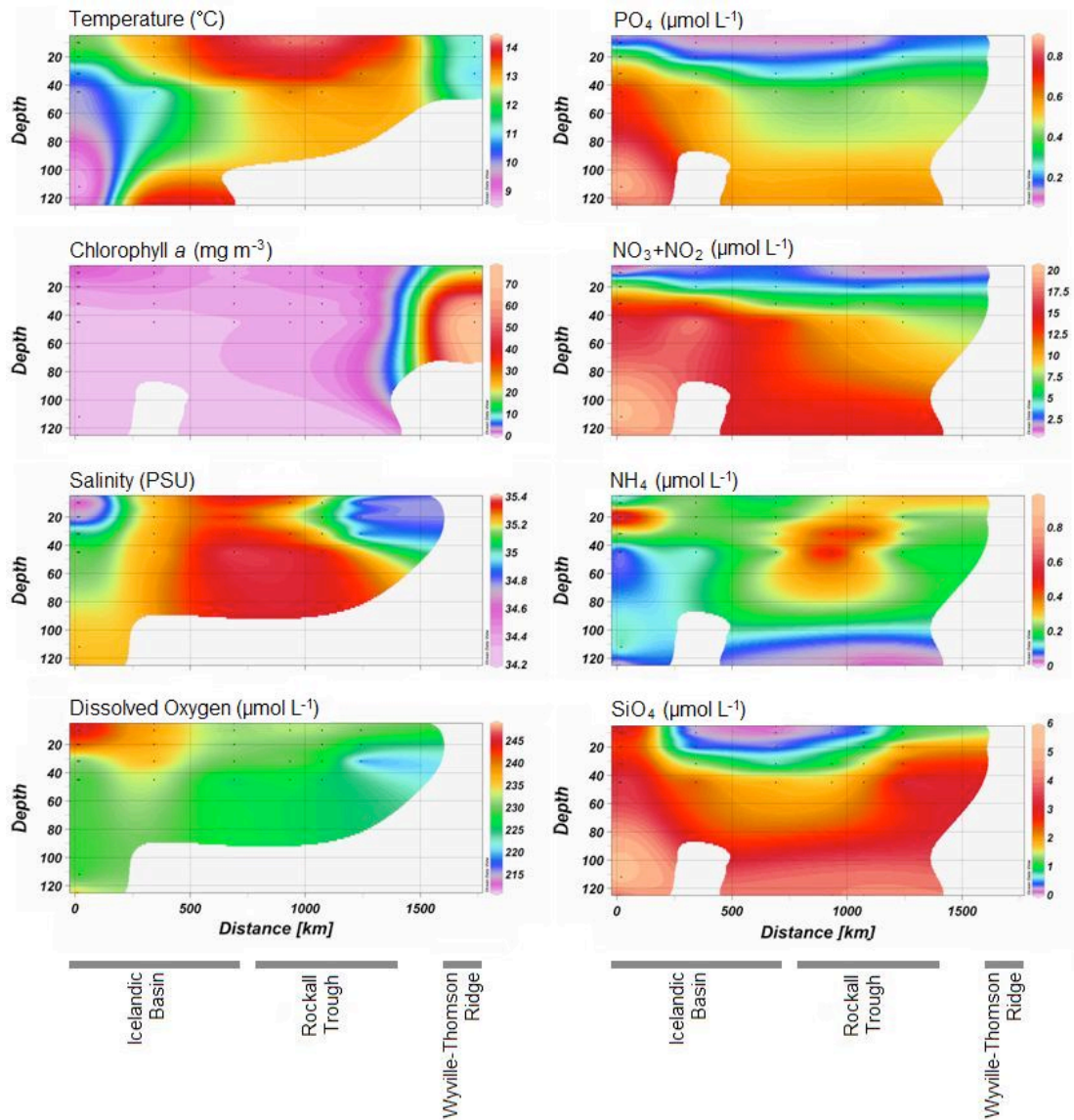


**Figure 4.3.** Contour plots showing chemical and physical parameters along the extended Ellett Line 2007. The distance along the transect, from Iceland to the Wyville-Thomson Ridge, is plotted on the x axis, against depth into the water column on the y axis. The colour represents the value of the environmental variable.

#### 4.2.2. Picophytoplankton abundance along the extended Ellett Line

Photosynthetic eukaryotes and *Synechococcus* cells were detected by flow cytometry (samples were not prefiltered through a 3  $\mu\text{m}$  pore-sized mesh and thus results may not strictly refer to the pico-sized organisms). These groups showed similar distribution patterns along the transect (Fig. 4.4). Photosynthetic eukaryote cell numbers were highest at the coastal Icelandic Basin site and at the easterly end of the Rockall Trough at the surface and at 10 m depth, peaking at  $<3.5 \times 10^4$  and  $<3.9 \times 10^4$  cells  $\text{ml}^{-1}$  respectively. *Synechococcus* peaked at  $<3.62 \times 10^5$  cells  $\text{ml}^{-1}$  in surface water at the coastal Icelandic Basin site, and reached over  $5 \times 10^5$  cells  $\text{ml}^{-1}$  towards the southern end of the Icelandic Basin sites sampled up to 20m deep. At the Wyville-Thomson Ridge sites, photosynthetic eukaryote and *Synechococcus* cell numbers were much lower at less than  $8 \times 10^3$  and  $5.5 \times 10^3$  cells  $\text{ml}^{-1}$  respectively. *Prochlorococcus* cells were not detected anywhere along the extended Ellett Line transect by flow cytometry.

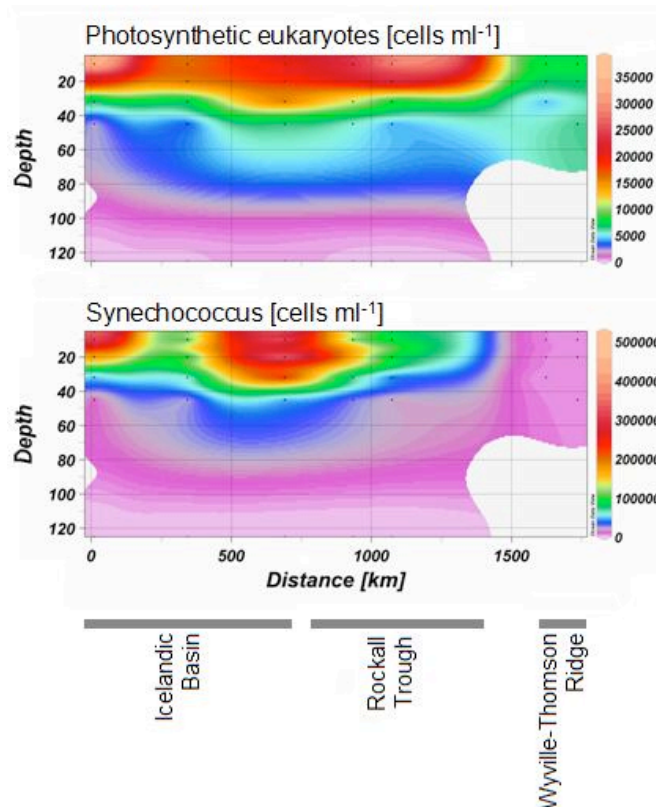


**Figure 4.4.** Contour plots of flow cytometry data along the extended Ellett Line. Cells  $\text{ml}^{-1}$  have been recorded for photosynthetic eukaryotes (top) and *Synechococcus* (bottom).

#### **4.2.3. Photosynthetic picoeukaryote community structure along the extended Ellett Line assessed using dot blot hybridisation analysis**

Of the ten class-specific probes used in dot blot hybridisations, five reached values above the arbitrarily defined background level of 2%. These were the probes targeting the Prymnesiophyceae, Chrysophyceae, Cryptophyceae, Pelagophyceae and Pinguiphyceae, (Fig. 4.5). The most 'abundant' class over the transect was Prymnesiophyceae (Fig. 4.5), with an average relative hybridisation value of 25% over the whole transect, and reached a maximum value of 65% at 32 m depth at station F towards the western end of the Rockall Trough (Fig. 4.6). Cryptophyceae also reached a maximum relative hybridisation of up to 65%, in this case at 32 m at station IB21S in the Icelandic Basin. The average hybridisation value for the Cryptophyceae was 10% relative hybridisation along the length of the transect, excluding the Wyville-Thomson Ridge where the signal for this probe remained below the level considered background (Fig. 4.6). Chrysophyceae reached a maximum value of 46% relative hybridisation at 32 m at station IB4 towards the southern end of the Icelandic Basin but was much lower over the rest of the transect (Fig. 4.6) at an average of 8%. Pelagophyceae reached a maximum of 35% relative hybridisation towards the southern end of the Icelandic Basin with an average value of 4% relative hybridisation over the transect. Pinguiphyceae reached 5% relative hybridisation in the Rockall Trough and although the average relative hybridisation of this probe was of 1%, the signal was regularly detected above the background level (Fig. 4.6).

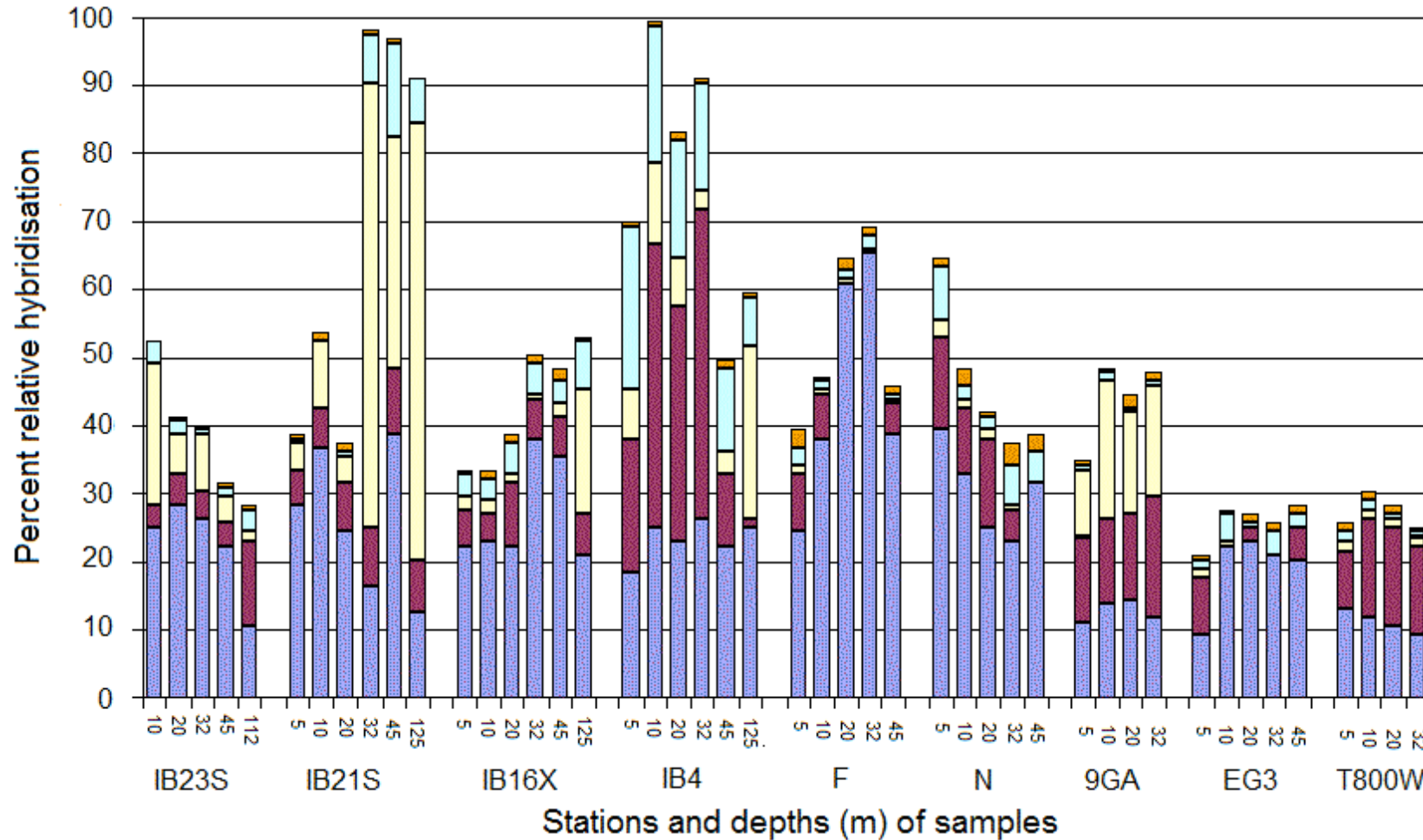


**Figure 4.5.** Histogram showing the percent relative hybridisation for probes which reached above 2% relative hybridisation along the extended Ellett Line, targeting the Prymnesiophyceae (■), Chrysophyceae (■), Cryptophyceae (□), Pelagophyceae (□) and Pinguiphyceae (■) for each station and depth analysed.

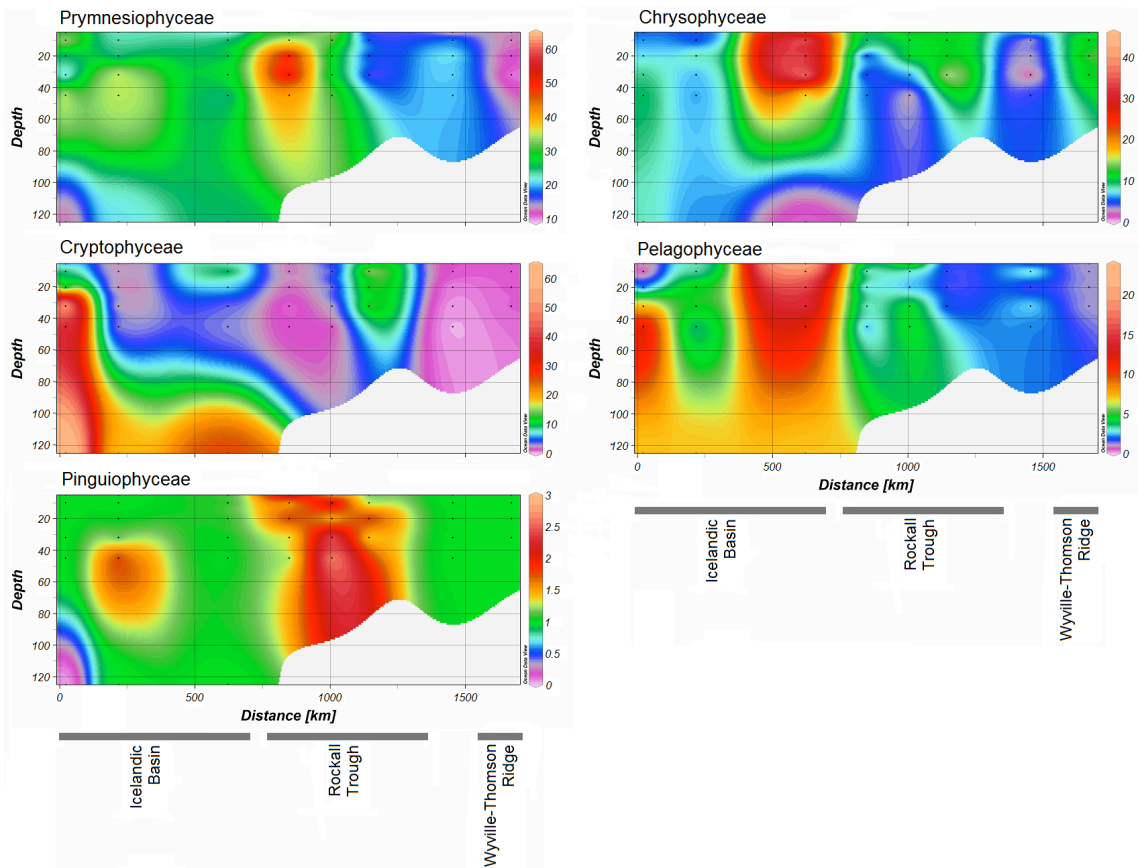


**Figure 4.6.** Contour plots of dot blot hybridisation data showing the distribution patterns of PPE classes along the extended Ellett Line transect. Contour plots indicate percentage relative hybridisation (as a proportion of all amplified by primers PLA491F and OXY1313R) of the different classes.

Twenty-four samples, for which dot blot hybridisation, chemical, physical and flow cytometry data were available, were used in statistical analysis. Canonical correspondence analysis (CCA) showed that 85% of dot blot hybridisation data could be explained by the measured environmental variables. Overall, the majority of variation is influenced by chemical parameters (concentrations of nitrate and nitrite, phosphate, silicate and dissolved oxygen as well as salinity) capable of explaining up to 69% of the variation in dot blot hybridisation data, with less influence of biological parameters (photosynthetic eukaryote and *Synechococcus* abundances and the concentration of chlorophyll *a*) explaining 39%, and physical parameters (temperature and depth) explaining 40% of the variation, much of which is overlapping with the influence of chemical parameters. The influence of these groups of parameters is illustrated by means of a Venn diagram (Fig. 4.7).

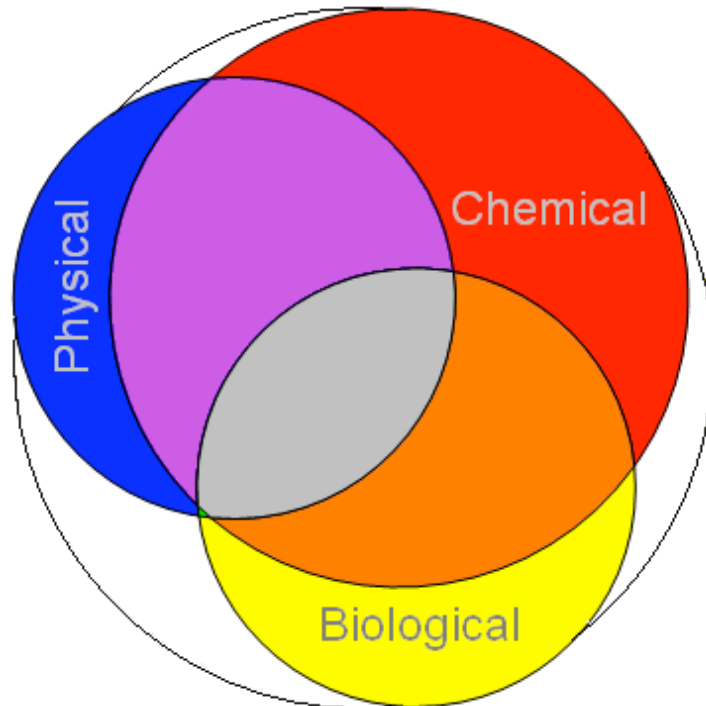


**Figure 4.7.** Venn diagram, drawn to scale by the eigenvalues calculated for the total variation in dot blot hybridisation along the extended Ellett Line (white) with the amount of variation that can be explained by physical (blue), chemical (red) and biological (yellow) parameters. The values for which were 40, 69 and 39% respectively. The overlap in the amount of variation explained by more than one set of parameters is also shown: physical and chemical parameters overlap by 31%, chemical and biological parameters overlap by 28% and physical and biological parameters overlap by 11% of the total variation. Physical parameters comprise temperature and depth; chemical parameters comprise concentrations of nitrate and nitrite, phosphate, silicate, dissolved oxygen and salinity; biological parameters comprise photosynthetic eukaryote and *Synechococcus* abundances and the concentration of chlorophyll *a*.

The majority of this variation could be explained in a 5-variable model with temperature, *Synechococcus* abundance, salinity, nitrate and nitrite concentration (measured together) and phosphate concentration as the key variables (Fig. 4.8). This model can explain up to 75% of the dot blot hybridisation data variation. Additional variables could only provide  $\leq 3\%$  increments in the amount of variance in dot blot hybridisation that was explained. Alone, the most important variable was temperature, which could explain up to 39% of the variation. Adding *Synechococcus* abundance to the model added 19% to the model, addition of salinity explained a further 8%, addition of  $\text{NO}_2 + \text{NO}_3$  3% and addition of  $\text{PO}_4$  a further 6%. The addition of  $\text{PO}_4$  only contributed considerably to the model in the presence of  $\text{NO}_2 + \text{NO}_3$ .

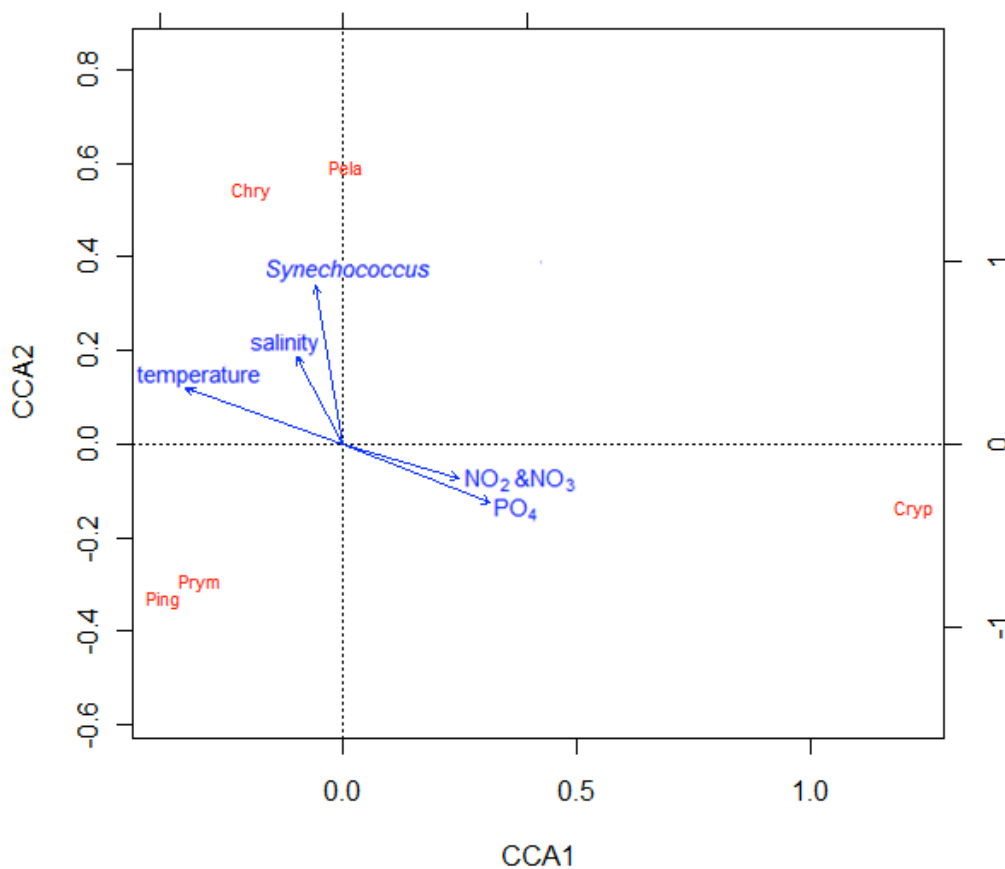


**Figure 4.8.** CCA plot of the environmental variables (blue) that are associated with the variation in dot blot hybridisation data (red) along the extended Ellett Line for classes Prymnesiophyceae (Prym), Chrysophyceae (Chry), Cryptophyceae (Cryp), Pelagophyceae (Pela) and Pinguiphyceae (Ping). Axis 1 (CCA1) can explain 50% of the total variation in dot blot hybridisation data, axis 2 (CCA2) can explain a further 25%. Two additional axes (not shown) can explain less than 1% extra.

#### **4.2.4. Taxonomic composition of photosynthetic picoeukaryotes at two sites along the extended Ellett Line transect**

Two clone libraries were constructed targeting the plastid 16S rRNA gene using samples from this transect (Fig. 4.2). One sample, from the Icelandic Basin (station IB4) at 32 m deep, was selected due to the noticeably high dot blot relative hybridisation signals for Chrysophyceae and Pelagophyceae of the sample (see Fig. 4.6). The other clone library was constructed with a sample from station EG3 at the Wyville-Thomson Ridge at 10 m deep, for which only two classes reached above the background level of 2%, Prymnesiophyceae and Pelagophyceae, and the total relative hybridisation signal for this sample was only 27%. The representation of classes in these clone libraries is illustrated (Fig. 4.10).

Both libraries were dominated by RFLP types with corresponding sequences assigned by BLAST analysis to Prymnesiophyceae (62% and 68% for the Icelandic Basin and Wyville-Thomson Ridge libraries respectively). Although dot blot hybridisation analysis indicated the Prymnesiophyceae to be more abundant than the other classes detected (Fig. 4.6), the clone libraries indicate this class to be more abundant than predicted by the dot blot hybridisation analysis (Fig. 4.9). The next most important class was Prasinophyceae (16% and 19% respectively), a class comprising several clades of which only one is targeted by a dot blot hybridisation probe. These two major classes were more diverse in the Wyville-Thomson Ridge library than the Icelandic Basin libraries as evidenced by the higher number of RFLP types assigned to these classes in the Wyville-Thomson Ridge library (Table 4.1). Aside from these two major classes, the community structure of these two samples seemed to vary. Chrysophyceae and Pelagophyceae related sequences were only detected in the Icelandic Basin library, although Pelagophyceae was predicted by the dot blot hybridisation data to be present in both libraries. The absence of Chrysophyceae at the Wyville-Thomson Ridge site was indicated by both clone library and dot blot hybridisation methods. Bacillariophyceae were detected only in the Wyville-Thomson Ridge library. A small number of clones relating to Dictyochophyceae and Cryptophyceae were present in both libraries.



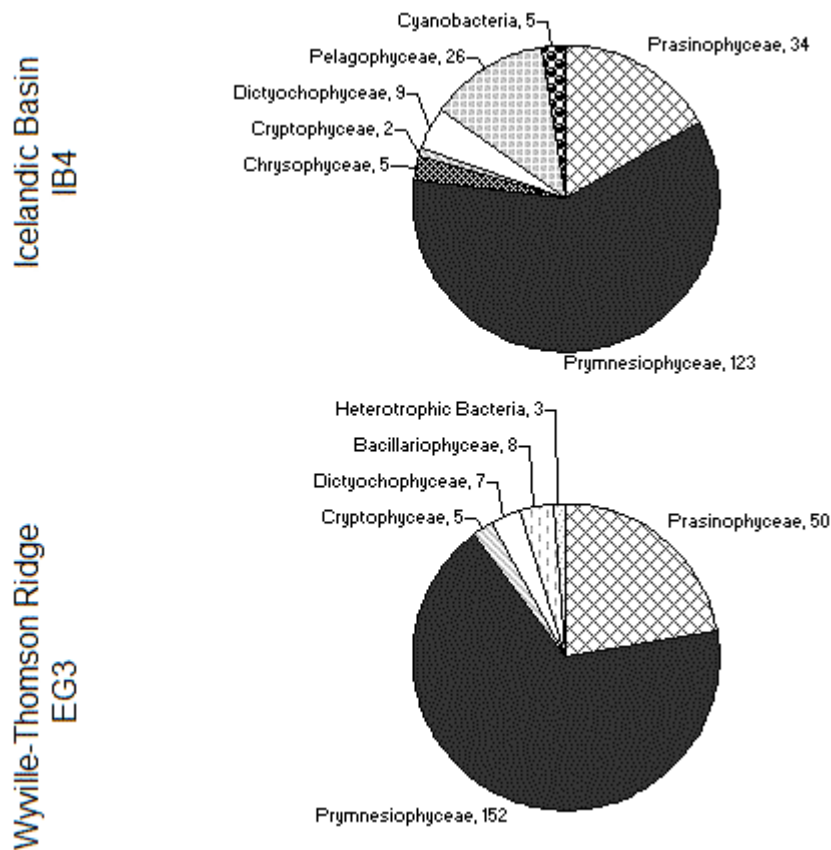


**Figure 4.9.** Pie-charts representing the proportion of clones assigned to different classes in clone libraries constructed for samples from the extended Ellett Line at station IB4 at 32 m depth and station EG3 at 10 m depth by RFLP analysis and BLAST and ARB alignments for representative sequences. The pie-charts are annotated with the class and number of clones assigned to each class.

**Table 4.1.** Number of RFLP types and clones identified within each algal class observed in the two plastid 16S rRNA gene clone libraries from the extended Ellett Line, constructed from the Iceland Basin station IB4 at 32 m depth and the Wyville-Thomson Ridge station EG3 at 10 m depth.

Class	Number of RFLP types (clones) in libraries	
	IB4, 32 m	EG3, 10 m
Prasinophyceae	3 (34)	10 (50)
Prymnesiophyceae	6 (123)	9 (152)
Chrysophyceae	1 (5)	-
Cryptophyceae	2 (2)	2 (5)
Dictyochophyceae	3 (9)	3 (7)
Pelagophyceae	3 (26)	-
Bacillariophyceae	-	1 (8)
Cyanobacteria	2 (5)	-
Heterotrophic Bacteria	-	1 (3)

Rarefaction analysis of these clone libraries (Fig. 4.10) shows that both are beginning to reach a plateau indicating that analysis of further clones would yield few novel RFLP types. This is confirmed by the high coverage values calculated for both clone libraries, at 90% for the Icelandic Basin library (IB4) and 89% for the Wyville-Thomson Ridge library (EG3).

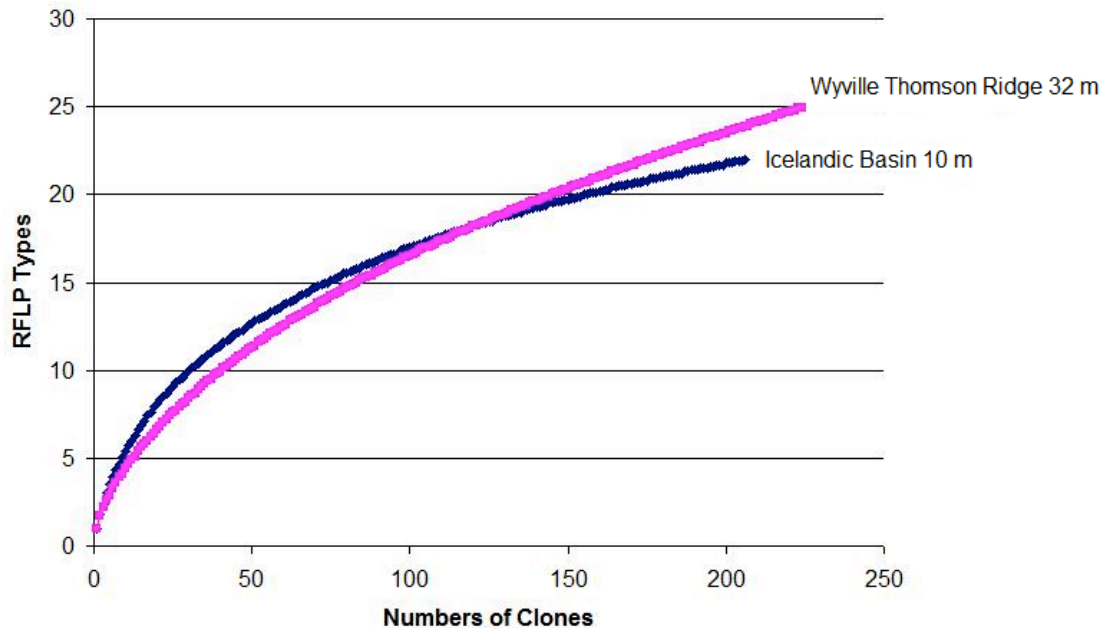


**Figure 4.10.** Rarefaction curves for clone libraries constructed from samples along the extended Ellett Line for station IB4 in the Icelandic Basin at 32 m depth and station EG3 at the Wyville Thomson Ridge at 10 m depth.

#### 4.2.5. Phylogenetic analysis

Analysis of RFLP patterns produced with the use of *Hae*III and *Eco*RI on PCR amplicons from the primers PLA491F and OXY1313R showed that some patterns observed in clone libraries from AMT15 (see section 3.2.4.1) were also present in the extended Ellett Line libraries. Thus, in the Prymnesiophyceae tree (Fig. 4.11), sequences from Ellett Line clones are grouped within the novel lineage containing clones from the AMT. Many of these sequences cluster into extensive, newly defined, lineages known as Prym16S-I and Prym16S-II (Lepère *et al.*, 2009).

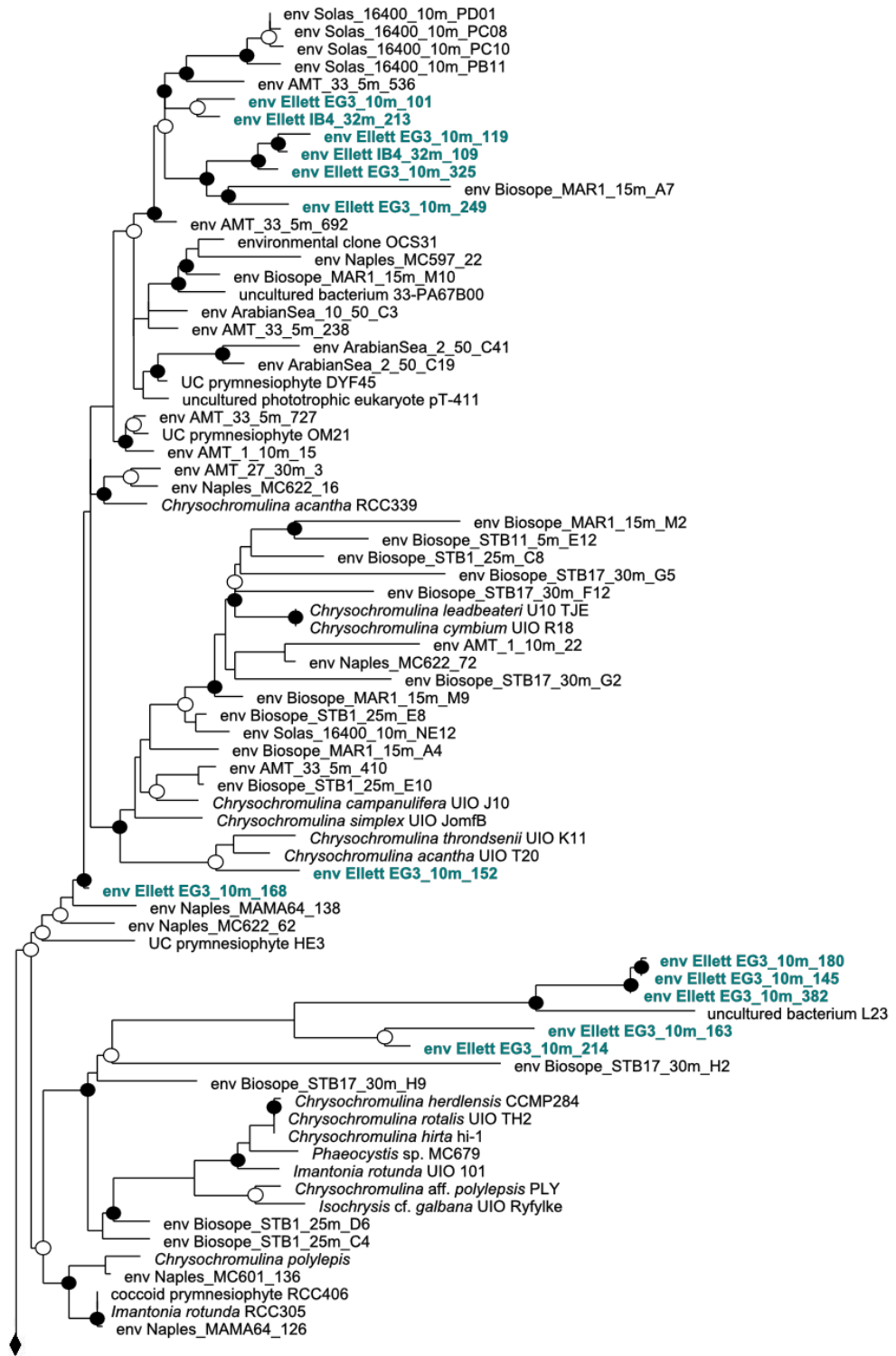


**Figure 4.11.** Phylogenetic relationships amongst the Prymnesiophyceae using plastid 16S rRNA gene sequences and a neighbour-joining algorithm. Sequences from the extended Ellett Line clone libraries are emboldened, highlighted in blue and labelled “Ellett”. Bootstrap analysis was performed by ARB parsimony method (Ludwig *et al.*, 2004). Open circles represent values above 70%; filled circles represent values above 90%. Continued next page.

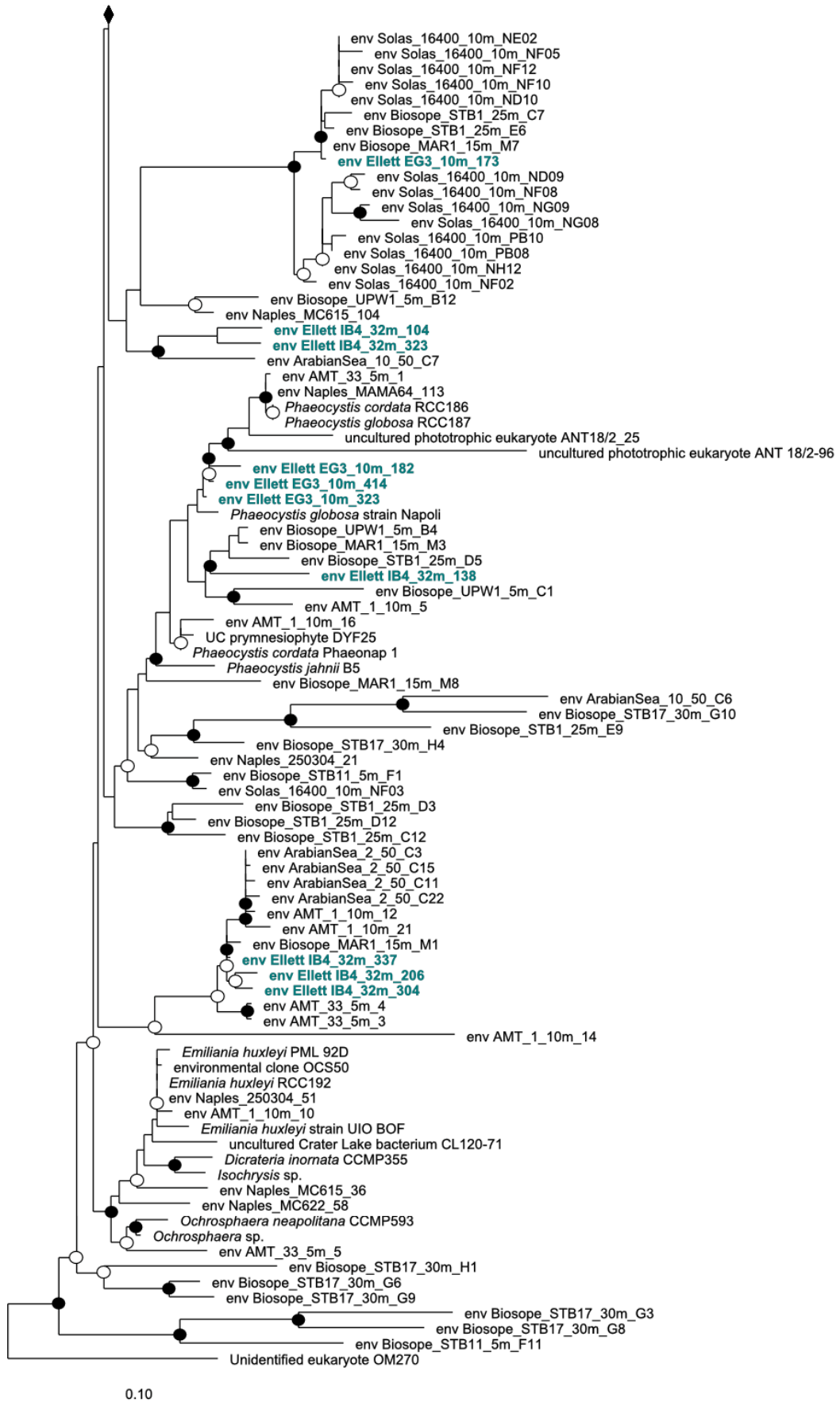
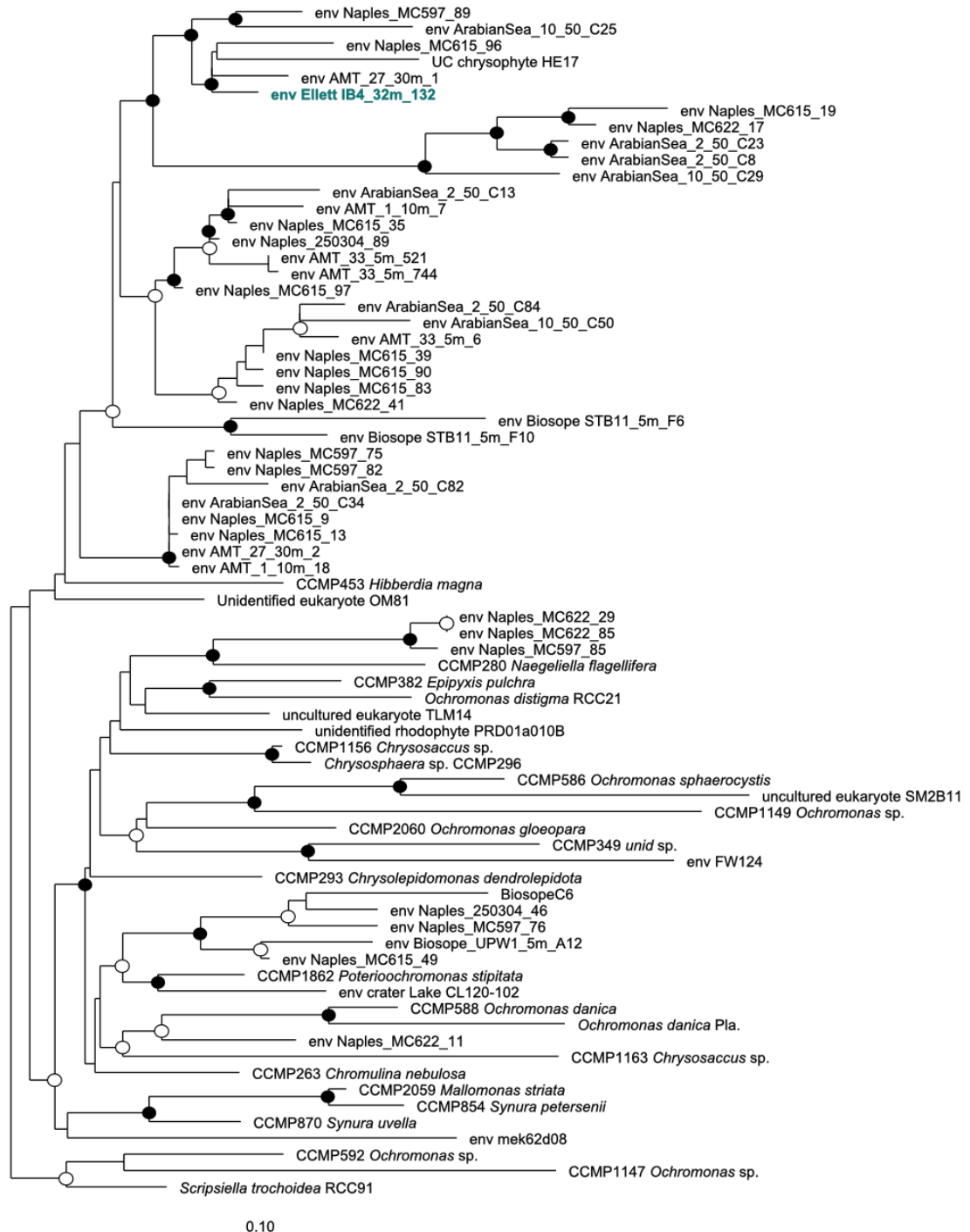


Figure 4.11. Continued.

Few clones were identified to be related to the Chrysophyceae. The five, from IB4 that were related to this class fell into a RFLP type also seen in the AMT southern gyre clone libraries (section 3.2.4.2), and indeed clustered with this sequence (Fig. 4.12).



**Figure 4.12.** Phylogenetic relationships amongst the Chrysophyceae using plastid 16S rRNA gene sequences and a neighbour-joining algorithm. Sequences from the extended Ellett Line are highlighted in blue. Bootstrap values above 70% are marked with an open circle, values above 90% are marked with a filled circle.

Three Dictyochophyceae RFLP types were observed in Ellett Line libraries, branching with other environmental sequences near to *Mesopedinella arctica* (Fig. 4.13). There are few plastid SSU rRNA sequences available as references for phylogenetic analysis of environmental samples at present.

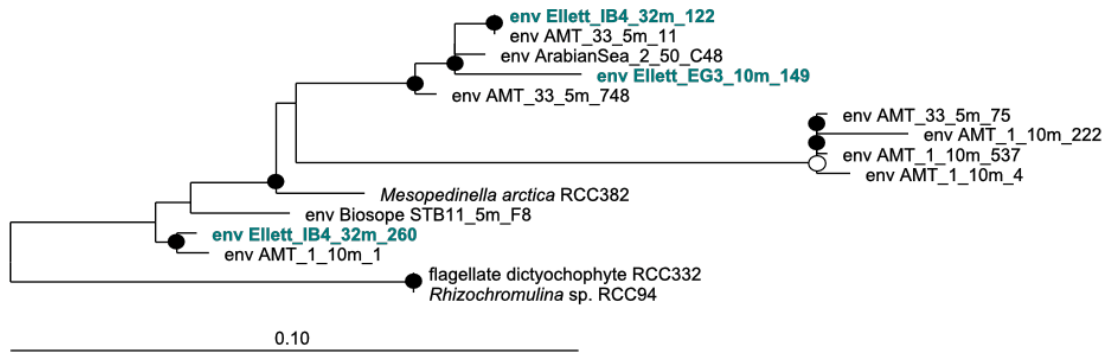


**Figure 4.13.** Phylogenetic relationships amongst the Dictyochophyceae using plastid 16S rRNA gene sequences and a neighbour-joining algorithm. Sequences from the extended Ellett Line are highlighted in blue. Bootstrap values above 70% are marked with an open circle, values above 90% are marked with a filled circle.

Two clones from the Ellett Line library EG3 branched within the Bacillariophyceae, in a cluster of environmental sequences. The nearest cultured sequence is of *Bacillaria paxillifer* (Fig. 4.14).

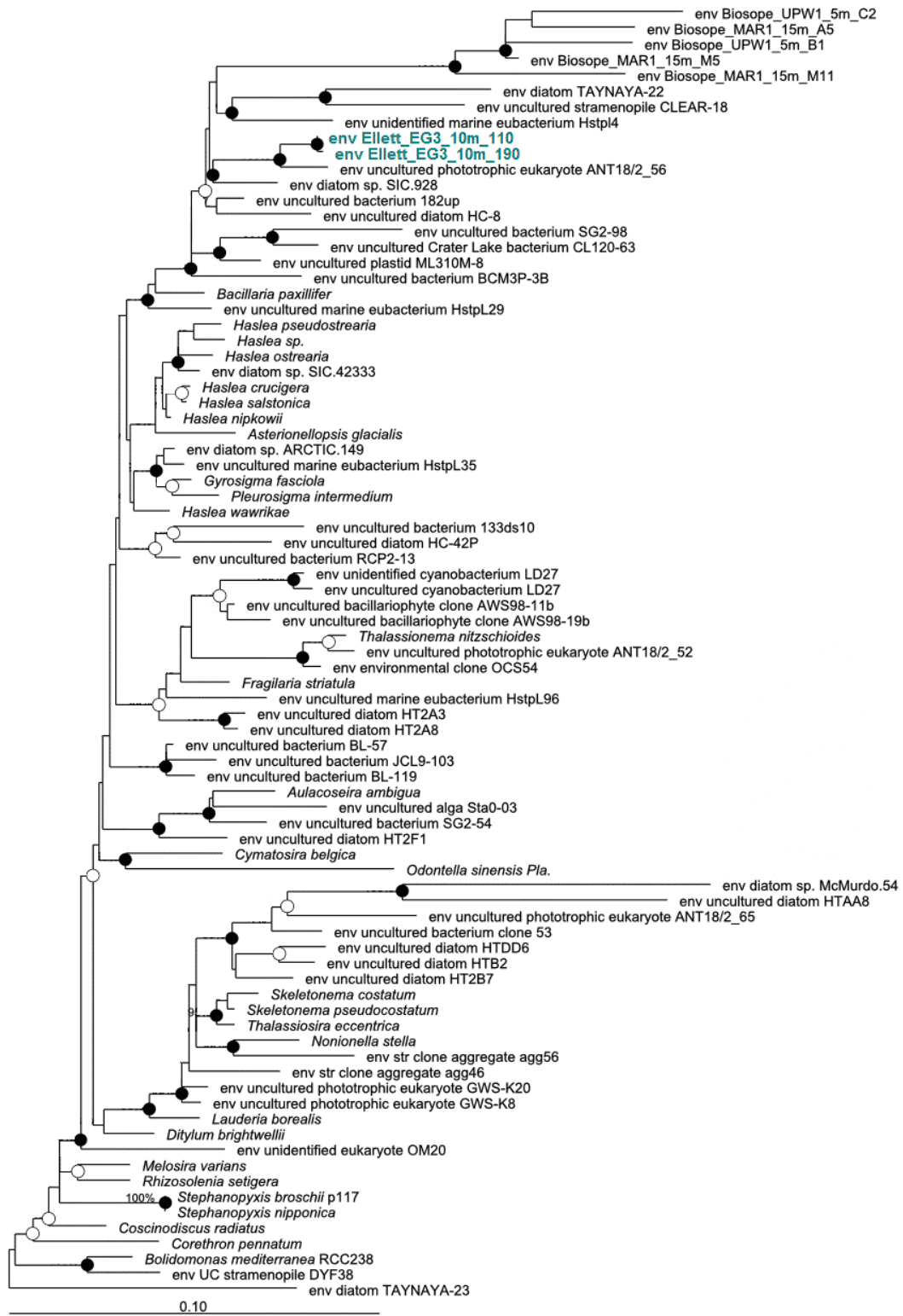


**Figure 4.14.** Phylogenetic relationships amongst the Bacillariophyceae using plastid 16S rRNA gene sequences and a neighbour-joining algorithm. Sequences from the extended Ellett Line are highlighted in blue. Bootstrap values above 70% are marked with an open circle, values above 90% are marked with a filled circle.

The Prasinophyceae appeared to be an important class in both libraries, and phylogenetic analysis showed that these Prasinophyceae-related sequences branched within a newly defined lineage designated Pras16S-VIII (Lepère *et al.*, 2009) (Fig. 4.15). The dot blot hybridisation method does not target this group.

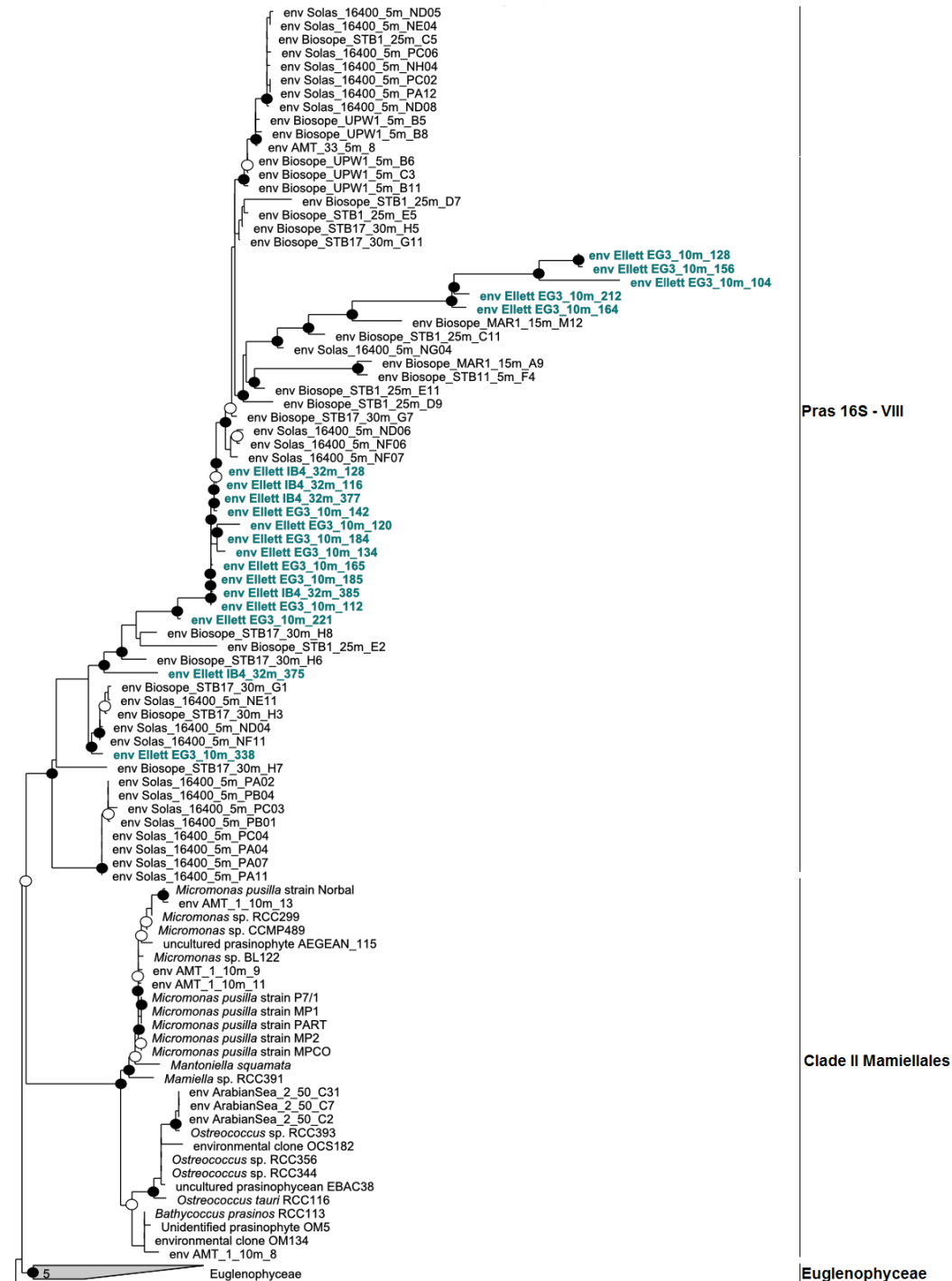


**Figure 4.15.** Phylogenetic relationships amongst the Chlorophyceae using plastid 16S rRNA gene sequences and a neighbour-joining algorithm. Sequences from the extended Ellett Line are highlighted in blue. Prasinophyte clades are shown. Bootstrap values above 70% are marked with an open circle, values above 90% are marked with a filled circle.



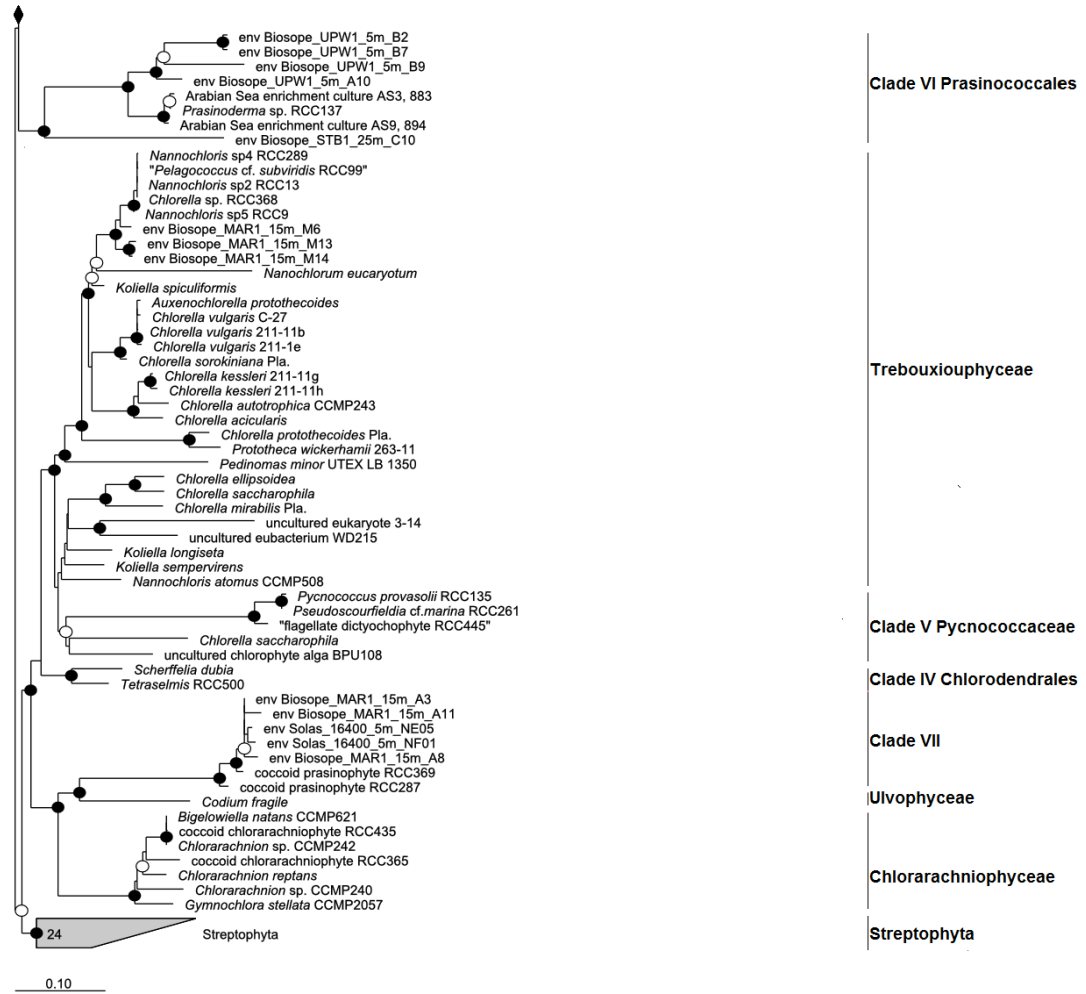
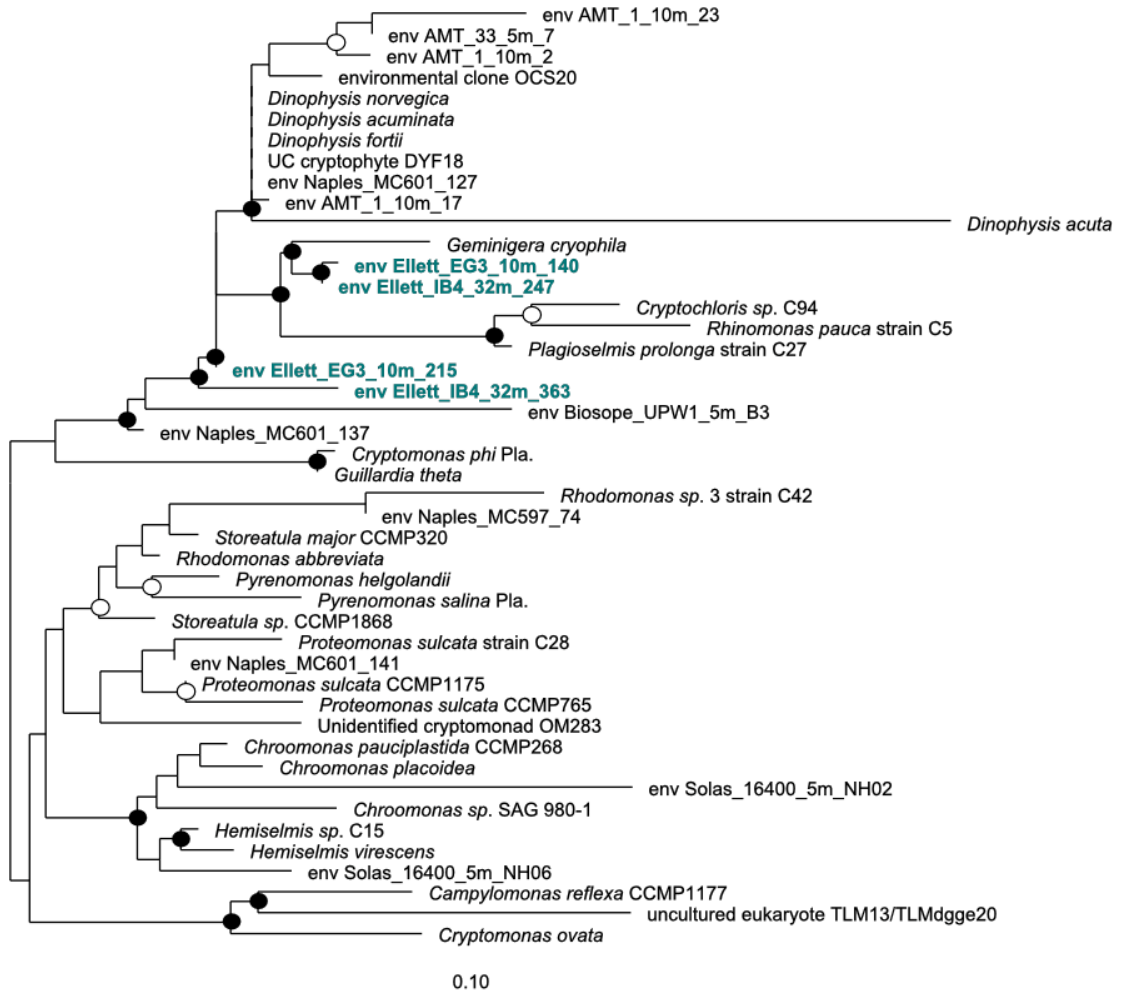


Figure 4.15. Continued.

Two sequences from EG3 and two from IB4 fell within the Cryptophyceae (Fig. 4.16), near to *Geminigera cryophila*. These sequences show some variation within this group which has not previously been observed for the plastid SSU rRNA gene.



**Figure 4.16.** Phylogenetic relationships amongst the Cryptophyceae using plastid 16S rRNA gene sequences and a neighbour-joining algorithm. Sequences from the extended Ellett Line are highlighted in blue. Bootstrap values above 70% are marked with an open circle, values above 90% are marked with a filled circle.

Pelagophyceae-related sequences from Ellett Line library IB4 form a cluster branching within the Pelagophyceae representing two RFLP types. This cluster appears separate from environmental sequences from the Atlantic Ocean (AMT), Arabian Sea (Fuller *et al.*, 2006b) and Pacific Ocean (Lepère *et al.*, 2009). A third RFLP type clusters separately, near to the Pacific Ocean (Lepère *et al.*, 2009) (Fig. 4.17).

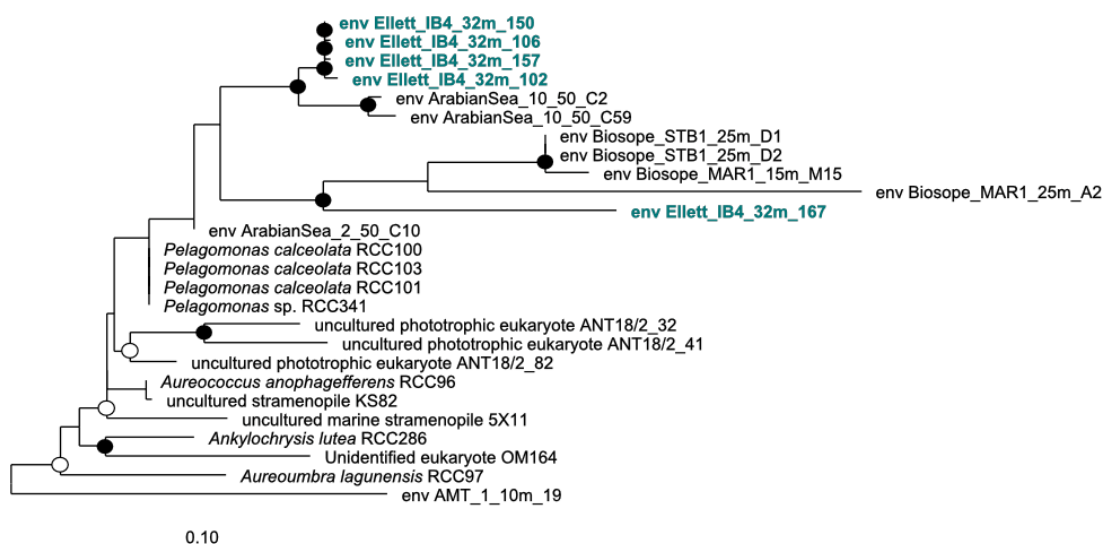


**Figure 4.17.** Phylogenetic relationships amongst the Pelagophyceae using plastid 16S rRNA gene sequences and a neighbour-joining algorithm. Sequences from the extended Ellett Line are highlighted in blue. Bootstrap values above 70% are marked with an open circle, values above 90% are marked with a filled circle.

#### 4.2.6. Photosynthetic picoeukaryote community composition along the extended Ellett Line transect evidenced by fluorescent *in situ* hybridisation (FISH) analysis

As a PCR-independent method, the use of FISH has given additional insight into some of the biases encountered when using PCR-dependent methods. Prymnesiophyceae, Prasinophyceae clade II, Chrysophyceae, Cryptophyceae and Pelagophyceae were all detected along the extended Ellett Line by fluorescent *in situ* hybridisation (FISH) (Table 4.2). As anticipated by dot blot hybridisation and clone library analysis, Prymnesiophyceae were very abundant in FISH samples (Table 4.2). Approximately one-third of positively labelled Prymnesiophyceae cells were larger than 3  $\mu\text{m}$  in diameter (Table 4.3), despite samples being pre-filtered through a 3  $\mu\text{m}$  pore-size mesh during preparation of the samples. However, cells which labelled with all other class-specific probe combinations were <3  $\mu\text{m}$  in size.

In 6 of the 13 samples, members of Prasinophyceae clade II were more abundant than the Prymnesiophyceae. Thus, FISH confirmed the bias against Prasinophyceae clade II using methods relying on PCR amplification of the partial plastid 16S SSU rRNA gene. This had been indicated in the comparison between AMT 18S and 16S SSU rRNA gene libraries (see section 3.2.6.) where Prasinophyceae clade II-related

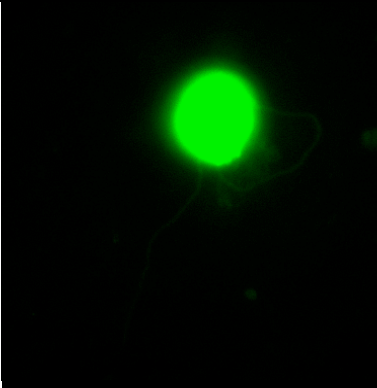
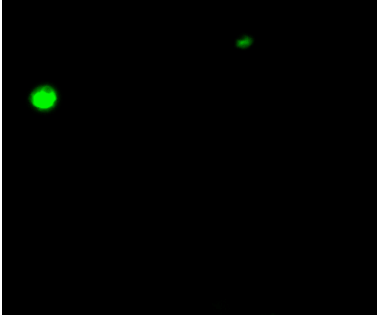
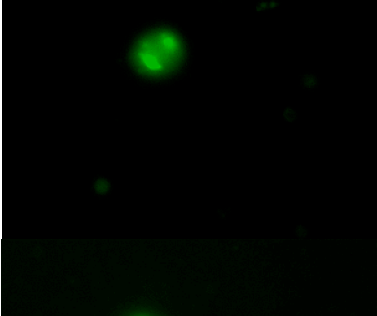
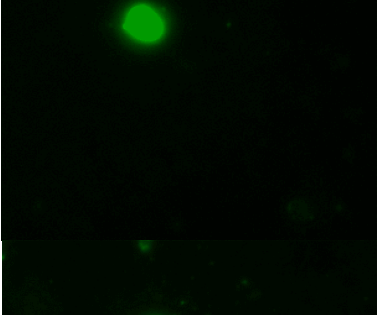
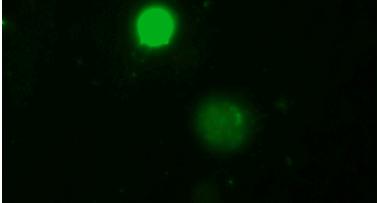
sequences were abundant in 18S SSU rRNA gene libraries, but only sparsely observed in 16S SSU rRNA gene libraries. Here, FISH showed that this group was as abundant as the Prymnesiophyceae along the extended Ellett Line, despite accounting for less than 20% of plastid 16S rRNA clones.

The Prymnesiophyceae and Prasinophyceae clade II were substantially more abundant than the other classes analysed. The Chrysophyceae, Cryptophyceae and Pelagophyceae appeared to be very minor components of the PPE community based on this FISH analysis. The use of a probe targeting the plastid 16S SSU rRNA of the Chrysophyceae revealed that these organisms generally appear to have two chloroplasts per cell (Table 4.3.).

**Table 4.2.** Results of fluorescent *in situ* hybridisation (FISH) along the extended Ellett Line. For each sample, total eukaryotes (including heterotrophs) cells ml<sup>-1</sup> as counted by FISH using probes EUK1209r, NCHLO01 and CHLO02 together are shown. The class-specific FISH results are expressed as cells ml<sup>-1</sup> (black) and as a percentage of total eukaryotes by FISH (blue).

Station	Depth	Total EUKS	Results = cells ml <sup>-1</sup> and % of total eukaryotes				
			Pras II	Prym	Chry	Cryp	Pela
IB21S	5 m	2.01×10 <sup>4</sup>	1.02×10 <sup>4</sup> 50.6	6.66×10 <sup>3</sup> 33.1	0 0.0	10 0.0	10 0.0
	10 m	2.85×10 <sup>4</sup>	2.07×10 <sup>3</sup> 7.3	2.32×10 <sup>3</sup> 8.1	28 0.1	9 0.0	17 0.1
	20 m	2.18×10 <sup>4</sup>	2.74×10 <sup>3</sup> 12.6	1.00×10 <sup>3</sup> 4.6	25 0.1	18 0.1	14 0.1
	32 m	7.19×10 <sup>3</sup>	9.51×10 <sup>2</sup> 13.2	6.31×10 <sup>2</sup> 8.8	0 0.0	5 0.1	16 0.2
Rockall F	5 m	1.13×10 <sup>4</sup>	3.11×10 <sup>2</sup> 2.8	1.96×10 <sup>3</sup> 17.4	4 0.0	1 0.0	70 0.6
	10 m	9.53×10 <sup>3</sup>	4.14×10 <sup>2</sup> 4.3	3.52×10 <sup>3</sup> 37.0	0 0.0	4 0.0	95 1.0
	20 m	1.67×10 <sup>4</sup>	2.13×10 <sup>2</sup> 1.3	4.80×10 <sup>3</sup> 28.7	12 0.1	2 0.0	39 0.2
Rockall N	5 m	2.47×10 <sup>4</sup>	1.11×10 <sup>4</sup> 44.8	1.19×10 <sup>4</sup> 48.0	96 0.4	7 0.0	63 0.3
	10 m	1.80×10 <sup>4</sup>	5.55×10 <sup>3</sup> 30.9	3.68×10 <sup>2</sup> 2.0	7 0.0	2 0.0	24 0.1
	20 m	1.99×10 <sup>3</sup>	1.75×10 <sup>2</sup> 8.8	32 1.6	5 0.3	0 0.0	3 0.2
9GA	5 m	1.30×10 <sup>3</sup>	0 0.0	44 3.4	0 0.0	0 0.0	1 0.1
	10 m	3.25×10 <sup>3</sup>	62 1.9	41 1.3	7 0.2	1 0.0	0 0.0
	20 m	3.84×10 <sup>2</sup>	16 4.2	16 4.2	0 0.0	0 0.0	2 0.5

**Table 4.3.** Fluorescent microscope images of cells observed for each class identified by FISH along the extended Ellett Line transect.

Class	Representative Fluorescent Microscope Image	Example Cell Dimensions	Probe Target
Prymnesiophyceae		6.9×6 μm	Nuclear SSU rRNA
Prasinophyceae II		3×2.6 μm and 1.4×1.2 μm	Nuclear SSU rRNA
Chrysophyceae		3.2×2.6 μm	Plastid SSU rRNA
Cryptophyceae		2.3×2.2 μm	Nuclear SSU rRNA
Pelagophyceae		2.8×2.4 μm	Nuclear SSU rRNA

### 4.3. Discussion

Average concentrations of chlorophyll *a* along the extended Ellett Line were comparable to those measured along AMT15 except in the Wyville-Thomson ridge area where chlorophyll concentrations were much higher. Average concentrations of silicate and phosphate were similar to the average along AMT15 and lower than those in the mesotrophic regions of AMT15. In contrast, the average combined concentration of nitrate and nitrite along the extended Ellett line are double that along AMT15, and a quarter higher than the average concentrations in the mesotrophic regions of AMT15.

Despite a fairly small difference in chemical concentration between the extended Ellett Line and AMT15, the flow cytometry data showed a very marked difference in PPE cell numbers between these two transects. *Prochlorococcus* was never detected along the extended Ellett Line by flow cytometry. This observation is in agreement with those in the PRIME study to the south of the Icelandic Basin (Tarran *et al.*, 2001). *Prochlorococcus* cells are generally only found between 40°N and 40°S and are not able to tolerate the temperatures encountered by the extended Ellett Line and PRIME transects (Partensky *et al.*, 1999).

*Synechococcus* and photosynthetic eukaryote abundances were substantially higher than along AMT15 where on average they were only one-fifth of the mean numbers detected along the extended Ellett Line. Even when only the mesotrophic regions of AMT15 are taken into account, cell numbers were less than half the average numbers along the Ellett Line for photosynthetic eukaryotes and *Synechococcus*. These cell numbers, peaking at  $3.9 \times 10^4$  cells ml<sup>-1</sup> at IB4 at 5 m depth for photosynthetic eukaryotes and  $5.26 \times 10^5$  cells ml<sup>-1</sup> at Rockall station N at 5 m depth for *Synechococcus*, were comparable, but slightly higher than those recorded for the northern end of the PRIME cruise, around 59°N 20°W in 1996 (Tarran *et al.*, 2001) where PPEs reached  $1.23 \times 10^4$  cells ml<sup>-1</sup> and *Synechococcus* reached  $2.18 \times 10^5$  cells ml<sup>-1</sup>.

As with dot blot hybridisation data from the AMT (see chapter 3), the sum of percentage relative hybridisation for individual samples was usually much lower than

100%, at approximately 50% on average over the transect. The clone library data for Ellett Line stations IB4 and EG3 showed that 24% and 30% of the clones were related to classes not targeted by the probes used for dot blot hybridisation, which may account for a substantial proportion of this discrepancy. In particular, almost 20% of clones in both libraries were affiliated with the Prasinophyceae.

Of the ten probes used in dot blot hybridisations, five reached percent relative hybridisation values of 2% considered to be above background levels. These class specific probes were the same as those considered above background along AMT15, with the exception of two minor classes along AMT15, Trebouxiophyceae and Eustigmatophyceae. A large proportion of the variation in dot blot hybridisation data could be explained by the environmental variables measured along the extended Ellett Line (84%), whereas only approximately half of the variation in dot blot hybridisation data could be explained by environmental variables along AMT15 (see section 3.2.5), despite fewer parameters being measured along the extended Ellett Line. This may simply be due to the much smaller number of samples included in the extended Ellett Line CCA ( $n=24$  for the extended Ellett Line in contrast to  $n=78$  for AMT15), and hence there is potentially less diversity to be explained by the model.

Prymnesiophyceae was the major class detected in dot blot hybridisation analysis along the extended Ellett Line. The Prymnesiophyceae was found to be a major class contributing to the nanophytoplankton in the same area (Moore *et al.*, 2005). The position of this class in the CCA plot of constrained axes 1 and 2, at right angles to the positions of the major environmental variables associated with the diversity data indicates the distribution of this class is not strongly influenced by the variables plotted on these axes (Fig. 4.7). The distribution of the Prymnesiophyceae is therefore primarily influenced by factors that have not been measured here and remain to be identified. The dominance of Prymnesiophyceae in the PPE community as evidenced by dot blot hybridisation data mirrors that found along AMT15 (see section 3.2), the pelagic Arabian Sea (Fuller *et al.*, 2006a), the coastal Mediterranean Sea (McDonald *et al.*, 2007) and in a transect through the South-East Pacific Ocean, including some of the most oligotrophic waters on Earth (Lèpere *et al.*, in press). In addition, sequences of Prymnesiophyceae origin have been frequently found in

nuclear SSU rRNA gene libraries from a range of locations including the Pacific Ocean (Moon van der Staay *et al.*, 2001), the mesotrophic coastal Pacific (Worden, 2006), Weddell Sea, Scotia Sea and Mediterranean Sea (Diez *et al.*, 2001), as well as the Arctic Ocean (Lovejoy *et al.*, 2006), Arctic-Atlantic convergence area (Hamilton *et al.*, 2008), English Channel (Vaulot *et al.*, 2002) and North West Mediterranean Sea (Massana *et al.*, 2004). The only exception was a nuclear SSU rRNA gene library constructed from a sample taken from the North Atlantic which did not contain any sequences related to the Prymnesiophyceae (Diez *et al.*, 2001). However, only 17 clones were analysed from this library so, given the apparent ubiquitous nature of the class indicated by numerous other studies, it seems very likely that, had more clones been analysed, sequences related to the Prymnesiophyceae would have been discovered. Whilst these libraries are usually dominated by sequences of heterotrophic lineages, when only suspected photosynthetic classes are considered, Prymnesiophyceae are often among the most abundant sequences. Furthermore, due to the high GC content of the nuclear genomes of Prymnesiophyceae, it is suggested the Prymnesiophyceae genes are not readily amplified by PCR with general eukaryotic primers, thus this class is often underestimated (Liu *et al.*, 2009). These authors suggest that exploitation of plastid genes may circumvent this bias as plastid genomes are rarely GC rich. Studies using the PCR independent FISH analysis of Norwegian and Barents Seas concluded the Prymnesiophyceae were important in Atlantic water masses and in particular open sea waters (Not *et al.*, 2005). This study suggested this class was less important in productive and coastal waters. However, their abundance in the productive extended Ellett Line waters and coastal Mediterranean Sea (McDonald *et al.*, 2007) as well as in a coastal Pacific clone library (Worden, 2006) supports the idea that the Prymnesiophyceae represent a ubiquitous, and abundant marine class within the PPE community and are therefore likely to be major players in global marine carbon cycling.

In contrast to the dot blot hybridisation data obtained for AMT15, the Cryptophyceae were the next most abundant class along the extended Ellett Line, reaching peak hybridisation values towards the coast of Iceland. Along AMT15, this class was restricted to the upwelling and coastal areas. Members of the Cryptophyceae have been found to be abundant at a number of coastal sites by various methods (Romari and Vaulot, 2004; McDonald *et al.*, 2007; Not *et al.*, 2007). Indeed, CCA showed



this class was highly associated with the nutrient variables nitrate, nitrite and phosphate both along the extended Ellett Line (Fig. 4.7) and AMT15 (see section 3.2.3).

The Chrysophyceae relative hybridisation values peaked at station IB4, but remained low over the rest of the transect. Hence, this class appears to be of less importance to the PPE community along the extended Ellett Line than along AMT15, or in the Gulf of Naples (McDonald *et al.*, 2007) or the Arabian Sea (Fuller *et al.*, 2006a). Even so, this class still appears to be a fairly important contributor to the PPE community along the transect. In contrast, Chrysophyceae have rarely been observed in nuclear SSU rRNA libraries, though when found these are from diverse sampling regions (Díez *et al.*, 2001; Worden *et al.*, 2006). Recently however, Shi *et al.* (submitted) demonstrated the presence of large numbers of nuclear SSU rRNA gene sequences affiliated to the Chrysophyceae from oligotrophic waters in the South-East Pacific Ocean. These sequences were derived from pico-sized ‘photosynthetic’ eukaryotic cells sorted by flow cytometry prior to DNA extraction and PCR amplification. This reiterates the problem of previous nuclear SSU rRNA libraries over-representing heterotrophic sequences, to the detriment of obtaining a ‘complete’ picture of the PPE community. Hence, it appears that the Chrysophyceae can be detected using a range of methods and across a plethora of different ocean regions indicating that they are an important class in marine systems and reinforcing the need to study this group further. Interestingly, the CCA analysis showed Chrysophyceae distribution patterns along the extended Ellett Line to be associated with higher values of temperature and *Synechococcus* abundance, but low nutrient concentrations. However, along AMT15, Chrysophyceae abundance was largely unrelated to these variables, potentially suggesting different Chrysophyceae populations in these regions.

Other classes detected along the extended Ellett Line were substantially less abundant than the Prymnesiophyceae, Cryptophyceae and Chrysophyceae. Minor classes were the Pelagophyceae, reaching 25% relative hybridisation at station IB4; and the Pinguiphyceae reaching 3% at Rockall station N. Pelagophyceae reached a peak of 6.75% in the Gulf of Naples in February 2004, but remained undetected over most of the rest of that time series whilst Pinguiphyceae were also undetected in the Naples study (McDonald *et al.*, 2007). Pelagophyceae and Pinguiphyceae are

largely absent from many 18S rRNA gene clone library studies (e.g. Moon van der Staay *et al.*, 2001, Romari and Vaultot, 2004; Massana *et al.*, 2004). However, 18S rRNA gene clone libraries from the Sargasso Sea contained a small number of sequences closely related to the Pelagophyceae (Not *et al.*, 2007b). The extended Ellett Line appears to include an unusually high abundance of Pelagophyceae. CCA showed this class to be most strongly associated with axis 3 linked with higher salt levels and nitrate, nitrite and phosphate concentrations. The Pinguiphyceae are most strongly associated with axis 4, which is not strongly linked with any of the measured environmental variables.

Overall, CCA showed the variation in PPE class diversity to be fairly strongly influenced by the environmental variables of temperature, *Synechococcus*, salinity, nitrate and nitrite and phosphate. Temperature and salinity at the sea surface have been shown to be quite strongly related to the assemblages of the photosynthetic nanoeukaryotes coccolithophores and dinocysts inferred from fossils in the sediment in a very similar area to that studied here (Solignac *et al.*, 2008). Salinity and temperature are indicators of different water masses, and many water masses come together in the hydrographically complex Rockall channel. In particular, warm saline water of the Gulf Stream crosses the channel from the south in addition to North Atlantic central water, cooler, lower salinity north western oceanic polar front water and higher salinity water of Mediterranean origin (Ellett *et al.*, 1986). Similarly, factors including salinity were important in determining the PPE community structure of a region of convergence of water masses in the Arctic (Hamilton *et al.*, 2008). Salinity may have an increased effect on the ecology of the northern north Atlantic as climate change in the Arctic causes reduced ice cover and discharge of low salinity, colder water into the Atlantic. This has been shown to expand the biogeographic ranges of phytoplankton as well as fish species northwards from the subtropics in the east and southwards for boreal species in the western north Atlantic (Greene *et al.*, 2008). The abundance of *Synechococcus* cells appeared to be an important factor shown by CCA to be potentially linked to the distribution of PPE classes. This may be a proxy for phototrophic biomass, found to be an important determinant in PPE assemblages in the Arctic. The concentration of chlorophyll *a* was included in the CCA separately, but added little to the model's ability to explain the dot blot hybridisation data. Correlation analysis showed chlorophyll *a*

concentration was closely correlated with *Synechococcus* abundance and thus was redundant in the model. As with the AMT data (see section 3.2.4) the addition of either nitrate or phosphate to the model has little effect on the amount of variation in dot blot hybridisation data that could be explained in the absence of the other. This is likely to be explained by the notion that both of these nutrients can limit growth of PPEs. Thus, if the concentration of one of these increases the PPE growth will remain limited unless the other nutrient increases. This has also been asserted for a freshwater pond with experimentally altered nitrate and phosphate concentrations (Fried *et al.*, 2003).

Clone libraries generally supported the dot blot hybridisation data, with the presence of sequences related to Chrysophyceae and Pelagophyceae being present in the library from station IB4 at 32 m, but not station EG3 at 10 m where relative hybridisation values had been 46% and 0% respectively for Chrysophyceae and 16% and 4% for Pelagophyceae. Both libraries were dominated by sequences related to the Prymnesiophyceae, in agreement with the dominance of this class along the extended Ellett Line as evidenced by dot blot hybridisation. However, at station IB4 32 m there is some discrepancy between the composition of the clone libraries and the hybridisation data which is more difficult to explain, though perhaps reflecting some bias against the Prymnesiophyceae of the dot blot hybridisation method.

Sequences related to the Prymnesiophyceae were phylogenetically diverse in the extended Ellett Line clone libraries with eight RFLP types observed that were not seen in libraries from AMT15. A number of sequences from the EG3 library (Wyville-Thomson Ridge) fell within a cluster containing *Chrysochromulina polylepsis* and *Imantonia rotunda* and environmental sequences from the Pacific within a clade designated Prym16S\_II (Lepère *et al.*, 2009) as well as sequences from the Mediterranean Sea (McDonald *et al.*, 2007). The *Chrysochromulina* are a very diverse group with some picoplanktonic species (Vaulot *et al.*, 2008), and sequences related to this group are common in nuclear rRNA gene clone libraries from various regions (e.g. see Moon van der Staay *et al.*, 2001; Not *et al.*, 2007b). Collectively, there are several lineages within the Prymnesiophyceae (Fig. 4.12) containing no cultured representatives. This is likely to be due to lack of cultured organisms, but also to an incomplete inventory of plastid rRNA genes in this class.

These lineages contain environmental sequences from the extended Ellett Line as well as the Atlantic Ocean (see section 3.2.6.1), Mediterranean Sea (McDonald *et al.*, 2007), Arabian Sea (Fuller *et al.*, 2006b), Pacific Ocean (Lepère *et al.*, 2009) and equatorial Atlantic Ocean (Jardillier *et al.*, submitted) illustrating the globally widespread nature of these lineages. Sequencing the plastid SSU rRNA genes of remaining available cultures, as well as a continued effort to culture Prymnesiophyceae from the pico-size range may clarify the identity of organisms represented by these environmental sequences.

Five clones from station IB4 represented an RFLP type seen in the AMT northern temperate clone library, phylogenetically branching within the Chrysophyceae. Environmental sequences from other cruises, e.g. the Arabian Sea (Fuller *et al.*, 2006b) appear to show the same level of micro-diversity within the Chrysophyceae. However, the extended Ellett Line stands apart from other cruises as libraries contained few clones related to Chrysophyceae and these all fell into the same RFLP type.

Several RFLP types in both libraries from stations IB4 and EG3 belonged to sequences related to the Prasinophyceae. These clones accounted for approximately 19% of the clones analysed, but 25% of the RFLP types observed in the library for station EG3 (Wyville-Thomson Ridge). This group were less diverse in the library for station IB4 (Icelandic Basin), accounting for 17% of clones analysed and 15% of RFLP types observed. This class accounts for the largest proportion of picoeukaryote cultures currently maintained (Vaulot *et al.*, 2008). However, the major lineage identified here designated Pras16S-VIII in the plastid phylogeny (Fig. 4.16) contains no sequences from cultured organisms. Similarly, there are lineages defined by sequencing of the nuclear SSU gene e.g. VIII and IX that also contain no cultured counterparts (see Viprey *et al.*, 2008). Hence, one or more of these may correspond to the lineages reported here. Certainly, the microdiversity observed within the Prasinophyceae may arise from niche exploitation of high- and low-light adapted ecotypes similar to that observed within *Ostreococcus* strains (e.g. see Rodriguez *et al.*, 2005).

FISH confirmed the dominance of Prymnesiophyceae (Table 4.1) along the extended Ellett Line transect, which had been indicated by dot blot hybridisation. However, the overwhelming dominance of this class using FISH technology perhaps indicates that the Prymnesiophyceae may be under-represented by dot blot hybridisation methodology. Indeed, libraries also indicated a higher abundance of members of the Prymnesiophyceae than was predicted by dot blot hybridisation analysis, although still much lower than the abundance indicated by FISH. Thus, although dot blot hybridisation analyses were dominated by Prymnesiophyceae, members of this class may be even more abundant than this method suggests. Indeed, *19'-hexanoyloxyfucoxanthin*, a diagnostic accessory pigment for the Prymnesiophyceae has been found to be omnipresent in the world ocean and recent data suggest that prymnesiophytes contribute 30-50% of the total photosynthetic standing stock of the world's oceans (Liu *et al.*, 2009). FISH analysis revealed that approximately one third of cells that labelled with the Prymnesiophyceae probe were larger than 3  $\mu\text{m}$  (Table 4.2). These cells hence appear to be capable of passing through 3  $\mu\text{m}$  pore-sized filters whilst still intact. Indeed, many of these larger cells observed by FISH had clearly intact flagella. This appears to be a common phenomenon and has been observed elsewhere (F. Not personal communication).

Also well represented by FISH analysis were members of Prasinophyceae clade II. This group dominates the PPE community in coastal and nutrient-rich areas (Not *et al.*, 2004), whereas Prymnesiophyceae members of the picoplankton community are widespread in open ocean environments (Not *et al.*, 2005). The fact that these two classes co-occur at similar levels along the extended Ellett Line transect, perhaps suggests the physical and chemical environments here show features intermediate between coastal and open ocean waters.

Despite being a major component of the PPE community by dot-blot hybridisation analysis, Cryptophyceae were only detected in small numbers by FISH. In particular, station IB21S had a dot blot hybridisation value of 70% for Cryptophyceae at 32 m depth whereas FISH analysis indicated this class was present at an abundance of only 5 cells  $\text{ml}^{-1}$  in this sample. Similarly, a study of the phytoplankton diversity of North-

west Iberian coastal sites found that the same FISH probe for Cryptophyceae identification labelled only a minor fraction of cells, although pigment analysis indicated that cryptophytes were a major contributor to chlorophyll *a* concentration of the region (Not *et al.*, 2007a). This may be due to the presence of Cryptophyceae plastids in the dinoflagellate genus *Dinophysis*, consisting of cells usually around 50 µm in length and commonly found in cold temperate waters of the northern hemisphere (Okolodkov, 2005). *Dinophysis* cells would not be detected by the nuclear 18S rRNA-targeted FISH probes, but methods targeting Cryptophyceae plastids such as the 16S rRNA gene dot blot hybridisations, and the pigment analysis described by Not *et al.* (2007a) would detect *Dinophysis* species. Indeed, comparisons of nuclear and plastid SSU rRNA gene libraries along AMT15 (section 3.2.4) yielded slightly more Cryptophyceae-related sequences in plastid than nuclear SSU rRNA gene clone libraries, though the class was far less abundant along AMT15 than along the extended Ellett line by all methods.

Similarly, FISH data indicated that the Chrysophyceae were a minor class along the extended Ellett line. However, filters collected at station IB4, where relative hybridisation values for the Chrysophyceae were highest, were not used due to paraformaldehyde precipitation. Along the rest of the transect relative hybridisation values for the class were lower. The use of the FISH probe targeting the 16S rRNA highlighted the presence of two plastids in the positively labelled cells (table 4.3), which may result in methods relying on PCR amplification of plastid SSU rRNA genes overstating the abundance of this class.

**Chapter 5:**

**Photosynthetic picoeukaryote community structure  
across major ocean basins**

## 5.1. Introduction

PPE community structure in the Arctic and Indian Oceans or along the Beagle cruise transect which circumnavigated the world has not previously been determined using the plastid 16S rRNA gene marker with dot blot hybridisation analysis. These, together with data from the Atlantic Meridional Transect and extended Ellett Line (presented in chapters 3 and 4 respectively), and published data from the Arabian Sea (Fuller *et al.*, 2006a) and the Pacific Ocean (Lepère *et al.*, 2009) are collated in order to identify general trends over this range of ocean regimes. In addition, multivariate statistics are performed on this extended dataset, to link these trends to some of the physical, chemical and biological parameters recorded during the studied cruises.

### 5.1.1. Introduction to the Arctic Ocean cruise

The Arctic Ocean was sampled in August 2002. The cruise (Fig. 5.1) was mainly in the Atlantic Arctic province (ARCT), briefly crossing into the boreal polar province (BPLR) defined by Longhurst (2007). These provinces are characterised by low temperatures, high salinity and an extreme irradiance cycle as summers are perpetually light and winters perpetually dark. The ARCT province experiences a spring bloom dominated by diatoms and large prymnesiophytes. Thus, the province is highly productive, but the picophytoplankton are considered to be relatively unimportant compared with lower latitudes (Longhurst, 2007). The BPLR province includes permanently ice-covered water and water that freezes over winter, causing higher variability in salinity than other provinces.

The ice and cavities within it provides a habitat for phytoplankton. Phytoplankton can also grow under ice when light is not stopped from passing through by snow cover. A study of partial 16S rRNA genes amplified from sea ice in both the Arctic and Antarctic retrieved many algal plastid sequences in addition to heterotrophic bacterial sequences (Brown and Bowman, 2001). Photosynthesis even occurs within snow, in the high Arctic where irradiance is high, the nano-sized (approximately 10 µm diameter) Chlorophyceae *Chlamydomonas nivalis* grows in the liquid water within pack snow between the surface and up to 3 cm deep (Stibal *et al.*, 2007). At the ice edge interface, the centric diatom *Melosira arctica* dominates the algal



biomass but with an uneven distribution (Gosselin *et al.*, 1997). This study found that algal cells of  $>5 \mu\text{m}$  dominated the algal biomass of sea ice whereas small cells ( $0.7\text{--}5 \mu\text{m}$ ) dominated the algal biomass of the water column underneath sea ice (Gosselin *et al.*, 1997). Where ice is only present at certain times of the year, an interesting phenomenon is observed where algal cells become trapped in ice crystals as ice forms and, later in the year, as the ice melts, these cells either sink as large flocs or seed the new phytoplankton community (Gradinger and Ikävalko, 1998; Longhurst, 2007).

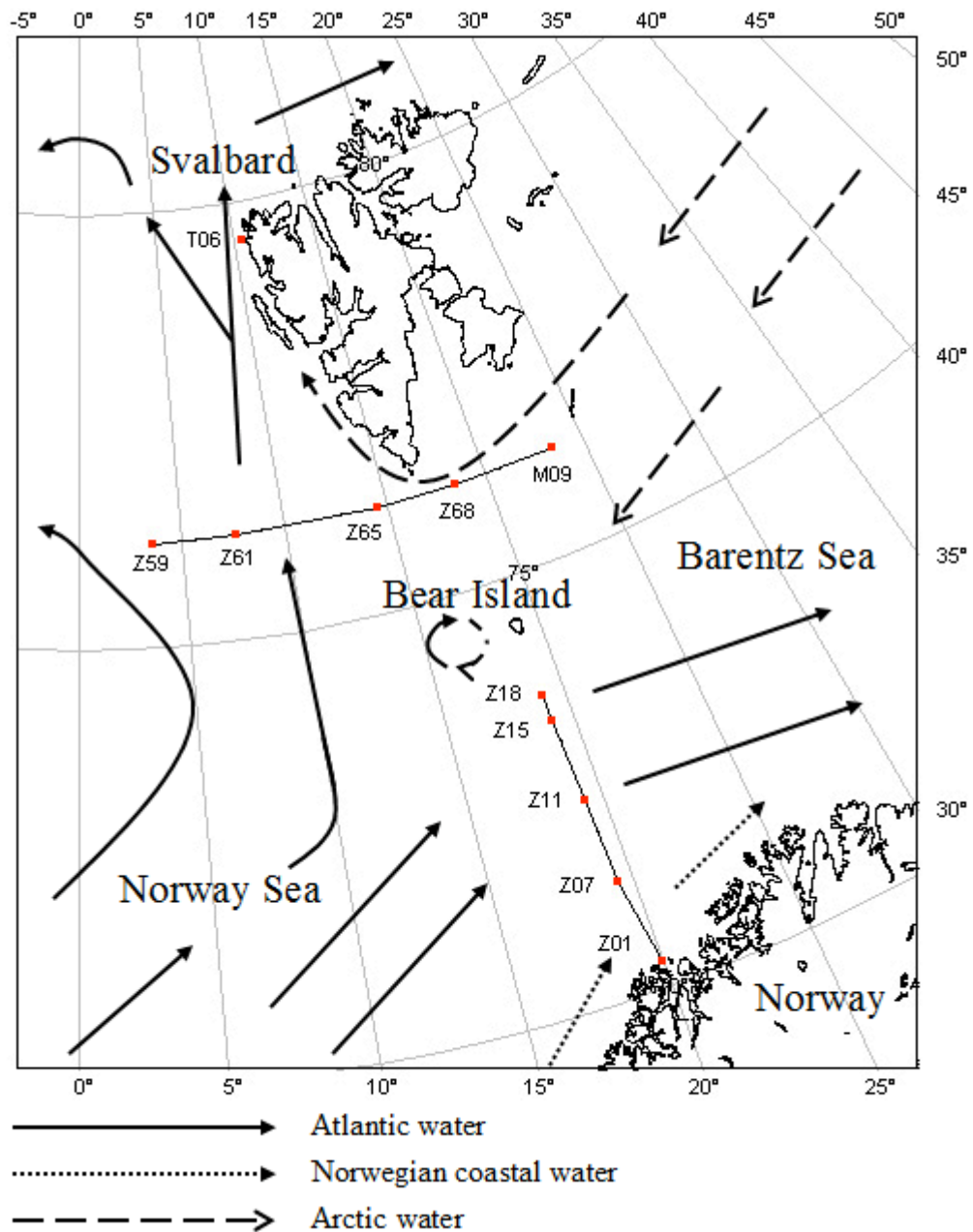


**Figure 5.1.** Map illustrating the position of stations sampled in the Arctic Ocean in 2002 used for dot blot hybridisation analysis.

Members of the Arctic Ocean marine microbial community have been studied by molecular methods. In particular the bacterioplankton and archaeal community structure has been studied (Bano and Hollibaugh, 2002; Bano *et al.*, 2004 respectively) and the latter compared between the Arctic and Antarctic. Many archaeal groups were found to be present in both locations, but with differences in the relative abundance of key groups, in addition to the observation of higher diversity at greater depths in Arctic waters (Bano *et al.*, 2004).

The photosynthetic prokaryotic community structure has been studied by dot blot hybridisation using ecotype-specific *Synechococcus* and *Prochlorococcus* probes by Zwirgmaier *et al.* (2007), who found that *Synechococcus* clades I and IV dominated these samples with very little contribution from other clades. Due to the high latitude, *Prochlorococcus* cells were undetected, as found along the Ellett Line by flow cytometry (see section 4.2.2). The dominance of clades I and IV was also found in the coastal boundary province of higher latitudes in this global study (Zwirgmaier *et al.*, 2007). Although Longhurst (2007) does not consider the coastal regions of the Arctic Ocean to be part of the global coastal province, this study shows that the provinces (excluding the coastal province of the tropical and subtropical regions) share similarity in their photosynthetic prokaryotic community structures.

In contrast to other regions, the photosynthetic microbial community in the Canadian Arctic Ocean has been found to be numerically dominated by eukaryotes (Tremblay *et al.*, 2009). The PPE community structure has been studied previously in the Arctic, by various methods. Pigment and fluorescent *in situ* hybridisation analyses suggest that the dominant PPEs in the Arctic Ocean belong to Prasinophyceae clade II (Not *et al.*, 2005; Lovejoy *et al.*, 2007; Tremblay *et al.*, 2009). However, this is not strictly supported by studies using PCR-based methods targeting the nuclear SSU rRNA gene. Clone libraries constructed from four sites in the Arctic Ocean contained many clones related to the Dinophyceae whose trophic mode could not be resolved. Clones related to photosynthetic classes belonged to the Prasinophyceae, Prymnesiophyceae, Cryptophyceae, Chrysophyceae, Chlorarachniophyceae and a novel class, probably the Picobiliphyceae (Lovejoy *et al.*, 2006), but were not found in all the libraries. In the north of Baffin Bay, denaturing gradient gel electrophoresis (DGGE) analysis was used targeting the nuclear SSU rRNA gene (Hamilton *et al.*, 2008). This study

revealed the dominance of the newly discovered Picobiliphyceae, which were represented by 17 sequences, whereas Prasinophyceae and Prymnesiophyceae, which dominate sequence analyses targeting the nuclear SSU rRNA genes of communities sampled from diverse regions of the world (Moon van der Staay *et al.*, 2001; Díez *et al.*, 2001; Vaultot *et al.*, 2002; Massana *et al.*, 2004; Worden, 2006), were represented by only 5 and 3 sequences respectively (Hamilton *et al.*, 2008).

### **5.1.2. Introduction to the Indian Ocean Cruise VANC10MV**

The Indian Ocean is the third largest ocean basin, stretching from Africa in the west to Australia in the east. However, it has been relatively neglected in studies except for the north-western section occupied by the Arabian Sea (Longhurst, 2007). The stretch traversed by the VANC10MV cruise (Fig. 5.2) mostly fell into the Indian South Subtropical Gyre province (ISSG), with a small number of stations sampled in the Eastern Africa Coastal province (EAFR) as defined by Longhurst (2007). The ISSG province has characteristically clear waters with low chlorophyll *a* concentrations. Unique open-ocean upwelling patterns lead to areas of elevated chlorophyll concentration as a result of unusual wind action (Xie *et al.*, 2002). Higher chlorophyll regions are observed along the South Equatorial Current, an eddy field to the west of Australia during late austral winter, in the Madagascar Basin which usually experiences a phytoplankton bloom in February, dendritic in shape due to the dynamics of the water caused by a fairly dense eddy field, and at shallow banks which are the site of distinct seasonal blooms (Longhurst, 2007).

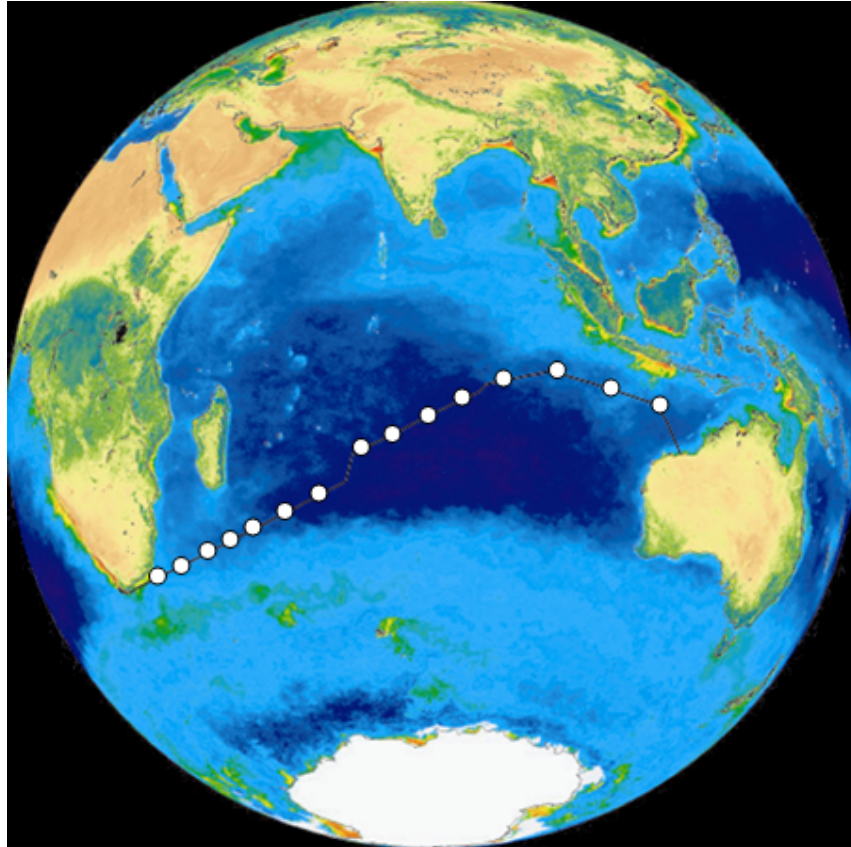


**Figure 5.2.** Map illustrating the position of stations sampled in the Indian Ocean in 2003 used for dot blot hybridisation analysis.

There are few studies of microbial ecology in the southern Indian Ocean, although the Arabian Sea has been relatively well studied. Samples from the VANC10MV cruise have already been analysed by molecular methods, providing some insights into the ecology of small eukaryotes and picophytoplankton in the region. The uncultured heterotrophic flagellates of marine stramenopiles group 4 (MAST-4) were studied by quantitative-PCR (Q-PCR) for a number of cruises including VANC10MV. They were found to be abundant around the deep chlorophyll maximum level and less abundant at the surface, possibly due to sensitivity to UV radiation. They were also not found much deeper than the photic zone and thus may represent important grazers of the photosynthetic plankton (Rodríguez-Martínez *et al.*, 2009).

Along the VANC10MV transect, 90% of chlorophyll *a* was accounted for by picophytoplankton. As was the case along AMT15 (see section 3.2.2), *Prochlorococcus* dominated the picophytoplankton of the oligotrophic gyre region, whilst *Synechococcus* dominated higher nutrient regions, and PPEs co-varied with

the *Synechococcus* (Not *et al.*, 2008). A more detailed study into *Prochlorococcus* and *Synechococcus* ecotype biogeography showed that three *Prochlorococcus* ecotypes were detected with distinct partitioning in the ISSG province: the low light ecotype was found over the province at approximately 75 m and deeper, high-light group I was found above 100 m deep in the west of the transect and high-light group II was primarily found above 50 m deep in the east of the transect. The EAFR province was dominated by *Synechococcus* clades II and V/VI/VII (detected together), particularly in surface waters (Zwirgmaier *et al.*, 2008).

A variety of molecular approaches as well as pigment analyses were used to assess the protist community structure, focusing on picoeukaryotes. This found Chlorophyceae (in particular belonging to Prasinophyceae clade II) to be important in the EAFR, whilst the Prymnesiophyceae were dominant in the ISSG (Not *et al.*, 2008). This coastal importance of Prasinophyceae and open ocean importance of Prymnesiophyceae has also been observed in other regions (Not *et al.*, 2005).

### **5.1.3. Introduction to the ‘Blue EArth GLobal Expedition’ (BEAGLE) cruise**

The Beagle cruise was a multidisciplinary expedition which circumnavigated the southern hemisphere (Uchida and Fukasawa, 2005). The cruise was achieved in 6 legs. Leg 1 occupied stations in the Pacific ocean between Brisbane, Australia and Tahiti; leg 2 occupied Pacific stations from Tahiti to South America; leg 3 bounded the coast line of South America; leg 4 occupied Atlantic stations between America and Africa; leg 5 occupied Indian Ocean stations between Africa and Freemantle, Australia; and finally leg 6 occupied an area to the south west of Australia, stretching to 58°S (Fig. 5.3).

The BEAGLE cruise legs 1, 2, 4 and 5 resampled 493 stations explored by the World Ocean Circulation Experiment (WOCE) of the early 1990’s so that data could be compared with that collected a decade earlier (Uchida and Fukasawa, 2005). Furthermore, 62 Argo floats were deployed to allow monitoring of temperature and circulation changes which may be associated with global climate change (Uchida and Fukasawa, 2005).

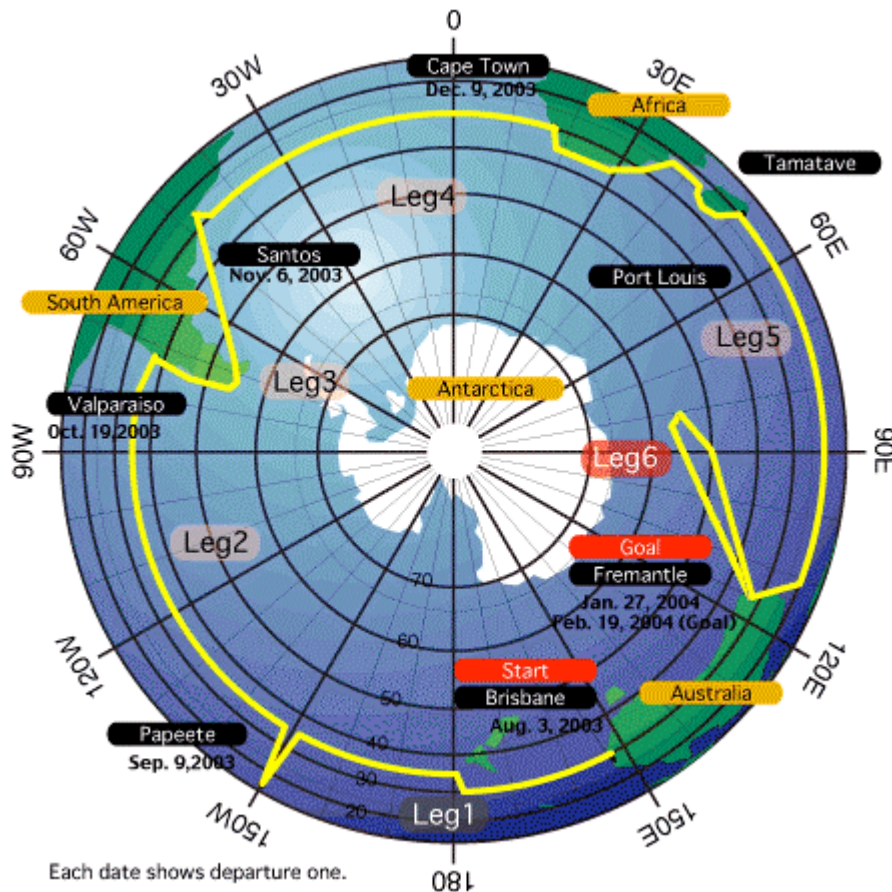


**Figure 5.3.** Map displaying the cruise track (yellow line) taken by the BEAGLE project August 2003 - January 2004. Image retrieved from IOCCP.org.

Whilst the BEAGLE cruise was largely focussed on chemical and physical oceanography, samples from legs 1, 2, 4 and 5 of the expedition have been analysed by marine ecologists interested in picophytoplankton community structure. In particular, along leg 2 of the cruise, picoplankton distribution was determined by flow cytometry (Grob *et al.*, 2007). Although, as found in other studies, *Prochlorococcus* was numerically dominant in the oligotrophic gyre, PPEs dominated the pico-sized autotrophic biomass and even contributed more to the <2  $\mu\text{m}$  biomass than the heterotrophic bacteria (Grob *et al.*, 2007). This is a surprising finding as cyanobacteria were expected to dominate primary production in the South Pacific gyre.

The phytoplankton community has also been studied along the BEAGLE transect by analysis of diagnostic pigments, allowing conclusions to be drawn both on the community structure and acclimation of the component cells to environmental parameters, in particular the acclimation to irradiance illustrated by photoprotective

carotenoids (Barlow *et al.*, 2007). This study found that the phytoplankton biomass was greater in the South Pacific gyre than in the Atlantic and Indian Ocean gyres, indicating that the Pacific gyre was less oligotrophic than the others, this may be explained by seasonal differences as the Pacific gyre was sampled during winter-spring whilst the Atlantic and Indian Oceans were sampled in early and mid summer respectively. These summer samples had higher proportions of prokaryotic phytoplankton and revealed a high proportion of photoprotective carotenoids, whereas in the Pacific Ocean small flagellates were dominant (Barlow *et al.*, 2007).

The distribution of specific *Prochlorococcus* ecotypes were analysed along legs 1, 2, 4 and 5 using dot blot hybridisation analysis of surface samples (Bouman *et al.*, 2006), finding that the *Prochlorococcus* high light II (HLII) ecotype dominated the surface of regions with high stratification in the Indian Ocean, whereas the high light I (HLI) ecotype was more prevalent in waters with moderate stratification in the mid Pacific Ocean basin and Atlantic Ocean basin. Low light (LL) ecotypes were found in the well mixed water column of the Pacific Ocean, as this cruise only sampled the surface waters and LL ecotypes would normally be found at the bottom of the photic zone. Phosphate concentration appeared to influence the distribution patterns, correlating positively with LL ecotypes and negatively with the HLII ecotype (Bouman *et al.*, 2006). In order to provide enough material for dot blot hybridisations, the surface samples used in this study were pooled from consecutive sets of three stations (see Fig 5.4). These pooled samples were analysed in this work using PPE class-specific probes in dot blot hybridisation experiments.

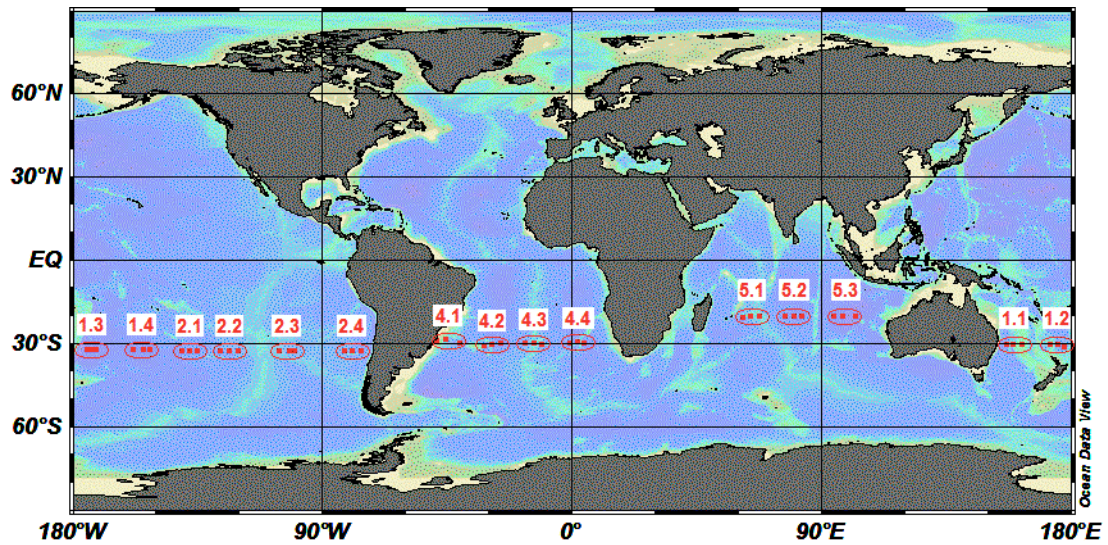


**Figure 5.4.** Map showing the position of stations sampled at the surface of the BEAGLE cruise transect for dot blot hybridisation analysis, drawn using OceanDataView. To provide ample material for analysis, samples were pooled in groups of three stations. Stations are circled in groups indicating this pooling of samples, and labelled with the leg and sample number.

#### 5.1.4. The ‘Analysing the Microbial BiodiveriTy of the Indian Ocean’ (AMBITION) and ‘Biogeochemistry and Optic South Pacific Experiment’ (BIOSOPE) cruises.

Analysis of the distribution patterns of PPE classes has already been examined for the AMBITION cruise in the Arabian Sea (North West Indian Ocean) and for the BIOSOPE cruise in the Pacific Ocean (Fuller *et al.*, 2006a; Lepère *et al.*, 2009).

The AMBITION cruise crossed the Arabian Sea upwelling province (ARAB) and Indian Monsoon gyres province (MONS) (Longhurst, 2007). The Arabian Sea has relatively high chlorophyll *a* biomass compared with other tropical open ocean regions. Seasonality in the phytoplankton community results from monsoon activity. Upwelling and algal blooms occur in the summer as a result of reversing monsoon wind, particularly in the North whereas the Southern Arabian Sea is relatively unaffected. Inter-monsoonal periods represent oligotrophic seasons (Longhurst, 2007). At the time of the cruise the water column was strongly stratified. The most abundant class detected was the Chrysophyceae, reaching up to 80% relative hybridisation whereas the Prymnesiophyceae reached only 35%. The Chrysophyceae



relative hybridisation appeared to correlate positively with dissolved oxygen and downwelling photosynthetically active radiation (Fuller *et al.*, 2006a). In addition, the distribution of *Prochlorococcus* and *Synechococcus* ecotypes were analysed along the transect, revealing dominance of *Synechococcus*, particularly of clade II, in the northern region of the transect and dominance of *Prochlorococcus* in the south transect showing distinct vertical partitioning of HL and LL ecotypes (Fuller *et al.*, 2006c).

The BIOSOPE cruise crossed the most oligotrophic waters in the world in the South Pacific Subtropical Gyre SPSG (Longhurst, 2007). In terms of physical oceanography, this is the most poorly-described region of the oceans. However, it is comparably an extremely uniform and stable region, with weak and consistent winds and no obvious seasonality (Longhurst, 2007). Chlorophyll biomass is always very low in this region, but blooms of the filamentous cyanobacterium *Trichodesmium* occur in the southwest of the province in the summer (Longhurst, 2007). Dot blot hybridisations indicated that Prymnesiophyceae and Chrysophyceae dominated the PPE community through the length of the transect, more minor classes were most abundant in the more mesotrophic regions with very low relative hybridisation values in the most oligotrophic regions (Lepère *et al.*, 2009). *Synechococcus* abundance was low along the BIOSOPE cruise, particularly in the oligotrophic gyre (Zwirgmaier *et al.*, 2008). *Prochlorococcus* abundance was highest adjacent to the oligotrophic gyre and slightly lower within the gyre. Dot blot hybridisations indicated that LL *Prochlorococcus* ecotypes were fairly broadly distributed deep in the water column along the whole transect. The HLII ecotype dominated over the HLI ecotype particularly in the gyre (Zwirgmaier *et al.*, 2008).

#### **5.1.5. Aims of this work**

This work is intended to characterise the distribution patterns of PPEs in the understudied southern Indian Ocean and the Arctic Ocean. By putting this data together with that from the BEAGLE, AMT (chapter 3), extended Ellett Line (chapter 4), AMBITION (Fuller *et al.*, 2006a) and BIOSOPE (Lepère *et al.*, 2009) cruises (Table 5.1; Fig. 5.5), this work is expected to provide insights into PPE community structure and their associations with environmental parameters at the global scale. Thus, this

data is expected to provide an unparalleled breadth of study of PPE class distribution patterns.

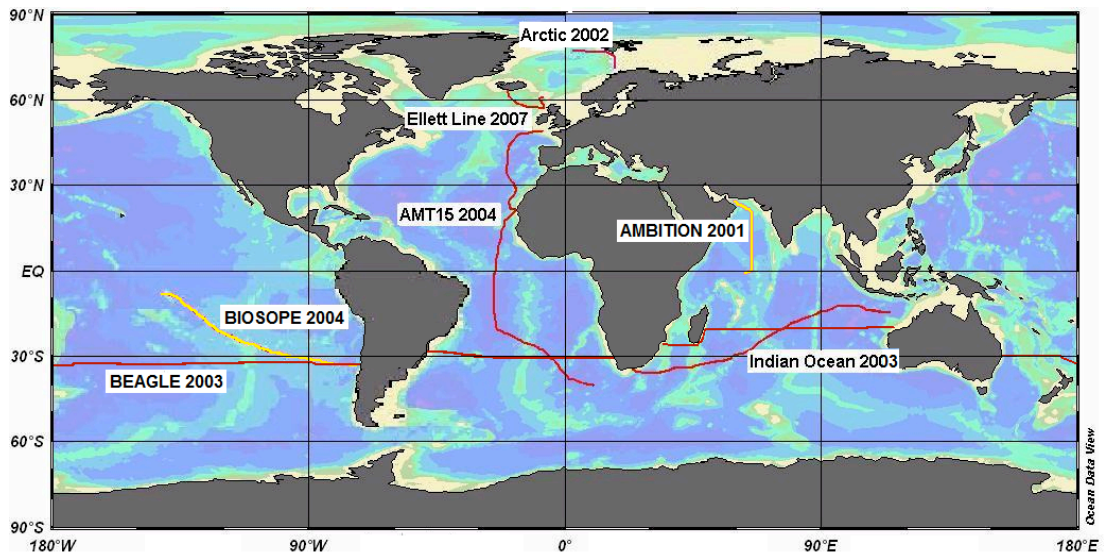


**Figure 5.5.** Map showing the location of cruises analysed by dot blot hybridisations to give global perspectives on PPE community structure. Dot blot hybridisation analyses for the BIOSOPE and AMBITION cruises (yellow) have been published previously (Fuller *et al.*, 2006a, and Lepère *et al.*, 2009 respectively). All other cruises (red) have been analysed in this work.

**Table 5.1.** Summary of cruises sampled in this work.

<b>Cruise</b>	<b>Date</b>	<b>Geographic Region</b>	<b>Latitude/Longitude</b>	<b>Sampling</b>	<b>Reference</b>
AMBITION	Sept 2001	Arabian Sea	1°S-26°N/ 56-67°E	11 stations 6 depths	Fuller <i>et al.</i> , 2006a
AMT15	Sept-Oct 2004	Atlantic Meridional Transect	48°N-40°S/ 25°W-10°E	21 stations 6 depths	Chapter 3
ARCTIC	Aug 2002	Arctic Ocean	70-79°N/3-23°E	11 Stations 5 depths	This work
ELLETT	Aug-Sept 2007	Northern North Atlantic	63-57°N/20-7°W	9 Stations 5-6 depths	Chapter 4
BEAGLE	Aug 2003-Jan 2004	Circumnavigation of the Southern Hemisphere	20-32°S	15 Stations surface only	This work
BIOSOPE	Oct-Dec 2004	Eastern South Pacific Ocean	8-34°S/141-72°W	11 Stations 6 depths	Lepère <i>et al.</i> , 2009
VANC10MV	May-Jun 2003	Indian Ocean	35-43°S/24-113°E	15 Stations 6 depths	This work

## 5.2. Results

### 5.2.1. The Arctic Ocean cruise

#### 5.2.1.1. Arctic Ocean environmental parameters

Samples analysed from the Arctic Ocean cruise had been collected at six depths from the surface of the water column to >60 m deep. Temperature measured along the cruise ranged from 12.5°C at the surface of the southernmost station, to 1.75°C at station Z18 at a depth of 60 m. Chlorophyll *a* concentration was between 0.03 and 3.04 mg m<sup>-3</sup>, and salinity was between 33.29 and 35.14 PSU. Nutrient concentrations were not measured at many of the sites which were sampled for dot blot hybridisation analysis, but where performed values between 0.01-0.3 µmol L<sup>-1</sup> nitrite, 0.01-6.23 µmol L<sup>-1</sup> nitrate, 0.05-0.54 µmol L<sup>-1</sup> phosphate, and 0.39-3.31 µmol L<sup>-1</sup> silicate were measured (Fig. 5.6).

#### 5.2.1.2. Picophytoplankton community structure in the Arctic Ocean

The picophytoplankton community was measured by flow cytometry along the Arctic Ocean transect (Fig. 5.7). As expected, *Prochlorococcus* cells were not detected. *Synechococcus* cells peaked at  $>6 \times 10^4$  cells ml<sup>-1</sup> at the surface of station Z01, the southernmost station of the cruise whilst photosynthetic eukaryotes peaked at  $>2 \times 10^4$  cells ml<sup>-1</sup> at the surface of station Z65 in the middle of the transect. In the south of the transect *Synechococcus* cells outnumbered photosynthetic eukaryotes, but north of 74°N, photosynthetic eukaryotes were more numerous than *Synechococcus*.

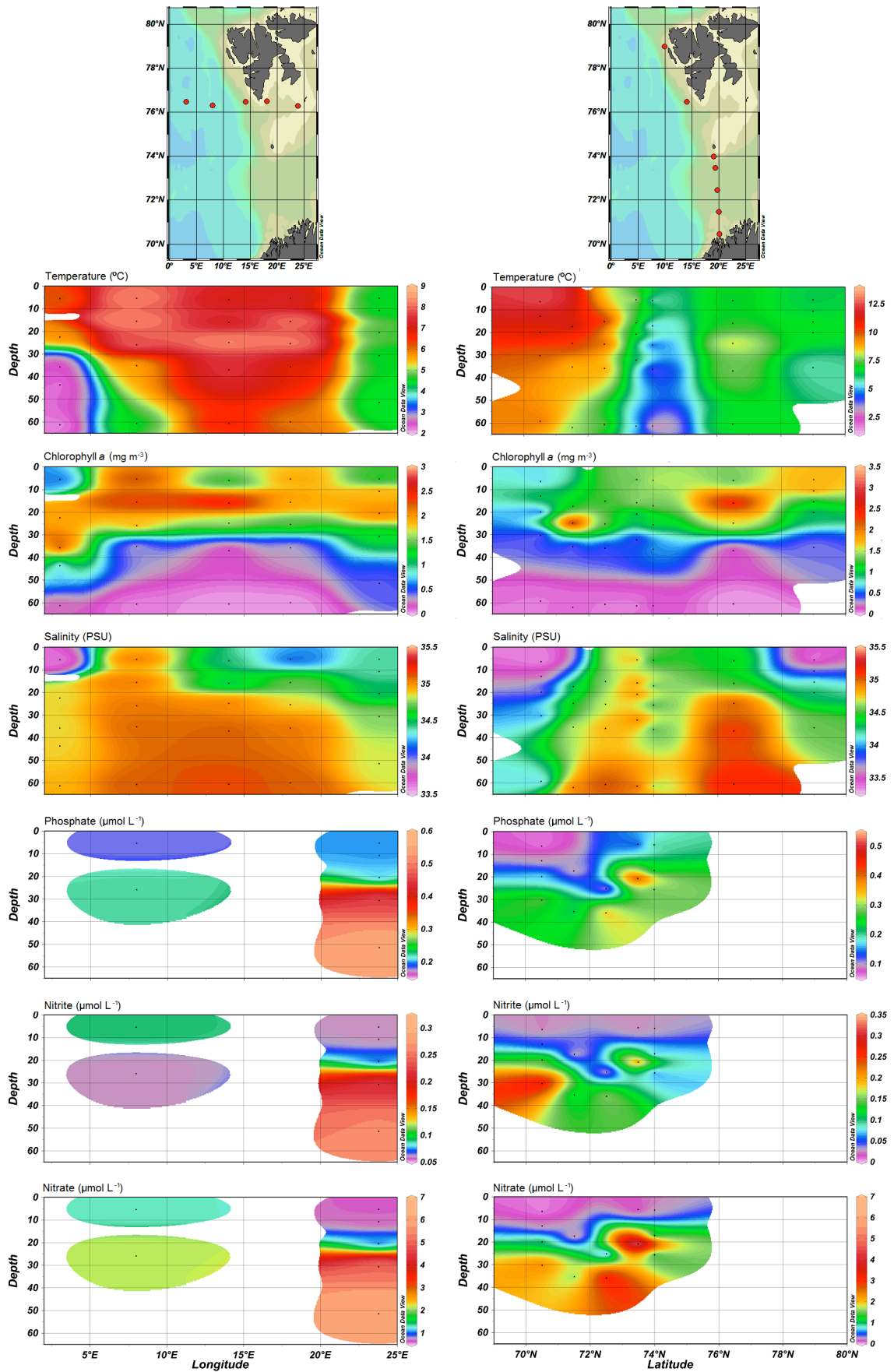


**Figure 5.6.** Contour plots showing chemical and physical parameters along the Arctic cruise by longitude (left) and latitude (right). Continued next page.

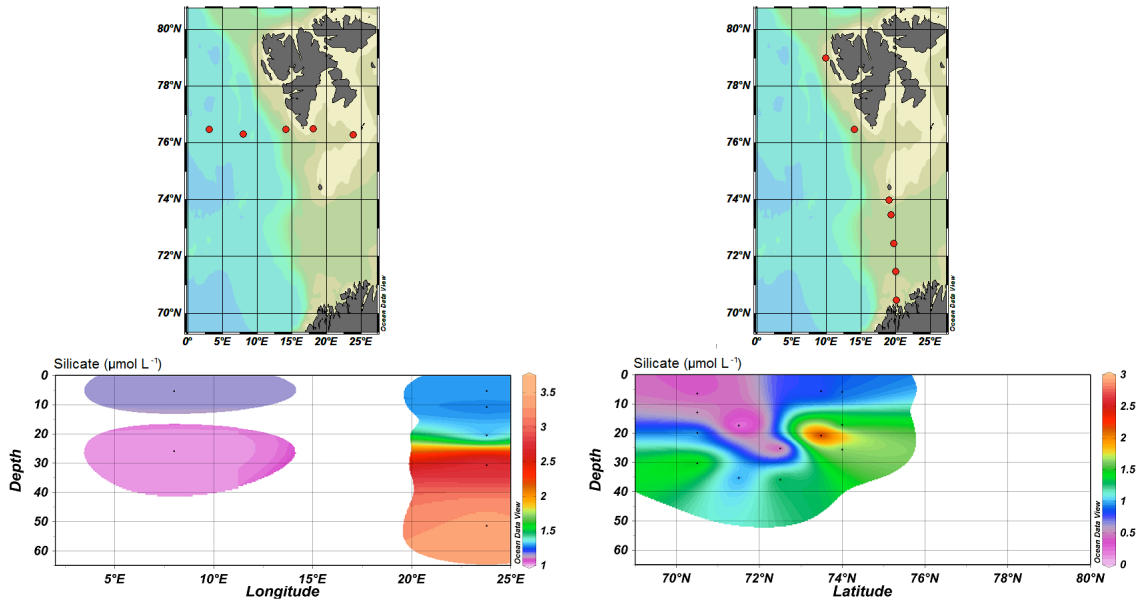
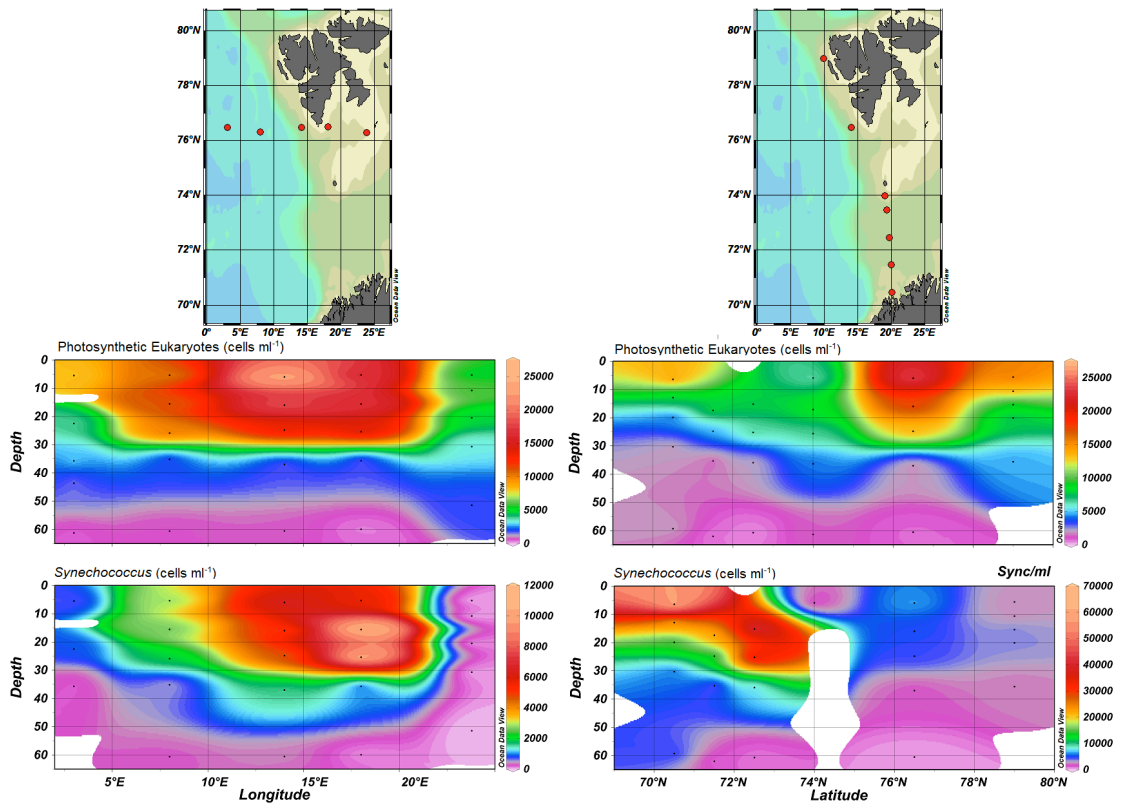


Figure 5.6. Continued

### 5.2.1.3. PPE distribution patterns in the Arctic Ocean

The PPE class with the highest relative hybridisation values was Prymnesiophyceae, peaking at 58% (Fig. 5.8). On average, Chrysophyceae were slightly lower and the peak value was 39%. Cryptophyceae and Pinguiphyceae peaked at 18 and 10% respectively. The Pavlovophyceae and Chlorarachniophyceae probes occasionally reached above background levels of hybridisation. The complementary distribution patterns of Prymnesiophyceae and Chrysophyceae, seen for AMT15 (section 3.2.4) is visible here, particularly for the longitudinal transect between 3 and 24°E at approximately 76.5°N (Fig. 5.8).



**Figure 5.7.** Contour plots of flow cytometry data along the Arctic cruise. Cells  $\text{ml}^{-1}$  are measured for photosynthetic eukaryotes (top), and *Synechococcus* (bottom) by longitude (left) and latitude (right).

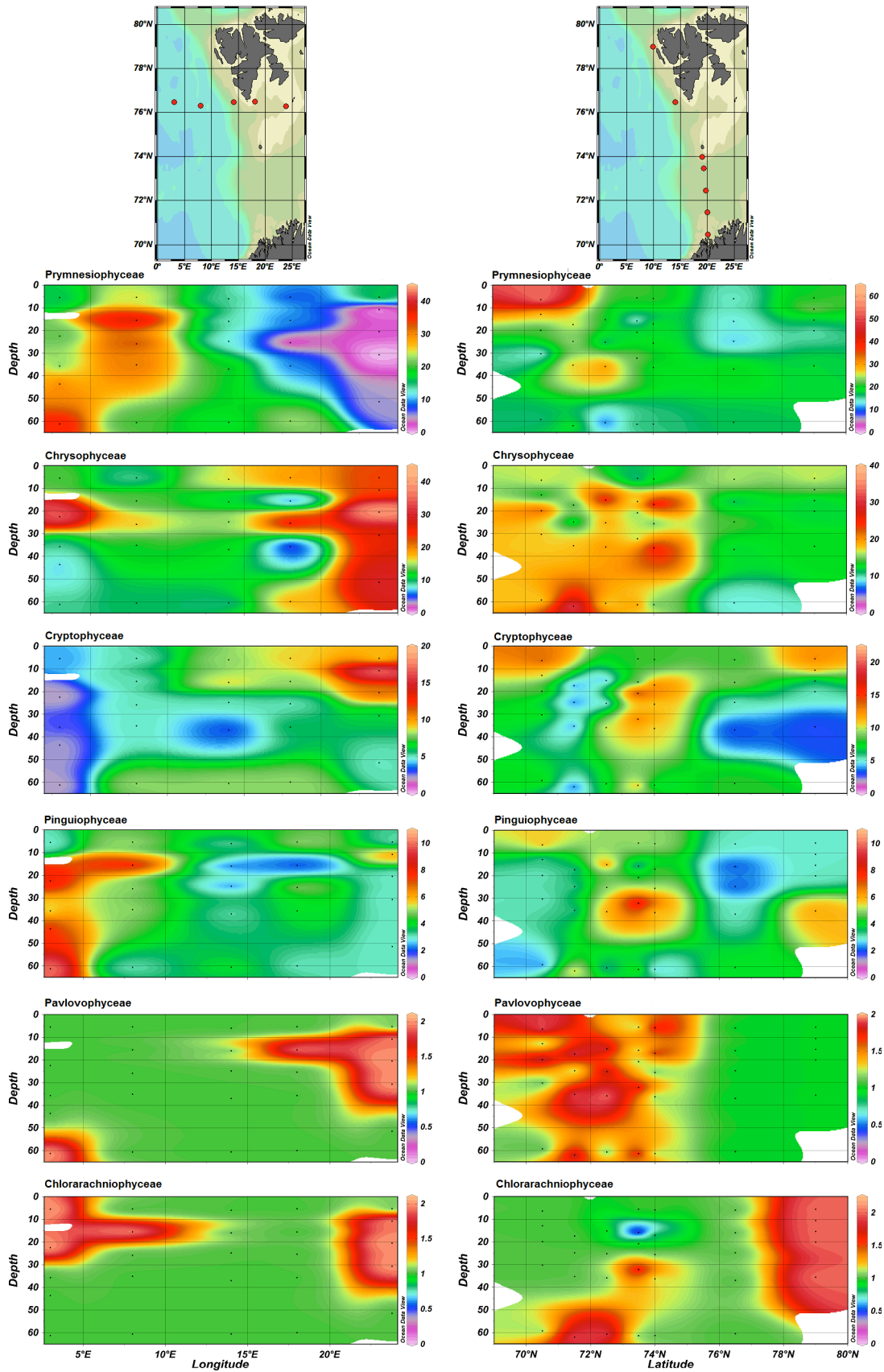


**Figure 5.8.** Contour plots of dot blot hybridisation data showing the distribution patterns of PPE classes along the Arctic cruise for stations illustrated (top) by longitude (left) and latitude (right). Contour plots indicate percentage relative hybridisation of the different classes.



Canonical correspondence analysis (CCA) showed that up to 85% of the variation in distribution patterns of PPE classes could be explained by measured environmental factors. Due to the disparity in environmental measurements for samples analysed by dot blot hybridisations, particularly nutrient concentrations, the sample size used in the CCA was small ( $n=16$ ). This possibly resulted in a larger proportion of variation being explained by environmental parameters. Chemical parameters (salinity and concentrations of nitrate, nitrite, phosphate and silicate) were able to explain up to 53% of the variation in dot blot hybridisation data. Physical parameters (temperature and depth) could explain up to 48% of the variation with an overlap with chemical parameters of 28% of the variation in dot blot hybridisation data. Biological parameters (abundances of photosynthetic eukaryotes and *Synechococcus*, and chlorophyll *a* concentration) could explain up to 46% of the variation overlapping with chemical parameters by 16% and with physical parameters by 30% of the variation in dot blot hybridisation data (Fig. 5.9).

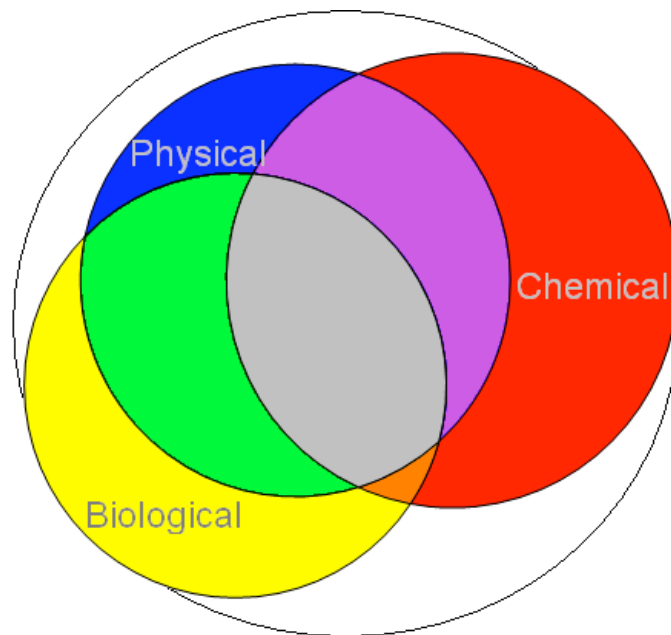


**Figure 5.9.** Venn diagram, drawn to scale by the eigenvalues calculated for the total variation in dot blot hybridisation along the Arctic Ocean cruise (white) with the amount of variation that can be explained by physical (blue), chemical (red) and biological (yellow) parameters. These groups of parameters explain 48%, 53% and 46% of the total variation in dot blot hybridisation data respectively. The overlap in the amount of variation explained by both physical and chemical parameters is 28% of the total variation in dot blot hybridisation data, the overlap between physical and biological parameters is 30% and between chemical and biological parameters is 16%. Physical parameters encompass depth and temperature; chemical parameters encompass concentrations of nitrate, nitrite, phosphate, silicate, and salinity; biological parameters encompass chlorophyll *a* concentration and flow cytometry counts of photosynthetic eukaryotes and *Synechococcus*.

Up to 82% of the variation in dot blot hybridisation data could be explained by a seven-variable model. The single variable that was able to explain the most variation was temperature which explained 40%. Addition of salinity increased the amount explained to 48%, addition of depth increased it to 60%, fluorescence to 67%, photosynthetic eukaryote abundance to 71%, *Synechococcus* abundance to 77%, and finally addition of nitrite concentration increased the amount of variation in dot blot hybridisation that could be explained by the model to 82%. Additional variables had very little effect on the amount of data explained. Plotting this model showed that different classes were associated with different environmental variables. Key classes Prymnesiophyceae and Chrysophyceae appeared to be associated with temperature, where Prymnesiophyceae showed positive correspondence and Chrysophyceae showed negative correspondence. Cryptophyceae appeared to be positively associated with chlorophyll *a* concentration (Fig. 5.10).

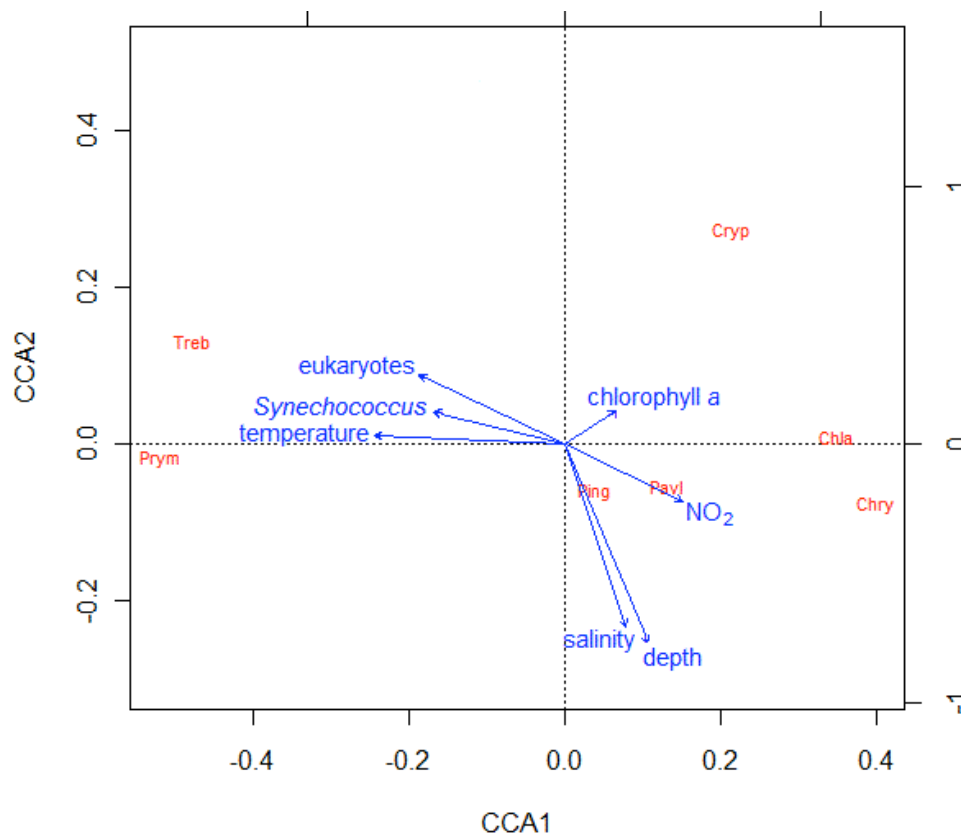


**Figure 5.10.** Canonical correspondence analysis (CCA) plot for PPE class distribution in the Arctic Ocean in relation to environmental variables, from dot blot hybridisation results for classes: Prymnesiophyceae (Prym), Chrysophyceae (Chry), Cryptophyceae (Cryp), Pinguiphyceae (Ping), Pelagophyceae (Pela), Chlorarachniophyceae (Chla) and Trebouxiophyceae (Treb). Axis 1 (CCA1) can explain 73% of the total variation in dot blot hybridisation data, axis 2 (CCA2) can explain a further 6%. A third axis (not shown) can explain a further 2%. Three additional axes (not shown) can explain a further 1% between them.

## 5.2.2. The Indian Ocean transect (VANC10MV)

### 5.2.2.1. Environmental parameters along the Indian Ocean transect

Few environmental parameters were measured along this transect. In particular, nutrient concentrations were not recorded. Temperatures ranged from 20.9 to 28.5°C at the surface, with highest values towards the eastern end of the transect, and reaching as low as 15.5°C at a depth of 200 m. An apparent thermocline is observed along the transect at between 60 and 160 m depth, which appears to correlate with peaks in chlorophyll *a* concentration of between 0.5 and 1 mg m<sup>-3</sup>. At the surface, chlorophyll *a* concentration ranged between 0.07 and 1.3 mg m<sup>-3</sup>. Salinity was lowest at the eastern end of the transect, dipping as low as 33.87 PSU and reaching a maximum of 35.8 PSU near the middle of the transect (Fig. 5.11).

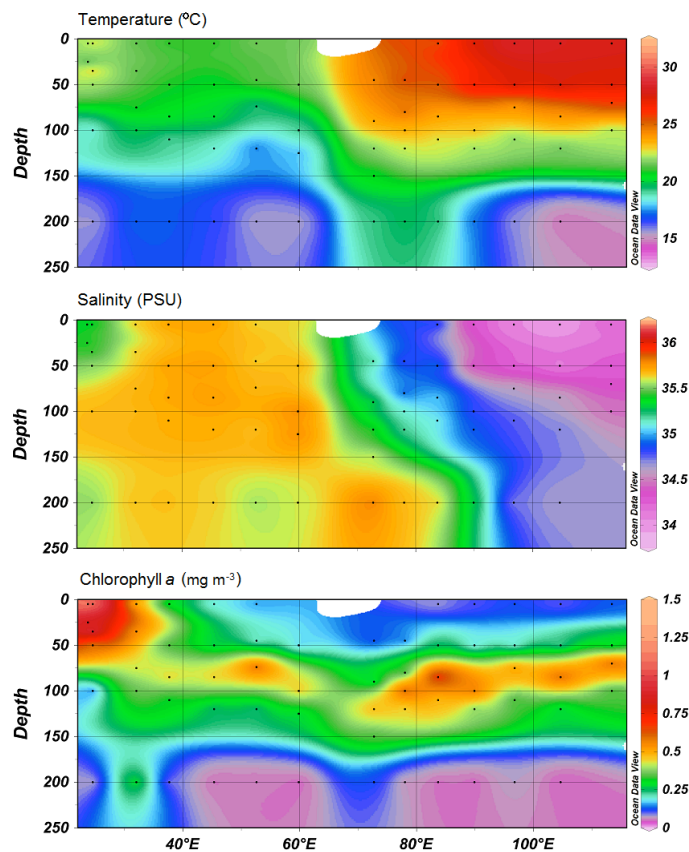


**Figure 5.11.** Contour plots showing the chemical and physical parameters measured along the Indian Ocean cruise.

### 5.2.2.2. Picophytoplankton community structure along the Indian Ocean transect

The picophytoplankton community was measured by ship-board flow cytometry and found to be dominated by *Prochlorococcus* over most of the transect peaking at  $2.8 \times 10^5$  cells  $\text{ml}^{-1}$ . *Synechococcus* and photosynthetic eukaryote cell numbers were highest at the westernmost stations of the transect corresponding to the highest values for chlorophyll *a* concentration, peaking at  $5.8 \times 10^4$  cells  $\text{ml}^{-1}$  and  $1.3 \times 10^4$  cells  $\text{ml}^{-1}$  respectively (Fig. 5.12). An area in the east of the transect is characterised by elevated numbers of photosynthetic eukaryotes between 50 and 85 m depth corresponding with the deep chlorophyll maximum observed in the area (Fig. 5.11).

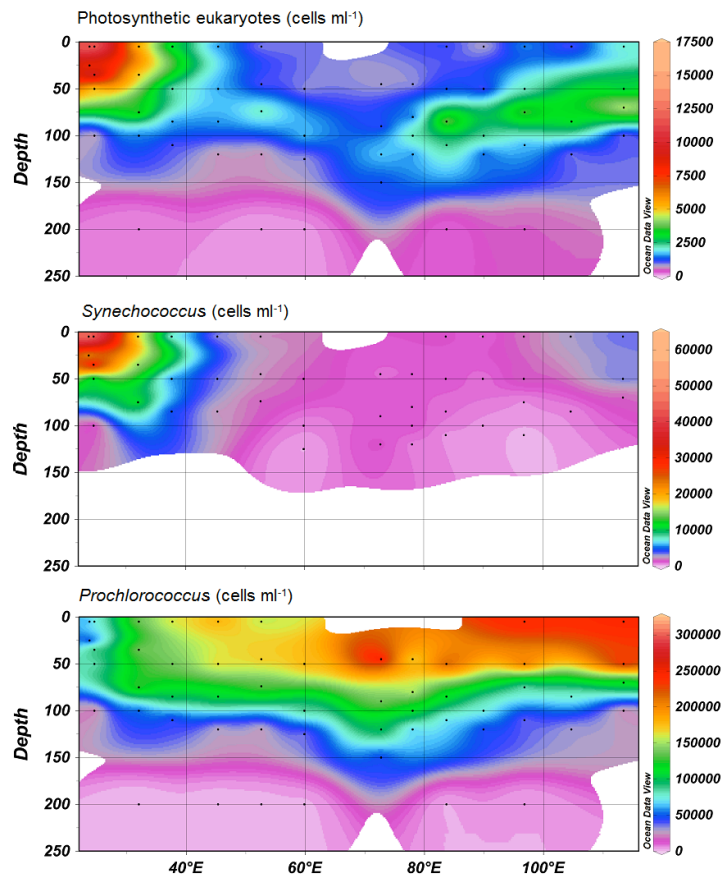


**Figure 5.12.** Contour plots of flow cytometry data along the Indian Ocean cruise. Cells  $\text{ml}^{-1}$  have been measured for photosynthetic eukaryotes (top), *Synechococcus* (middle) and *Prochlorococcus* (bottom).

### 5.2.2.3. PPE distribution patterns along the Indian Ocean transect

Dot blot hybridisation analysis indicated that the Indian Ocean transect was dominated by the Prymnesiophyceae with an average relative hybridisation value of 20% over the whole cruise and a peak of 58% at a couple of stations along the transect (Fig. 5.13). The second most dominant class appeared to be Chrysophyceae which despite a much lower average value of 11% relative hybridisation over the cruise reached a peak of 49% at the eastern end of the transect. Other classes appeared to be far less abundant; Cryptophyceae reached a maximum of 32% relative hybridisation, but beyond the easternmost station remained very low, only occasionally rising above background levels. Pinguiphyceae, Pelagophyceae and Trebouxiophyceae relative hybridisation values were generally below background levels with a peak at 200 m depth in the western section of the transect (Fig.5.13).

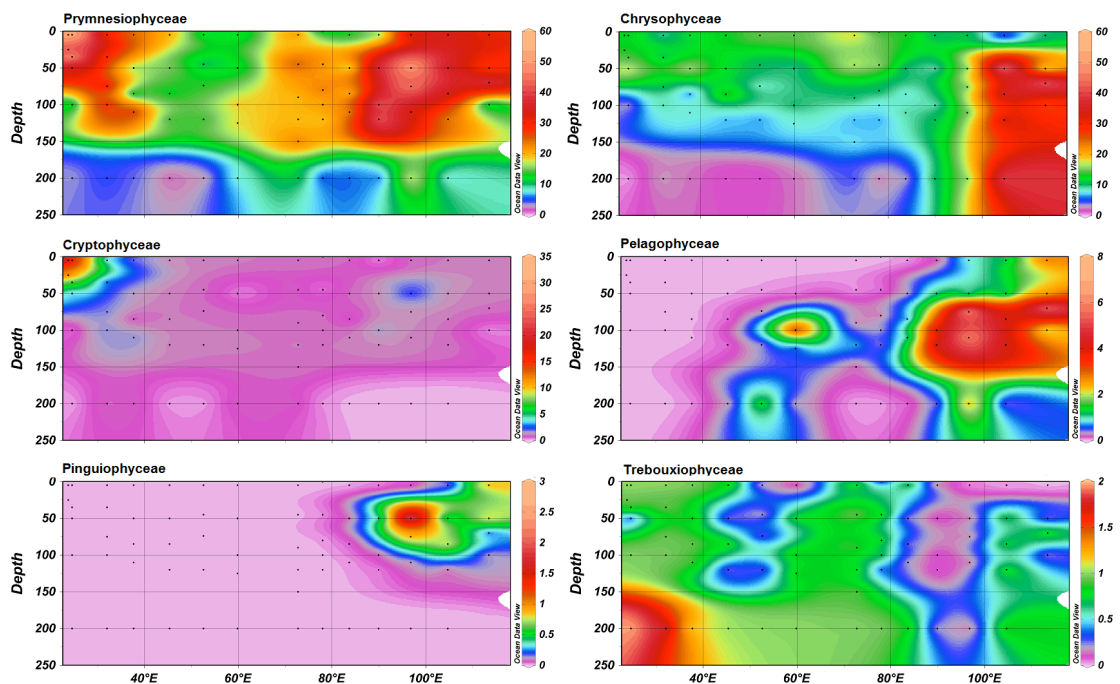


**Figure 5.13.** Contour plots of dot blot hybridisation data showing the distribution patterns of PPE classes along the Indian Ocean transect. Colour represents the % relative hybridisation.

CCA analysis showed that up to 53% of the variation in dot blot hybridisation data could be explained by variables measured along the Indian Ocean cruise (n=40). When divided into physical, chemical and biological parameters, biological parameters (chlorophyll *a* concentration and photosynthetic eukaryote,

*Synechococcus* and *Prochlorococcus* abundances) explained the most at 36% of the variation in dot blot hybridisation data. Physical parameters (temperature and depth) explained 19% of the variation in dot blot hybridisation data with an overlap of 12% of variation in dot blot hybridisation data with biological parameters. As nutrient concentrations were not measured along this cruise, chemical parameter comprised only salinity. This was able to explain up to 10% of the variation in dot blot hybridisation data with an overlap of 3% of dot blot hybridisation variation with biological data and no overlap with physical parameters (Fig. 5.14).

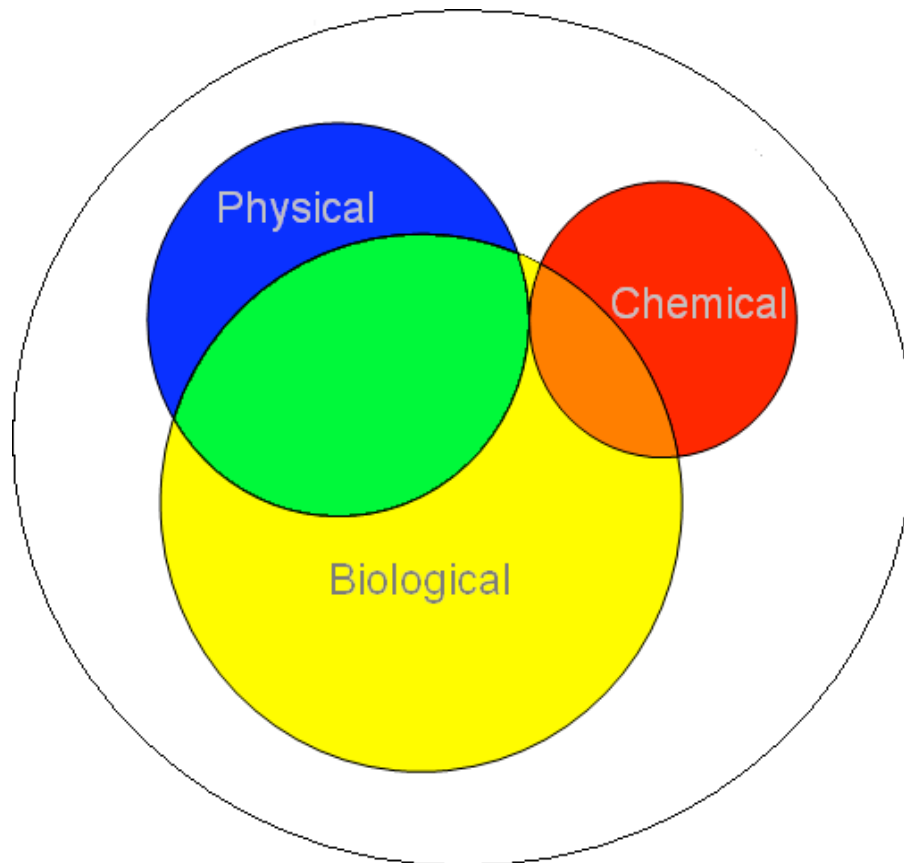


**Figure 5.14.** Venn diagram, drawn to scale by the eigenvalues calculated for the total variation in dot blot hybridisation along the Indian Ocean cruise (white) with the amount of variation that can be explained by physical (blue), chemical (red) and biological (yellow) parameters. These groups of parameters explain 19%, 10% and 36% of the total variation in dot blot hybridisation data. The overlap in the amount of variation explained by both physical and biological parameters is 12% and the overlap between chemical and biological parameters is 3%. Physical parameters encompass depth and temperature; chemical parameters encompass only salinity; biological parameters encompass chlorophyll *a* concentration and flow cytometry counts of photosynthetic eukaryotes and *Synechococcus* and *Prochlorococcus*.

A three-variable model explained 44% of the variation in dot blot hybridisation data. *Synechococcus* abundance was able to explain the most data alone at 26% of

variation in dot blot hybridisation data. When salinity was added to the model this rose to 34% of the variation, and with temperature as well it rose to 44%. Additional variables only caused small increments in the amount of dot blot hybridisation data that could be explained. *Synechococcus* abundance was associated with Cryptophyceae relative hybridisation, Chrysophyceae was negatively associated with *Synechococcus* abundance on axis one and three (data not shown). Salinity was associated positively with Trebouxioephyceae and negatively with Pinguioephyceae and Pelagophyceae relative hybridisation. Temperature is positively associated with Pinguioephyceae (Fig. 5.15). The variation in dot blot hybridisation data for Prymnesioephyceae positioned in the middle of the graph indicates that it is associated with average levels of the environmental variables.

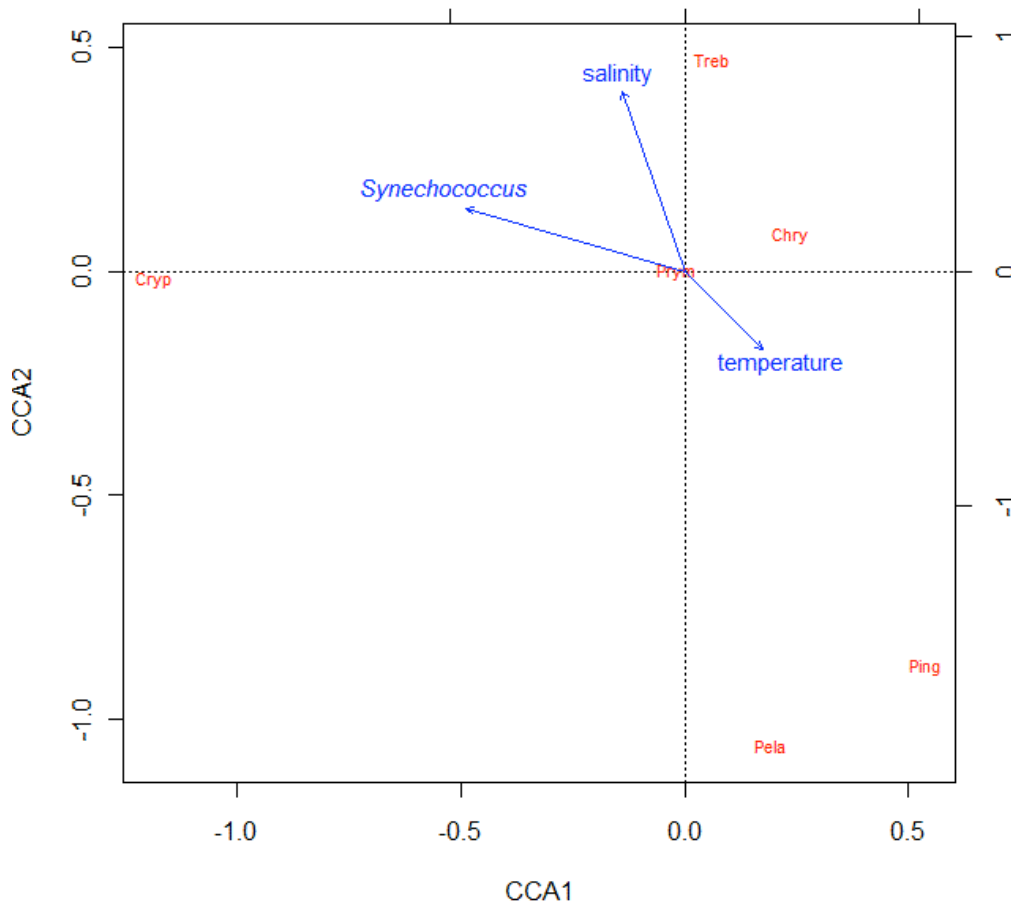


**Figure 5.15.** CCA plot for PPE class distribution in the Indian Ocean in relation to environmental variables, from dot blot hybridisation results for classes: Prymnesioephyceae (Prym), Chrysophyceae (Chry), Cryptophyceae (Cryp), Pinguioephyceae (Ping), Pelagophyceae (Pela) and Trebouxioephyceae (Treb). Axis 1 (CCA1) can explain 29% of the total variation in dot blot hybridisation data, axis 2 (CCA2) can explain a further 11%. A third axis (not shown) can explain a further 4%.

### **5.2.3. The BEAGLE transect**

#### **5.2.3.1. Environmental parameters along the BEAGLE transect**

The BEAGLE transect was sampled only at the surface of the water column. Temperature was highest in the Indian Ocean, sampled in mid summer, peaking at 26.5°C, and lowest in the Pacific Ocean, sampled in the winter and spring, at a minimum of 16°C. Salinity ranged between 34.4 PSU in the east of the Pacific Ocean and 36.3 PSU in the west of the Atlantic Ocean. Chlorophyll *a* concentration was highest in the Pacific Ocean, peaking at 0.37 mg m<sup>-3</sup>, and lowest in the Indian Ocean at a minimum of 0.02 mg m<sup>-3</sup>. Nutrient concentrations varied with nitrate concentration ranging between undetectable levels and 0.78 µmol L<sup>-1</sup>, nitrite between undetectable levels and 0.19 µmol L<sup>-1</sup>, phosphate between 0.07 and 0.34 µmol L<sup>-1</sup> and silicate between 0.3 and 2.2 µmol L<sup>-1</sup>. Nutrient concentrations were generally slightly higher in the Pacific Ocean than in the Atlantic and Indian Ocean, except silicate which was much higher in the Indian Ocean (Fig. 5.16).

#### **5.2.3.2. Picophytoplankton community structure along the BEAGLE transect**

Flow cytometry showed that photosynthetic eukaryote and *Synechococcus* abundances ranged from  $4.3 \times 10^2$  to  $7 \times 10^3$  and from  $9.2 \times 10^2$  to  $4.2 \times 10^4$  cells ml<sup>-1</sup> respectively, and both peaked in the most coastal regions of the Pacific Ocean. *Prochlorococcus* abundance ranged from  $8.7 \times 10^3$  to  $1.3 \times 10^5$  cells ml<sup>-1</sup>, and was highest in the Indian Ocean (Fig. 5.17).



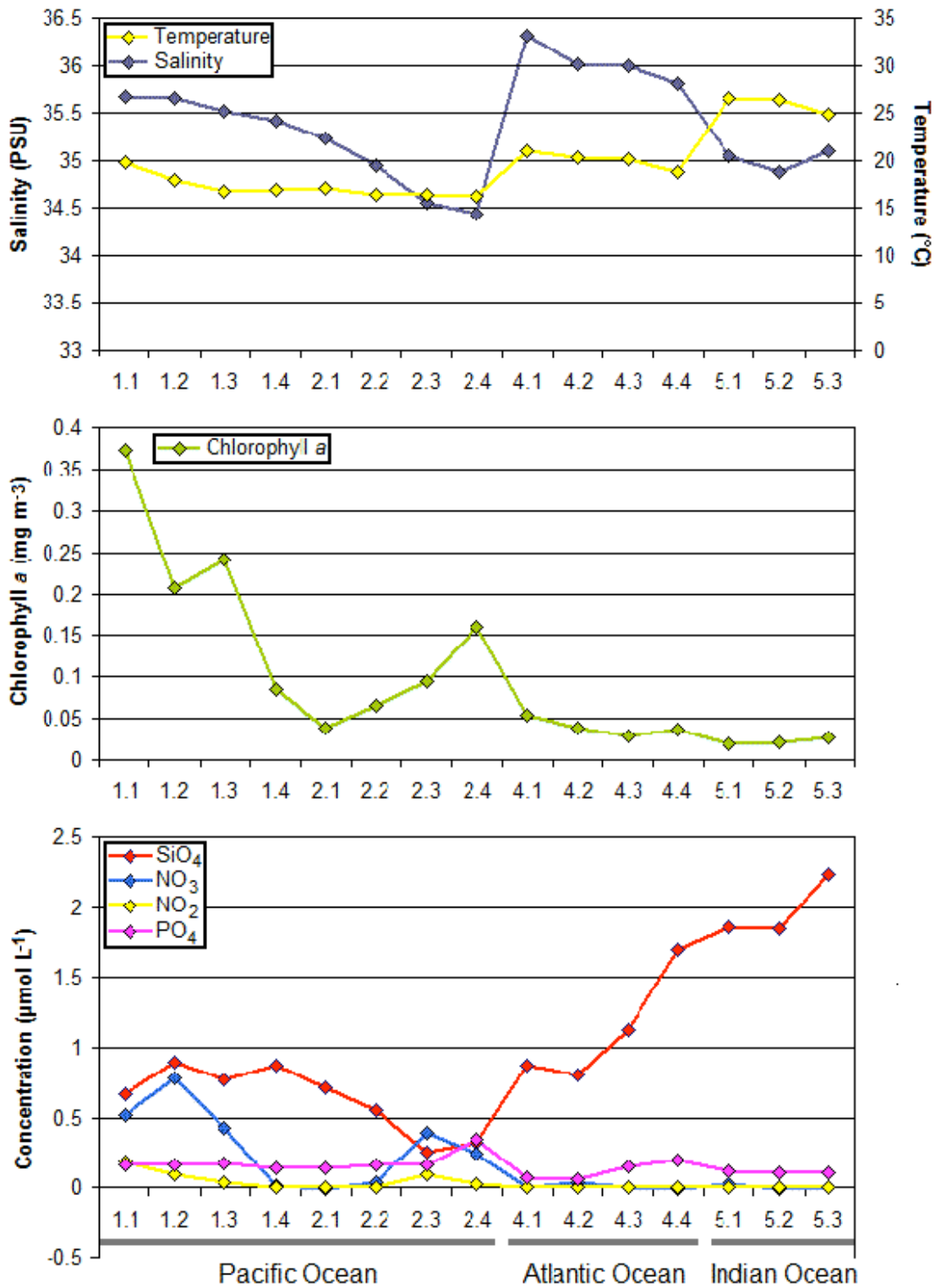


**Figure 5.16.** Physical and chemical parameters measured along the BEAGLE transect. Temperature and salinity (top), chlorophyll *a* concentration (middle) and nutrient concentrations (bottom) are shown.

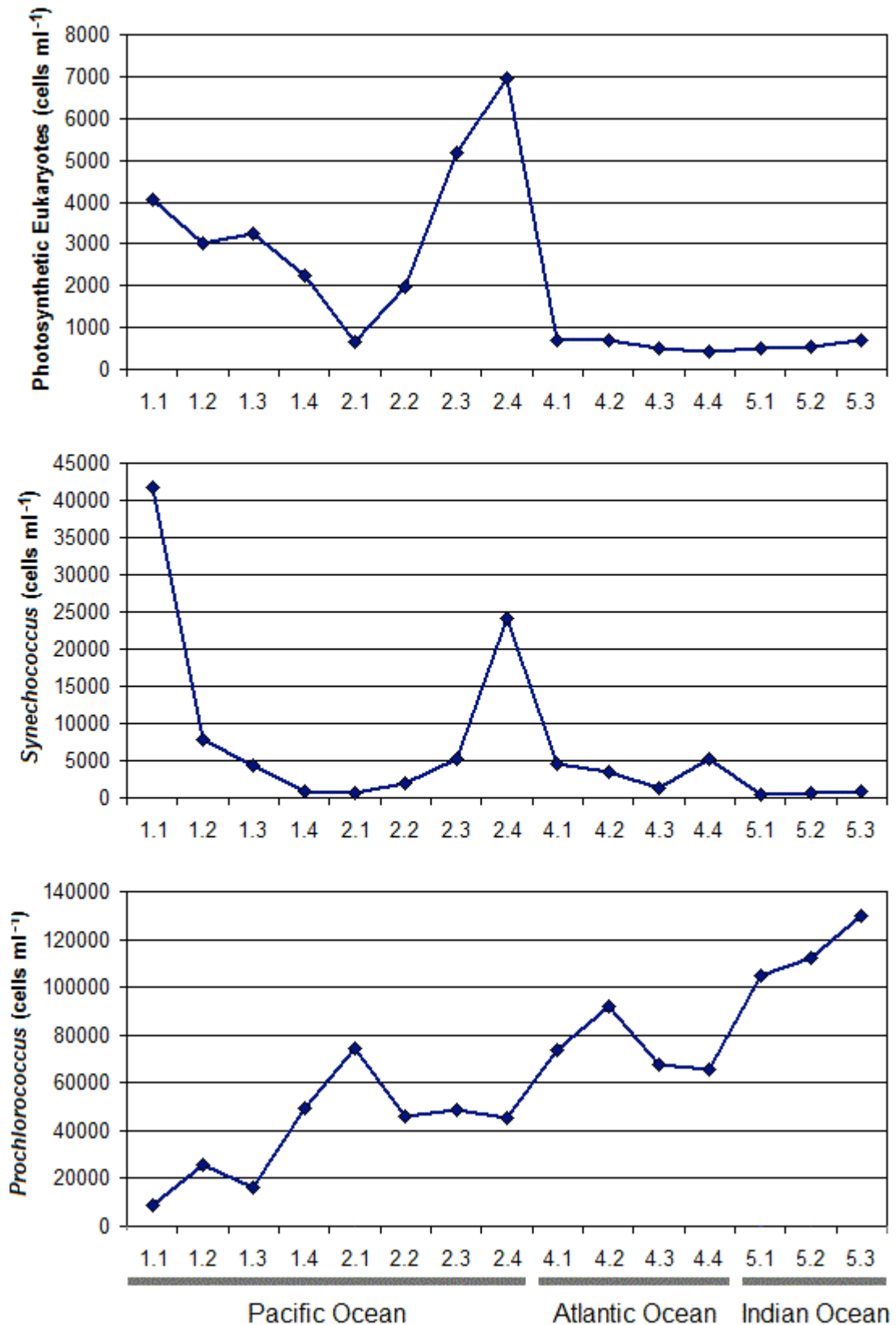


**Figure 5.17.** Flow cytometry data along the BEAGLE cruise. Cells ml<sup>-1</sup> have been measured for photosynthetic eukaryotes (top), *Synechococcus* (middle) and *Prochlorococcus* (bottom).

### 5.2.3.3. PPE distribution patterns along the BEAGLE transect

Dot blot hybridisation analyses indicated that all stations along the BEAGLE transect were dominated by the Prymnesiophyceae and Chrysophyceae, with more minor contributions from the Cryptophyceae, Pinguiphyceae, Pavlovophyceae and Chlorarachniophyceae (Fig. 5.18). The Pavlovophyceae and Chlorarachniophyceae featured in the Pacific and were largely absent from the Atlantic and Indian Oceans.

CCA showed that up to 87% of the variation in dot blot hybridisation data along the BEAGLE transect could be explained by environmental parameters measured on the cruise (n=15). When divided into physical, chemical and biological parameters, chemical parameters (salinity and concentrations of silicate, nitrite, nitrate and phosphate) explained the most at 52% of the variation in dot blot hybridisation data. Biological parameters (chlorophyll concentration and abundances of photosynthetic eukaryotes, *Synechococcus*, *Prochlorococcus* and heterotrophic bacteria) explained 43% of the variation in dot blot hybridisation data with an overlap of 11% of variation in dot blot hybridisation data with biological parameters. The single physical parameter used (temperature) was able to explain up to 12% of the variation in dot blot hybridisation data with an overlap of 7% of dot blot hybridisation variation with biological data and 3% overlap with physical parameters (Fig. 5.19).

A seven-variable model explained 77% of the variation in the dot blot hybridisation data. *Prochlorococcus* abundance was able to explain the most data alone at 21% of variation in dot blot hybridisation data. When silicate concentration was added to the model this rose to 34% of the variation, addition of temperature increased it to 45%, nitrate to 52%, photosynthetic eukaryote abundance to 61%, salinity to 70% and heterotrophic bacteria abundance to 77%. Additional variables only caused small increments in the amount of dot blot hybridisation data that could be explained. *Prochlorococcus* abundance and temperature was associated with Chrysophyceae relative hybridisation and strongly negatively associated with Cryptophyceae, Pavlovophyceae and Chlorarachniophyceae, whereas these classes were associated with nitrate concentrations. Silicate concentration was associated positively with Chrysophyceae, and photosynthetic eukaryote abundance negatively, and *vice versa* for Pavlovophyceae relative hybridisation. Prymnesiophyceae relative hybridisation

was largely unexplained by the measured parameters, but was fairly weakly associated with heterotrophic bacteria abundance (Fig. 5.20).

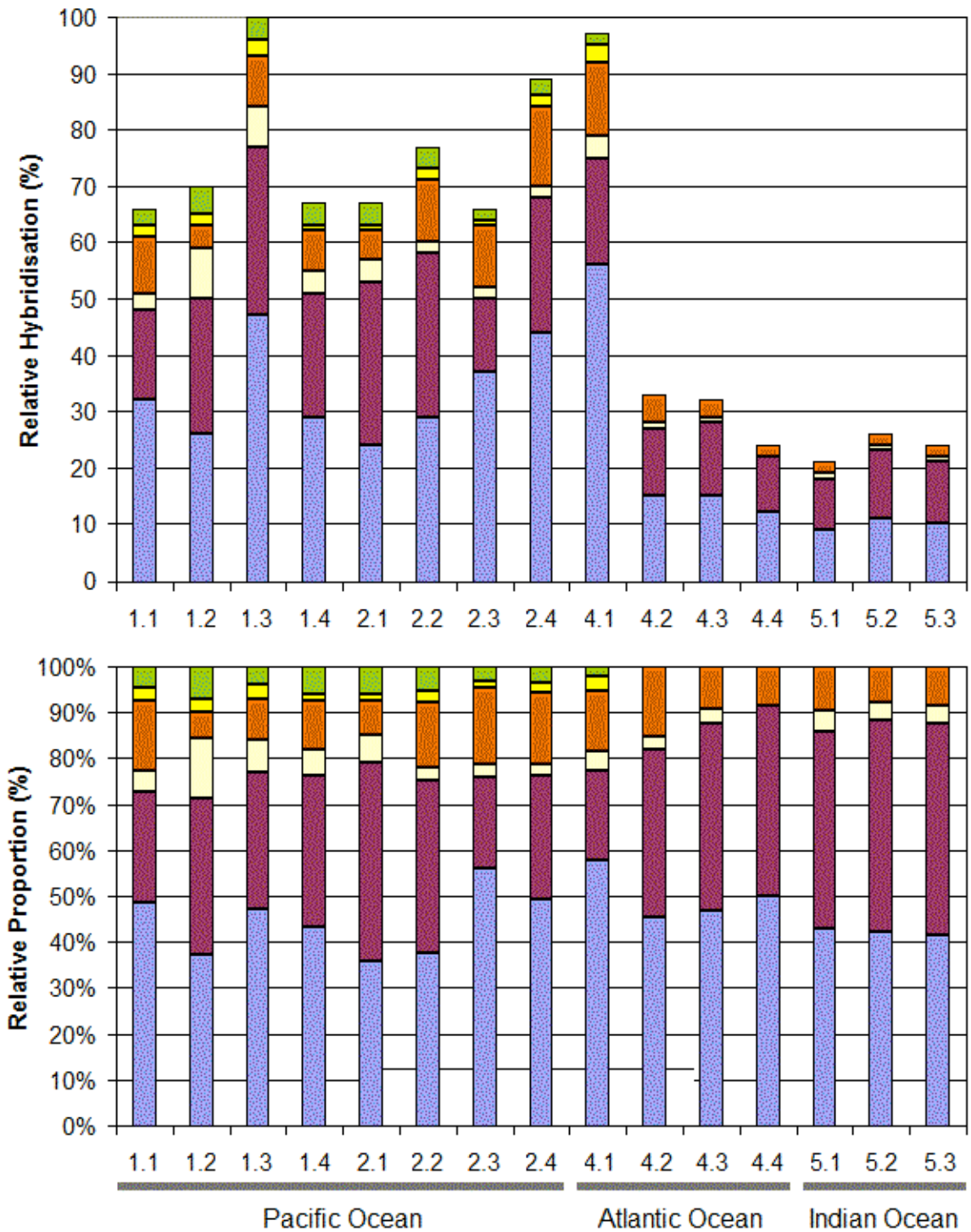


**Figure 5.18.** Percent relative hybridisation (top) and relative proportion (bottom) for probes which reached above 2% relative hybridisation for the BEAGLE transect, targeting the Prymnesiophyceae (■), Chrysophyceae (■), Cryptophyceae (■), Pinguiphyceae (■), Pavlovophyceae (■) and Chlorarachniophyceae (■) for each station set along the BEAGLE cruise.

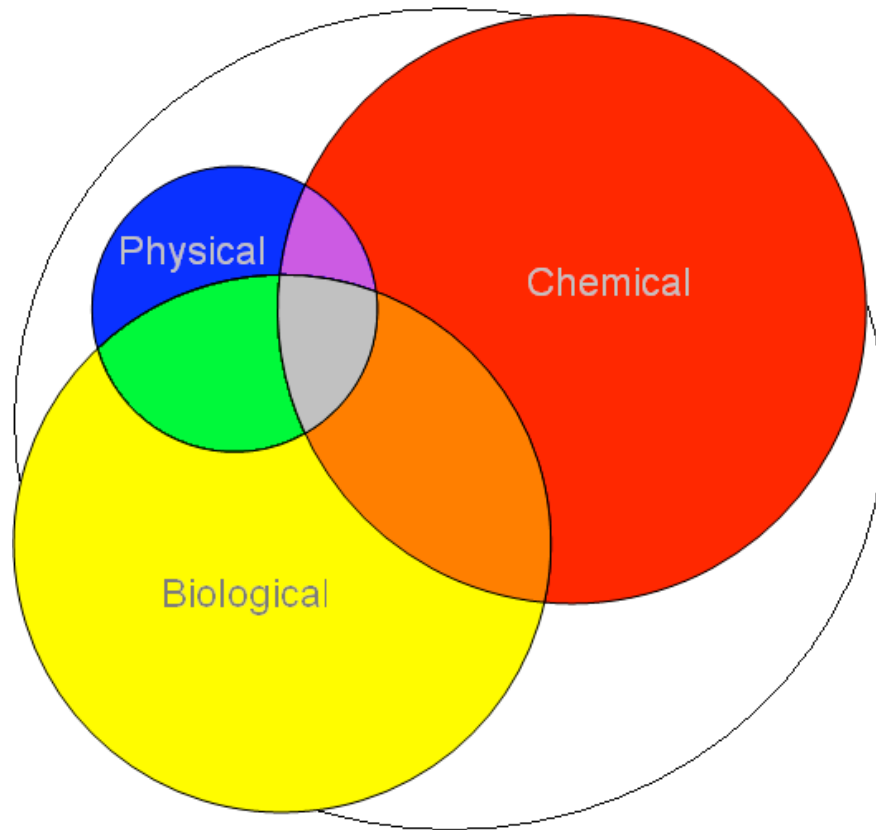


**Figure 5.19.** Venn diagram, drawn to scale by the eigenvalues calculated for the total variation in dot blot hybridisation along the BEAGLE transect (white) with the amount of variation that can be explained by physical (blue), chemical (red) and biological (yellow) parameters. These groups of parameters explain 12%, 52% and 43% of the total variation in dot blot hybridisation data. The overlap in the amount of variation explained by both physical and chemical parameters is 3% of the total variation in dot blot hybridisation data. The overlap between physical and biological parameters is 7% and between chemical and biological parameters is 11%. Physical parameters encompass temperature; chemical parameters encompass concentrations of nitrate, nitrite, phosphate, silicate, and salinity; biological parameters encompass chlorophyll *a* concentration and flow cytometry counts of photosynthetic eukaryotes, *Synechococcus*, *Prochlorococcus* and heterotrophic bacteria.

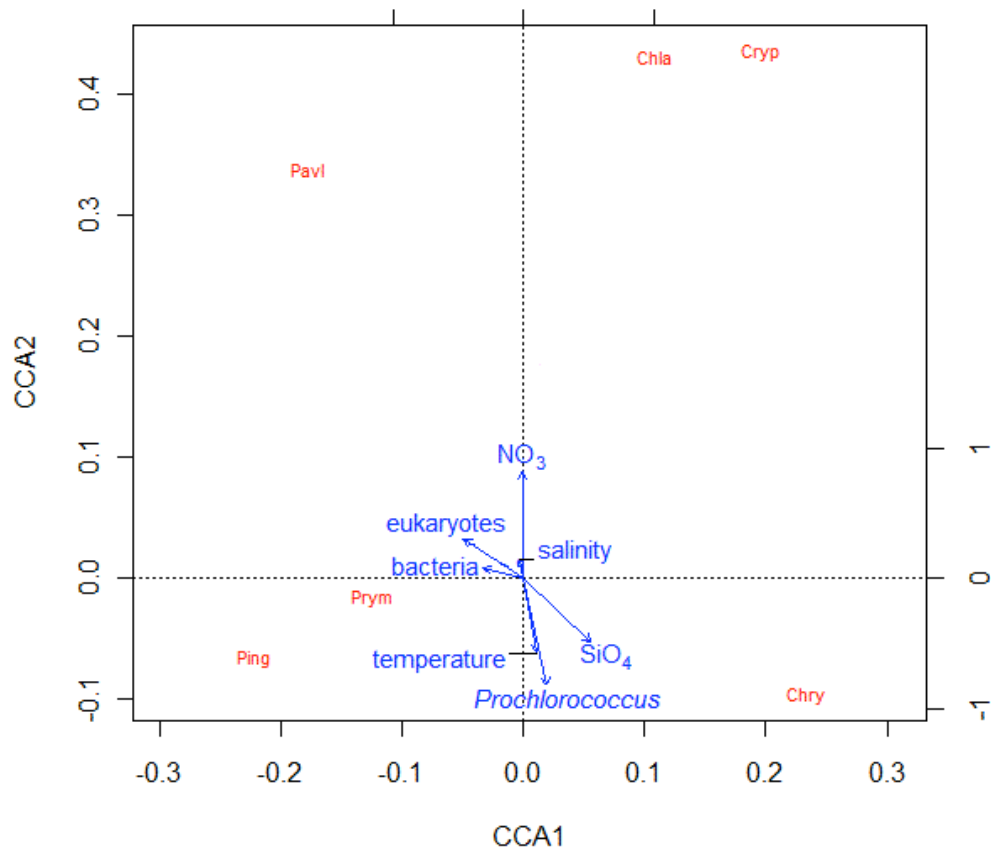


**Figure 5.20.** CCA plot for PPE class distribution along the BEAGLE transect in relation to environmental variables, from dot blot hybridisation results for classes: Prymnesiophyceae (Pym), Chrysophyceae (Chry), Cryptophyceae (Cryp), Pinguiphyceae (Ping), Pavlovophyceae (Pavl) and Chlorarachniophyceae (Chla). Axis 1 (CCA1) can explain 42% of the total variation in dot blot hybridisation data, axis 2 (CCA2) can explain a further 28%. A third axis (not shown) can explain a further 7%. Two additional axes (not shown) can explain less than 1%.

#### 5.2.4. Global perspectives on PPE class distributions

Comparison of dot blot hybridisation data from the cruises used here reveals the persistent importance of the Prymnesiophyceae and Chrysophyceae over the range of ocean environments analysed. These two classes comprise at least 58% of the total relative hybridisation values for PPE classes over all seven transects considered (Fig. 5.21). The third most important class detected appears to be the Cryptophyceae as this is frequently observed. However, this is at values rarely exceeding 5% relative hybridisation in individual samples. Global distribution patterns are different for each PPE class detected (Fig. 5.22).

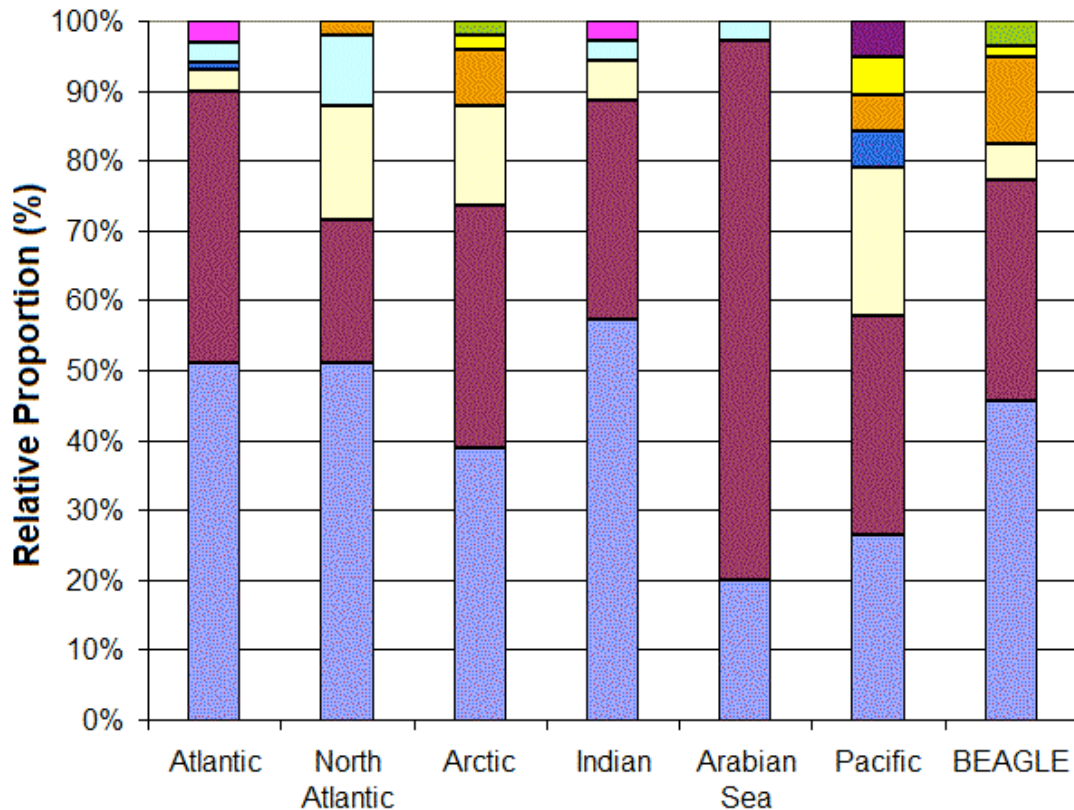


**Figure 5.21.** Average relative proportion of PPE classes detected by dot blot hybridisations for each cruise used in this study. Pymnesiophyceae (■), Chrysophyceae (■), Cryptophyceae (■), Eustigmatophyceae (■), Trebouxiophyceae (■), Pinguiophyceae (■), Pavlovophyceae (■), Chlorarachniophyceae (■) and Prasinophyceae clade VI (■).

CCA was performed for the global dataset, excluding the Indian Ocean cruise for which little data was available on chemical parameters ( $n=239$ ). Data for nine environmental parameters were available for all the other cruises, comprising phosphate concentrations, nitrate and nitrite concentrations measured together, salinity, depth, temperature, photosynthetic eukaryotes, *Synechococcus* and *Prochlorococcus* abundances. With this dataset, only 28% of the total variation in dot blot hybridisation could be explained by the environmental parameters. When divided into physical, chemical and biological parameters, chemical parameters (salinity and concentrations of phosphate, and nitrite and nitrate considered together) explained the most at 19% of the variation in dot blot hybridisation data. Physical parameters (temperature and depth) explained 13% of the variation in dot blot hybridisation data with an overlap of 8% of variation in dot blot hybridisation data with chemical parameters. Biological parameters (chlorophyll *a* concentration and abundances of photosynthetic eukaryotes, *Synechococcus* and *Prochlorococcus*)

were able to explain up to 10% of the variation in dot blot hybridisation data with an overlap of 4% of dot blot hybridisation variation with chemical parameters and 5% overlap with physical parameters (Fig. 5.23).

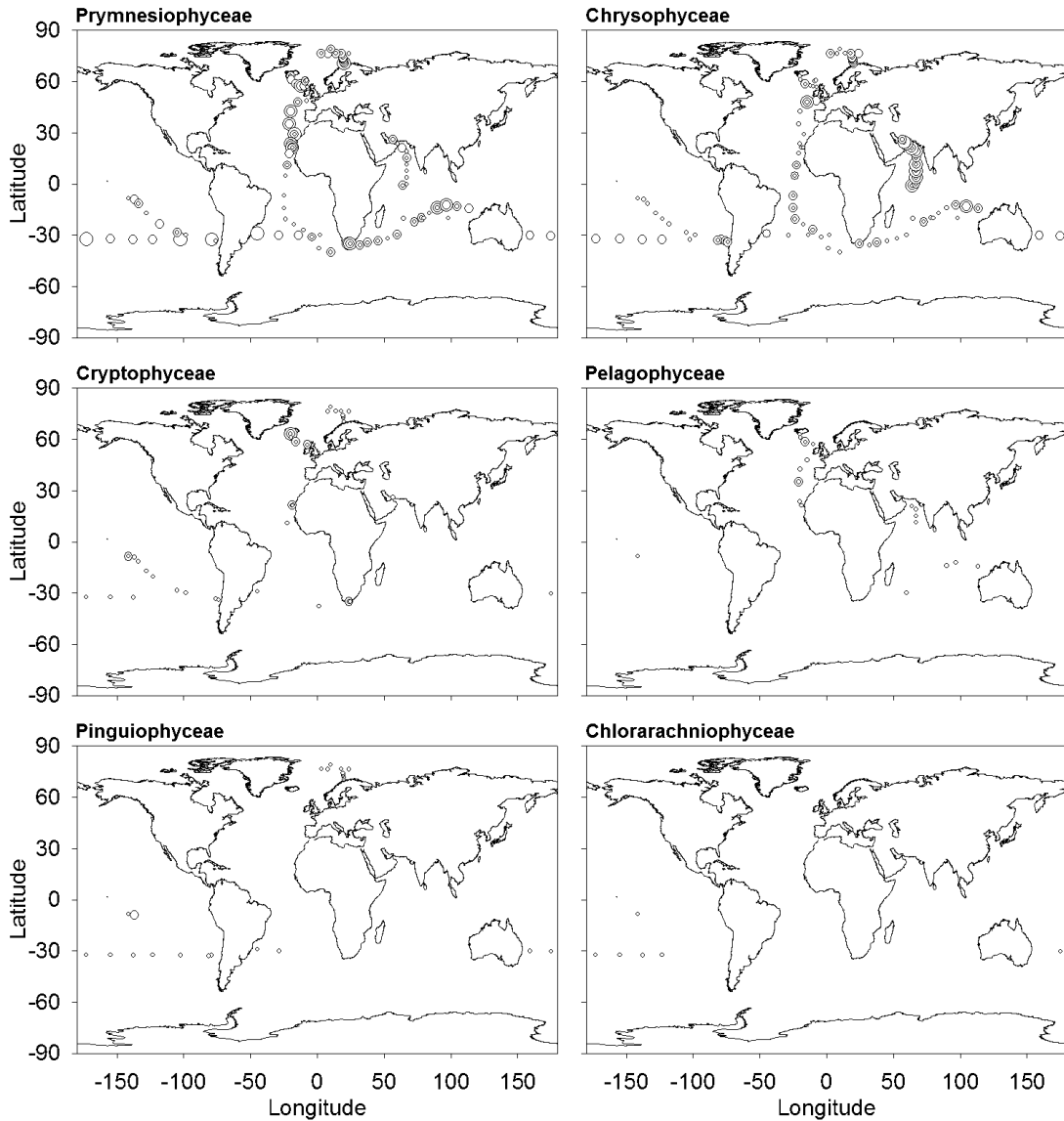


**Figure 5.22.** Global distribution patterns of PPE classes in samples as determined by dot blot hybridisations (relative hybridisation of class specific probes as a proportion of all amplified by primers PLA491F and OXY1313R). Circle sizes represent percent relative hybridisation values: small = 5-20%, medium = 20-50%, large = >50%. Values below 5% are not shown. Continued next page.



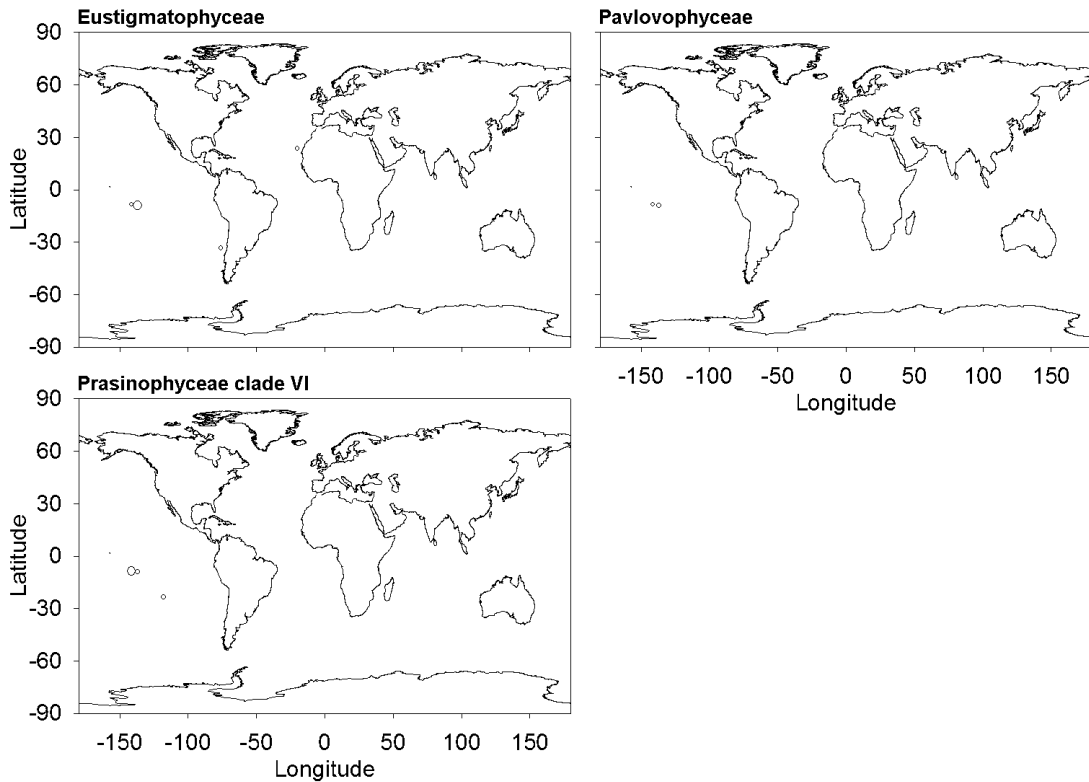


**Figure 5.22.** Continued.

A three-variable model explained over 22% of the variation in dot blot hybridisation data (Fig. 5.24). Phosphate concentration was able to explain the most data alone at 14% of variation in dot blot hybridisation data. When temperature was added to the model this rose to 20% of the variation and addition of nitrite and nitrate concentration increased it to 22.3%. Additional variables only caused very small increments in the amount of dot blot hybridisation data that could be explained. Temperature seems to be independent of the two chemical gradients as the plot shows these variables at right angles to each other (Fig. 5.24). Phosphate and nitrate + nitrite concentration is associated with Prasinophyceae clade VI and negatively associated with Eustigmatophyceae. Chrysophyceae and Eustigmatophyceae were associated with average to elevated temperatures and temperature was negatively associated with most of the other classes detected, most strongly with Chlorarachniophyceae, Cryptophyceae and Pinguiphyceae.

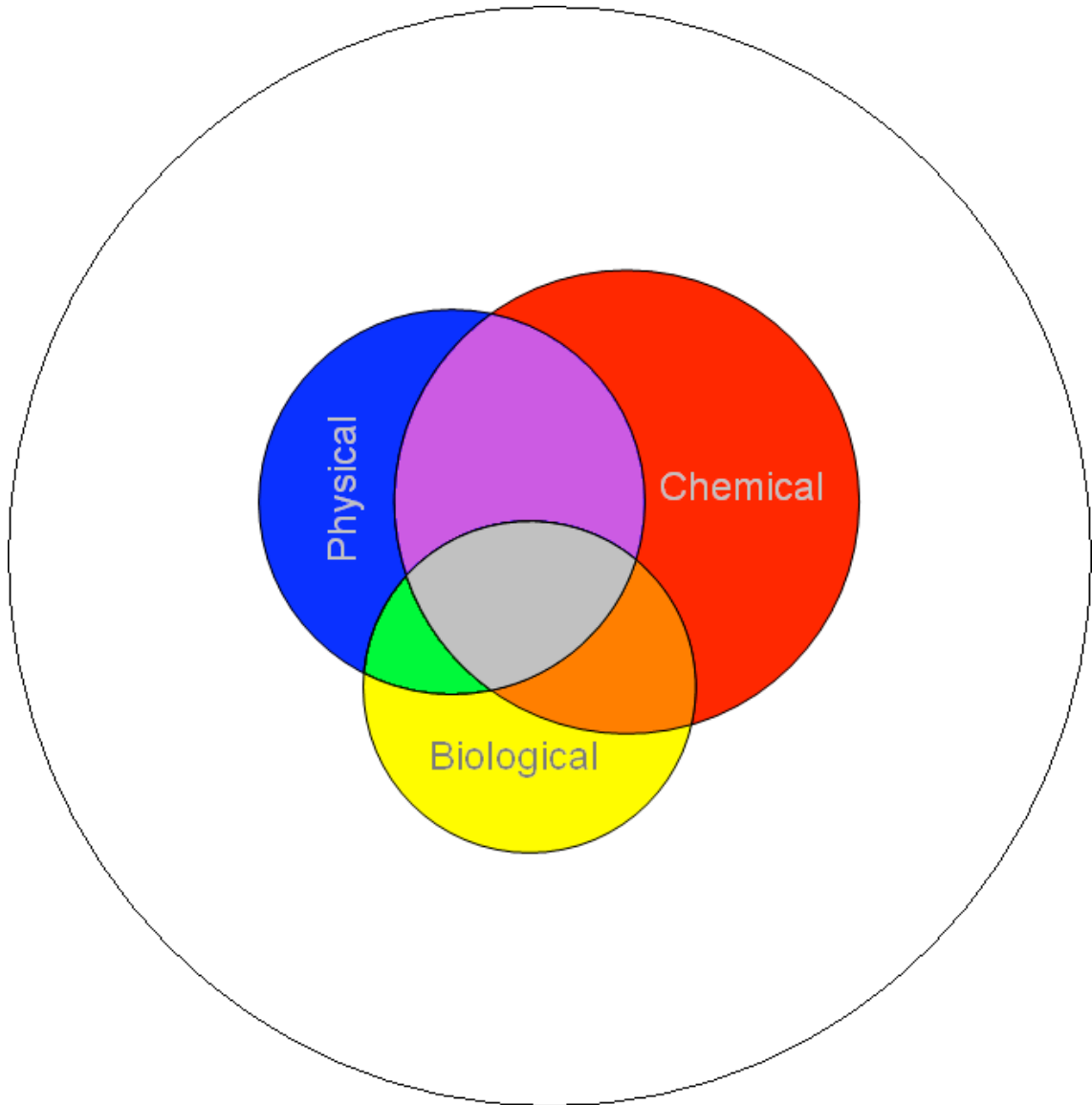


**Figure 5.23.** Venn diagram, drawn to scale by the eigenvalues calculated for the total variation in dot blot hybridisation in the global dataset (white) with the amount of variation that can be explained by physical (blue), chemical (red) and biological (yellow) parameters. These groups of parameters explain 14%, 20% and 9% of the total variation in dot blot hybridisation data respectively. The overlap in the amount of variation explained by both physical and chemical parameters is 8% of the total variation in dot blot hybridisation data. The overlap between chemical and biological parameters is 3% of the total variation and the overlap between physical and biological parameters is 4% of the total variation. Physical parameters encompass depth and temperature; chemical parameters encompass concentrations of nitrate and nitrite measured together, phosphate concentration and salinity; biological parameters encompass chlorophyll *a* concentration and flow cytometry counts of *Prochlorococcus*, *Synechococcus* and photosynthetic eukaryotes.

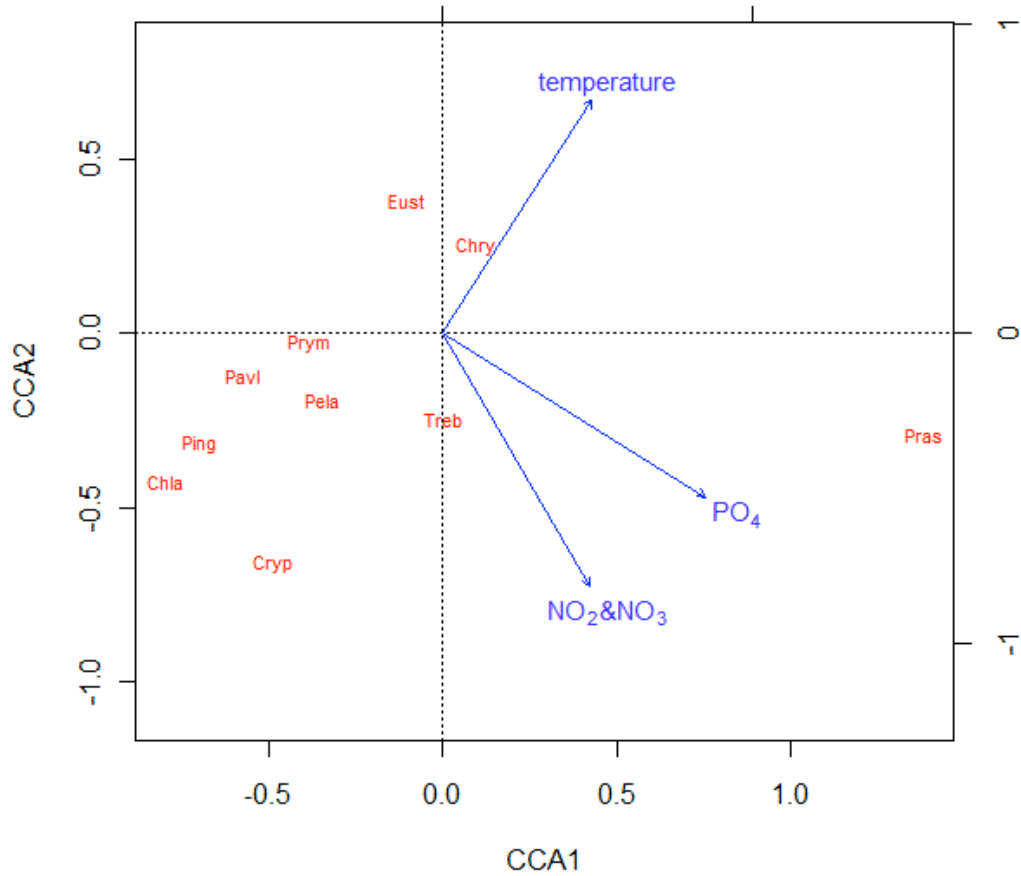


**Figure 5.24.** CCA plot for global PPE class distribution in relation to environmental variables, from dot blot hybridisation results for classes: Prymnesiophyceae (Prym), Chrysophyceae (Chry), Cryptophyceae (Cryp), Pinguiphyceae (Ping), Pelagophyceae (Pela), Eustigmatophyceae (Eust), Trebouxiophyceae (Treb), Pavlovophyceae (Pavl), Chlorarachniophyceae (Chla) and Prasinophyceae clade VI (Pras). Axis 1 (CCA1) can explain 17% of the total variation in dot blot hybridisation data, axis 2 (CCA2) can explain a further 4%. A third axis (not shown) can explain a further 1%.

### 5.2.5. Phylogenetic analysis of environmental sequences from the Arctic Ocean

A clone library was constructed for station Z59 at a depth of 60 m. 204 clones were examined by RFLP analysis and representatives of each RFLP type were sequenced. Only one clone was found to be chimeric. The majority of clones were related to Prymnesiophyceae (Fig. 5.25). With others related to Chrysophyceae, Cryptophyceae, cyanobacteria and one related to Bacillariophyceae. Notable in their absence were clones related to any clades of the Prasinophyceae.

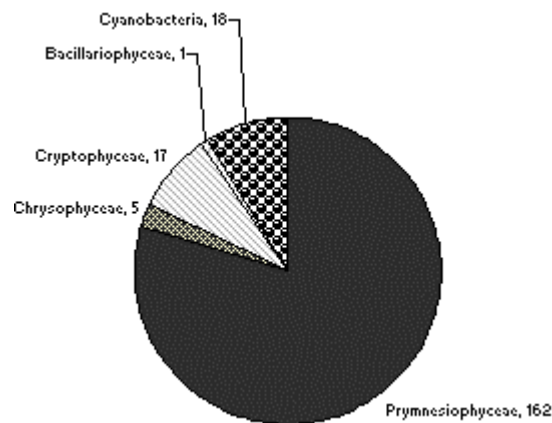


**Figure 5.25.** Pie-chart representing the proportion of clones assigned to different classes in the clone library constructed for station Z59 of the Arctic cruise by RFLP analysis and BLAST and ARB alignments. The class names and the number of clones assigned to each class are shown.

Sequences related to the Prymnesiophyceae were within the *Phaeocystis* genus (Fig. 5.26). Sequences related to the Chrysophyceae were in two clusters, one near to *Poterioochromonas stipitata*, a freshwater chrysophyte of approximately 6  $\mu\text{m}$  diameter with a small chloroplast, but dependent on mixotrophy by engulfing bacteria (Andersen, 2006). The second branched within the extensive cluster of environmental sequences from various marine systems, containing no described representatives (Fig. 5.27). Sequences related to Cryptophyceae clustered near to *Geminigera cryophila*, a cryptophyte associated with kleptoplasmy by dinoflagellates and ciliates (Takishita *et al.*, 2002; Johnson *et al.*, 2007). Thus, it is possible that the presence of sequences related to this species may indicate either the presence of *Geminigera* species or the presence of host cells which have temporarily sequestered plastids of *Geminigera* origin.

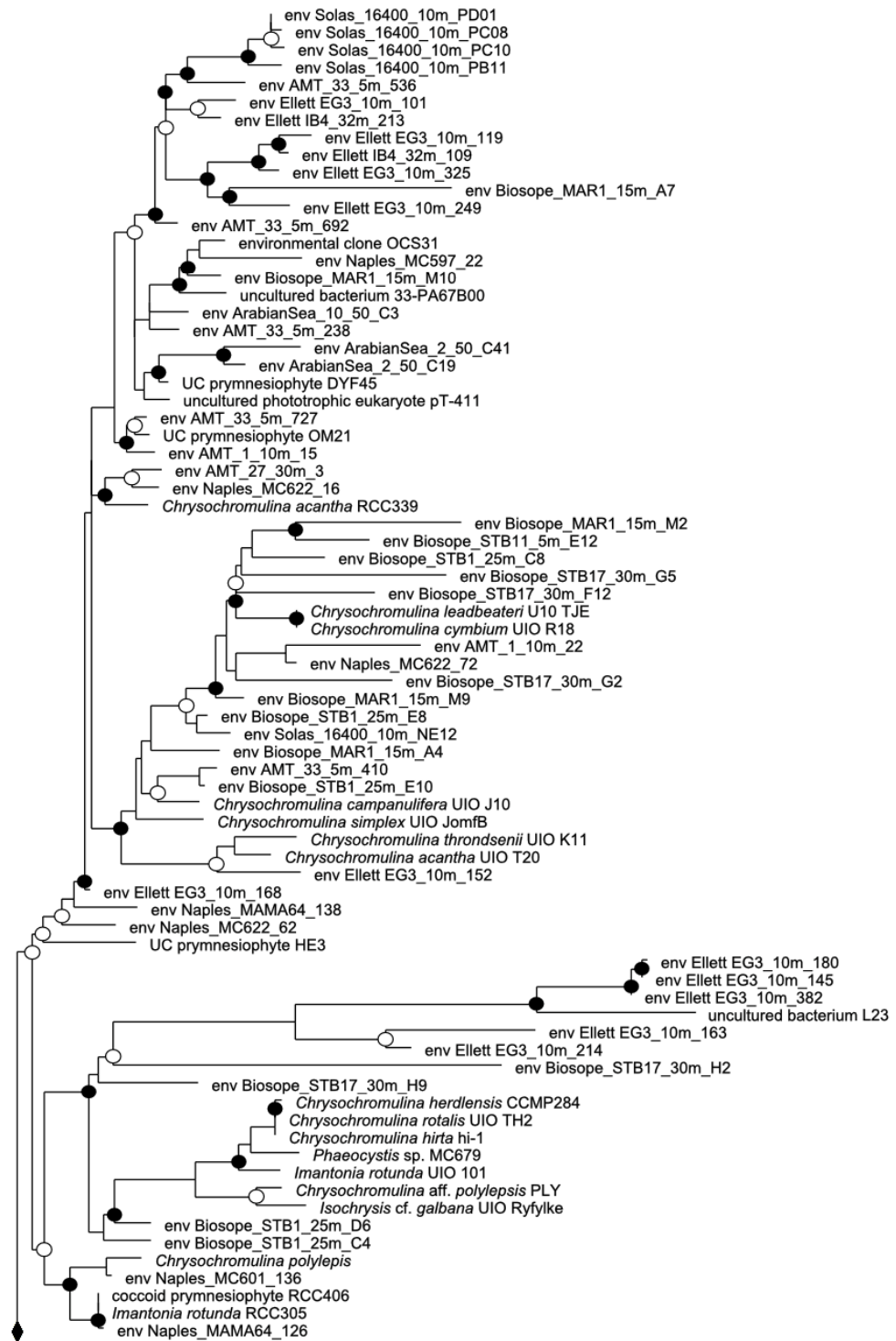


**Figure 5.26.** Phylogenetic relationships amongst the Prymnesiophyceae using plastid 16S rRNA gene sequences and a neighbour-joining algorithm. Environmental sequences from the Arctic Ocean station Z59 are indicated in blue. Bootstrap values above 70% are marked with an open circle, values above 90% are marked with a filled circle. Continued next page.

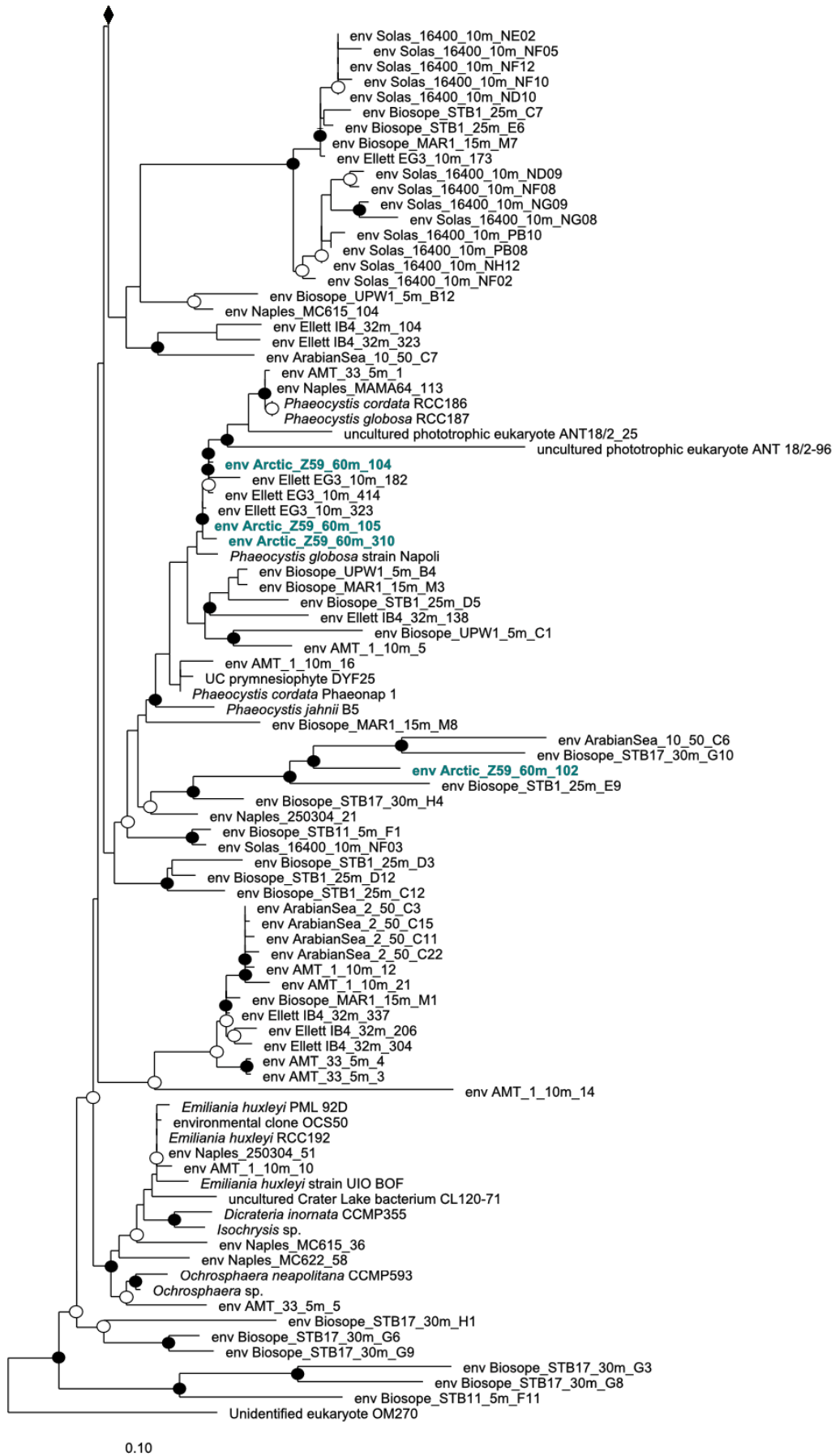
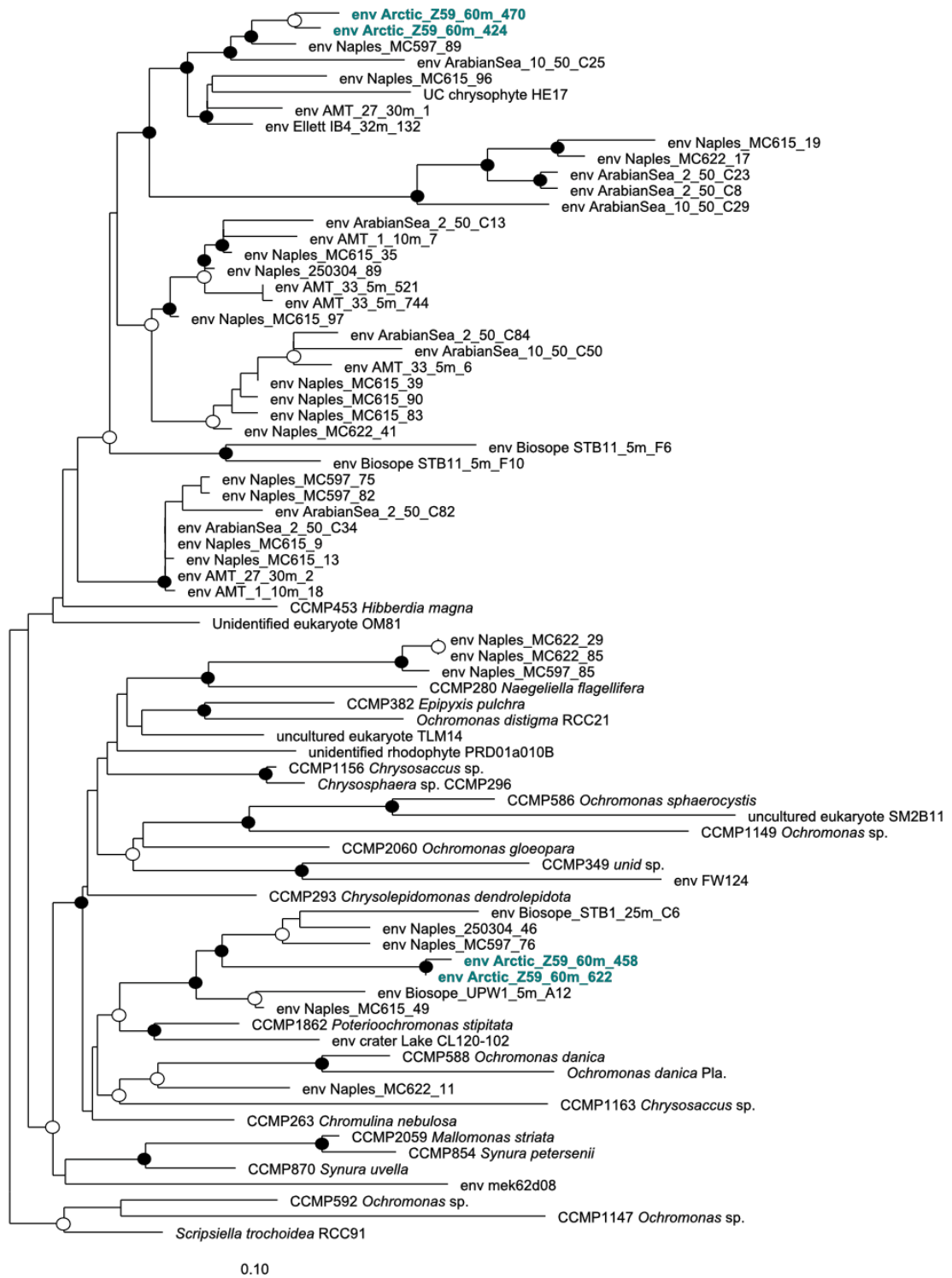
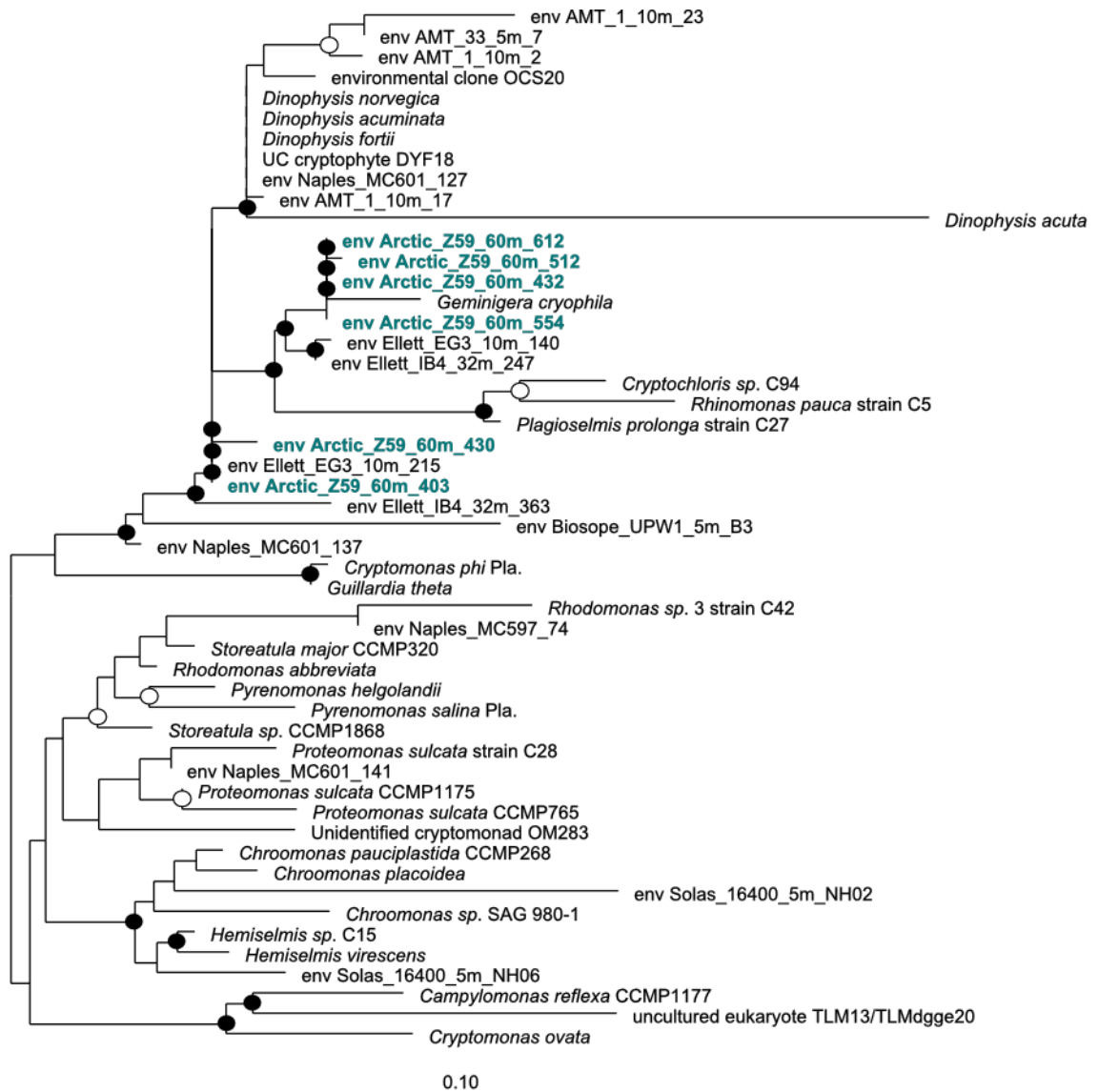


Figure 5.26. Continued



**Figure 5.27.** Phylogenetic relationships amongst the Chrysophyceae using plastid 16S rRNA gene sequences and a neighbour-joining algorithm. Environmental sequences from the Arctic Ocean station Z59 are indicated in blue. Bootstrap values above 70% are marked with an open circle, values above 90% are marked with a filled circle.



**Figure 5.28.** Phylogenetic relationships amongst the Cryptophyceae using plastid 16S rRNA gene sequences and a neighbour-joining algorithm. Environmental sequences from the Arctic Ocean station Z59 are indicated in blue. Bootstrap values above 70% are marked with an open circle, values above 90% are marked with a filled circle.

### 5.3. Discussion

#### 5.3.1. PPE class distribution patterns along the Arctic Ocean transect

Members of the Prymnesiophyceae and the Chrysophyceae were the dominant PPE classes detected by dot blot hybridisation analysis along the Arctic Ocean transect, and along the longitudinal transect these classes showed a complementary distribution as seen along the Atlantic Meridional Transect (section 3.2.4). CCA



indicated that the Prymnesiophyceae were associated with higher temperatures along the transect, indeed the highest relative hybridisation values for this class are at the most southerly stations of the transect. Chrysophyceae were associated with lower temperatures, photosynthetic eukaryote and *Synechococcus* abundances and higher nitrite concentrations, although this latter variable was relatively unimportant in explaining variation in dot blot hybridisation data. In contrast, the CCA performed on the AMT dataset (section 3.2.3) showed that the Chrysophyceae appeared not to be influenced by temperature, however the Prymnesiophyceae were associated with higher temperatures as seen here. Prymnesiophyceae are known to be important primary producers in the Arctic Ocean (Longhurst, 2007). However, they are usually larger than 5 µm in diameter and picophytoplankton are considered relatively unimportant at these high latitudes (Longhurst, 2007). Whilst prymnesiophyte sequences have featured in molecular studies of the picophytoplankton, they appear to be a minor contributor to this community (Lovejoy, 2006; Hamilton, 2008). This low importance of Prymnesiophyceae to the community may have resulted from the underestimation of the class observed for methods exploiting the nuclear SSU rRNA gene (Liu *et al.*, 2009). However, pigment analysis in the Arctic Ocean revealed a low concentration of chlorophyll *c*<sub>3</sub>, associated with Prymnesiophyceae and Pelagophyceae indicating a low abundance of Prymnesiophyceae in the Arctic Ocean (Lovejoy *et al.*, 2007). In contrast, Prymnesiophyceae were found to be important in Atlantic-type waters of the Arctic by FISH analysis (Not *et al.*, 2005).

Recent studies have indicated the importance of Prasinophyceae clade II to the picophytoplankton of the Arctic Ocean (Not *et al.*, 2005; Lovejoy *et al.*, 2007). However, the PLA491F-1313R primer pair (Fuller *et al.*, 2006b) seems to poorly amplify this group (McDonald *et al.*, 2007), and there are no plastid probes available for dot blot hybridisation which detect Prasinophyceae clade II. The fact that a clone library constructed from station Z59 revealed no sequences of any clade within the Chlorophyceae, suggests that, if present, Arctic Prasinophyceae are likely to be largely members of clade II. A further study indicated dominance of the recently discovered Picobiliphyceae in the Arctic Ocean (Hamilton *et al.*, 2008), again not detected by dot blot hybridisation as representatives of this class have not yet been cultured so plastid SSU rRNA gene sequences are not available for probe

development. Thus, the dominance of the Prymnesiophyceae indicated by the dot blot hybridisations performed here needs to be put into this context.

CCA showed that a great deal of variation in the dot blot hybridisation data could be explained by the environmental variables measured. However, it is unfortunate that nutrient data was available for only sixteen of the fifty-three samples analysed. Thus, there was a lot less variation in dot blot hybridisation data for the CCA to explain. Interestingly, the most useful variables in explaining variation in the dot blot hybridisation data were temperature and salinity, also found to be useful in explaining Arctic community structure by DGGE analysis (Hamilton *et al.*, 2008). These factors are likely to become increasingly important as both are associated with global climate change, as the temperature increases and ice cover is reduced, freshening the adjacent seawater (Greene *et al.*, 2008).

Nutrient data appeared to be largely unimportant in explaining the variation in dot blot hybridisation data in the Arctic Ocean, in comparison to the other variables measured. This may have been due to redundancy as nutrient concentrations are associated with other variables, such as depth. Nonetheless other parameters were much more strongly associated with dot blot hybridisation data than nutrient concentrations. Sea-ice algae, particularly diatoms, were found not to be limited by nitrogen or phosphorus source, but were seasonally limited by silicon availability (Gosselin *et al.*, 1990). Whilst silicate concentration is able to explain 34% of the variation in dot blot hybridisation data when considered alone, second only to temperature (data not shown), in the presence of other variables becomes unimportant. Pearson correlation analysis indicated that silicate concentration was significantly negatively correlated with temperature ( $p=0.005$ ) and positively correlated with phosphate, nitrate and nitrite concentration ( $p<0.001$ ) (data not shown). When considered alone, this variable correlates most strongly with Chrysophyceae. Whilst no marine Chrysophyceae have been characterised, well-known freshwater Chrysophyceae and Synurophyceae have a requirement for silicate due to their siliceous cyst stage, and some such as members of the order Parmales are also known to have silica scales although others are naked or have organic scales or loricae (Andersen, 2007).

### 5.3.2. PPE class distribution patterns along the Indian Ocean transect

The Indian Ocean transect appeared to be dominated by the Prymnesiophyceae as assessed by dot blot hybridisation analysis. However, CCA did not reveal any associations between this class and any of the environmental parameters measured, possibly as a result of the lack of data concerning nutrient availability along the transect. This dominance of Prymnesiophyceae is supported by pigment analysis along the same transect, where approximately half of the picoeukaryotic pigments at open ocean stations were attributed to this class (Not *et al.*, 2008). This study found the Prasinophyceae, particularly *Micromonas*, to be more important in the coastal stations comprising approximately a fifth of picoeukaryotic cell numbers. However, as mentioned above, clade II prasinophytes are not detected by the probes used in dot blot hybridisations. The second and third most abundant classes detected by dot blot hybridisation analysis were Chrysophyceae and Cryptophyceae, respectively. This is supported by sequences from photosynthetic classes obtained in nuclear rRNA gene clone libraries for samples from the cruise (Not *et al.*, 2008).

Although little data was available to describe the physical and chemical characteristics of the transect, a striking observation appears to be the presence of a thermocline along the length of the transect corresponding with peaks in chlorophyll *a* concentration. The thermocline separates the mixed surface layer and the deep water, thus a strong thermocline and shallow surface mixed layer limits the nutrient flux from deeper waters in turn limiting the phytoplankton growth (Sharples *et al.*, 2001).. The turbulence of the water column is therefore an important influence in phytoplankton ecology but is a complex characteristic. For example, multiple zones within the mixed layer have been observed with different physical characteristics and community structures (Joint and Pomroy, 1986). Therefore, collaboration between ecologists and physical oceanographers would be necessary to appreciate the interactions of these variables.

Key parameters found to be linked with variation in dot blot hybridisation data along the Indian Ocean transect were revealed by CCA to be *Synechococcus* abundance, salinity and temperature. In the same region, temperature was found to be linked with heterotrophic stramenopile flagellates of the MAST-4 group and secondarily to

irradiance (Rodríguez-Martínez *et al.*, 2009). Higher temperature waters appeared to be associated with lower salinities. Temperature was positively, and salinity negatively linked with variations in Pinguiphyceae and Pelagophyceae dot blot hybridisation data. Chrysophyceae appears not to be associated with temperature, but rather weakly associated with low abundances of *Synechococcus*. The lack of data for nutrient concentrations may have precluded other insights into the association of PPE classes with environmental parameters from being drawn. In the northern Indian Ocean (Arabian Sea) nitrogen availability and dissolved oxygen were found to have associations with PPE classes, including an association between Chrysophyceae and higher levels of dissolved oxygen and lower concentrations of nitrogen (Fuller *et al.*, 2006a). However, this analysis also leaves the distribution of Prymnesiophyceae largely unexplained (Fuller *et al.*, 2006a).

### **5.3.3. PPE class distribution patterns along the BEAGLE transect**

This circumnavigation of the southern hemisphere was also dominated by Prymnesiophyceae and Chrysophyceae. Such a phenomenon was also found in the Pacific Ocean (where eight of the fifteen stations of the BEAGLE transect were located) along the BIOSOPE transect (Lepère *et al.*, 2009), as well as along the Indian Ocean transect which covered a similar area of the Indian Ocean as leg 5 of the BEAGLE transect (section 5.2.3.3). A study of the pigment content of surface water samples showed that the small phytoplankton community of the Pacific Ocean was dominated by flagellates, based on a combination of diagnostic pigments, whereas prokaryotic phytoplankton were more important in the Atlantic and Indian Oceans (Barlow *et al.*, 2007). The combination of pigments considered for flagellates comprised 19'hexanoyloxyfucoxanthin, diagnostic for Prymnesiophyceae; alloxanthin, diagnostic for Cryptophyceae; chlorophyll *b*, diagnostic for green flagellates including Prasinophyceae and 19'butanoyloxyfucoxanthin, a controversial pigment as its specificity is not adequately resolved. However, it has been associated with both the Chrysophyceae and Prymnesiophyceae (Barlow *et al.*, 2007). Similarly, dot blot hybridisation values were higher in the Pacific Ocean than in the Atlantic and Indian Oceans. In particular, the dot blot hybridisation values for Prymnesiophyceae and Chrysophyceae were both much higher in the Pacific Ocean than in the Atlantic and Indian Oceans. The prymnesiophyte pigment,

19'hexanoyloxyfucoxanthin, often dominates over other diagnostic pigments in several different regions (Liu *et al.*, 2009).

The pigment based study found that the dominance of flagellates in the Pacific Ocean was associated with the cooler temperature and higher inorganic nitrogen concentration (Barlow *et al.*, 2007). CCA of PPE dot blot hybridisation data indicated that temperature and nitrate concentration were useful in explaining the variation in the data obtained. However, other parameters were more strongly associated with the dot blot hybridisation data. In particular, *Prochlorococcus* abundance explained the largest proportion of PPE dot blot hybridisation data, itself correlated with temperature, and associated with Chrysophyceae and Pinguiphyceae and low levels of Pavlovophyceae, Cryptophyceae and Chlorarachniophyceae. Chrysophyceae was also associated with elevated silicate level, possibly as a result of a silicate requirement for maintenance of silica scales. It is necessary for marine picochrysoytes to be isolated and characterised so that these nutrient requirements can be elucidated.

#### **5.3.4. Global perspectives on PPE class distributions**

The classes detected by dot blot hybridisation analysis appear to be ubiquitous, but with different distribution patterns at both the basin and global scale. The Prymnesiophyceae and Chrysophyceae were consistently the most abundant classes detected by dot blot hybridisation analysis over all seven cruises considered. Furthermore, these classes showed complementary distribution patterns along many cruises, although this was more obvious in some transects than others. This observation supports the suggestion that Prymnesiophyceae have been consistently underestimated by molecular studies of PPEs as a result of PCR bias against the group when using primers targeting the nuclear SSU rRNA gene (Liu *et al.*, 2009). This is particularly significant in the light of data suggesting that the Prymnesiophyceae are among the most active primary producers in the Ocean, and this activity is disproportionately large compared to their abundance (Jardillier *et al.*, submitted). Together this data suggests that pico-sized prymnesiophytes may be among the most important primary producers in the global ocean.

More minor classes also showed varying distribution patterns. Members of the Cryptophyceae appeared to be fairly ubiquitous, but had consistently, relatively low percent relative hybridisation values. Members of the Pinguiphyceae were also fairly widespread whilst the Pelagophyceae, Pavlovophyceae, Eustigmatophyceae, Trebouxiophyceae and Prasinophyceae clade VI were only detected in certain regions. Whilst members of the Pelagophyceae are very easily cultivated from a variety of marine environments (LeGall *et al.*, 2008), the data presented here indicates they are in fact a minor class in the global ocean.

Multivariate statistics consistently showed that chemical variables were able to explain more variation in dot blot hybridisation data than physical and biological parameters. Indeed, marine production is vulnerable to constraint by nutrient availability, and phytoplankton nitrogen:phosphorus (N:P) ratios differ with group. For example, green algae have higher ratios than red algae and more specifically, growth strategies also alter this ratio with generalist strategies having near Redfield ratios of 16:1 N:P, opportunistic strategies relying on low N:P ratios and survivalist strategy relying on high N:P ratios (Arrigo, 2005). However, probably as a result of redundancy of variables in the statistical models constructed, physical and biological parameters were often among those able to explain the most variation when considered on their own.

Temperature appears to be a key variable in explaining variation in PPE dot blot hybridisation data. This parameter is among the most useful in multivariate statistics for all cruises except the AMBITION transect (Fuller *et al.*, 2006a). When the global dataset was analysed, temperature remained an important parameter. Temperature is a fairly complex variable, it varies with latitude, seasonality and depth down the water column, and is associated with global climate change. The seasonality of temperature is associated with stratification of the water column and thus is associated with nutrient availability, as a shallow mixed layer precludes the introduction of nutrients from deeper waters (Tait and Dipper, 1998; Williams and Follows, 2003). A 20-year study of the plankton (larger than the pico-size fraction) showed that global climate change, resulting in sea-surface warming altered the phytoplankton distribution in the North Atlantic Ocean (Richardson and Schoeman, 2004). This accentuated the difference in productivity between warm and cool

waters, with cooler regions becoming the site of greater phytoplankton abundance whereas warmer regions had lower abundance (Richardson and Schoeman, 2004). Overall, increasing surface water temperature is expected to result in reduced productivity (Behrenfeld *et al.*, 2006). In the CCA calculations performed in this work, some of the associations of temperature with classes are different between cruises, probably as a result of the complexity of this variable. In the Arctic cruise, where the average temperature was just 7°C, the higher temperatures encountered are associated with higher Prymnesiophyceae and lower Chrysophyceae dot blot hybridisation values, whereas along the BEAGLE transect, the average temperature was 20°C and higher temperatures were associated with higher values for the Chrysophyceae, whilst Prymnesiophyceae appeared relatively unaffected. At the global scale, Chrysophyceae was associated with average to high temperatures.

The low proportion of variation in dot blot hybridisation explained by the CCA on the global dataset indicates that other factors may influence these distribution patterns. Viruses and predators are important in shaping marine microbial communities. Top down pressures had a strong influence over the picoeukaryote community of a freshwater lake (Lepère *et al.*, 2006). However, these different sets of variables are in fact closely linked. Viral lysis is an important factor in the regeneration of nutrients in the microbial loop (Azam *et al.*, 1983; Wilson and Mann, 1997). The infection of cells and the mode of infection (i.e. lytic or lysogenic infection) is affected by the nutritional condition of the host cells (Wilson and Mann, 1997) and the productivity of a region is dependent on availability of nutrients which may be released as a result of viral lysis (Azam *et al.*, 1983).

A further reason for the small proportion of variation that could be explained by CCA is that analysis of PPEs at the class level excludes analysis of distribution patterns of PPEs at a higher taxonomic distribution. By assessing the prokaryotic picophytoplankton at the ecotype level, Zwirgmaier *et al.* (2008) were able to give global insights into the association of distribution patterns with environmental parameters. Indeed, specifically specialised ecotypes within Prasinophyceae were found to be influenced by nutrient levels (Viprey *et al.*, 2008). The Prymnesiophyceae, found to be the most important class detected by dot blot hybridisations is known to contain a vast diversity that had previously been

underestimated (Liu *et al.*, 2009), and it is likely that the clades harboured within this diversity exhibit unique distribution patterns and associations with external parameters.



## **Chapter 6:**

### **General discussion and future perspectives**

## 6.1. General discussion

In this work, three different methods were used to assess the PPE community: construction of clone libraries, dot blot hybridisations and fluorescent *in situ* hybridisations (FISH). The use of such a combined approach allowed various findings to be made. For example, the comparison of nuclear and plastid SSU rRNA gene clone libraries supported the assertion of Liu *et al.* (2009), that the nuclear rRNA gene based approach underestimates diversity within the prymnesiophyte community. Furthermore, FISH analyses indicated that members of this class were more abundant along the extended Ellett Line than was suggested in dot blot hybridisation analysis. Conversely, the Cryptophyceae appeared to be much less abundant by FISH than by dot blot hybridisations. This is likely to be as a result of the Cryptophyceae plastid SSU rRNA gene-targeted dot blot hybridisation probe also detecting the Cryptophyceae-derived plastids that are present in members of the dinoflagellate genus *Dinophysis*, whereas the nuclear SSU rRNA-targeted FISH probe would not detect members of this group.

The use of FISH has the advantage that individual cells can be discriminated and the number of cells per milliliter of sample can be calculated. This may be a more meaningful measure of abundance than the percent relative hybridisation calculated from dot blot hybridisation data. FISH is also PCR independent and as such is free from the biases that may be introduced in by PCR amplification. However, a recent study comparing nuclear SSU rRNA gene clone library construction with a PCR-free approach by analysis of Global Ocean Survey (GOS) metagenome data showed very similar results, indicating that the PCR step involved in clone library construction did not impose significant bias (Not *et al.*, 2009).

The use of dot blot hybridisation analysis allowed a larger number of samples to be processed than would have been possible by alternative methods. The approach allowed PPE class level distribution patterns to be identified. That the total class-specific signal rarely reached 100% indicates that these samples contained amplicons from classes not targeted by the probes used. These may have belonged to classes such as the Prasinophyceae clade II, Dictyochophyceae or non-PPE sequences such

as those belonging to cyanobacteria or other prokaryotes. Sequences with such affiliations were found in all plastid SSU rRNA gene libraries constructed. This effect is likely to be particularly marked in samples with low abundances of PPEs as a lack of target sequence may increase the proportion of non-specific PCR amplification.

Both the dot blot hybridisation and FISH approaches were limited by the use of probes specific to the class level. A higher taxonomic resolution may have yielded further information and clearer patterns of distribution. Furthermore, probes may miss target organisms due to differences in the DNA (dot blot hybridisations) or RNA (FISH) sequence targeted by the probe. Probe design may be limited by the availability of sequence data, and we cannot be sure that the probes will target all organisms of a class as there may be some variation in their DNA sequences.

Clone library construction is an approach that is not limited to a particular taxonomic level and, rather than providing data on the distribution on PPEs, clone libraries are more useful for assessment of the diversity of the group. Novel lineages have been discovered by this type of analysis, and the amassed sequence data can be used in the development of new probes. However, the use of restriction fragment length polymorphism (RFLP) screening is necessary to restrict the sequence data to a manageable level, but may mask some of the diversity present. It is also prohibitive to construct clone libraries for large numbers of samples as clone library construction, RFLP screening and sequence analysis is more time consuming than other approaches.

All of the approaches used, in all of the different regions studied, indicated that the Prymnesiophyceae were a highly abundant class in the world ocean. This work provided a lot of support for the notion that previous work with nuclear SSU rRNA gene libraries has underestimated the abundance and diversity of this class (Liu *et al.*, 2009). Here plastid 16S rRNA gene clone libraries constructed for AMT15 revealed more diversity than their nuclear 18S rRNA gene counterparts (Section 3.2.6). Furthermore, dot blot hybridisation analyses indicated that the Prymnesiophyceae were a key class in all major ocean basins. Coupled to the finding of Jardillier *et al.* (submitted) that Prymnesiophyceae were disproportionately important in CO<sub>2</sub>

fixation despite low numerical contribution to the total picophytoplankton at the study site, this work highlighting their globally widespread abundance may indicate that pico-sized prymnesiophytes may be among the most important primary producers in the world's oceans.

This work also confirmed Fuller *et al.*'s (2006a) argument that the Chrysophyceae were abundant in the marine environment despite never having been isolated in culture. This work extended this observation from the Arabian Sea to all major ocean basins. In addition to this, the distribution of this class was found to have an inverse relationship with the distribution of the Prymnesiophyceae. Furthermore, the use of fluorescent *in situ* hybridisation, utilising a probe targeted to the plastid gave some morphological information on the class, as labelled cells appeared to contain two plastids. It is often necessary to maintain members of a class in culture in order to make morphological observations.

The phylogenetic analyses revealed lineages within both the Prymnesiophyceae and the Chrysophyceae which contained no cultured members, but which did contain environmental sequences from a broad range of geographical locations. Furthermore, an extensive lineage within the Prasinophyceae was also found to contain many sequences from the Atlantic Ocean cruises (AMT15 and the extended Ellett Line) as well as sequences that had been obtained from the Pacific Ocean (Lepère *et al.*, 2009). This suggests that novel lineages within these three classes are widely distributed.

Other classes did not appear to be ubiquitous and certainly were only found above the detection limits for dot blot hybridisations at particular sites. The different classes had clearly different distribution patterns (see Fig. 5.22) and thus were likely to have been influenced by different parameters. The classes may have also contained clades with different growth strategies which would influence their distributions.

Canonical correspondence analyses (CCAs) could explain most of the variation for small datasets, as there was little variation present within these datasets. However, in datasets with larger sample numbers such as AMT15 (section 3.2.2) and the global dataset (section 5.2.4), a lot of the variation in dot blot hybridisation data was

unexplained. This is likely to result from the lack of taxonomic resolution in the dot blot hybridisation method. A large proportion of the variation in dot blot hybridisations targeting ecotypes within the prokaryotic picophytoplankton could be explained by the parameters used in this work (Zwirglmaier *et al.*, 2008). However, the CCA calculations provided some insights into the environmental parameters that may influence the distribution patterns of PPE classes. When divided into physical, chemical and biological parameters, chemical parameters were consistently able to explain the most variation, suggesting that PPE distribution patterns are influenced by nutrient availability and salinity. Within the physical parameters, temperature was a key variable which appeared to influence PPE distributions in every dataset studied. Mixing of the water column is a factor which may be related to the PPE community structure. This is a factor associated with variables such as temperature, density structure and salinity. However the complexity of some of these variables, such as the association of temperature with latitude and depth as well as the depth of the mixed layer confuses this association. Therefore, data on mixed layer depth may be potentially useful in explaining PPE community structure. Some of the variation in dot blot hybridisation data may potentially be explained by environmental factors for which data were not available. In freshwater studies, zooplankton grazing has been shown to influence small eukaryote assemblages (Lepère *et al.*, 2006). Marine viruses are known to be an important controlling factor over their host communities (Fuhrman, 1999) so it is possible that data on parameters of this nature may help to explain more of the variation in PPE distribution patterns. Furthermore, it has recently been shown that in the North Atlantic Ocean PPEs perform unexpectedly high rates of bacterivory (Zubkov and Tarran, 2008). If this is a global phenomenon it is likely that PPEs are less dependent on the availability of inorganic nutrients than previously thought. It may also result in PPE distribution patterns being influenced by the availability of bacterioplankton prey.

The large volumes of water collected and analysed in this work will have masked any small-scale patchiness of PPE distributions. Indeed the marine environment is unlikely to be homogenous as nutrient availability for pico-sized plankton is likely to be strongly variable over very small scales due to inputs from cell lysis. Such nutrient patches have been observed as small areas containing large numbers of chemotactic bacteria (Blackburn *et al.*, 1998). Thus, by considering distributions of

PPEs on much smaller scales, it is likely that close associations with environmental factors can be resolved.

## 6.2. Future perspectives

Limitations of this work were that the dot blot hybridisation analysis was constrained to the class level, whereas studying at a higher taxonomic resolution is likely to yield more information, particularly with reference to the association of PPE distributions with environmental parameters. It is probable that clades within PPE classes are yet to be discovered. Given findings in prokaryotic picophytoplankton and within Prasinophyceae clade II, it is likely that different PPE ecotypes exist associated with specific depths down the water column. In the CCA analyses at the class level performed in this work, depth was not found to be particularly important. This would be expected if beyond the class level, different depth-adapted clades were present.

Differently-adapted clades can be found by detailed study of depth profiles, particularly of stratified water columns. It may be useful to design PCR primers to specifically target, for example, the Prymnesiophyceae or Chrysophyceae and use DNA sequencing to look for depth-specific clusters. Furthermore, it has been asserted that it is imperative that pico-sized marine Prymnesiophyceae and Chrysophyceae be isolated in culture in order for these classes to be fully appreciated. This effort could yield information on the organisms represented by the clusters of environmental sequences seen by phylogenetic analysis. It would be particularly interesting to isolate pico-sized members of these classes from different depths of a stratified water column and, if indeed present, characterise different ecotypes within the classes.

It may be possible to design ‘cluster-specific’ probes from the 16S rRNA gene sequence data that has been amassed through this work and that of others (Fuller *et al.*, 2006b; McDonald *et al.*, 2007; Lepère *et al.*, 2009; Jardillier *et al.*, submitted). However, these are likely to begin to fall below the detection limits of dot blot hybridisation, which require percent relative hybridisation values above 2%. Thus, it may be necessary to shift to a more sensitive method such as quantitative PCR (qPCR). However, a major drawback of this technique would be that analysing large

numbers of samples would be much more costly and time consuming, precluding such a broad study as that presented here.

The use of high throughput sequencing has the potential to analyse large numbers of samples quickly, with data being made available for both qualitative diversity studies and quantitative abundance and distribution studies. The latter can be achieved by searching sequence data for the presence of sequence signatures, diagnostic to the group of interest. This approach would be advantageous as it would be more sensitive than dot blot hybridisation analysis, whilst still allowing rapid analysis of large numbers of samples.

In order to address the issue of the bias associated with the plastid SSU rRNA gene primers used against Prasinophyceae clade II, the bias could potentially be quantified by experimentally amplifying known ratios of classes (for example, Prymnesiophyceae and Prasinophyceae clade II). This may help to translate the proportion of amplicons of each class in a sample into the proportion of organisms that they represent in the environment.

The use of plastid-targeted FISH probes opens doors for quantifying heterotrophic members of potentially photosynthetic classes. For example, what proportions of the prymnesiophytes found in the extended Ellett Line FISH analysis (section 4.2.6) using the 18S SSU rRNA gene prymnesiophyte probe contained a plastid? It may also be useful in determining the number of plastids per cell, as was revealed for the Chrysophyceae with this approach. This has implications for how readily the targetted class is likely to be amplified from an environmental sample by the 16S rRNA primers.

## **Bibliography**



- Aiken, J. and Bale, A.J.** (2000). An introduction to the Atlantic Meridional Transect (AMT) programme. *Prog. Oceanogr.* **45**, 251-256.
- Aiken, J., Rees, N., Hooker, S., Holligan, P., Bale, A.J., Robins, D., Moore, G., Harris, R. and Pilgrim, D.** (2000). The Atlantic Meridional Transect: overview and synthesis of data. *Prog. Oceanogr.* **45**, 257-312.
- Andersen, R.A.** (2007). Molecular systematics of the Chrysophyceae and Synurophyceae. In: Brodie, J. and Lewis, J. *Unravelling the Algae: the past, present and future of algae systematics*. CRC Press, Boca Raton, USA. 283-311.
- Andersen, R.A.** (2006) <http://starcentral.mbl.edu/mv/PDF/buildPDF.php?imageid=2645>.
- Andersen, R.A., Saunders, G.W., Paskind, M.P. and Sexton, J.** (1993). Ultrastructure and 18S rRNA gene sequence for *Pelagomonas calceolata* gen. and sp. nov. and the description of a new algal class the Pelagophyceae *classis nov.* *J. Phycol.* **29**, 701-715.
- Andersen, R.A., Van der Peer, Y., Potter, D., Sexton, J.P., Kawachi, M. and LaJeunesse, T.** (1999). Phylogenetic analysis of the SSU rRNA from members of the Chrysophyceae. *Protist* **150**, 71-84.
- Archibald, J.M.** (2009). The puzzle of plastid evolution. *Current Biology.* **19**, 81-88.
- Archibald, J.M. and Keeling, P.J.** (2002). Recycled plastids: a 'green movement' in eukaryotic evolution. *Trends Genet.* **18**, 577-584.
- Arrigo, K.R.** (2005). Marine microorganisms and global nutrient cycles. *Nature.* **437**, 349-355.
- Azam, F., Fenchel, T., Field, J.G., Gray, J.S., Meyer-Reil, L.A. and Thingstad, F.** (1983). The ecological role of water-column microbes in the sea. *Mar. Ecol. Prog. Ser.* **10**, 257-263.
- Baldauf, S.L.** (2003). The deep root of eukaryotes. *Science* **300**, 1703-1706.
- Bano, N., and Hollibaugh, J.T.** (2002). Phylogenetic composition of bacterioplankton assemblages from the Arctic Ocean. *Appl. Environ. Microbiol.* **68**, 505-518.
- Bano, N., Ruffin, S., Ransom, B. and Hollibaugh, J.T.** (2004). Phylogenetic composition of Arctic Ocean archaeal assemblages and comparison with Antarctic assemblages. *Appl. Environ. Microbiol.* **70**, 781-789.
- Barlow, R.G., Mantoura, R.F.C. and Cummings, D.G.** (1999). Monsoonal influence on the distribution of phytoplankton pigments in the Arabian Sea. *Deep-Sea Res. II* **46**, 677-699.

- Barlow, R., Stuart, V., Lutz, V., Sessions, H., Sathyendranath, S., Platt, T., Kyewalyanga, M., Clementson, L., Fukasawa, M., Watanabe, S. et al.** (2007). Seasonal pigment patterns of surface phytoplankton in the subtropical southern hemisphere. *Deep-Sea Res. I* **54**, 1687-1703.
- Behrenfeld, M.J., O'Malley, R.T., Siegel, D.A., McClain, C.R., Sarmiento, J.L., Feldman, G.C., Milligan, A.J., Falkowski, P.G., Letelier, R.M. and Boss, E.S.** (2006). Climate-driven trends in contemporary ocean productivity. *Nature* **444**, 752-755.
- Biegala, I. C., Not, F., Vaultot, D. and Simon N.** (2003). Quantitative assessment of picoeukaryotes in the natural environment using taxon-specific oligonucleotide probes in association with tyramide signal amplification-fluorescent in situ hybridization and flow cytometry. *Appl. Environ. Microbiol.* **69**, 5519–5529.
- Blackburn, N., Fenchel, T., and Mitchell, J.** (1998). Microscale Nutrient Patches in Planktonic Habitats Shown by Chemotactic Bacteria. *Science* **282**, 2254-2256.
- Blanchot, J. Andre, J.M., Navarette, C., Neveux, J. and Radenac, H.** (2001). Picophytoplankton in the equatorial Pacific: Vertical distributions in the warm pool and in the high nutrient low chlorophyll conditions. *Deep-Sea Res.* **48**, 297-314.
- Booth, B.C. and Marchant, H.J.** (1987). Parmales, a new order of marine chrysophytes, with descriptions of 3 new genera and 7 new species. *J. Phycol.* **23**, 245-260.
- Bouman, H.A., Ulloa, O., Scanlan, D.J., Zwirgmaier, K., Li, W.K.W., Platt, T., Stuart, V., Barlow, R., Leth, O., Clementson, L., Lutz, V., Fukasawa, M., Watanabe, S. and Sathyendranath S.** (2006). Oceanographic Basis of the Global Surface Distribution of *Prochlorococcus* Ecotypes. *Science*. **312**, 918 – 921.
- Bravo-Sierra, E. and Hernández-Becerril, D.U.** (2003). Parmales (Chrysophyceae) from the Gulf of Tehuantepec, Mexico, including the description of a new species, *Tetraparma Insecta* Sp. Nov., and a proposal to the taxonomy of the group. *J. Phycol.* **39**, 577-583.
- Brown, M.V., and Bowman, J.P.** (2001). A molecular phylogenetic survey of sea-ice microbial communities (SIMCO). *FEMS Microbiol. Ecol.* **35**, 267–275.
- Butcher, R.W.** (1952). Contributions to our knowledge of the smaller marine algae. *J. Mar. Biol. Assoc. UK* **31**, 175-191.
- Campbell, L. and Vaultot, D.** (1993). Photosynthetic picoplankton community structure in the subtropical North Pacific Ocean near Hawaii (station ALOHA). *Deep-Sea Res. I* **40**, 2043-2060.
- Caron, D.A., Gast, R.J., Lim, E.L. and Dennett, M.R.** (1999). Protistan community structure: molecular approaches for answering ecological questions. *Hydrobiologica* **401**, 215-227.

- Cavalier-Smith, T.** (2006). The tiny enslaved genome of a rhizarian alga. *Proc. Natl. Acad. Sci.* **103**, 9379-9380.
- Chambouvet, A., Morin, P., Marie, D. and Guillou, L.** (2008). Control of toxic marine dinoflagellate blooms by serial parasitic killers. *Science* **322**, 1254-1257.
- Chesnick, J.M., Morden, C.W. and Schmieg, A.M.** (1996). Identity of the endosymbiont of *Peridinium foliaceum* (Pyrrophyta): analysis of the *rbcLS* operon. *J. phycol* **32**, 850-857.
- Cole J.R., Chai B., Marsh T.L., Farris R.J., Wang Q., Kulam S.A., Chandra S., McGarrell D.M., Schmidt T.M., Garrity G.M., et al.** (2003). The Ribosomal Database Project (RDP-II): previewing a new autoaligner that allows regular updates and the new prokaryotic taxonomy. *Nucl. Acids Res.* **31**, 442-3.
- Derelle, E., Ferraz, C., Rombauts, S., Rouzé, P., Worden, A.Z., Robbens, A., Partensky, F., Degroeve, S., Echeynié, S., Cooke, R. et al.** (2006). Genome analysis of the smallest free-living eukaryote *Ostreococcus tauri* unveils many unique features. *Proc. Natl. Acad. Sci. USA* **103**, 11647-11652.
- Devred, E., Sathyendranath, S. and Platt, T.** (2007). Delineation of ecological provinces using ocean colour radiometry. *Mar Ecol Prog Ser* **346**, 1-13.
- Díez, B., Pedros-Alio, C. and Massana, R.** (2001). Study of genetic diversity of eukaryotic picoplankton in different oceanic regions by small-subunit rRNA gene cloning and sequencing. *Appl. Environ. Microbiol.* **67**, 2932-2941.
- Droop, M.R.** (1954). A note on the isolation of small marine algae and flagellates for pure cultures. *J. Mar. Biol. Assoc. UK* **33**, 511-514.
- Ducklow, H.W.** (2003). Biogeochemical Provinces: Towards a JGOFS Synthesis. In *Ocean Biogeochemistry: a synthesis of the Joint Global Ocean Flux Study (JGOFS)*, pp. 3-17. Edited by M.J.R. Fasham. Springer-Verlag Berlin Heidelberg.
- Ducklow, H.W., Steinberg D.K. and Buesseler K.O.** (2001). Upper Ocean Carbon Export and the biological pump. *Oceanography* **14**, 50-58.
- Edwards, U., Rogall, T., Blocker, H., Emide, M. and Bottger, E.C.** (1989). Isolation and direct complete nucleotide determination of entire genes. Characterization of a gene coding for 16S ribosomal RNA. *Nucleic Acids Res* **17**, 7843-7853.
- Ellett, D.J., Edwards, A. and Bowers, R.** (1986). The hydrography of the Rockall Channel – an overview. *Proc. Roy. Soc. Edinb. B* **88**, 61-81.
- Falkowski, P.G. and Owens, T.G.** (1978). Effects of light intensity on photosynthesis and dark respiration in six species of marine phytoplankton. *Mar. Biol.* **45**, 289-295.

- Falkowski, P.G., Katz, M.E., Knoll, A.H., Quigg, A., Raven, J.A., Schofield, O. and Taylor, F.J.R.** (2004). The evolution of modern eukaryotic phytoplankton. *Science* **305**, 354-360.
- Falkowski, P.G., Scholes, R.J., Boyle, E., Canadell, J., Canfield, D., Elser, J., Gruber, N., Hibbard, K., Högberg, P., Linder, S. *et al.*** (2000). The global carbon cycle: a test of our knowledge of Earth as a system. *Science* **290**, 291-296.
- Field, C.B., Behrenfeld, M.J., Randerson, J.T., Falkowski, P.G.** (1998). Primary production of the biosphere: integrating terrestrial and oceanic components. *Science* **281**, 237-240.
- Finlay, B.J.** (2002). Global dispersal of free-living microbial eukaryotic species. *Science* **296**, 1061-1063.
- Fried, S., Mackie, B. and Nothwehr, E.** (2003). Nitrate and phosphate levels positively affect the growth of algal species found in Perry Pond. *Tillers* **4**, 21-24.
- Fuhrman, J.A.** (1999). Marine viruses and their biogeochemical and ecological effects. *Nature* **399**, 541-548.
- Fuller, N.J., Tarran, G.A., Cummings, D.G., Woodward, E.M.S., Orcutt, K.M., Yallop, M., Le Gall, F. and Scanlan, D.J.** (2006a). Molecular analysis of photosynthetic picoeukaryote community structure along an Arabian Sea transect. *Limnol. Oceanogr.* **51**, 2502-2514.
- Fuller, N.J., Campbell, C., Allen, D.J., Pitt, F.D., Zwirgmaier, K., Le Gall, F., Vaulot, D. and Scanlan, D.J.** (2006b). Analysis of photosynthetic picoeukaryote diversity at open ocean sites in the Arabian Sea using a PCR biased towards marine algal plastids. *Aquat. Microb. Ecol.* **43**, 79-93.
- Fuller, N.J., Tarran, G.A., Yallop, M., Orcutt, K.M. and Scanlan, D.J.** (2006c). Molecular analysis of picocyanobacterial community structure along an Arabian Sea transect reveals distinct spatial separation of lineages. *Limnol. Oceanogr.* **51**, 2515–2526.
- Gast, R., Moran, D.M., Dennett, M.R. and Caron, D.A.** (2007). Kleptoplasty in an Antarctic dinoflagellate: caught in evolutionary transition? *Environ. Microb.* **9**, 39-45.
- Gibb, S.W., Barlow, R.G., Cummings, D.G., Rees, N.W, Trees C.C., Holligan, P. and Suggett, D.** (2000). Surface phytoplankton pigment distributions in the Atlantic Ocean: an assessment of basin scale variability between 50°N and 50°S. *Prog. Oceanogr.* **45**, 339-368.
- Giovannoni, S.J., Delong, E.F., Olsen, G.J. and Pace., N.R.** (1988). Phylogenetic group-specific oligodeoxynucleotide probes for identification of single microbial cells. *J. Bacteriol.* **170**, 720–726.

- Giovannoni, S.J. and Stingl, U.** (2005). Molecular diversity and ecology of microbial plankton. *Nature* **437**, 343-348.
- Gordon, J.D.M.** (2003). The Rockall Trough, Northeast Atlantic: the cradle of deep-sea biological oceanography that is now being subjected to unsustainable fishing activity. *J. Northw. Atl. Fish. Sci.* **31**, 57-83.
- Gosselin, M., Legendre L., Therriault, C. and Demers, S.** (1990) Light and nutrient limitation of sea-ice microalgae (Hudson Bay, Canadian Arctic). *J. Phycol.* **26**, 220-232.
- Gosselin, M., Levasseur, M., Wheeler, P.A., Horner, R.A. and Booth, B.C.** (1997). New measurements of phytoplankton and ice algal production in the Arctic Ocean. *Deep-Sea Res. II* **44**, 1623-1644.
- Gradinger, R. and Ikävalko J.** (1998). Organism incorporation into newly forming Arctic sea ice in the Greenland Sea. *J. Plankton Res.* **20**, 871-886.
- Greene, C.H., Pershing A.J., Cronin T.M. and Ceci, N.** (2008). Arctic climate change and its impacts on the ecology of the north Atlantic. *Ecology* **89**, supplement S24-S38.
- Grob, C., Ulloa, O., Li, W.K.W., Alarcon, G., Fukasawa, M., Watanabe, S.,** (2007). Picoplankton abundance and biomass across the eastern South Pacific Ocean along latitude 32.5 degrees S. *Mar. Ecol. Prog. Ser.* **322**, 53-62.
- Guillou, L., Chrétiennot-Dinet, M.-J., Medlin, L.K., Claustre, H., Loiseaux-de Goër, S. and Vault, D.** (1999). *Bolidomonas*: a new genus with two species belonging to a new algal class, the Bolidophyceae (Heterokonta). *J. Phycol.* **35**, 368-381.
- Guillou, L., Viprey, M., Chambouvet, A., Welsh, R.M., Kirkham, A.R., Massana, R., Scanlan, D.J. and Worden, A.Z.** (2008). Widespread occurrence and genetic diversity of marine parasitoids belonging to *Syndiniales* (Alveolata). *Environ. Microbiol.* **10**, 3349-3365.
- Hackett, J.D., Anderson, D.M., Erdner, D.L. and Bhattacharya, D.** (2004a). Dinoflagellates: a remarkable evolutionary experiment. *Am. J. Bot.* **91**, 1523-1534.
- Hackett, J.D., Yoon, H.S., Soares, M.B., Bonaldo, M.F., Casavant, T.L., Scheetz, T.E., Nosenko, T. and Bhattacharya, D.** (2004b). Migration of the plastid genome to the nucleus in a peridinin dinoflagellate. *Curr. Biol.* **14**, 213-218.
- Hamilton, A.K., Lovejoy, C., Galand, P.E. and Ingram, R.G.** (2008). Water masses and biogeography of picoeukaryote assemblages in a cold hydrographically complex system. *Limnol. Oceanogr.* **53**, 922-935.
- Herbland, A., Le Bouteiller, A. and Rimbault, P.** (1985). Size structure of phytoplankton biomass in the equatorial Atlantic Ocean. *Deep-Sea Res.* **32**, 819-836.

**Heywood, J.L., Zubkov, M.V., Tarran, G.A, Fuchs, B.M. and Holligan, P.M.** (2006). Prokaryoplankton standing stocks in oligotrophic gyre and equatorial provinces of the Atlantic Ocean: Evaluation of inter-annual variability. *Deep-Sea Res. II* **53**, 1530-1547.

**Higgins, H.W. and Mackay, D.J.** (2000). Algal class abundances estimated from chlorophyll and carotenoid pigments in the western Equatorial Pacific under El Niño and non-El Niño conditions. *Deep-Sea Res. I* **47**, 1461-1483.

**Holland, S.** (2003). <http://www.uga.edu/~strata/software/>.

**Holliday, N.P. and Reid, P.** (2001). Is there a connection between high transport of water through the Rockall Trough and ecological changes in the North Sea? *ICES Journal of Marine Science* **58**, 270-274.

**Holliday, N.P., Hughes, S.L., Bacon, S., Beszczynska-Möller, A., Hansen, B., Lavin, A., Loeng, H., Mork, K.A., Østerhus, S., Sherwin, T. et al.** (2008). Reversal of the 1960s to 1990s freshening trend in the northeast North Atlantic and Nordic Seas. *Geophys. Res. Lett.* **35**, L03614, doi: 10.1029/2007GL032675.

**Holliday, N.P., Yelland, M.J., Pascal, R., Swail, V.R., Taylor, P.K., Griffiths, C.R. and Kent, E.** (2006). Were extreme waves in the Rockall trough the largest ever recorded? *Geophys. Res. Lett.* **33**, L05613.

**Hooker, S.B., Rees, N.W. and Aiken, J.** (2000). An objective methodology for identifying oceanic provinces. *Prog. Oceanogr.* **45**, 313-338.

**Hughes, S.L., Holliday, N.P. and Beszczynska-Möller, A.** (Eds) (2008). ICES Report on Ocean Climate 2007. *ICES Cooperative Research Report* No. 291. 64 pp.

**Jardillier, L., Zubkov, M.V., Pearman, J. and Scanlan, D.J.** The importance of the smallest prymnesiophytes in oceanic CO<sub>2</sub> fixation. Submitted to *ISME J.*

**Johnson, M.D., Oldach, D., Delwiche, C.F. and Stoecker, D.K.** (2007). Retention of transcriptionally active cryptophyte nuclei by the ciliate *Myrionecta rubra*. *Nature* **445**, 426-428.

**Johnson, Z.I., Zinser, E.R., Coe, A., McNulty, N.P., Woodward, E.M.S. and Chisholm, S.W.** (2006). Niche partitioning among *Prochlorococcus* ecotypes along ocean-scale environmental gradients. *Science* **311**, 1737-1740.

**Joint, I.R. and Pipe, R.K.** (1984). An electron microscope study of a natural population of picoplankton from the Celtic Sea. *Mar. Ecol. Prog. Ser.* **20**, 113-118.

**Joint, I.R. and Pomroy, A.J.** (1986). Photosynthetic characteristics of nanoplankton and picoplankton from the surface mixed layer. *Mar. Biol.* **92**, 465-474.

**Katz, L.** (1998). Changing perspectives on the origin of eukaryotes. *Trends Ecol. Evol.* **13**, 493-497.

- Larsson, U. and Hagström, A.** (1982). Fractionated phytoplankton primary production, exudate release and bacterial production in a Baltic eutrophication experiment. *Marine Biology*. **67**, 57-70.
- Le Gall, F., Rigaut-Jalabert, F., Marie, D., Garczareck, L., Viprey, M., Godet, A. and Vaultot, D.** (2008). Picoplankton diversity in the South-East Pacific Ocean from cultured. *Biogeosciences* **5**, 203-214.
- Legendre, P. and Legendre, L.** (1998). *Numerical ecology*. (2nd edition). Elsevier Science BV, Amsterdam.
- Lepère, C., Boucher, D., Jardillier, L., Domaizon, I. and Debroas, D.** (2006). Succession and regulation factors of small eukaryote community composition in a lacustrine ecosystem (Lake Pavin). *Appl. Environ. Microbiol.* **72**, 2971-2981.
- Lepère, C., Domaizon, I. and Debroas, D.** (2008). Unexpected importance of potential parasites in the composition of the freshwater small-eukaryote community. *Appl. Environ. Microbiol.* **74**, 2940-2949.
- Lepère, C., Vaultot, D., and Scanlan, D. J.** (2009) Photosynthetic picoeukaryote community structure in the South East Pacific Ocean encompassing the most oligotrophic waters on Earth. *Environ. Microbiol.* **11**: 3105-3117.
- Li, W.K.W.** (1989). Shipboard analytical flow cytometry of oceanic ultraphytoplankton. *Cytometry* **10**, 564-579.
- Li, W.K.W.** (1994). Primary production of prochlorophytes, cyanobacteria, and eucaryotic ultraphytoplankton: Measurements from flow cytometric sorting. *Limnol. Oceanogr.* **39**, 169-175.
- Li, W.K.W., Subba Rao, D.V., Harrison, W.G., Smith, J.C., Cullen, J.J., Irwin, B. and Platt, T.** (1983). Autotrophic picoplankton in the tropical ocean. *Science* **219**, 292-295.
- Liu, H., Probert, I., Uits, J., Claustre, H., Aris-Brosou, S., Frada, M., Not, F. and de Vargas, C.** (2009). Extreme diversity in noncalcifying haptophytes explains a major pigment paradox in open oceans. *P. Natl. Acad. Sci.* **106**, 12803-12808.
- Longhurst, A.** (2007). *Ecological geography of the sea*, 2<sup>nd</sup> edn. Elsevier A.P.
- Lovejoy, C., Massana, R. and Pedrós-Alió, C.** (2006). Diversity and distribution of marine microbial eukaryotes in the Arctic Ocean and adjacent seas. *Appl. Environ. Microb.* **72**, 3085-3095.
- Lovejoy, C., Vincent, W.F., Bonilla, S., Roy, S., Martineau, M.J., Terrado, R., Potvin, M., Massana, R. and Pedros-Alio, C.** (2007). Distribution, phylogeny, and growth of cold-adapted picoprasinophytes in arctic seas. *J. Phycol.* **43**, 78-89.
- Lovell, C.R. and Konopka, A.** (1985). Primary and Bacterial production in two dimictic Indiana Lakes. *Appl. Environ. Microb.* **49**, 485-491.

- Ludwig, W., Strunk, O., Westram, R., Richter, L., Meier, H. Yadhukumar, Buchner, A., Lai, T., Steppi, S., Jobb, G *et al.*** (2004). Arb: a software environment for sequence data. *Nucl. Acids Res.* **32**, 1363-1371.
- Malone, T.** (1971). The relative importance of nannoplankton and netplankton as primary producers in tropical oceanic and neritic phytoplankton communities. *Limnol. Oceanogr.* **16**, 633-639.
- Mann, N.H., Cook, A., Millard, A., Bailey, S. and Clokie, M.** (2003). Marine ecosystems: Bacterial photosynthesis genes in a virus. *Nature* **424**, 741.
- Marañón, E. and Holligan, P.M.** (1999). Photosynthetic parameters of phytoplankton from 50°N to 50°S in the Atlantic Ocean. *Mar. Ecol. Prog. Ser.* **176**, 191-203.
- Marañón, E., Holligan, P.M., Barciela, R., Gonzalez, N., Mourino, B., Pazo, M.J. and Varela, M.** (2001). Patterns of phytoplankton size structure and productivity in contrasting open-ocean environments. *Mar. Ecol. Prog. Ser.* **216**, 43-56.
- Massana, R., Balagúe, V., Guillou, L. and Pedrós-Alió, C.** (2004). Picoeukaryotic diversity in an oligotrophic coastal site studied by molecular and culturing approaches. *FEMS Microb. Ecol.* **50**, 231-243.
- Mauchline, J.** (1988). Growth and breeding of meso- and bathypelagic organisms of the Rockall Trough, northeastern Atlantic Ocean and evidence of seasonality. *Mar. Biol.* **98**, 387-393.
- McDonald, S.M., Sarno, D., Scanlan, D.J. and Zingone, A.** (2007). Genetic diversity of eukaryotic ultraphytoplankton in the Gulf of Naples during an annual cycle. *Aquat. Microb. Ecol.* **50**, 75-89.
- McFadden, G. and Gilson, P.** (1995). Something borrowed, something green: lateral transfer of chloroplasts by secondary endosymbiosis. *Trends Ecol. Evol.* **10**, 12-17.
- Medlin, L.K., Metfies, K., Mehl, H., Wiltshire, K. and Valentin, K.** (2006). Picoeukaryotic plankton diversity at the Helgoland time series site as assessed by three molecular methods. *Microb. Ecol.* **52**, 53-71.
- Mommaerts, J.** (1973). The relative importance of nannoplankton in the North Sea primary production. *Br. Phycol. J.* **8**, 13-20.
- Moon van der Staay, S.Y., De Watchter, R. and Vaultot, D.** (2001). Oceanic 18S rDNA sequences from picoplankton reveal unsuspected eukaryotic diversity. *Nature* **409**, 607-610.



- Moore, C.M., Lucas, M.I., Sanders, R. and Davidson, R.** (2005). Basin-scale variability of phytoplankton bio-optical characteristics in relation to bloom state and community structure in the Northeast Atlantic. *Deep-Sea Res. I* **52**, 401-419.
- Moreira, D. and López-García, P.** (2002). The molecular ecology of microbial eukaryotes unveils a hidden world. *TRENDS Microbiol.* **10**, 31-38.
- Moreira, D. and Philippe, H.** (2001). Sure facts and open questions about the origin and evolution of photosynthetic plastids. *Res. Microbiol.* **152**, 771-780.
- Not, F., del Campo, J., Balagué, V., de Vargas, C. and Massana, R.** (2009) New insights into the diversity of marine picoeukaryotes. *Plos One* **4**, e7143.
- Not, F., Gausling, R., Azam, F., Heidelberg, J.F. and Worden, A.Z.** (2007b). Vertical distribution of picoeukaryotic diversity in the Sargasso Sea. *Environ. Microb.* **9**, 1233-1252.
- Not, F., Latasa, M., Marie, D., Cariou, T., Vaultot, D. and Simon, N.** (2004). A single species *Micromonas pusilla* (Prasinophyceae) dominates the eukaryotic picoplankton in the Western English Channel. *Appl. Environ. Microbiol.* **70**, 4064-4072.
- Not, F., Latasa, M., Scharek, R., Viprey, M., Karleskind, P., Balague, V., Ontoriaoviedo, I., Cumino, A., Goetze, E. and Vaultot, D.** (2008). Protistan assemblages across the Indian Ocean, with a specific emphasis on the picoeukaryotes. *Deep Sea Res. I.* **55**, 1456-1473.
- Not, F., Massana, R., Latasa, M., Marie, D., Colson, C., Eikrem, W., Pedrós-Alió, C., Vaultot, D. and Simon, N.** (2005). Late summer community composition and abundance of photosynthetic eukaryotes in Norwegian and Barents Seas. *Limnol. Oceanogr.* **50**, 1677-1686.
- Not, F., Valentin, K., Romari, K., Lovejoy, C., Massana, R., Töbe, K., Vaultot, D. and Medlin, L.** (2007). Picobiliphytes: a marine picoplanktonic algal group with unknown affinities to other eukaryotes. *Science* **315**, 252-254.
- Not, F., Zapata, M., Pazos, Y., Campaña, E., Doval, M. and Rodríguez, F.** (2007a). Size-fractionated phytoplankton diversity in the NW Iberian coast: a combination of microscopic, pigment and molecular analyses. *Aquat. Microb. Ecol.* **49**, 255-265.
- Nübel, U., Garcia-Pichel, F. and Muyzer, G.** (1997). PCR primers to amplify 16S rRNA genes from cyanobacteria. *Appl. Environ. Microbiol.* **63**, 3327-3332.
- Odum, H.T.** (1956). Efficiencies, size of organisms, and community structure. *Ecology* **37**, 592-597.
- Okolodkov, Y. B.** (2005) The global distribution patterns of toxic, bloom dinoflagellates recorded from the Eurasian Arctic. *Harmful Algae* **4**, 351-369.

- Olson, R.J., Vaultot, D. and Chisholm, S.W.** (1985). Marine phytoplankton distributions measured using shipboard flow cytometry. *Deep Sea Res. I.* **32**, 1273-1280.
- Palenik, B., Grimwood, J., Aerts, A., Rouzé, P., Salamov, A., Putnam, N., Dupont, C., Jorgensen, R., Derelle, E., Rombauts, S. et al.** (2007). The tiny eukaryotes *Ostreococcus* provides genomic insights into the paradox of plankton speciation. *Proc. Natl. Acad. Sci.* **104**, 7705-7710.
- Partensky, F., Blanchot, J., Lantoine, F., Neveux, J. and Marie, D.** (1996). Vertical structure of picophytoplankton at different trophic sites in the northeastern Atlantic Ocean. *Deep-Sea Res. I.* **43**, 1191-1213.
- Partensky, F., Hess, W.R. and Vaultot, D.** (1999). *Prochlorococcus*, a marine photosynthetic prokaryote of global significance. *Microbiol. Mol. Biol. R.* **63**, 106-127.
- Pauly, D. and Christensen, V.** (1995). Primary production required to sustain global fisheries. *Nature.* **374**, 255-257.
- Pidwirny, M. and Duffy, E.** (2008) "Ocean" In: Encyclopedia of Earth. Eds. Cleveland, C.J. (Washington, D.C.: Environmental Information Coalition, National Council for Science and the Environment). [First published in the Encyclopedia of Earth October 2, 2006; revised June 5 2008; retrieved July 21, 2009]. <<http://www.eoearth.org/article/Ocean>>.
- Post, W.M., Peng, T.H., Emanuel, W.R., King, A.W., Dale, V.H. and DeAngelis, D.L.** (1990). The global carbon cycle. *American Scientist* **78**, 310-326.
- Poulton, A.J., Holligan, P.M., Hickman, A., Kim, Y.-M., Adey, T.R., Stinchcombe, M.C., Holeton, C., Root, S. and Woodward, E.M.S.** (2006). Phytoplankton carbon fixation, chlorophyll-biomass and diagnostic pigments in the Atlantic Ocean. *Deep-Sea Res. II* **53**, 1593-1610.
- Raven, J.A.** (1998). The twelfth Tansley Lecture. Small is beautiful: The picophytoplankton. *Functional Ecol.* **12**, 503-513.
- Raymond, J., Zhaxybayeva, O., Gogarten, J.P., Gerdes, S.Y. and Blankenship, R.E.** (2009). Whole-genome analysis of photosynthetic prokaryotes. *Science.* **298**, 1616-1620.
- Richardson, T.L. and Jackson, G.A.** (2007). Small phytoplankton and carbon export from the surface ocean. *Science* **315**, 838-840.
- Richardson, A.J. and Schoeman, D.S.** (2004). Climate impact on plankton ecosystems in the northeast Atlantic. *Science* **305**, 1609-1612.
- Robinson, C., Poulton, A.J., Holligan, P.M., Baker, A.R., Forster, G., Gist, N., Jickells, T.D., Malin, G., Upstill-Goddard, R., Williams, R.G. et al.** (2006). The

Atlantic Meridional Transect (AMT) Programme: a contextual view 1995-2005. *Deep-Sea Res. II* **53**, 1485-1515.

**Rodríguez, F., Derelle, E., Guillou, L., Le Gall, F., Vaultot, D. and Moreau, H.** (2005). Ecotype diversity in the marine picoeukaryote *Ostreococcus* (Chlorophyta, Prasinophyceae). *Environ. Microb.* **7**, 853-859.

**Rodríguez-Martínez, R., Labrenz, M., del Campo, J., Forn, I., Jürgens, K. and Massana, R.** (2009). Distribution of the uncultured protist MAST-4 in the Indian Ocean, Drake Passage and Mediterranean Sea assessed by real-time quantitative PCR. *Environ. Microbiol.* **11**, 397-408.

**Romari, K. and Vaultot, D.** (2004). Composition and temporal variability of picoeukaryote community at a coastal site of the English Channel from 18S sequences. *Limnol. Oceanogr.* **49**, 784-798.

**Rost, B., Riebesell, U. and Sültemeyer, D.** (2006). Carbon acquisition of marine phytoplankton: effect of photoperiod length. *Limnol. Oceanogr.* **51**, 12-20.

**Saijo, Y.** (1964). Size distribution of photosynthesizing phytoplankton in the Indian Ocean. *J. Oceanogr. Soc. Japan* **19**, 187-189.

**Saldarriaga, J.F., Taylor, F.J.R., Keeling, P.J. and Cavalier-Smith, T.** (2001). Dinoflagellate nuclear SSU rRNA phylogeny suggests multiple plastid losses and replacements. *J. Mol. Evol.* **53**, 204-213.

**Sekiguchi, H., Moriya, M., Nakayama, T. and Inouye, I.** (2002). Vestigial chloroplasts in heterotrophic Stramenopiles *Pteridomonas danica* and *Ciliophrys infusionum* (Dictyochophyceae). *Protist* **153**, 157-167.

**Sharples, J., Moore, C.M., Rippeth, T.P., Holligan, P.M., Hydes, D.J., Fisher, N.R. and Simpson, J.H.** (2001) Phytoplankton distribution and survival in the thermocline. *Limnol. Oceanogr.* **46**, 486-496.

**Sherwin, T., Baker, A., Brand, T., Fromlett, J., Gibson, R., Gieschen, L., Harden-Davies, H., Holland, R., Hinz, D., Inall, M. et al.** (2008). Cruise D321b: Reykjavik to Clyde, August and September 2007, *SAMS Internal Report 255*, Dunstaffnage Marine Laboratory, Oban, pp 160.

**Simon, N., Barlow, R.G., Marie, D., Partensky, F. and Vaultot, D.** (1994). Characterisation of oceanic photosynthetic picoeukaryotes by flow cytometry. *J. Phycol.* **30**, 922-935.

**Simon, N., Campbell, L., Ornlófsdóttir, E., Groben R., Guillou, L., Lange, M. and Medlin L.K.** (2000). Oligonucleotide probes for the identification of three algal groups by dot blot and fluorescent whole-cell hybridisation. *J. Eukaryot. Microbiol.* **47**, 76-84.

**Simon, N., Cras, A., Foulon, E. and Lemée, R.** (2009). Diversity and evolution of marine phytoplankton. *Biologies* **332**, 159-170.

- Simon, N., Lebot, N., Marie, D., Partensky, F. and Vaultot, D.** (1995) Fluorescent *in situ* hybridisation with ribosomal-RNA-targeted oligonucleotide probes to identify small phytoplankton by flow cytometry. *Appl. Environ. Microbiol.* **61**, 2506-2513.
- Six, C., Finckel, Z.V., Rodríguez, F., Marie, D., Parkensky, F. and Campbell, D.A.** (2008) Contrasting photoacclimation strategies in ecotypes of the eukaryotic picoplankter *Ostreococcus*. *Limnol. Oceanogr.* **53**, 255-265.
- Šlapeta, J., López-García, P. and Moreira, D.** (2006). Global dispersal and ancient cryptic species in the smallest marine eukaryotes. *Mol. Biol. Evol.* **23**, 23-29.
- Solignac, S., de Vernal, A. and Giraudeau, J.** (2008) Comparison of coccolith and dinocyst assemblages in the northern North Atlantic: how well do they relate with surface hydrography? *Mar. Micropaleontol.* **68**, 115-135.
- Stibal, M., Elster, J., Šabacká, M. and Kaštovská, K.** (2007). Seasonal and diel changes in photosynthetic activity of the snow alga *Chlamydomonas nivalis* (Chlorophyceae) from Svalbard determined by pulse amplitude modulation fluorometry. *FEMS Microbiol. Ecol.* **59**, 265-273.
- Stolte, W., Kraay, G.W., Noordeloos, A.M. and Riegman, R.** (2000). Genetic and physiological variation in pigment composition of *Emiliana huxleyi* (Prymnesiophyceae) and the potential use of its pigment ratios as a quantitative physiological marker. *J. Phycol.* **36**, 529-539.
- Suttle, C. A.** (2007) Marine viruses – major players in the global ecosystem. *Nat. Rev. Microbiol.* **5**, 801-812.
- Tait, R.V. and Dipper, F.A.** (1998). *Elements of marine ecology*. (4th edition.). Butterworth-Heinemann Oxford.
- Takishita, K., Koike, K., Maruyama, T. and Ogata, T.** (2002). Molecular Evidence for plastid robbery (kleptoplastidy) in *Dinophysis*, a dinoflagellate causing diarrhetic shellfish poisoning. *Protist* **153**, 293-302.
- Tarran, G.A., Heywood, J.L. and Zubkov, M.V.** (2006). Latitudinal changes in the standing stocks of nano- and picoeukaryotic phytoplankton in the Atlantic Ocean. *Deep-Sea Res. II* **53**, 1516-1529.
- Tarran, G.A., Zubkov, M.V., Sleight, M.A., Burkill, P.H. and Yallop, M.** (2001). Microbial community structure and standing stocks in the NE Atlantic in June and July of 1996. *Deep-Sea Res. II* **48**, 963–985.
- Teira, E., Mouriño, B., Marañón, E., Pérez, V., Pazó, M.J., Serret, P., Armas, D., Escáñez, J., Woodward, E.M.S. and Fernández, E.** (2005). Variability of chlorophyll and primary production in the Eastern North Atlantic Subtropical Gyre: potential factors affecting phytoplankton activity. *Deep-Sea Res. I* **52**, 569-588.

- Tremblay, G., Belzile, C., Gosselin, M., Poulin, M., Roy, S. and Tremblay, J.E.** (2009). Late summer phytoplankton distribution along a 3500 km transect in Canadian Arctic waters: strong numerical dominance by picoeukaryotes. *Aquat. Microb. Ecol.* **54**, 55-70.
- Turnton, J. and Fenna, P.** (2008). Observations of extreme wave conditions in the north-east Atlantic during December 2007. *Weather* **63**, 352-355.
- Uchida, H. and Fukasawa, M. Eds.,** (2005) *WHP P6, I3/I4 Revisit Data Book Blue Earth Global Expedition 2003* (JAMSTEC, Yokosuka, Kanagawa).
- van Leeuwe, M.A. and Stefels, J.** (1998). Effects of iron and light stress on the biochemical composition of Antarctic *Phaeocystis* species (Prymnesiophyceae) II: pigment composition. *J. Phycol.* **34**, 496-504.
- Vaulot, D., Eikrem, W., Viprey, M. and Moreau, H.** (2008). The diversity of small eukaryotic phytoplankton ( $\leq 3 \mu\text{m}$ ) in marine ecosystems. *FEMS Microb. Rev.* **32**, 795-820.
- Vaulot, D., Romari, K. and Not, F.** (2002). Are autotrophs less diverse than heterotrophs in the marine picoplankton? *Trends Microbiol.* **10**, 266-267.
- Viprey, M., Guillou, L., Ferréol, M. and Vaulot, D.** (2008). Wide genetic diversity of picoplanktonic green algae (Chloroplastida) in the Mediterranean Sea uncovered by a phylum-biased PCR approach. *Environ. Microbiol.* **10**, 1804-1822.
- Waterbury, J.B., Watson, S.W., Guillard, R.R.L. and Brand, L.E.** (1979). Widespread occurrence of a unicellular, marine, planktonic, cyanobacterium. *Nature.* **277**, 293-294.
- Watson, R., Pauly, D., Christensen, V., Froese, R., Longhurst, A., Platt, T., Sathyendranath, S., Sherman, K., O'Reilly J. and Celone, P.** (2003). Mapping fisheries onto marine ecosystems for regional, oceanic and global integrations. In *Large marine ecosystems of the world*, pp. 375-395, Edited by G. Hempel and K. Sherman. Elsevier B.V.
- West, N.J. and Scanlan, D.J.** (1999). Niche-partitioning of *Prochlorococcus* populations in a stratified water column in the eastern North Atlantic Ocean. *Appl. Environ. Microbiol.* **65**, 2585-2591.
- West, N.J., Schönhuber, W.A., Fuller, N.J., Amann, R.I., Rippka, R., Post, A.F. and Scanlan, D.J.** (2001). Closely related *Prochlorococcus* genotypes show remarkably different depth distributions in two oceanic regions as revealed by *in situ* hybridization using 16S rRNA-targeted oligonucleotides. *Microbiology* **147**, 1731-1744.
- Wheeler, A.J., Kozachenko, M., Masson, D.G. and Huvenne, V.A.I.** (2008). Influence of benthic sediment transport on cold-water coral bank morphology and growth: the example of the Darwin Mounds, north-east Atlantic. *Sedimentology* **55**, 1875-1887.

- Williams, R.G., and Follows, M.J.** (2003). Physical transport of nutrients and maintenance of biological production. In: Fasham, J.R. *Ocean Biogeochemistry, The Role of the Ocean Carbon Cycle in Global Change*. Berlin, Germany: Springer-Verlag. 19-51.
- Williams, R.B. and Murdoch, M.B.** (1966). Phytoplankton production and chlorophyll concentration in the Beaufort Channel North Carolina. *Limnol. Oceanogr.* **11**, 73-83.
- Wilson, W.H. and Mann, N.H.** (1997). Lysogenic and lytic viral production in marine microbial communities. *Aquat. Microb. Ecol.* **13**, 95-100.
- Worden, A.Z.** (2006). Picoeukaryote diversity in coastal waters of the Pacific Ocean. *Aquat. Microb. Ecol.* **43**, 165-175.
- Worden, A.Z., Lee, J., Mock, T., Rouzé, P., Simmons, M.P., Aerts, A.L., Allen, A.E., Cuvelier, M.L., Derelle, E., Everett, M. et al.** (2009). Green evolution and dynamic adaptations revealed by genomes of the marine picoeukaryotes *Micromonas*. *Science* **324**, 268-272.
- Worden, A.Z., Nolan, J.K. and Palenik, B.** (2004). Assessing the dynamics and ecology of marine picophytoplankton: the importance of the eukaryotic component. *Limnol. Oceanogr.* **49**, 168-179.
- Xie, S.P., Annamalai, H., Schott, F. and McCreary, J.P.** (2002) Structure and mechanisms of South Indian Ocean climate variability. *J. Climate.* **15**, 864-878.
- Yentsch, C.M. and Horan, P.K.** (1989). Cytometry in the aquatic sciences – Introduction. *Cytometry* **10**, 497-499.
- Yentsch, C.S. and Ryther, J.H.** (1959). Relative significance of the net phytoplankton and nannoplankton in the waters of Vinyard Sound. *J. Cons. Perm. Int. Explor. Mer.* **24**, 231-238.
- Yuan, J., Chen, M.-Y., Shao, P., Zhou, H., Chen, Y.-Q. and Qu, L.-H.** (2004). Genetic diversity of small eukaryotes from the coastal waters of Nansha Islands in China. *FEMS Microb. Lett.* **240**, 163-170.
- Zeidner, G., Preston, C.M., Delong, E.F., Massana, R., Post, A.F., Scanlan, D.J. and Béjà, O.** (2003). Molecular diversity among marine picophytoplankton as revealed by *psbA* analyses. *Environ. Microbiol.* **5**, 212-216.
- Zhu, F., Massana, R., Not, F., Marie, D. and Vaultot, D.** (2005). Mapping of picoeucaryotes in marine ecosystems with quantitative PCR of the 18S rRNA gene. *FEMS Microbiol. Ecol.* **52**, 79-92
- Zubkov, M.V., Sleight, M.A., Burkill, P.H. and Leakey, R.J.G.** (2000). Picoplankton community structure on the Atlantic Meridional Transect: a comparison between seasons. *Prog. Oceanogr.* **45**, 369-386.

**Zubkov, M.V., Sleigh, M.A., Tarran, G.A., Burkill, P.H. and Leakey, R.J.G.** (1998). Picoplanktonic community structure on an Atlantic transect from 50°N to 50°S. *Deep-Sea Res. I.* **45**, 1339-1355.

**Zubkov, M.V. and Tarran, G.A.** (2008). High bacterivory by the smallest phytoplankton in the North Atlantic Ocean. *Nature* **455**, 224-227.

**Zwirgmaier, K., Heywood, J.L., Chamberlain, K., Woodward, E.M.S., Zubkov, M.V. and Scanlan, D.J.** (2007). Basin-scale distribution patterns of picocyanobacterial lineages in the Atlantic Ocean. *Environ. Microbiol.* **9**, 1278-1290.

**Zwirgmaier, K., Jardillier, L., Ostrowski, M., Mazard, S., Garczarek, L., Vault, D., Not, F., Massana, R., Ulloa, O. and Scanlan, D.** (2008) Global phylogeography of marine *Synechococcus* and *Prochlorococcus* reveals a distinct partitioning of lineages among oceanic biomes. *Environ Microbiol* **10**, 147–161.

## **Appendix**



16S and 18S rRNA gene sequences generated by this work have been submitted to Genbank and are available on the CD attached to this thesis.

Plastid 16S rRNA gene sequences from AMT15 have been deposited in Genbank, accession numbers GQ863739-GQ863780.

See file: AMT15\_plastid\_16S\_sequences.fas.

Plastid 16S rRNA gene sequences from the extended Ellett Line have been deposited in Genbank, accession numbers GQ863828-GQ863884.

See file: Ellett\_plastid\_16S\_sequences.fas.

Plastid 16S rRNA gene sequences from the Arctic cruise have been deposited in Genbank, accession numbers GQ863885-GQ863899.

See file: Arctic\_plastid\_16S\_sequences.fas.

18S rRNA gene sequences of potential photosynthetic classes from AMT15 have been deposited in Genbank, accession numbers GQ863798-GQ863827.

See file: AMT15\_18S\_potential\_photosynthetic\_sequences.fas.

18S rRNA gene sequences of heterotrophic lineages (excluding alveolates) from AMT15 have been deposited in Genbank, accession numbers GQ863781-GQ863797.

See file: AMT15\_18S\_heterotroph\_sequence.fas.

18S rRNA gene sequences of alveolates have been published (Guillou *et al.*, 2008) and are in Genbank, accession numbers EU780589-EU780636.

See file: AMT\_18S\_alveolate\_sequences.fas.

Class-specific percent relative hybridisation values for samples from AMT15 by dot blot hybridisation analysis.

Sample	Station	Depth (m)	Total	Prym	Chry	Cryp	Eust	Pela	Treb	Ping
1A	1	2	11	6	4	0	0	0	1	0
1B	1	10	34	5	27	1	0	0	1	0
1C	1	25	41	2	35	2	0	0	1	0
1D	1	35	27	3	21	1	0	0	1	0
1E	1	50	55	3	49	2	0	0	2	0
1F	1	100	45	10	30	1	0	1	2	0
3A	3	2	82	11	65	1	1	3	2	0
3B	3	10	100	25	72	1	0	0	2	0
3C	3	20	27	15	6	0	0	5	0	0
3D	3	35	41	27	6	0	0	6	0	0
3E	3	50	43	25	10	0	1	7	0	0
3G	3	80	36	6	28	1	1	0	0	0
5A	5	2	43	39	3	0	0	0	0	0
5B	5	10	41	38	2	0	0	0	0	0
5C	5	15	53	45	6	0	0	0	0	0
5E	5	30	83	72	9	1	0	0	0	0
5F	5	50	40	31	7	1	0	0	0	1
5I	5	110	17	0	3	0	1	11	0	0
7A	7	2	54	47	6	0	0	0	0	0
7B	7	15	55	44	10	1	0	0	0	0
7C	7	25	27	21	4	0	1	0	0	0
7E	7	50	75	65	9	0	0	0	0	0
7G	7	75	80	56	2	0	0	22	0	0
7I	7	110	77	66	2	0	0	9	0	0
9A	9	2	19	0	18	0	0	0	1	0
9B	9	15	13	0	12	0	0	0	0	0
9C	9	30	64	58	5	0	0	0	0	0
9E	9	55	46	37	9	0	0	0	0	0
9G	9	115	19	18	1	0	0	0	0	0
9I	9	180	11	8	1	0	0	0	2	0
10B	10	10	44	32	5	1	2	1	0	2
10E	10	25	62	52	5	1	2	1	0	1
10G	10	50	99	66	2	1	15	14	0	1
10H	10	75	35	29	1	0	2	2	0	1
11A	11	2	46	34	4	0	0	7	1	0
11B	11	5	55	43	2	2	0	7	1	0
11C	11	10	52	45	4	2	0	1	0	0
11D	11	15	65	56	6	1	1	0	0	0
11F	11	30	54	25	4	16	0	7	2	0
11H	11	50	53	21	4	23	0	3	1	1
12A	12	2	56	43	2	9	0	0	0	2
12B	12	10	55	42	3	8	1	0	0	1
12C	12	15	45	32	3	8	1	1	0	1
12G	12	50	18	7	4	5	1	0	0	0
12I	12	75	8	4	3	1	0	0	0	0
13A	13	2	19	6	7	3	0	1	2	0
13B	13	5	19	5	9	1	0	0	4	0
13C	13	10	20	5	7	1	0	3	3	0
13D	13	15	15	4	8	1	0	2	0	0

Continued next page

Sample	Station	Depth (m)	Total	Prym	Chry	Cryp	Eust	Pela	Treb	Ping
13F	13	25	11	3	7	1	0	0	0	0
13H	13	50	18	7	7	4	0	0	0	0
14A	14	2	23	11	2	9	0	0	0	0
14C	14	10	28	21	2	4	0	0	0	1
14E	14	30	8	4	2	1	0	0	0	0
14G	14	45	12	7	2	1	0	0	0	1
14I	14	70	13	7	3	1	1	0	0	1
15B	15	10	31	22	7	2	0	0	0	1
15C	15	15	36	26	9	2	0	0	0	0
15E	15	30	43	22	19	1	0	0	0	0
15F	15	70	45	35	6	3	0	0	0	0
15I	15	100	42	35	2	4	0	0	0	0
17A	17	2	51	9	41	0	1	0	0	0
17B	17	10	38	8	28	0	0	0	0	1
17C	17	15	37	8	26	0	0	1	0	2
17D	17	25	43	12	30	0	0	0	0	0
17G	17	60	39	22	8	9	0	0	0	0
17I	17	80	17	10	5	1	0	0	0	0
19A	19	2	46	11	35	1	0	0	0	0
19C	19	20	47	9	37	0	1	0	0	0
19D	19	30	27	9	18	0	0	0	0	0
19F	19	75	24	8	14	1	0	0	0	1
19G	19	110	14	13	0	0	0	0	0	0
21A	21	2	26	6	16	0	0	0	0	3
21B	21	15	21	2	18	0	0	0	0	0
21C	21	25	15	4	11	0	0	0	0	0
21D	21	45	27	3	23	0	0	0	0	0
21F	21	100	22	9	11	1	1	0	0	0
21G	21	150	5	4	0	0	0	0	0	0
23A	23	2	51	7	43	0	0	0	0	1
23B	23	20	56	11	44	0	1	0	0	0
23C	23	35	47	5	35	0	1	3	0	3
23D	23	60	15	3	10	0	0	0	1	0
23F	23	140	7	4	2	0	0	0	0	0
23H	23	200	7	2	2	0	0	0	2	0
25A	25	2	36	9	26	0	0	0	1	0
25B	25	25	24	7	16	1	0	0	0	0
25C	25	45	27	7	19	0	0	0	1	0
25D	25	80	31	8	22	0	1	0	1	0
25F	25	170	31	13	17	0	0	0	1	0
25H	25	200	5	0	0	0	0	0	4	0
27A	27	2	15	3	10	0	0	0	1	0
27B	27	30	22	5	16	0	0	0	1	0
27C	27	50	21	2	17	1	0	0	1	0
27D	27	85	17	3	12	1	0	0	1	0
27G	27	180	18	9	6	1	0	0	1	0
27H	27	275	11	0	4	1	2	0	2	0
29A	29	2	58	12	44	1	0	0	1	0
29B	29	20	26	3	21	1	0	0	2	0
29C	29	35	44	2	39	0	0	0	3	0
29D	29	60	37	4	30	0	0	1	1	0

Continued next page

Sample	Station	Depth (m)	Total	Prym	Chry	Cryp	Eust	Pela	Treb	Ping
29H	29	220	5	0	1	1	0	0	3	0
31A	31	2	34	13	18	0	0	1	1	0
31B	31	15	27	9	16	1	0	0	1	0
31C	31	25	23	11	10	0	0	0	1	0
31E	31	45	31	22	8	1	0	0	0	0
31F	31	100	17	3	8	1	0	2	3	0
31H	31	150	6	2	3	0	0	0	2	0
33A	33	2	25	10	12	0	0	1	2	0
33B	33	5	30	18	11	1	1	0	1	0
33C	33	10	27	11	11	2	0	0	2	0
33D	33	20	31	14	15	1	0	0	2	0
33E	33	40	33	3	16	10	1	0	2	0
33G	33	70	21	11	8	1	0	0	2	0
35A	35	2	30	21	8	0	1	0	0	0
35B	35	10	34	26	7	1	0	0	0	0
35C	35	20	37	29	7	0	1	0	0	0
35D	35	30	33	27	5	1	0	0	0	1
35F	35	75	23	16	5	1	0	0	0	0
35H	35	110	18	15	2	1	0	0	0	0

Class-specific percent relative hybridisation values for samples from the extended Ellett Line cruise by dot blot hybridisation analysis.

Sample	Station	Depth (m)	Total	Prym	Chry	Cryp	Pela	Ping
E2	IB23S	10	52	25	3	21	3	0
E3	IB23S	20	42	28	5	6	2	1
E4	IB23S	32	41	26	4	9	1	1
E5	IB23S	45	31	22	3	4	1	1
E6	IB23S	112	27	10	12	1	3	1
E7	IB21S	5	39	28	5	4	1	1
E8	IB21S	10	56	39	6	10	0	1
E9	IB21S	20	37	24	7	4	1	1
E10	IB21S	32	98	16	9	65	7	1
E11	IB21S	45	98	39	10	34	14	1
E12	IB21S	125	91	12	8	64	7	0
E13	IB16X	5	33	22	5	2	3	1
E14	IB16X	10	33	23	4	2	3	1
E15	IB16X	20	38	22	9	1	5	1
E16	IB16X	32	51	38	6	1	5	1
E17	IB16X	45	48	35	6	2	3	2
E18	IB16X	125	53	21	6	18	7	1
E19	IB4	5	70	18	20	7	24	1
E20	IB4	10	100	25	42	12	20	1
E21	IB4	20	83	23	35	7	17	1
E22	IB4	32	92	26	46	3	16	1
E23	IB4	45	48	22	10	3	12	1
E24	IB4	125	60	25	1	26	7	1
E25	RockallF	5	39	23	9	1	3	3
E26	RockallF	10	48	38	7	1	1	1
E27	RockallF	20	65	61	0	1	1	2
E28	RockallF	32	69	65	1	0	2	1
E29	RockallF	45	47	39	5	1	1	1
E31	RockallN	5	65	39	14	3	8	1
E32	RockallN	10	49	33	10	1	2	3
E33	RockallN	20	42	25	13	1	2	1
E34	RockallN	32	38	23	5	1	6	3
E35	RockallN	45	39	31	0	0	5	3
E37	9GA	5	35	11	12	10	1	1
E38	9GA	10	48	14	12	20	1	1
E39	9GA	20	44	14	12	15	1	2
E40	9GA	32	48	12	18	16	1	1
E42	EG3	5	21	9	9	1	1	1
E43	EG3	10	28	22	0	1	4	1
E44	EG3	20	27	23	2	0	1	1
E45	EG3	32	25	21	0	0	3	1
E46	EG3	45	28	20	5	0	2	1
E47	T800W	5	25	13	9	1	1	1
E48	T800W	10	29	12	14	1	1	1
E49	T800W	20	27	10	14	1	1	1
E50	T800W	32	25	9	13	1	1	1

Class-specific percent relative hybridisation values for samples from the Arctic Ocean cruise by dot blot hybridisation analysis.

Sample	Station	Depth (m)	Total	Prym	Chry	Cryp	Treb	Ping	Pavl	Chla
A1	Z01	6.4	99	58	17	14	1	6	2	1
A2	Z01	12.9	54	25	12	11	1	3	1	1
A3	Z01	19.9	59	20	24	9	0	3	2	1
A4	Z01	30.3	42	11	18	8	0	3	1	1
A5	Z01	59.3	44	16	16	8	0	2	1	1
A7	Z07	17.4	48	27	12	3	0	3	2	1
A8	Z07	24.8	42	25	9	3	0	3	1	1
A9	Z07	35.3	56	28	18	3	1	3	2	1
A10	Z07	62.0	68	20	34	3	1	6	2	2
A12	Z11	15.2	63	21	29	3	0	7	2	1
A13	Z11	25.2	45	14	20	3	0	5	2	1
A14	Z11	35.9	73	32	20	11	1	6	2	1
A15	Z11	60.7	38	9	16	7	0	3	1	2
A16	Z15	5.6	45	21	9	8	0	5	1	1
A17	Z15	15.8	30	9	12	6	0	2	1	0
A18	Z15	20.8	55	19	12	18	0	4	1	1
A19	Z15	32.2	65	23	14	14	0	10	2	2
A20	Z15	61.4	58	16	21	13	0	5	2	1
A21	Z18	5.9	50	21	13	8	0	5	2	1
A22	Z18	17.1	77	21	34	14	0	5	2	1
A23	Z18	25.6	50	19	14	10	0	5	1	1
A24	Z18	36.3	64	18	28	10	1	5	1	1
A25	Z18	61.3	38	16	13	5	0	2	1	1
A26	M09	5.3	55	17	23	9	1	3	1	1
A27	M09	10.8	50	0	23	17	0	6	2	2
A28	M09	20.5	59	2	39	11	0	3	2	2
A29	M09	30.7	39	0	26	6	0	3	2	2
A30	M09	51.4	44	5	29	5	0	3	1	1
A31	Z68	5.3	43	8	19	9	0	5	1	1
A32	Z68	15.6	28	9	6	8	0	2	2	1
A33	Z68	25.4	41	1	27	5	1	5	1	1
A34	Z68	35.7	24	9	3	6	0	4	1	1
A35	Z68	59.9	54	23	18	8	0	3	1	1
A36	Z65	6.0	43	14	16	8	0	3	1	1
A37	Z65	16.0	37	13	11	9	0	2	1	1
A38	Z65	24.8	35	12	14	5	0	2	1	1
A39	Z65	37.0	40	20	12	3	0	3	1	1
A40	Z65	60.5	40	17	9	8	0	4	1	1
A41	Z61	5.4	46	25	9	5	0	5	1	1
A42	Z61	15.5	67	38	13	5	0	8	1	2
A43	Z61	25.9	62	33	17	5	0	5	1	1
A44	Z61	35.1	55	31	12	5	0	5	1	1
A45	Z61	60.6	43	20	10	8	0	3	1	1
A46	Z59	5.5	39	16	13	4	0	3	1	2
A47	Z59	22.5	68	21	34	2	0	8	1	2
A48	Z59	35.7	40	21	9	3	0	5	1	1
A49	Z59	43.6	50	31	7	2	0	8	1	1
A50	Z59	61.2	60	36	9	2	0	10	2	1
A51	T06	5.6	57	20	17	13	1	3	1	2
A52	T06	10.6	57	24	15	12	0	3	1	2

Continued next page.

Sample	Station	Depth (m)	Total	Pym	Chry	Cryp	Treb	Ping	Pavl	Chla
A53	T06	15.4	39	17	11	5	0	3	1	2
A54	T06	20.1	37	14	12	5	0	3	1	2
A55	T06	35.6	43	18	13	3	0	6	1	2

Class-specific percent relative hybridisation values for samples from the Indian Ocean cruise VANC10MV by dot blot hybridisation analysis.

Sample	Station	Depth (m)	Prym	Chry	Cryp	Pela	Ping	Treb
I1	1	5	54	11	32	0	0	1
I2	1	25	37	13	15	0	0	1
I7	2	5	57	15	6	0	0	1
I8	2	35	58	14	6	0	0	1
I9	2	50	29	20	2	0	0	0
I10	2	100	6	1	0	0	0	1
I11	2	200	3	0	0	0	0	2
I13	3	5	25	7	1	0	0	1
I14	3	35	26	8	1	0	0	1
I15	3	75	39	12	2	0	0	1
I16	3	100	34	10	2	0	0	1
I17	3	200	5	3	1	0	0	2
I19	4	5	23	12	1	0	0	1
I20	4	50	12	20	1	0	0	1
I21	4	85	0	1	0	0	0	1
I22	4	110	34	8	2	0	0	1
I23	4	200	4	2	1	0	0	1
I24	4	800	6	6	0	0	0	1
I25	5	5	21	13	1	0	0	1
I26	5	50	16	11	1	0	0	0
I27	5	85	11	19	1	0	0	1
I28	5	120	11	6	1	0	0	0
I29	5	200	1	1	0	0	0	1
I30	5	800	0	2	0	0	0	1
I31	6	5	9	15	1	0	0	0
I32	6	45	8	10	1	0	0	0
I33	6	74	13	6	1	0	0	0
I34	6	120	12	5	1	0	0	0
I35	6	200	1	1	0	2	0	1
I36	6	800	1	2	0	0	0	2
I38	7	50	11	9	0	0	0	1
I39	7	100	20	11	1	5	0	1
I40	7	125	19	8	1	0	0	1
I41	7	200	9	2	1	0	0	1
I42	7	800	1	1	0	0	0	1
I43	8	5	11	14	1	0	0	0
I44	8	5	25	20	1	0	0	1
I45	8	45	27	18	1	0	0	1
I46	8	90	18	11	1	0	0	1
I47	8	120	19	6	1	1	0	1
I48	8	150	25	8	1	0	0	1
I49	8	200	13	5	1	0	0	1
I50	8	800	0	1	0	0	0	1
I51	9	0	8	12	1	0	0	0
I52	9	45	22	18	0	0	0	1
I53	9	80	26	12	1	0	0	1
I54	9	100	21	6	1	0	0	1
I55	9	120	16	5	1	0	0	0
I56	9	200	2	1	0	0	0	1
I57	9	1000	18	5	1	0	0	1

Continued next page.



Sample	Station	Depth (m)	Prym	Chry	Cryp	Pela	Ping	Treb
I58	10	5	12	14	1	0	0	1
I59	10	50	9	8	1	0	0	0
I60	10	85	12	6	0	0	0	0
I61	10	110	17	10	1	0	0	0
I62	10	200	5	1	0	0	0	1
I63	10	1000	8	6	0	0	0	1
I64	11	5	12	9	0	0	0	0
I65	11	50	42	6	1	1	0	0
I66	11	100	53	6	2	5	0	0
I67	11	120	49	11	1	5	0	0
I68	11	200	3	11	0	0	0	0
I69	11	1000	2	11	0	0	0	0
I70	12	5	37	12	1	1	0	0
I71	12	50	58	11	3	0	3	0
I72	12	75	50	11	1	8	1	0
I73	12	110	29	12	1	7	0	0
I74	12	200	21	13	0	3	0	0
I75	12	1000	2	28	0	1	0	0
I76	13	5	35	1	1	1	0	0
I77	13	50	33	58	1	0	0	1
I78	13	85	35	41	1	4	1	1
I79	13	120	22	37	1	4	0	1
I80	13	200	6	44	0	0	0	1
I82	14	5	30	11	1	3	1	0
I83	14	50	23	7	1	2	1	0
I84	14	70	43	49	1	7	0	1
I85	14	100	2	23	0	1	0	0

Class-specific percent relative hybridisation values for samples from the BEAGLE cruise by dot blot hybridisation analysis.

Sample	Depth (m)	Total	Prym	Chry	Cryp	Ping	Pavl	Chla
1.1	5	66	32	16	3	10	2	3
1.2	5	70	26	24	9	4	2	5
1.3	5	100	47	30	7	9	3	4
1.4	5	67	29	22	4	7	1	4
2.1	5	67	24	29	4	5	1	4
2.2	5	77	29	29	2	11	2	4
2.3	5	66	37	13	2	11	1	2
2.4	5	89	44	24	2	14	2	3
4.1	5	97	56	19	4	13	3	2
4.2	5	33	15	12	1	5	0	0
4.3	5	32	15	13	1	3	0	0
4.4	5	24	12	10	0	2	0	0
5.1	5	21	9	9	1	2	0	0
5.2	5	26	11	12	1	2	0	0
5.3	5	24	10	11	1	2	0	0